Analyse pflanzlicher Proteinkinasen

und ihrer nachgeschalteten Komponenten

Dissertation

der Mathematisch-Naturwissenschaftlichen Fakultät

der Eberhard Karls Universität Tübingen

zur Erlangung des Grades eines

Doktors der Naturwissenschaften

(Dr. rer. nat.)

vorgelegt von

Janika Witthöft

aus Rottweil

Tübingen

2011

Tag der mündlichen Qualifikation:	29.11.2011
Dekan:	Prof. Dr. Wolfgang Rosenstiel
1. Berichterstatter:	Prof. Dr. Klaus Harter
2. Berichterstatter:	Prof. Dr. Claudia Oecking

INHALTSVERZEICHNIS

ABKÜRZUNGSVERZEICHNIS

A	Alanin
aa	*amino acid*
ABA	Abscisinsäure
AHA1	ARABIDOPSIS H^+-ATPASE 1
AHK	*Arabidopsis* Histidinkinase
AHP	*Arabidopsis* HPt Protein
APRR	*Arabidopsis* Pseudo-Responseregulator
ARR	*Arabidopsis* Responseregulator
Atrboh	*Arabidopsis thaliana* respiratory burst oxidase homologue
BAK1	BRI1-ASSOCIATED KINASE 1
BES1	*bri1*-EMS SUPPRESSOR 1
BiFC	Bimolecular fluorescence complementation
BIN2	BRASSINOSTEROID INSENSITIVE 2
BKI1	BRI1 KINASE INHIBITOR 1
BL	Brassinolid
BR	Brassinosteroide
BRI1	BRASSINOSTEROID INSENSITIVE 1
BSK	BR SIGNALING KINASE
BSU1	*bri1*-SUPPRESSOR 1
BZR1	BRASSINAZOLE RESISTANT 1
CHASE	c*yclase/ histidine kinase-associated sensing extracellular*
CKI1	CYTOKININ INSENSITIVE 1
CSSM	*confocal sample scanning microscopy*
CTR1	CONSTITUTIVE TRIPLE RESPONSE 1
DREPP	DEVELOPMENTALLY REGULATED PLASMAMEMBRANE POLYPEPTIDE
EIN4	ETHYLENE INSENSITIVE 4
elf26	EF-Tu peptide 26
E_m	Membranpotential
EndoH	Endoglykosidase H
ER	Endoplasmatisches Retikulum
ERS	Ethylene response sensor
ETR	Ethylene resistant
Fc	Fusicoccin
flg22	Flagellin 22
FLS2	FLAGELLIN SENSITIVE 2
FLT	*fluorescence lifetime*; Fluoreszenzlebensdauer
FRET	Förster-Resonanzenergietransfer
GFP	grün fluoreszierendes Protein
H_2O_2	Wasserstoffperoxid
HPts	*histidine-containing phosphotransfer proteins*
ID	Inseldomäne
K	Lysin
kDa	Kilodalton
LRR-RLKs	*leucine rich-repeat receptor-like kinases*
MAPKKK	*Mitogen-activated protein kinase kinase kinase*
mbSUS	*mating-based split-ubiquitin system*
NLS	*nuclear localization signal*; Kernlokalisationssignal
NO	Stickstoffmonoxid
oV	Orthovanadat
PAMP	*pathogen-associated molecular pattern*
R	Arginin
ROS	*reactive oxygen species*
SERK	SOMATIC EMBRYOGENESIS RECEPTOR-LIKE KINASE
SLN1	SYNTHETIC LETHAL OF N-END RULE 1

SSK1	SUPPRESSOR OF SENSOR KINASE 1
T	Threonin
TCS	*two component system*; Zweikomponentensystem
TCSA	3,3',4',5-tetrachlorosalicylanilide
YPD1	TYROSINE (Y) PHOSPHATASE DEPENDENT 1

1 SUMMARY

In order to elucidate the mechanisms of plant signal transduction pathways, it is essential to analyze in detail the molecular function of the different signalling components and to determine whether aspects such as their subcellular localization or phosphorylation state play an important role in regulating their function.

Here, the subcellular localization of the cytokinin receptors AHK3 and AHK4 was analyzed. They are representatives of the histidine kinase family of the two-component system (TCS) which is an important signalling mechanism in *Arabidopsis*, based on a histidine to aspartate phosphorelay. Until now, it has been assumed that the cytokinin receptors reside at the plasma membrane (Kim *et al.* 2006). However, we showed that GFP- and RFP-fusions of AHK3 and AHK4, respectively, are localized at the endoplasmic reticulum (ER) of transiently transformed tobacco epidermal leaf cells and *Arabidopsis* cotyledon cells. Furthermore, the N- and C-terminal GFP fusions of AHK3 represent functional cytokinin receptors since they complement the cytokinin insensitive phenotype of the *ahk2ahk3* double mutant. The observed ER-localization of AHK3-GFP in transiently transformed leaves could be confirmed in these *Arabidopsis* lines. The sensitivity of AHK3-GFP and GFP-AHK3 to the endoglycosidase H substantiates their ER localization and leads to the assumption that the cytokinin-binding CHASE domain of AHK3 is exposed to the ER lumen. Apparently, the current model of cytokinin signal perception at the plasma membrane needs to be reconsidered.

Apart from the cytokinin receptors, the subcellular localization of the A-type response regulators (ARRs), representing output elements of the TCS, was examined. Although they do not have an obvious nuclear localization signal (NLS), they are mainly localized in the nucleus (Grefen & Harter 2004). It could be shown by single amino acid exchanges (lysine to alanine) that ARR3, 4, 7 and 15, which are representatives of the A-type ARRs, have short sequence motifs, whose mutation led to a mainly cytoplasmic localization of the corresponding GFP-fusions and, therefore serve as NLSs. Interestingly, the determined NLS positions are not conserved even between phylogenetically tightly related A-type ARRs and are located in the C-terminus of the proteins. Therefore, it can be assumed that this less examined C-terminal part of the A-type ARRs is relevant for their subcellular distribution, in contrast to the receiver domain which confers signalling.

Furthermore, AHK5, the least characterized histidine kinase of the TCS, was analyzed regarding its functional relevance in the stomatal closure response. Until now, AHK5 has only been identified as a negative regulator of ABA- and ethylene-induced root growth inhibition (Iwama *et al.* 2007). Here, it could be shown that stomatal closure, mediated by H_2O_2, which is produced in response to exogenous or endogenous stimuli, depends on AHK5. Stomata of different *ahk5* mutants did neither respond to exogenously applied H_2O_2 nor to factors like darkness, NO or ethylene that are known to enhance the endogenous H_2O_2 production. By protein-protein interaction studies of AHK5 with *downstream* elements of the TCS – phosphotransfer proteins (AHPs) and ARRs – it was possible to identify further components of the pathway, namely AHP1, AHP2 and ARR4. Using different *ahp* mutants as well as an *arr4* mutant, it could be confirmed that AHP1, AHP2 and ARR4 are crucial for stomatal closure in response to

different stimuli. Furthermore, it could be shown that the stomatal closure in response to H_2O_2 is depending on the phosphorylation state of ARR4. The complexity of this pathway leads to the conclusion that fine-tuning of the stomatal movement has a high impact on the plant's response to environmental stimuli.

Independently of the TCS, other phytohormones like brassinosteroids (BR) are also perceived by membrane bound receptors, namely BRI1 in the case of BR. Here, a fast BR-induced and BRI1-depending process in the plasma membrane (PM) of *Arabidopsis* could be described. BR leads to the hyperpolarisation of the PM accompanied by a cell wall expansion. This was shown by recording the fluorescence lifetime of BRI1-GFP which responds to changes in the physico-chemical environment of fluorescent proteins. The observed processes depend on the activity of the PM-bound H^+-ATPase (P-ATPase), which is in this case not regulated by the phosphorylation of a conserved threonine residue (T948) in its C-terminal auto-inhibitory domain. The BR-induced hyperpolarisation of the PM and the cell wall expansion are therefore early events in the BR-regulated cell elongation that are described for the first time *in planta* with high spatio-temporal resolution.

2 ZUSAMMENFASSUNG

Zum tieferen Verständnis pflanzlicher Signaltransduktionswege ist es essentiell, die molekulare Wirkungsweise ihrer einzelnen Komponenten im Detail zu untersuchen. Außerdem stellt sich die Frage, ob molekulare Eigenschaften wie deren subzelluläre Lokalisation oder ihr Phosphorylierungszustand für ihre Funktion ausschlaggebend sind.

Dafür wurde exemplarisch die subzelluläre Lokalisation der Cytokininrezeptoren AHK3 und AHK4 untersucht. Diese sind Vertreter der Familie der Histidinkinasen des Zweikomponentensystems (*two component system*, TCS), einem bedeutenden Signaltransduktionsmechanismus in Pflanzen, basierend auf einem Histidin zu Aspartat *Phosphorelay*. Bisher wurde angenommen, dass die Cytokininrezeptoren an der Plasmamembran lokalisiert sind (Kim *et al.* 2006). In dieser Arbeit wurde jedoch gezeigt, dass GFP- beziehungsweise RFP-Fusionsproteine von AHK3 und AHK4 in transient transformierten Tabakblättern sowie *Arabidopsis* Keimlingen am ER lokalisiert sind. Außerdem sind die GFP-Fusionen von AHK3 funktional, da sie den cytokinininsensitiven Phänotyp der *ahk2ahk3* Doppelmutante komplementieren. AHK3-GFP wurde auch in stabil transformierten *Arabidopsis*-Linien am ER detektiert. Die gezeigte Sensitivität von AHK3-GFP und GFP-AHK3 auf die Endoglykosidase H untermauert deren ER-Lokalisation und lässt ferner vermuten, dass AHK3 so orientiert ist, dass die cytokininbindende CHASE-Domäne ins ER-Lumen reicht. Aufgrund der hier erzielten Ergebnisse muss der Cytokininsignalweg neu überdacht werden.

Abgesehen von der subzellulären Lokalisation der Cytokininrezeptoren, war die der A-Typ Responseregulatoren (ARRs) von Interesse. Diese gehören zu den *Output*-Elementen des TCS und sind, obwohl sie kein offensichtliches Kernlokalisationssignal (*nuclear localization signal*, NLS) besitzen, größtenteils im Zellkern lokalisiert (Grefen & Harter 2004). Durch gezielte Einzelaminosäureaustausche (Lysin zu Alanin) konnte gezeigt werden, dass ARR3, 4, 7 und 15, typische Vertreter der A-Typ ARRs, kurze Sequenzmotive besitzen, deren Mutation zur einer überwiegend zytoplasmatischen Lokalisation der entsprechenden GFP-Fusionen führt und die daher als NLSs dienen. Die NLS-Sequenzen und ihre intramolekulare Lokalisation sind interessanterweise auch zwischen eng verwandten A-Typ ARRs nicht konserviert und befinden sich ausschließlich im C-Terminus der Proteine. Es ist daher zu vermuten, dass der bisher wenig untersuchte C-terminale Bereich der A-Typ ARRs für deren subzelluläre Lokalisation verantwortlich ist und ihm daher eine größere Bedeutung zukommt als bislang angenommen.

Des Weiteren wurde die bis dahin am wenigsten charakterisierte Histidinkinase des TCS, AHK5, hinsichtlich ihrer Funktion beim Schließen der Stomata untersucht. Bisher war AHK5 nur als negativer Regulator der ABA- und ethyleninduzierten Hemmung des Wurzelwachstums bekannt (Iwama *et al.* 2007). In der vorliegenden Arbeit konnte jedoch gezeigt werden, dass das Schließen der Stomata als Reaktion auf H_2O_2, welches aufgrund exo- oder endogener Auslöser gebildet wird, von AHK5 abhängt. *ahk5*-Mutanten reagierten weder mit Schließen der Stomata auf exogen appliziertes H_2O_2 noch auf Faktoren wie Dunkelheit, NO oder Ethylen, die die endogene H_2O_2-Produktion stimulieren. Durch Interaktionsstudien mit weiteren Elementen des TCS – Phosphotransferproteine (AHPs) und ARRs – wurden außerdem Komponenten des Signalwegs *downstream* von AHK5 identifiziert und zwar AHP1, AHP2 und ARR4. Durch die

Analyse verschiedener *ahp*- und einer *arr4*-Mutante konnte bestätigt werden, dass AHP1, AHP2 und ARR4 für die Reaktion der Stomata auf verschiedene exo- oder endogene Faktoren essentiell sind. Darüber hinaus konnte gezeigt werden, dass das Schließen der Stomata in Reaktion auf H_2O_2 vom Phosphorylierungszustand von ARR4 abhängt. Die Komplexität dieses Signalwegs unterstreicht die Bedeutung einer präzisen Feinregulierung des Stomataschlusses für die Pflanze.

Unabhängig vom TCS, werden auch andere Phytohormone wie die Brassinosteroide (BR) durch membrangebundene Rezeptoren wie in diesem Fall BRI1, perzipiert. In dieser Arbeit konnte ein früher BR-induzierter und BRI1-abhängiger Signaltransduktionsvorgang in der Plasmamembran (PM) charakterisiert werden. BR führt zur Hyperpolarisation der PM und zu einer damit verbundenen Verbreiterung der Zellwand, was durch die Aufzeichnung der Fluoreszenzlebensdauer von BRI1-GFP gezeigt werden konnte, die auf Änderungen der physikochemischen Umgebung eines Fluoreszenzproteins reagiert. Die beobachteten Prozesse stehen mit der Aktivität der PM-gebundenen H^+-ATPase (P-ATPase) in Zusammenhang, die jedoch offensichtlich in diesem Fall nicht durch Phosphorylierung eines konservierten Threoninrestes (T948) in ihrer C-terminalen autoinhibitorischen Domäne reguliert wird. Die BR-induzierte Hyperpolarisation der PM und die Verbreiterung der Zellwand sind daher frühe Ereignisse bei der BR-regulierten Zellstreckung, welche hier zum ersten Mal mit hoher räumlich-zeitlicher Auflösung *in planta* beschrieben werden konnten.

3 EINLEITUNG

Pflanzen sind in allen Entwicklungsstadien einer Vielzahl von Umwelteinflüssen ausgesetzt, an die sie sich anpassen müssen. Dabei spielen Signalmoleküle wie z.B. Phytohormone eine zentrale Rolle, die in einem komplexen Zusammenspiel die pflanzliche Entwicklung regulieren. Zu den Phytohormonen zählen Cytokinin, Auxin, Ethylen, Abscisinsäure (ABA) und Giberelline (klassische Phytohormone) sowie Brassinosteroide, Salicylsäure, Jasmonsäure und Strigolactone. Dabei werden beispielsweise Cytokinin, Ethylen und Brassinosteroide von membrangebundenen Kinasen perzipiert und führen über eine komplexe Signalkaskade reversibler Proteinphosphorylierungen zu einer zellulären Antwort, die meist auf einer veränderten Genexpression beruht. Um ein Signal bis zur Transkriptionsmaschinerie im Zellkern weiterzuleiten, ist oft ein geregelter Kerntransport bestimmter Proteine erforderlich. Für das tiefere Verständnis dieser Signalwege ist die Analyse der molekularen Wirkungsweise sowie der subzellulären Lokalisation der einzelnen Komponenten von zentraler Bedeutung.

3.1 Kernlokalisationssignale

Um in den Zellkern zu gelangen, müssen kernlokalisierte Proteine den Kernporenkomplex überwinden. Proteine, die kleiner als 40-60 kDa sind, können in der Regel passiv in den Zellkern diffundieren (Mattaj & Englmeier 1998; Moore 1998), größere Proteine erfordern dagegen einen aktiven Kernimport und damit ein funktionales Kernlokalisationssignal (*nuclear localization signal*, NLS), das durch Kernimportfaktoren wie Karyopherine erkannt wird (Macara 2001; Peters 2009). NLS können in zwei Hauptgruppen unterteilt werden: Klassische und nicht klassische NLS. Klassische NLS sind kurze Peptidmotive bestehend aus basischen Aminosäuren, meist Lysin (K) und Arginin (R). Sie können weiter in mono- und bipartite NLS unterteilt werden (Raikhel 1992; Hicks *et al.* 1995; Macara 2001). Ein monopartites NLS besteht aus mindestens vier basischen Aminosäuren in Folge wie z.B. das des großen Antigens des SV40 Virus (KKKRK) (Kalderon *et al.* 1984). Andere monopartite NLS sind die c-myc ähnlichen NLS (KRVK) mit einem basischen Abschnitt, der durch mindestens eine ungeladene Aminosäure unterbrochen wird (Dang & Lee 1988). Ein bipartites NLS definiert sich durch zwei basische Regionen, die durch eine Zwischensequenz unterschiedlicher Länge und Zusammensetzung, meist 10-30 Aminosäuren, voneinander getrennt sind (Lange *et al.* 2007; Pawlowski *et al.* 2010). Ein Beispiel dafür ist das bipartite NLS von Nukleoplasmin (KAVKRPAATKKAGQAKKKKL) (Robbins *et al.* 1991). Nicht klassische NLS sind hingegen weniger gut charakterisiert und haben unterschiedliche Sequenzmuster (Mattaj & Englmeier 1998).

Auch in Pflanzen existieren NLS, die den verschiedenen Kategorien zugeordnet werden können. Das Opaque2-Protein (O2) aus Mais enthält z.B. zwei verschiedene NLS-Typen. Das NLS A (NAIL**RRK**LEEDLE) kann den SV40-ähnlichen NLS zugeordnet werden während das NLS B (**RKRK**ESNRESA**RR**S**R**Y**RK**) ein bipartites NLS darstellt (Varagona *et al.* 1992).

3.2 Signalwege verschiedener Phytohormone

3.2.1 Cytokinine

Cytokinine wurden in den 1950er Jahren aufgrund ihrer Fähigkeit entdeckt, die Zellteilung in Tabakgewebekulturen zu fördern (Miller *et al.* 1955). Allgemein lassen sich Cytokinine als N^6-substituierte Adeninderivate mit einer isoprenoiden oder einer aromatischen Seitenkette beschreiben. In Pflanzen finden sich überwiegend Cytokinine mit isoprenoider Seitenkette, wobei *trans*-Zeatin und Isopentenyladenin als wichtigste Vertreter zu nennen wären (Sakakibara 2006).

Cytokinine sind an den meisten pflanzlichen Entwicklungsprozessen beteiligt – oft im Zusammenspiel mit anderen Hormonen. So hängt es in Gewebekulturen vom Verhältnis zwischen Cytokinin und Auxin ab, ob die Wurzel- oder die Sprossbildung induziert wird (Skoog & Miller 1957). Auch außerhalb von Gewebekulturen üben Cytokinin und Auxin antagonistische Wirkungen aus. So hemmt Cytokinin die Seitenwurzelbildung (Li *et al.* 2006; Laplaze *et al.* 2007), fördert jedoch das Austreiben von Seitenknospen am Spross. Auxin hingegen fördert die Apikaldominanz und hemmt damit das Austreiben von Seitenknospen (Tanaka *et al.* 2006; Shimizu-Sato *et al.* 2009). Bei der Spross- und Wurzelentwicklung hat Cytokinin einen positiven Effekt auf die Aktivität des Sprossmeristems, hingegen einen negativen auf das Wurzelmeristem und hemmt daher das Wurzelwachstum (Werner *et al.* 2003). Nach Infektion einer Pflanze mit *Agrobacterium tumefaciens* werden aufgrund von gesteigerter Cytokininproduktion und Zellteilung Wurzelhalstumoren gebildet (Costacurta & Vanderleyden 1995). Cytokinine sind außerdem für die Entwicklung der Leitgewebe in der Wurzel essentiell (Mähönen *et al.* 2006a; Mähönen *et al.* 2006b) und spielen bei der ABA-Signaltransduktion sowie bei der Reaktion auf osmotischen Stress eine Rolle (Tran *et al.* 2007; Tran *et al.* 2010). Licht- und Cytokininsignaltransduktion sind über den *Arabidopsis* Responseregulator 4 (ARR4) miteinander verbunden, sodass Cytokinin auch die photomorphogenetische Entwicklung einer Pflanze beeinflusst (Sweere *et al.* 2001; Mira-Rodado *et al.* 2007). Außerdem verzögern Cytokinine die Blattseneszenz (Richmond & Lang 1957; Gan & Amasino 1995) und scheinen mit exogenen Faktoren wie der Nährstoffversorgung in Verbindung zu stehen (Franco-Zorrilla *et al.* 2002; Franco-Zorrilla *et al.* 2005). Die Cytokininperzeption und -signaltransduktion verlaufen über ein sogenanntes *Multi-Step* Zweikomponentensystem.

3.2.2 Das Zweikomponentensystem

Das Zweikomponentensystem (*two component system*, TCS) ist ein Signaltransduktionsmechanismus, der auf einem Phosphotransfer zwischen Histidin und Aspartat basiert. In seiner einfachen Form besteht es aus zwei Komponenten: Einer Histidinkinase und einem Responseregulator. Die Histidinkinase setzt sich aus einer *Input*- und einer *Transmitter*-Domäne zusammen, der Responseregulator aus *Receiver*- und *Output*-Domäne. Durch ein Signal, das an der *Input*-Domäne der Histidinkinase wahrgenommen wird, kommt es zur Autophosphorylierung ihrer *Transmitter*-Domäne an einem konservierten Histidinrest. Von dort wird die Phosphorylgruppe auf ein Aspartat in der *Receiver*-Domäne des Responseregulators übertragen, wodurch dieser aktiviert wird und eine spezifische zelluläre Reaktion in Gang setzt. Beim sogenannten *Multi-Step* TCS ist zwischen Histidinkinase und Responseregulator noch eine weitere Komponente

geschaltet, die HPts (*Histidine-containing phosphotransfer proteins*). Die beteiligten Histidinkinasen werden Hybrid-Histidinkinasen genannt und bestehen aus *Input*- und *Transmitter*-Domäne sowie einer *Receiver*-Domäne. Von der *Transmitter*-Domäne kommend wird die Phosphorylgruppe erst intramolekular auf einen Aspartatrest in der *Receiver*-Domäne weitergeleitet. Von dort aus wird das Phosphat auf ein konserviertes Histidin in den HPts übertragen und schließlich auf ein Aspartat in der *Receiver*-Domäne der Responseregulatoren, die in phosphoryliertem Zustand die zelluläre Antwort steuern (Horak *et al.* 2011).
Es wurde lange vermutet, dass Zweikomponentensysteme ausschließlich in Prokaryoten vorkommen. Dies wurde jedoch durch die Entdeckung von zwei eukaryotischen Histidinkinasen widerlegt: Der Osmosensor SLN1 aus Hefe (Ota & Varshavsky 1993; Maeda *et al.* 1994), sowie der Ethylenrezeptor ETR1 aus *Arabidopsis* (Chang et al. 1993) sind Hybrid-Histidinkinasen.

Die Familie der Hybrid-Histidinkinasen in *Arabidopsis* umfasst elf Mitglieder. AHK2, AHK3 und AHK4 (ARABIDOPSIS HISTIDINKINASE) dienen als Cytokininrezeptoren, wobei die Cytokininbindung an ihrer CHASE-Domäne (c*yclase/histidine kinase-associated sensing extracellular*) erfolgt (Inoue *et al.* 2001; Suzuki *et al.* 2001; Ueguchi *et al.* 2001; Yamada *et al.* 2001; Wulfetange *et al.* 2011b). Eine Funktion als Cytokininrezeptor wurde zuerst für AHK4 gezeigt und zwar in der letalen Hefemutante *Sln1*, in der das für die einzige Histidinkinase der Hefe codierende Gen, *SLN1*, defekt ist (Maeda *et al.* 1994; Posas *et al.* 1996). Durch Expression von *AHK4* in dieser Mutante, wird deren Letalität cytokininabhängig aufgehoben (Inoue *et al.* 2001; Ueguchi *et al.* 2001).
Die Cytokininrezeptoren haben teilweise überlappende, jedoch auch deutlich voneinander unterscheidbare Expressionsmuster, die mit ihrer Funktion korrelieren. *AHK4* ist verstärkt in Wurzeln exprimiert *AHK2* und *AHK3* dagegen in Blättern (Higuchi *et al.* 2004; Nishimura *et al.* 2004). Dementsprechend ist z.B. hauptsächlich AHK3 für die Verzögerung der Blattseneszenz durch Cytokinin verantwortlich (Kim *et al.* 2006) und AHK4 spielt eine Rolle bei der Entwicklung der Wurzel (Nishimura *et al.* 2004). AHK4 scheint außerdem den Cytokininsignalweg über einen bidirektionalen *Phosphorelay* zu regulieren: Sie kann AHPs (*Arabidopsis* HPts) nicht nur phosphorylieren sondern in Abwesenheit von Cytokinin auch dephosphorylieren, was zur Inaktivierung des Signalwegs führt (Mähönen *et al.* 2006a; Mähönen *et al.* 2006b).
Einzelmutanten der Cytokininrezeptoren lassen sich phänotypisch nicht von Wildtyppflanzen unterscheiden und erst eine *ahk2,3,4*-Tripelmutante ist cytokinininsensitiv und stark zwergwüchsig, was auf eine redundante Funktion der Rezeptoren schließen lässt (Higuchi *et al.* 2004; Nishimura *et al.* 2004; Riefler *et al.* 2006).
Auch das Phytohormon Ethylen wird von Histidinkinasen perzipiert. Neben dem bereits erwähnten ETR1 finden sich in *Arabidopsis* vier weitere Ethylenrezeptoren: ERS1, ETR2, ERS2 und EIN4 (Hwang *et al.* 2002; Grefen & Harter 2004; Guo & Ecker 2004). Aufgrund von Sequenzunterschieden können diese in zwei Unterfamilien unterteilt werden: Unterfamilie I besteht aus ETR1 und ERS1, welche Histidinkinaseaktivität besitzen. ETR2, ERS2 und EIN4 gehören zur zweiten Unterfamilie, der für die Histidinkinaseaktivität essentielle Aminosäurereste fehlen (Hall & Bleecker 2003). Der Ethylensignalweg läuft in weiten Teilen unabhängig vom TCS über CTR1 (CONSTITUTIVE TRIPLE RESPONSE 1), eine

Raf-ähnliche MAPKKK (*Mitogen-activated protein kinase kinase kinase*) ab (Gao *et al.* 2003). Ob die Signalweiterleitung *downstream* von CTR1, einem negativen Regulator der Ethylensignaltransduktion, über eine herkömmliche MAPK-Kaskade verläuft, wird derzeit intensiv diskutiert (Hahn & Harter 2009). Jedoch auch der Weg über das TCS ist nicht bedeutungslos, da beispielsweise die ETR1-abhängige Phosphorylierung von ARR2 die Transkription ethylenregulierter Gene aktiviert (Hass *et al.* 2004).
Weitere Histidinkinasen dienen als Osmosensor (AHK1) (Urao *et al.* 1999; Tran *et al.* 2007; Wohlbach *et al.* 2008) oder sind essentiell für die Entwicklung des weiblichen Gametophyten (CKI1) (Pischke *et al.* 2002; Hejatko *et al.* 2003). AHK5 ist die einzige Histidinkinase, die keine Transmembrandomäne besitzt, weshalb eine zytoplasmatische Lokalisation angenommen wird (Grefen & Harter 2004). Welches Signal die Autophosphorylierung von AHK5 initiiert ist noch nicht eindeutig geklärt, jedoch scheint sie an der Integration verschiedener Signalwege beteiligt zu sein. So ist AHK5 beispielsweise ein negativer Regulator des Signalweges, bei dem Ethylen und ABA das Wurzelwachstum hemmen, d.h. die Wurzeln einer *ahk5*-Mutante reagieren hypersensitiv auf Ethylen und ABA (Iwama *et al.* 2007).

Die AHPs stellen die Bindeglieder zwischen Histidinkinasen und Responseregulatoren dar. AHP1-5 sind positive Regulatoren des Cytokininsignalweges und in ihrer Funktion redundant (Hutchison *et al.* 2006). Ihnen wird eine *Shuttle*-Funktion zwischen Zellkern und Zytoplasma zugeschrieben, wodurch die Phosphorylgruppe von den membrangebundenen Histidinkinasen zu den im Kern lokalisierten Responseregulatoren weitergeleitet wird. Bisher wurde angenommen, dass AHP1 und AHP2 cytokininabhängig im Zellkern akkumulieren (Hwang & Sheen 2001), wobei kürzlich jedoch gezeigt wurde, dass eine nukleozytoplasmatische Verteilung dauerhaft aufrechterhalten wird (Punwani *et al.* 2010). AHP6 ist ein Pseudo-AHP, bei dem das konservierte, für den Phosphotransfer notwendige, Histidin durch ein Asparagin ersetzt ist und das daher nicht phosphoryliert werden kann. AHP6 kommt eine Sonderfunktion zu, da es ein negativer Regulator der Cytokininantwort und für die Entwicklung der Leitgewebe von Bedeutung ist (Mähönen *et al.* 2006a).

Die Endglieder des *Multi-Step* Zweikomponentensystems bilden die *Arabidopsis* Responseregulatoren (ARRs), die sich in vier Gruppen einteilen lassen: A-Typ (ARR3-9, ARR15-17), B-Typ (ARR1, ARR2, ARR10-14, ARR18-21) und C-Typ ARRs (ARR22 und ARR24) sowie die Pseudo-ARRs (APRR1-9) (Imamura *et al.* 1999; Horák *et al.* 2008).
A-Typ ARRs bestehen aus einer hoch konservierten *Receiver*-Domäne und einem kurzen C-terminalen Bereich mit unterschiedlicher Aminosäurezusammensetzung (D'Agostino *et al.* 2000). Die Transkription der A-Typ ARRs wird durch Cytokinin induziert (Brandstatter & Kieber 1998; D'Agostino *et al.* 2000; Hwang & Sheen 2001), wobei eine Hauptfunktion der A-Typ ARRs die negative Regulation der Cytokininantwort darstellt (To *et al.* 2004). Einige A-Typ ARRs werden nach Phosphorylierung über das Zweikomponentensystem, cytokininabhängig stabilisiert, was sich in einer erhöhten Proteinhalbwertszeit widerspiegelt (To *et al.* 2007).

A-Typ ARRs sind an vielen pflanzlichen Entwicklungs- und Wachstumsprozessen beteiligt. So ist z.B. ARR4 in der Lage, die Licht- und die Cytokininsignaltransduktion miteinander zu verknüpfen, indem es mit Phytochrom B interagiert und den Photorezeptor in seiner aktiven Form stabilisiert (Sweere *et al.* 2001; Mira-Rodado *et al.* 2007). ARR3, ARR4 und ARR9 spielen außerdem bei der Regulation der circadianen Rhythmik eine Rolle (Salome *et al.* 2006; Zheng *et al.* 2006; Ishida *et al.* 2008) und ARR7 hat eine Funktion bei der Antwort auf Kältestress (Jeon *et al.* 2010). Weiter ist bekannt, dass das Homöodomänenprotein WUSCHEL die Transkription von *ARR5*, *ARR6*, *ARR7* und *ARR15* direkt unterdrückt, wodurch eine korrekte Meristementwicklung ermöglicht wird (Leibfried *et al.* 2005). Die Transkription von *ARR7* und *ARR15* wird außerdem durch Auxin aktiviert, was für die Bildung von Wurzelstammzellen während der Embryonalentwicklung entscheidend ist (Müller & Sheen 2008). Im Sprossmeristem hingegen wird die Expression von *ARR7* und *ARR15* durch Auxin unterdrückt (Zhao *et al.* 2010).

Die B-Typ ARRs bestehen aus einer *Receiver*-Domäne und einer ausgedehnten C-terminalen *Output*-Domäne mit einem GARP DNA-Bindemotiv (Riechmann *et al.* 2000), einer Transaktivierungsdomäne und mindestens einem NLS (Grefen & Harter 2004). Sie sind aktive Transkriptionsfaktoren und daher im Zellkern lokalisiert, wobei sie cytokininabhängig die Transkription der A-Typ ARRs steuern (Sakai *et al.* 2000; Hwang & Sheen 2001; Imamura *et al.* 2001; Lohrmann *et al.* 2001; Sakai *et al.* 2001; Imamura *et al.* 2003). B-Typ ARRs sind positive Regulatoren der Cytokininantwort, was sich darin widerspiegelt, dass z.B. eine *arr1*-Mutante eine verminderte Cytokininsensitivität zeigt (Sakai *et al.* 2001). Mehrfachmutanten von B-Typ ARRs reagieren sukzessive weniger sensitiv auf Cytokinin, wobei die *arr1,10,12*-Tripelmutante fast komplett insensitiv ist (Mason *et al.* 2005) und auch die transkriptionelle Aktivierung vieler cytokininregulierter Gene ausbleibt (Argyros *et al.* 2008). Daher scheinen besonders diese drei B-Typ ARRs eine entscheidende Rolle in der Cytokininsignaltransduktion zu spielen.

Die C-Typ ARRs sind speziell in reproduktiven Organen exprimiert und haben eine *Receiver*-Domäne, die der der Histidinkinasen ähnelt. Betrachtet man allerdings ihre Struktur und Funktion gleichen sie eher den A-Typ ARRs, wobei ihre Expression nicht durch Cytokinin induziert wird. Die ektopische Expression des C-Typ ARRs *ARR22* in anderen Geweben führt zu einem zwergenhaften Phänotyp mit schwach ausgebildetem Wurzelsystem und einer Störung des Cytokininsignalweges. Auch der Phänotyp eines ARR22-Überexprimierers lässt vermuten, dass ARR22 auf bisher noch ungeklärte Weise in die Cytokininsignaltransduktion eingreift (Kiba *et al.* 2004; Gattolin *et al.* 2006; Horák *et al.* 2008).

Den APRR fehlt der für ihre Phosphorylierung notwendige Aspartatrest und sie haben eine Funktion bei der Regulierung der circadianen Uhr (McClung 2006).

3.2.3 Brassinosteroide

Brassinosteroide (BR) sind pflanzliche Steroidhormone, die die vegetative und reproduktive Entwicklung der Pflanze steuern. Sie fördern die Zellstreckung und Zellteilung, regulieren Fruchtreife und Seneszenz sowie die Pollenentwicklung und deren Fertilität. Außerdem sind sie an der Reaktion auf vielfältige Umwelteinflüsse beteiligt – oft im Zusammenspiel mit anderen Phytohormonen wie Cytokininen, Giberellinen und Auxinen (Mandava 1988; Clouse & Sasse 1998; Altmann 1999; Bishop 2003). Ihren Namen

verdanken sie der Tatsache, dass das erste pflanzliche Steroidhormon, Brassinolid (BL), aus Pollen von *Brassica napus* (Raps) isoliert wurde (Grove *et al.* 1979).

Eine Hauptfunktion der Brassinosteroide ist die Regulation des vegetativen Wachstums. Dies kann über verstärkte Zellstreckung oder eine Erhöhung der Zellenanzahl erreicht werden, wobei Ähnlichkeiten zur auxininduzierten Zellstreckung bestehen. Diese erfolgt über die Ansäuerung des Apoplasten und eine damit verbundene Aktivierung pH-abhängiger Expansine, was zur Lockerung der Zellwand führt. Dadurch wird der Zellwanddruck vermindert und Wasser kann in die Vakuole aufgenommen werden, wodurch sich das Volumen der Zelle erhöht (Rayle & Cleland 1970, 1977; Cleland *et al.* 1991; Rayle & Cleland 1992). Als Antwort auf BL erfolgt vor Beginn der Zellstreckung eine Protonenausschüttung in den apoplastischen Raum sowie die Hyperpolarisation der Plasmamembran (Romani *et al.* 1983; Cerana *et al.* 1985; Mandava 1988). Kürzlich konnte gezeigt werden, dass wenige Minuten nach BL-Behandlung in Zellen von *Arabidopsis*-Keimlingen, die eine GFP-Fusion des BR-Rezeptors BRI1 (BRASSINOSTEROID INSENSITIVE 1) exprimieren, eine Zellwandexpansion auftritt, die mit der vorhandenen Menge an BRI1-GFP in Zusammenhang steht (Elgass *et al.* 2009; Elgass *et al.* 2010a). Das bedeutet, dass die Gesamtmenge an BRI1 oder seine Dichte von regulatorischer Relevanz ist, was auch der Grund dafür sein könnte, dass Wurzel- und Hypokotylzellen hinsichtlich der Zellwandverbreiterung unterschiedlich auf BL reagieren (Elgass *et al.* 2010b). Die Zellwandverbreiterung wird der Zellwandlockerung, verbunden mit einer Wasseraufnahme in den Apoplasten und einem Anschwellen der Zellwand, zugeschrieben, welche der Zellstreckung voraus gehen (Clouse & Sasse 1998; Haubrick & Assmann 2006; Elgass *et al.* 2009) und wurde von einer Änderung der Fluoreszenzlebensdauer (*fluorescence lifetime*, FLT) von BRI1-GFP begleitet, was eine Änderung dessen physikochemischer Umgebung widerspiegelt (Elgass *et al.* 2009).

3.2.4 Der Brassinosteroidsignalweg

Der Brassinosteroidrezeptor BRI1 ist an der Plasmamembran lokalisiert und gehört zur Familie der *leucine rich-repeat receptor-like kinases* (LRR-RLKs) (Clouse *et al.* 1996; Li & Chory 1997). Er besitzt eine extrazelluläre Domäne bestehend aus 25 LRRs und einer Inseldomäne (ID) zwischen LRR 21 und 22, gefolgt von einer Transmembrandomäne und einem zytoplasmatischen Teil. Dieser enthält die sogenannte Juxtamembranregion, eine Kinasedomäne und einen C-terminalen Bereich (Kim & Wang 2010; Clouse 2011; Yang *et al.* 2011). Die BR-Bindung findet an der extrazellulären Domäne statt. Diese bildet eine rechts gewundene, stark verdrillte Superhelix, wobei die ID in ihr Inneres hineinragt, wo sie polare und hydrophobe Wechselwirkungen mit LRR 13-25 eingeht. BL bindet in nächster Nähe zur ID und führt zu deren Konformationsänderung (Hothorn *et al.* 2011). Dadurch entsteht eine stabile Plattform für Protein-Protein Interaktionen innerhalb der BRI1-Superhelix, die für die Aktivierung des Rezeptors und die Signalkaskade notwendig ist (Hothorn *et al.* 2011). BRI1 interagiert nach BR-Bindung mit seinem Korezeptor BAK1 (BRI1 ASSOCIATED KINASE 1), was zur Transphosphorylierung zwischen den beiden Proteinen führt (Li *et al.* 2002; Nam & Li 2002; Russinova *et al.* 2004; Wang *et al.* 2005; Wang *et al.* 2008). BAK1 gehört zur Familie der SERKs (SOMATIC EMBRYOGENESIS RECEPTOR-LIKE

KINASE) und wird daher auch als SERK3 bezeichnet. SERKs sind ebenfalls LRR-RLKs mit einer kleinen extrazellulären Domäne bestehend aus fünf LRRs (Schmidt *et al.* 1997; Hecht *et al.* 2001).
Der vollen Aktivierung des BRI1/BAK1-Rezeptorkomplexes liegt ein Mechanismus zugrunde, der sowohl die Interaktion ihrer extrazellulären Domänen als auch die Assoziation ihrer Kinasedomänen erfordert (Jaillais *et al.* 2011a). In Abwesenheit von BR wird BRI1 durch die Interaktion mit BKI1 (BRI1 KINASE INHIBITOR 1), einem negativen Regulator der BR-Signaltransduktion, in einem inaktiven Zustand gehalten (Wang & Chory 2006). Zu diesem Zeitpunkt findet vermutlich noch keine Interaktion mit BAK1 statt. Die BR-Bindung führt zur Bildung einer Interaktionsplattform innerhalb der BRI1-Superhelix mit hoher Affinität zur extrazellulären Domäne von BAK1 und zur Tyrosinphosphorylierung von BKI1 (Jaillais *et al.* 2011b). Dadurch wird BKI1 von BRI1 entlassen und BAK1 an die Plattform rekrutiert (Jaillais *et al.* 2011a).
Die BSKs (BR SIGNALLING KINASES) vermitteln die Signaltransduktion *downstream* von BRI1/BAK1. In Abwesenheit von BR sind sie an BRI1 gebunden. Nach BR-Bindung werden die BSKs von BRI1 phosphoryliert und vom Rezeptorkomplex entlassen (Tang *et al.* 2008). Dies führt zur Aktivierung von BSU1 (*bri1*-SUPPRESSOR 1), welches anschließend mit BIN2 (BRASSINOSTEROID INSENSITIVE 2), einem negativen Regulator des BR-Signalweges, interagiert, und diesen durch Dephosphorylierung inaktiviert (Mora-Garcia *et al.* 2004; Peng *et al.* 2008; Kim *et al.* 2009). In Abwesenheit von BR phosphoryliert BIN2 die Transkriptionsfaktoren BES1 (*bri1*-EMS SUPPRESSOR 1) und BZR1 (BRASSINAZOLE RESISTANT), was zu deren proteosomaler Degradation führt. Ist BIN2 inaktiv, werden BES1 und BZR1 nicht phosphoryliert, wodurch sie im Kern akkumulieren und die BR-abhängige Genexpression in Gang setzen (He *et al.* 2002; Wang *et al.* 2002; Yin *et al.* 2002; Zhao *et al.* 2002; He *et al.* 2005; Yin *et al.* 2005; Vert & Chory 2006). Durch BES1 und BZR1 wird die Expression einer Vielzahl von Genen reguliert. Diese sind in Wasseraufnahme, Ionentransport, und Änderungen des Zytoskeletts involviert (Kim & Wang 2010; Clouse 2011), alles Prozesse, die für das vegetative Wachstum nötig sind. Mit *DEVELOPMENTALLY REGULATED PLASMAMEMBRANE POLYPEPTIDE* (*DREPP*) wurde ein neues BR-reguliertes Gen identifiziert, dessen Produkt in die Regulation des BR-vermittelten Längenwachstums an der Grenzfläche zwischen Plasmamembran und Zytoplasma involviert ist. Es wird vermutet, dass DREPP zur Reorganisation des Zytoskeletts beiträgt (Sun *et al.* 2010).

3.3 Die H_2O_2-vermittelte Schließreaktion der Stomata

Die Signalwirkung und kontrollierte Produktion reaktiver Sauerstoffspezies (*reactive oxygen species*, ROS) wie H_2O_2 ist für viele Vorgänge in der Pflanze von großer Bedeutung. H_2O_2 wird beispielsweise bei der Photosynthese und Atmung, sowie bei der Reaktion auf äußere Einflüsse wie Wassermangel, Kälte, Hitze, Schadstoffe, UV-Licht und Pathogenbefall gebildet. Es dient als Signalmolekül oder *second messenger* (Apel & Hirt 2004) und ist an der Regulation vieler molekularer und zellulärer Prozesse wie der Genexpression, dem programmierten Zelltod, der Zellteilung, dem Längenwachstum und auch dem Schließen der Stomata beteiligt (Neill *et al.* 2002).

Unterschiedliche Faktoren wie z.B. ABA, Dunkelheit oder Ethylen, induzieren das Schließen der Stomata jeweils über die Bildung von H_2O_2, weshalb H_2O_2 auch als Schlüsselkomponente bei der Regulation der Stomata gilt (Pei *et al.* 2000; Zhang *et al.* 2001; Desikan *et al.* 2004; Desikan *et al.* 2006). Das ethyleninduzierte Schließen der Stomata weist darauf hin, dass Signalwege des TCS auch in Stomata eine Rolle spielen. Ethylen wird dabei über ETR1 perzipiert und induziert die H_2O_2-Produktion *via* AtrbohF, eine ROS-produzierende NADPH-Oxidase, was anschließend zum Schließen der Stomata führt (Desikan *et al.* 2006). Interessanterweise scheint ETR1 allerdings auch *downstream* des gebildeten H_2O_2 von Nöten zu sein, da *etr1*-Mutanten nicht mit Schließen der Stomata auf exogen appliziertes H_2O_2 reagieren (Desikan *et al.* 2005). ETR1 hat daher in Schließzellen eine Doppelfunktion: Es ist erstens zur Ethylenperzeption erforderlich und dient zweitens als Ziel von H_2O_2, wodurch die nachstehenden Signalprozesse vermittelt werden, die zum Schließen der Stomata führen. Für das ETR1-abhängige Schließen der Stomata ist allerdings nicht dessen Histidinkinasedomäne erforderlich sondern ein Cysteinrest (Cys65) in der zweiten Transmembrandomäne (Desikan *et al.* 2005). Cys65 könnte dabei ein Angriffsziel von H_2O_2 sein, da dieses unter anderem durch die Oxidation von Cysteinresten auf Proteine wirkt (Cooper *et al.* 2002).

Die meisten ethylenabhängigen Signalwege laufen über die MAPKKK CTR1 ab, was jedoch in Schließzellen nicht zu gelten scheint, da hier weitere Elemente des TCS involviert sind. Eine *arr2*-Mutante ist beispielsweise nicht in der Lage, ihre Stomata in Reaktion auf Ethylen oder H_2O_2 zu schließen, weshalb ARR2 *downstream* von H_2O_2 in diesem Signalweg zu positionieren ist (Desikan *et al.* 2006). Auch in Hefe wurde gezeigt, dass Elemente des Zweikomponentensystems als H_2O_2-Sensoren fungieren (Singh 2000; Buck *et al.* 2001). Die *sln1/ssk1*-Mutante (SLN1 als Hybrid-Histidinkinase und SSK1 als Responseregulator) ist nicht in der Lage, auf Medium mit H_2O_2 zu wachsen (Singh 2000), was jedoch durch den Ethylenrezeptor ETR1 komplementiert werden kann (Desikan *et al.* 2005).

Da *etr1*-Stomata normal auf ABA reagieren, haben der ABA- und der Ethylensignalweg in Schließzellen – obwohl beide über die Bildung von H_2O_2 ablaufen – scheinbar nur manche Komponenten wie z.B. AtrbohF gemein, wohingegen andere wie z.B. ETR1 spezifisch für einen der beiden Wege sind. Die H_2O_2-vermittelte Schließreaktion der Stomata wird daher offensichtlich über ein komplexes Zusammenspiel verschiedener Signalwege reguliert.

3.4 Ziele der Arbeit

Da Phytohormone für die pflanzliche Entwicklung eine zentrale Rolle spielen, sind ihre Signalwege und deren Komponenten Gegenstand intensiver Forschung. Manche Komponenten sind hinsichtlich ihrer Funktion und ihrer subzellulären Lokalisation bereits detailliert untersucht worden. Viele Fragen sind jedoch bislang unbeantwortet, deren Aufklärung zum vollständigeren Verständnis der Signalwege fehlt. In dieser Arbeit sollten daher noch ungeklärte Abschnitte verschiedener Signalwege in Pflanzen untersucht und somit einige offene Fragen beantwortet werden.

Die Cytokininrezeptoren wurden beispielsweise hinsichtlich ihrer Funktion bereits intensiv untersucht. Ihre subzelluläre Lokalisation wurde jedoch noch nicht eindeutig bestimmt. Bisher wurde angenommen, dass sie an der Plasmamembran lokalisiert sind (Kim *et al.* 2006). Weitergehende Untersuchungen deuteten jedoch auf ein anderes Lokalisierungsmuster hin (Dortay *et al.* 2008). Daher sollte in dieser Arbeit zunächst die subzelluläre Lokalisation der Cytokininrezeptoren, insbesondere die von AHK3, mittels verschiedener GFP-Fusionen und Kolokalisationsstudien mit verschiedenen Markerproteinen geklärt werden.

Darüber hinaus sollte die bisher am wenigsten charakterisierte Histidinkinase, AHK5, analysiert werden. AHK5 ist ein negativer Regulator des Signalweges, in dem die Phytohormone ABA und Ethylen das Wurzelwachstum hemmen (Iwama *et al.* 2007). Da der Ethylenrezeptor ETR1 auch für das H_2O_2-induzierte Schließen der Stomata erforderlich ist (Desikan *et al.* 2005), sollte über die Analyse verschiedener *ahk5*-Mutanten untersucht werden, ob AHK5 auch diesen Signalweg mit ETR1 gemein hat. Um Komponenten *downstream* von AHK5 zu identifizieren, sollten darüber hinaus Interaktionsstudien mit weiteren Elementen des TCS (AHPs und ARRs) durchgeführt und mit Hilfe von *ahp*- und *arr*-Mutanten deren eventuelle Funktion im H_2O_2-Signalweg in Schließzellen näher beleuchtet werden.

Nach Analyse verschiedener Eigenschaften einiger Histidinkinasen sollte eine Gruppe von ARRs, die A-Typ ARRs, auf das Vorhandensein von Kernlokalisationssignalen (*nuclear localization signal*, NLS) analysiert werden. Die A-Typ ARRs sind überwiegend im Zellkern lokalisiert, die Existenz eines NLS wurde jedoch bisher nur vermutet, aber nicht intensiver untersucht (Imamura *et al.* 2001; Kiba *et al.* 2002). Repräsentativ für die Familie der A-Typ ARRs galt es daher, in ARR3, 4, 7 und 15 mittels gezielten Einzelaminosäureaustauschs putative NLS zu mutieren und anschließend die subzelluläre Lokalisation entsprechender GFP-Fusionen zu bestimmen. Dies könnte die Frage beantworten, welche Bedeutung der Kernimport dieser Proteine für die zelluläre Antwort auf ein bestimmtes, über Histidinkinasen perzipiertes Eingangssignal hat.

Neben der Analyse verschiedener Elemente des TCS, sollten frühe Prozesse des Brassinosteroidsignalwegs untersucht werden. Obwohl Brassinosteroide (BR) nicht zu den klassischen Phytohormonen gehören, ist der BR-Signalweg einer der bestuntersuchten in Pflanzen. Trotzdem sind auch hier noch Fragen unbeantwortet, vor allem hinsichtlich BR-induzierter Reaktionen, die unabhängig von Änderungen der Genexpression ablaufen. Es ist z.B. noch nicht bekannt, welche Vorgänge unmittelbar nach BR-Bindung in der Plasmamembran ablaufen und damit die ersten Schritte der BR-induzierten Zellstreckung darstellen.

Die Messung der Fluoreszenzlebensdauer (*fluorescence lifetime*, FLT) einer GFP-Fusion des Brassinosteroid-rezeptors BRI1 hat sich als geeignete Methode erwiesen, die unmittelbare Umgebung von BRI1 zu untersuchen, da sich die FLT z.B. mit dem pH-Wert oder dem elektrischen Feld ändert und daher Information über die physikochemische Umgebung des Rezeptors liefert (Elgass *et al.* 2009; Elgass *et al.* 2010a). Auf diese Weise sollten frühe, BR-induzierte Prozesse in der Plasmamembran von BRI1-GFP exprimierenden Keimlingen untersucht werden.

4 ERGEBNISSE UND DISKUSSION

4.1 Die *Arabidopsis* Cytokininrezeptoren AHK3 und AHK4 sind am Endoplasmatischen Retikulum lokalisiert

Caesar, K., Thamm, A. M. K., Witthöft, J., Elgass, K., Huppenberger, P., Grefen, C., Horák, J., Harter, K. (2011) Evidence for the Localization of the *Arabidopsis* Cytokinin Receptors AHK3 and AHK4 at the Endoplasmic Reticulum. *J Exp Bot* DOI:10.1093/jxb/err238.

Cytokinine sind Adeninderivate und gehören zu den fünf klassischen Phytohormonen. Sie sind an vielen wesentlichen Prozessen der pflanzlichen Entwicklung beteiligt (Müller & Sheen 2007; Werner & Schmülling 2009) und spielen bei der Reaktion auf osmotischen sowie Kältestress eine Rolle (Tran *et al.* 2007; Jeon *et al.* 2010). Die Cytokininperzeption und -signaltransduktion verlaufen über ein *Multi-Step* Zweikomponentensystem – ein Histidin zu Aspartat *Phosphorelay*, der sich aus AHKs, AHPs und ARRs zusammensetzt. In *Arabidopsis thaliana* dienen drei membrangebundene Histidinkinasen – AHK2, AHK3 und AHK4 – als Cytokininrezeptoren, wobei die Cytokininbindung an der sogenannten CHASE-Domäne erfolgt, woraufhin die Autophosphorylierung des Rezeptors an einem konservierten Histidinrest in der *Transmitter*-Domäne initiiert wird (Kieber & Schaller 2010; Müller 2011). Im *Multi-Step* Zweikomponentensystem wird die Phosphatgruppe anschließend über einen konservierten Aspartatrest in der *Receiver*-Domäne des Rezeptors und die HPts an die Responseregulatoren weitergeleitet (To & Kieber 2008). Obwohl die Cytokininrezeptoren hinsichtlich ihrer Funktion und biochemischen Eigenschaften bereits intensiv untersucht wurden (Higuchi *et al.* 2004; Nishimura *et al.* 2004; Riefler *et al.* 2006; Romanov *et al.* 2006), wurde ihre subzelluläre Lokalisation bisher noch nicht eindeutig bestimmt.

Um die subzelluläre Lokalisation der Cytokininrezeptoren endgültig aufzuklären, wurden zunächst C- und N-terminale GFP-Fusionsproteine von AHK3 transient in *Nicotiana benthamiana* Blättern und *Arabidopsis* Keimlingen exprimiert. Alle Fusionsproteine waren unabhängig vom Promotor (*35S* oder *UBQ10*) am Endoplasmatischen Retikulum (ER) lokalisiert, was durch Kolokalisation mit ER-Markerproteinen bestätigt wurde. Sie kolokalisierten hingegen weder mit der plasmamembrangebundenen Histidinkinase AHK1 noch mit einem Golgi-Marker. Um Überexpressionsartefakte durch konstitutiv aktive Promotoren ausschließen zu können, fand auch ein induzierbares Promotorsystem Anwendung, durch welches sich die Expression der Fusionsproteine kontrollieren ließ. Die so exprimierten Proteine waren auch am ER lokalisiert.

Des Weiteren enthält die Aminosäuresequenz von AHK3 Sortierungssignale für den sekretorischen Pfad, sowie den ER-Export, welche durch das jeweilige Fluoreszenzprotein maskiert sein könnten. Es wurde daher ein Konstrukt angefertigt, bei dem GFP zwischen die erste und zweite Transmembrandomäne inseriert wurde (AHK3intGFP), was jedoch keine Änderung der Lokalisation zur Folge hatte.

Um die ER-Lokalisation der AHK3 GFP Fusionsproteine weiter zu untermauern, wurden diese auf ihre EndoH-Sensitivität überprüft. EndoH ist eine Glykosidase, die mannosereiche Oligosaccharide spaltet, welche für Proteine am ER typisch sind (Maley *et al.* 1989). In der AHK3-Aminosäuresequenz befinden sich fünf mögliche Glykosylierungsstellen, weshalb bei ER-Lokalisation eine EndoH-Sensitivität zu erwar-

ten wäre, was für AHK3-GFP und GFP-AHK3 bestätigt werden konnte. AHK1 diente als Negativkontrolle, da es zwar neun mögliche Glykosylierungsstellen besitzt, jedoch an der Plasmamembran lokalisiert ist und daher bereits im sekretorischen Pfad prozessiert wurde, weshalb es kein Substrat mehr für EndoH darstellte (Hong *et al.* 2008).
Die Applikation von Cytokinin änderte ebenfalls nichts an der ER-Lokalisation von AHK3, weshalb eine ligandenabhängige Verlagerung des Rezeptors an die Plasmamembran unwahrscheinlich ist. Auch die Koexpression mit AHK4, einem weiteren Cytokininrezeptor, blieb ohne sichtbare Wirkung. Beide Rezeptoren kolokalisierten am ER. Mittels mbSUS (Grefen *et al.* 2009) konnte darüber hinaus gezeigt werden, dass AHK3 Homodimere bildet und *in vivo* mit AHK4 interagiert.
Des Weiteren sind die GFP-Fusionen von AHK3 funktional, da sie den Zwergwuchs und das cytokininsensitive Wurzelwachstum der *ahk2ahk3* Doppelmutante komplementierten. AHK3-GFP konnte in den komplementierten *Arabidopsis* Linien in netzartigen Strukturen und dem perinukleären Raum detektiert werden und war außerdem EndoH-sensitiv. AHK3-GFP war daher nicht nur bei transienter Expression am ER angesiedelt, sondern auch in transgenen *Arabidopsis* Linien.

Die Lokalisation der Cytokininrezeptoren am ER hat weitreichende Konsequenzen für den Begriff der Cytokininperzeption und -signaltransduktion. Die hier gezeigte EndoH-Sensitivität sowie Daten anderer Arbeiten deuten darauf hin, dass die cytokininbindende CHASE-Domäne zum ER-Lumen orientiert ist und die C-terminale Kinasedomäne zum Zytoplasma (Dortay *et al.* 2006). Dies stimmt mit der Beobachtung überein, dass z.B. die Cytokininbindung an AHK4 ein pH-Optimum um 6,5 hat (Romanov *et al.* 2006), welches im ER-Lumen vorherrscht (Kim *et al.* 1998) und dass bei einem apoplastischen pH-Wert von 5,5 (Li *et al.* 2005) zumindest an AHK3 fast keine Bindung mehr stattfindet (Romanov *et al.* 2006). Sind die Cytokininrezeptoren also am ER lokalisiert und zwar so, dass ihre CHASE-Domäne ins Lumen reicht, binden sie ihren Liganden mit wesentlich höherer Affinität.
Des Weiteren sind Cytokinine relativ gut membrangängig und es sind mehrere plasmamembranständige Transporter beschrieben, die Cytokinin in die Zelle transportieren können (Burkle *et al.* 2003; Wormit *et al.* 2004; Hirose *et al.* 2005; Cedzich *et al.* 2008). Außerdem kommen Enzyme, die in Cytokininbiosynthese und -abbau involviert sind, in verschiedensten Zellkompartimenten, einschließlich dem ER, vor (Sakakibara 2006), was auf Mechanismen schließen lässt, die einen Metabolismus von Cytokinin in unterschiedlichen Kompartimenten ermöglichen und/oder Cytokinin (-derivate) in der Zelle verteilen. Es ist daher nicht auszuschließen, dass die zelluläre Cytokininwirkung (z.B. Regulation der Zellteilung) einen autokrinen Effekt darstellt.
Da zwei weitere unabhängige Arbeiten, die Lokalisation der Cytokininrezeptoren am ER bestätigt haben (Lomin *et al.* 2011; Wulfetange *et al.* 2011a), muss das aktuelle Modell der Cytokininperzeption an der Plasmamembran neu überdacht werden.
Neuere Analysen haben außerdem gezeigt, dass auch Proteine, die mit anderen Hormonsignalwegen in Zusammenhang stehen, am ER lokalisiert sind (Friml & Jones 2010). Es lässt sich daher spekulieren, dass das ER den intrazellulären Umschlagplatz für Phytohormone und deren Zusammenspiel darstellt.

4.2 Ein schneller, brassinolidregulierter Signalweg in der Plasmamembran von *Arabidopsis thaliana*

Caesar, K., Elgass, K., Chen, Z., Huppenberger, P., Witthöft, J., Schleifenbaum, F., Blatt, M. R., Oecking, C., Harter, K. (2011) A fast brassinolide-regulated response pathway in the plasma membrane of *Arabidopsis thaliana*. *Plant J* 66, 528-540.

Witthöft, J., Caesar, K., Elgass, K., Huppenberger, P., Kilian, J., Schleifenbaum, F., Oecking, C., Harter, K. (2011) The activation of the Arabidopsis P-ATPase 1 by the brassinosteroid receptor BRI1 is independent of threonine 948 phosphorylation. *Plant Signal Behav* 6, 1063-1066.

Witthöft, J., Harter, K. (2011) Latest news on *Arabidopsis* brassinosteroid perception and signaling. *Front Plant Sci* 2:58, doi:10.3389/fpls.2011.00058.

Brassinosteroide wie z.B. Brassinolid (BL) sind Phytohormone, die an der Regulation des Zellstreckungswachstums und der Reaktion auf biotischen und abiotischen Stress beteiligt sind (Clouse & Sasse 1998). Ihre Bindung an den Brassinosteroidrezeptor BRI1 führt zu dessen Autophosphorylierung und zur anschließenden Rekrutierung des Korezeptors BAK1. Darauf folgt die Transphosphorylierung zwischen BRI1 und BAK1, was die Signalkaskade und damit die zelluläre Reaktion in Gang setzt (Kim & Wang 2010; Clouse 2011; Yang *et al.* 2011). Obwohl detaillierte *in planta* Analysen bisher fehlen gelten eine Protonenausschüttung in den apoplastischen Raum und die Hyperpolarisation der Plasmamembran als Auslöser für die Zellstreckung in Reaktion auf Brassinosteroide (Romani *et al.* 1983; Cerana *et al.* 1985; Mandava 1988; Haubrick & Assmann 2006).

Für die Untersuchung molekularer Prozesse in lebenden Pflanzenzellen ist es notwendig, die zu analysierenden Proteine sichtbar zu machen und Informationen über deren Umgebung zu gewinnen. Hierbei hat der Einsatz autofluoreszierender Proteine wie z.B. GFP die Zellbiologie revolutioniert, da sich durch Fusion mit GFP die subzelluläre Lokalisation und Dynamik eines Proteins *in vivo* bestimmen lässt (Dixit *et al.* 2006; Giepmans *et al.* 2006; Suzuki *et al.* 2007). Für die nähere Analyse dessen physikochemischer Umgebung bzw. deren Änderung als Reaktion auf ein bestimmtes Signal ist allerdings die reine Bestimmung der Lokalisation oder der Intensität des GFP-Signals nicht ausreichend. Dafür müssen andere Eigenschaften fluoreszierender Proteine wie z.B. die Fluoreszenzlebensdauer (*fluorescence lifetime*, FLT) herangezogen werden (Harter *et al.* 2011). Diese ändert sich mit dem pH-Wert, dem Brechungsindex oder dem elektrischen Feld (Ohta *et al.* 2010) und liefert daher Informationen über die physikochemische Umgebung eines fluoreszenzmarkierten Proteins. Die Messung der FLT wurde bereits für die Analyse einer GFP-Fusion des plasmamembrangebundenen Brassinosteroidrezeptors BRI1 herangezogen (Elgass *et al.* 2009). In *Arabidopsis* Keimlingen, die BRI1-GFP exprimieren (Friedrichsen *et al.* 2000), wurde durch die Kombination aus FLT-Spektroskopie und CSSM (*confocal sample scanning microscopy*) wenige Minuten nach BL-Gabe eine Zellwandverbreiterung beobachtet. Diese ging mit einer Änderung der FLT von BRI1-GFP einher, was eine Veränderung dessen physikochemischer Umgebung widerspiegelt (Elgass *et al.* 2009). Der Auslöser dafür könnte eine Änderung des Membranpotentials (E_m) der Plasmamembran sein (Elgass *et al.* 2010a).

Um diese Hypothese weiter zu festigen, wurden *Arabidopsis* Keimlinge, die BRI1-GFP exprimieren, mit Natriumacetat behandelt, was zum Ausgleich des pH-Gradienten über der Plasmamembran führt

(Grainger *et al.* 1979; Johnson & Epel 1981; Dupré & Schaaf 1996; Bobik *et al.* 2010). Eine BL-Behandlung zeigte in Gegenwart von Natriumacetat keinen Effekt mehr auf die FLT von BRI1-GFP und die Zellwandbreite. Dies deutet darauf hin, dass für beide zellphysiologischen Prozesse ein elektrochemischer Protonengradient über der Plasmamembran erforderlich ist. Daher wurden die Keimlinge mit Substanzen behandelt, die das Membranpotential der Plasmamembran verändern. Auxin reguliert beispielsweise die Zellstreckung und die Dehnbarkeit der Zellwand, was mit einer Hyperpolarisation der Plasmamembran verbunden ist (Cleland 2004). Durch Applikation von Auxin wurden eine Verkürzung der FLT von BRI1-GFP sowie eine Zellwandverbreiterung nachgewiesen. Elektrophysiologische Messungen in Wurzelepidermiszellen von BRI1-GFP exprimierenden sowie Wildtyp Keimlingen haben außerdem ergeben, dass BL die Plasmamembran aller untersuchten Wurzelzellen hyperpolarisierte wodurch sich die FLT von BRI1-GFP änderte und eine Zellwandverbreiterung zu beobachten war.

Im Gegensatz dazu hatte die Ansäuerung des extrazellulären Raums auf pH 5,5 – ein pH-Wert, der zur Aktivierung apoplastischer Expansine, Lockerung der Zellwand, Wasseraufnahme in den Apoplasten und Anschwellen der Zellwand führen könnte (Cho & Cosgrove 2004; Zhang *et al.* 2005; Sanchez-Rodriguez *et al.* 2010) – keinen nennenswerten Effekt auf die Expansion der Zellwand. Eine Kombination hingegen aus Ansäuerung des Apoplasten und Hyperpolarisation der Plasmamembran verstärkte den Effekt der Hyperpolarisation, was auf ein Zusammenspiel zwischen pH- und E_m-abhängigen Mechanismen hindeutet. Der Effekt von BL auf die Zellwand war allerdings noch bedeutend stärker als der von Ansäuerung und Hyperpolarisation zusammen. Daher ist BL entweder in der Lage, eine noch stärkere lokale Ansäuerung und Hyperpolarisation zu induzieren oder es gibt eine dritte Komponente, die dazu beiträgt. Dies könnte ein weiteres Phytohormon wie z. B. Auxin sein, da bereits gezeigt wurde, dass Auxin zusammen mit Brassinosteroiden die Zellstreckung fördert (Mandava 1988; Halliday 2004; Nemhauser *et al.* 2004; Sanchez-Rodriguez *et al.* 2010), was auch im Einklang mit der hier gezeigten Zellwandverbreiterung durch Auxin stünde.

Die Ursache für die beobachtete Hyperpolarisation der Plasmamembran durch BL könnte eine erhöhte Protonenausschüttung sein, die mit einer gesteigerten Aktivität der plasmamembrangebundenen H^+-ATPase (P-ATPase) in Zusammenhang steht (Friedrichsen & Chory 2001). Daher wurde vor BL-Gabe entweder Fusicoccin (Fc) eingesetzt, was die Aktivität der P-ATPase erhöht (Wurtele *et al.* 2003) oder *ortho*-Vanadat (*o*V), ein Inhibitor der P-ATPase (MacLennan *et al.* 1997; Schaller & Oecking 1999). Nach Vorbehandlung mit *o*V, konnte keine BL-induzierbare Zellwandverbreiterung und Änderung der FLT von BRI1-GFP beobachtet werden. Wurde *o*V allerdings vor der BL-Behandlung ausgewaschen, fanden beide Prozesse wieder statt. Fc hingegen reichte aus, um auch ohne BL eine Änderung der FLT von BRI1-GFP zu induzieren und den Effekt von *o*V aufzuheben. Die Daten zeigen, dass die Hyperpolarisation der Plasmamembran Voraussetzung für die Zellwandverbreiterung und die Verkürzung der FLT von BRI1-GFP nach BL-Gabe ist, und dass die beobachteten Änderungen im Membranpotential durch die P-ATPase kontrolliert werden. Da BL die Expression der P-ATPase innerhalb des Messzeitraums von 30 min nicht erhöht (Goda *et al.* 2008), muss die Aktivierung posttranslational ablaufen.

Es wurde bereits gezeigt, dass für die BL-regulierte Genexpression die Kinaseaktivität von BRI1 nötig ist (Wang *et al.* 2005), was zu der Frage führt, ob dies auch für die hier gezeigte Regulierung der P-ATPase Aktivität und die Hyperpolarisation der Plasmamembran gilt. Daher wurde eine mutante Variante von BRI1-GFP generiert, die keine Kinaseaktivität mehr besitzt (BRI1^{KE}-GFP)(Oh *et al.* 2000; Wang *et al.* 2005). Die BRI1-GFP Fusionen wurden zusammen mit der *Arabidopsis* P-ATPase 1 (AHA1) in *Nicotiana benthamiana* Blättern exprimiert. Durch BL-Gabe war eine Verkürzung der FLT von BRI1-GFP zu beobachten, nicht jedoch von BRI1^{KE}-GFP. Die Kinaseaktivität von BRI1 ist demnach für die Regulierung von AHA1 und die BL-abhängige Hyperpolarisation der Plasmamembran erforderlich. Möglicherweise aktiviert BRI1 die P-ATPase über direkte Interaktion verbunden mit ihrer Phosphorylierung. Es wurden daher Interaktionsstudien mittels mbSUS (Grefen *et al.* 2009) und *in planta* FRET-Analysen durchgeführt. AHA1 und BRI1 interagierten miteinander, nicht jedoch AHA1 und LTI6b, welches ebenfalls an der Plasmamembran lokalisiert ist (Cutler *et al.* 2000). Dies deutet auf eine spezifische Wechselwirkung zwischen BRI1 und der P-ATPase hin und stützt damit die Vermutung, dass deren Aktivierung mit einer direkten Interaktion einhergeht.

Es ist bekannt, dass die Phosphorylierung konservierter Serin- oder Threoninreste in der C-terminalen autoinhibitorischen Domäne der P-ATPasen deren enzymatische Aktivität beeinflusst, indem sie die Assoziation mit 14-3-3 Proteinen begünstigt, was wiederum die Wirkung der autoinhibitorischen Domäne aufhebt (Speth *et al.* 2010). Da die Interaktion mit 14-3-3 Proteinen eine Phosphorylierung der vorletzten Aminosäure der ATPase erfordert (T948), wurde untersucht ob dieser Threoninrest für die BL-regulierte Aktivierung von AHA1 notwendig ist. BRI1 aktivierte jedoch nicht nur die wildtypische P-ATPase sondern auch AHA1^{T948A}, was durch eine signifikante Änderung in der FLT von BRI1-GFP belegt wurde. Die Aktivierung von AHA1 durch BRI1 läuft demnach nicht über Phosphorylierung von T948 und auch die Interaktion der beiden Proteine war davon unabhängig. Eventuell könnten andere Serin- oder Threoninreste durch BRI1 phosphoryliert werden oder es liegt ein bisher nicht erforschter Mechanismus zugrunde.

Neben ihrer Eignung als molekularer Sensor zur Messung des Membranpotentials in lebenden Pflanzenzellen mit hoher räumlich-zeitlicher Auflösung, kann die FLT von BRI1-GFP auch zur *in planta* Analyse eines BL-Signals über längere Distanzen herangezogen werden. Durch Applikation von BL an der Wurzel änderte sich die FLT von BRI1-GFP in Zellen des oberen Hypokotyls. Die Änderung der FLT war allerdings erst 25 min nach BL-Applikation detektierbar, da die Hypokotylzellen nicht direkt mit BL in Berührung kamen. Waren die Wurzeln allerdings von Wasser umgeben, konnte keine Änderung der FLT beobachtet werden. Es muss daher ein mobiles Signal geben, das ausgehend von den Wurzelzellen die Hyperpolarisation der Plasmamembran in unbehandelten oberen Hypokotylzellen induzieren kann. Ob es sich dabei um BL selbst handelt, bleibt offen. Nichtsdestotrotz eignet sich die Messung der FLT von BRI1-GFP auch zur Analyse systemischer Prozesse, die Änderungen im Membranpotential des Zielgewebes hervorrufen. Sie ist damit vielseitig anwendbar, nicht invasiv und kann im intakten Gewebeverband durchgeführt werden, weshalb sie besonders zuverlässige Aussagen über Vorgänge im lebenden Organismus liefert.

4.3 Kernlokalisationssignale in *Arabidopsis* A-Typ Responseregulatoren

Heunemann, M., Mira-Rodado, V., Harter, K., Witthöft, J. (2011) Nuclear localization signals in A-type response regulators of *Arabidopsis thaliana*. In Vorbereitung.

Die *Arabidopsis* Responseregulatoren (ARRs) bilden die Endglieder eines *Multi-Step* Zweikomponentensystems (Hwang *et al.* 2002; Grefen & Harter 2004) und werden in drei Gruppen unterteilt: A-, B- und C-Typ ARRs. Die B-Typ ARRs bestehen aus einer *Receiver*-Domäne und einer C-terminalen *Output*-Domäne mit DNA-Bindemotif, Transaktivierungsdomäne und mindestens einem NLS (Lohrmann *et al.* 1999; Sakai *et al.* 2000; Lohrmann *et al.* 2001). Die A- und C-Typ ARRs haben mit den B-Typ ARRs nur die *Receiver*-Domäne gemein, wohingegen die ausgedehnte C-terminale *Output*-Domäne fehlt.
Obwohl A-Typ ARRs kein offensichtliches NLS besitzen, sind sie im Zellkern und im Zytoplasma lokalisiert (Sweere *et al.* 2001) oder akkumulieren sogar überwiegend im Zellkern (Imamura *et al.* 2001; Kiba *et al.* 2002; Dortay *et al.* 2008), wie Versuche mit GFP-Fusionsproteinen gezeigt haben. Da das Molekulargewicht der GFP-Fusionen jedoch 50-60 kDa beträgt und dies die Grenze für passive Diffusion in den Zellkern überschreitet (Mattaj & Englmeier 1998; Moore 1998), ist zu vermuten, dass die A-Typ ARRs NLS besitzen, die allerdings bisher noch nicht genau beschrieben wurden.

Die Aminosäuresequenzen der A-Typ ARRs sind hoch konserviert und unterscheiden sich lediglich in ihrer kurzen C-terminalen Region signifikant voneinander, wobei mögliche NLS-Sequenzen in diesen weniger konservierten Bereichen zu finden sind.
Zunächst wurden anhand charakteristischer Merkmale fünf mögliche NLS in der ARR4-Proteinsequenz bestimmt, an deren Anfang jeweils ein für NLS typisches Lysin (K) steht. Im Gegensatz zu GFP-ARR4, welches hauptsächlich im Zellkern lokalisiert war, war GFP-ARR4$^{K108/147/155/172/252A}$, bei dem alle fünf Lysinreste zu Alanin (A) mutiert wurden, in transient transformierten *Nicotiana benthamiana* Blättern und *Arabidopsis* Keimlingen überwiegend im Zytoplasma lokalisiert. Um zu untersuchen, welche der Punktmutationen für die Änderung in der subzellulären Lokalisation verantwortlich ist, wurden Varianten von ARR4 generiert, die jeweils nur eine der Mutationen tragen. Lediglich die Lokalisation von GFP-ARR4^{K172A} unterschied sich von der des wildtypischen GFP-ARR4, was bedeutet, dass das KRK-Motiv (Aminosäuren 172-174) höchstwahrscheinlich ein funktionales NLS darstellt.
Unter Verwendung von DRONPA, einem Fluoreszenzprotein, dessen Fluoreszenz sich durch Licht verschiedener Wellenlängen, reversibel „aktivieren“ und „deaktivieren“ lässt (Lummer *et al.* 2011), konnte außerdem der Kernimport von ARR4 visualisiert werden. Hierfür wurde die Fluoreszenz von ARR4-DRONPA im Zellkern selektiv „ausgeschaltet“ und der Kern über einen Zeitraum von 20 min beobachtet. Aufgrund einer Fluoreszenzzunahme in diesem Kern innerhalb weniger Minuten wurde deutlich, dass fluoreszierendes ARR4-DRONPA aus dem Zytoplasma in den Zellkern importiert wurde. Für ARR4^{K172A}-DRONPA konnte hingegen kein Kernimport nachgewiesen werden, was die Beobachtung der überwiegend zytoplasmatischen Lokalisation von GFP-ARR4^{K172A} stützt.
ARR3 – das zu ARR4 am nächsten verwandte Protein – war nach Fusion mit GFP im Zellkern und im Zytoplasma lokalisiert. Das KRK-Motiv, welches in ARR4 als NLS fungiert, ist in ARR3 an derselben

Position zu finden. Die Lokalisation von GFP-ARR3^{K172A} unterschied sich allerdings nicht von der des wildtypischen GFP-ARR3. Da das NLS Vorhersageprogramm *cNLS Mapper* (Kosugi *et al.* 2009) für ARR3 ein bipartites NLS ab Position 152 vorhersagt hat (DV**KRLR**SYLTRDVKVAAEGN**KRK**LTTPP), wurde zusätzlich noch Lysin 154 mutiert, was zu einer überwiegend zytoplasmatischen Lokalisation von GFP-ARR3$^{K154/172A}$ führte. Die subzelluläre Lokalisation der einfach mutierten Variante GFP-ARR3^{K154A} unterschied sich ebenfalls nicht von GFP-ARR3. Das bedeutet, dass – im Gegensatz zu ARR4 – in ARR3 zwei Lysinreste (K154 und K172) für dessen Kernlokalisation ausschlaggebend sind.

Weiter gibt es Hinweise, dass die A-Typ Responseregulatoren ARR7 und ARR15 ebenfalls ein NLS in ihren C-Termini enthalten (Imamura *et al.* 2001; Kiba *et al.* 2002). Für ARR7 wird KRMK (Aminosäuren 193-196) als NLS diskutiert. Die Mutation von Lysin 193 änderte aber ebenso wenig an der überwiegend nukleären Lokalisation, wie die des in ARR7 ebenfalls enthaltenen KRK-Motivs (Aminosäuren 167-169; siehe ARR3 und 4). Erst nach Mutation beider Lysinreste (167 und 193) war das entsprechende GFP-Fusionsprotein überwiegend im Zytoplasma lokalisiert.

ARR3 und ARR7 haben also zwei basische Motive, die für deren Kernlokalisation verantwortlich und durch eine Verbindungssequenz getrennt sind, wie es für bipartite NLS häufig der Fall ist. Für bipartite NLS wurde jedoch auch gezeigt, dass die Mutation eines der basischen Bereiche ausreicht, um die Funktion des NLS zu zerstören (Munoz-Fontela *et al.* 2003; Pawlowski *et al.* 2010). Da bei ARR3 und 7 aber zwei Mutationen erforderlich waren, um eine zytoplasmatische Lokalisation hervorzurufen, ist davon auszugehen, dass diese zwei monopartite NLS besitzen, die in ihrer Funktion redundant sind.

Für ARR15 wurde spekuliert, dass das KRIK-Motiv (Aminosäuren 198-201) als NLS fungieren könnte (Kiba *et al.* 2002), was durch die überwiegend zytoplasmatische Lokalisation von GFP-ARR15^{K198A} bestätigt wurde. Mittels Western Blot konnte ausgeschlossen werden, dass die beobachteten Unterschiede in der subzellulären Lokalisation von Expressionsunterschieden der verschiedenen GFP-ARR Fusionsproteine oder freiem GFP herrühren.

Da die Einzelaminosäureaustausche in ARR3, 4, 7 und 15 zu einer drastischen Änderung der subzellulären Lokalisation führten, deren Molekulargewicht aber nicht nennenswert veränderten, ist davon auszugehen, dass der Kernimport der A-Typ ARRs aktiv und selektiv *via* NLS erfolgt und dass sie nicht durch passive Diffusion in den Zellkern gelangen.

Wie bereits erwähnt unterscheiden sich die A-Typ ARRs nur in ihren C-terminalen Bereichen signifikant voneinander. ARR5/6 und 8/9 enthalten wie ARR3, 4, 7 und 15 ein basisches Motiv im C-Terminus (KRAK bzw. KRK) und sind als GFP-Fusionen im Zellkern lokalisiert (Kiba *et al.* 2002; Dortay *et al.* 2008). ARR16 fehlt hingegen nahezu der gesamte C-terminale Bereich, und es ist fast ausschließlich im Zytoplasma lokalisiert (Kiba *et al.* 2002; Dortay *et al.* 2008)

Es scheint daher naheliegend, dass der C-terminale Bereich der A-Typ ARRs für deren subzelluläre Lokalisation ausschlaggebend ist und ihm daher eine größere Bedeutung zukommt als bisher angenommen.

4.4 Die Funktion der *Arabidopsis* Histidinkinase 5 und ihrer untergeordneten Komponenten beim Schließen der Stomata

Desikan, R., Horák, J., Chaban, C., Mira-Rodado, V., Witthöft, J., Elgass, K., Grefen, C., Cheung, M.-K., Meixner, A. J., Hooley, R., Neill, S. J., Hancock, J. T., Harter, K. (2008) The Histidine Kinase AHK5 Integrates Endogenous and Environmental Signals in *Arabidopsis* Guard Cells. *PLoS ONE* 3, e2491.

Mira-Rodado, V., Veerabagu, M., Witthöft, J., Teply, J., Harter, K., Desikan, R. (2011) Identification of two-component system elements downstream of AHK5 in the stomatal closure response. In Revision.

Wasserstoffperoxid (H_2O_2) ist eine Form reaktiver Sauerstoffspezies und wird von Pflanzen als Antwort auf biotischen und abiotischen Stress gebildet (Apel & Hirt 2004). H_2O_2 dient dabei als Signal oder *second messenger* und setzt Prozesse in Gang, die dem Schutz vor und der Anpassung an bestimmte Umwelteinflüsse dienen. Es reguliert zudem Vorgänge, wie Genexpression, programmierten Zelltod, Zellteilung, Längenwachstum und Schließen der Stomata (Neill *et al.* 2002). Des Weiteren wurde gezeigt, dass der Ethylenrezeptor ETR1 in der H_2O_2-Signaltransduktion in Schließzellen eine Rolle spielt, wobei er als mögliches Angriffsziel von H_2O_2 gilt (Desikan *et al.* 2005). ETR1 gehört zu den Hybrid-Histidinkinasen des Zweikomponentensystems (Grefen & Harter 2004). Für einige Mitglieder des Zweikomponentensystems ist noch nicht bekannt, bei welchen Signalwegen sie involviert sind und wie diese miteinander in Verbindung stehen, wobei *second messenger* wie z.B. H_2O_2 als Bindeglieder in Frage kommen (Desikan et al 2005b). Da gezeigt wurde, dass AHK5 – die bisher am wenigsten untersuchte Histidinkinase – den ETR1-abhängigen Ethylensignalweg hinsichtlich des Wurzelwachstums hemmt (Iwama *et al.* 2007), liegt die Vermutung nahe, dass AHK5 auch an der ETR1-abhängigen H_2O_2-Signaltransduktion beteiligt ist.

Zur näheren Charakterisierung von AHK5 wurde zunächst ihre, in Ermangelung einer Transmembrandomäne, vorhergesagte zytoplasmatische Lokalisation (Grefen & Harter 2004) überprüft. GPF-AHK5 und AHK5-GFP waren im Zytoplasma von transient transformierten *Nicotiana benthamiana* Blättern und *Arabidopsis* Protoplasten lokalisiert. Ebenfalls durchgeführte Zellfraktionierungen sowie die Erstellung eines Fluoreszenzintensitätsprofils über den Plasmamembran-Zellwand-Bereich zweier benachbarter Zellen wiesen aber auf eine Lokalisation im Zytosol und an der Plasmamembran hin.

Um zu prüfen, ob AHK5 eine Funktion beim Schließen der Stomata haben könnte, wurde deren Expression in einer mit Schließzellen angereicherten Probe untersucht. Es konnte nachgewiesen werden, dass *AHK5* in Schließzellen exprimiert und die Expression durch H_2O_2 verstärkt wird, was auf eine Funktion von AHK5 bei der H_2O_2-Signaltransduktion in Schließzellen hinweist. Dies wurde durch die H_2O_2-Insensitivität der Stomata zweier *ahk5*-Mutanten – *ahk5-3* (Samson *et al.* 2002) und *ahk5-1* (Sessions *et al.* 2002) – weiter gestützt.

Ähnliche Beobachtungen wurden bei der Reaktion auf Dunkelheit und Ethylen gemacht, die normalerweise das Schließen der Stomata über die Bildung von H_2O_2 induzieren (Desikan *et al.* 2004; Desikan *et al.* 2006). Die Stomata der *ahk5*-Mutanten blieben geöffnet, wohingegen wildtypische Pflanzen mit Schließen der Stomata reagierten. In diesem Zusammenhang konnte auch gezeigt werden, dass die für die Loka-

lisationsstudien verwendeten Konstrukte funktional sind, da diese den Phänotyp der *ahk5*-Mutanten komplementierten.

H_2O_2 induziert außerdem die Bildung von NO bei der Reaktion von Schließzellen auf ABA (Bright *et al.* 2006). Falls AHK5 also tatsächlich *downstream* von H_2O_2 agiert, könnte in den Mutanten auch die Reaktion auf NO beeinträchtigt sein. Tatsächlich zeigten sie eine verminderte Sensitivität auf NO. Interessanterweise war aber die Reaktion der *ahk5*-Mutanten auf ABA nicht nennenswert verändert, weshalb zu vermuten ist, dass der ABA-Signalweg weitestgehend ohne AHK5 abläuft und dass nicht ABA sondern ein anderes Signal zur Bildung von jenem H_2O_2 oder NO führt, das durch AHK5 wahrgenommen wird. Hierbei gibt es Parallelen zu der H_2O_2-insensitiven *etr1*-Mutante, welche ebenfalls normal auf ABA reagiert (Desikan *et al.* 2006).

Während die NADPH-Oxidasen ATRBOHD und ATRBOHF in Reaktion auf ABA H_2O_2 generieren (Kwak *et al.* 2003) sowie ATRBOHF in Reaktion auf Ethylen (Desikan *et al.* 2006), ist die Herkunft des aufgrund von Dunkelheit gebildeten H_2O_2 bisher nicht bekannt. Um zu analysieren, ob AHK5 die Redoxhomöostase der Stomata beeinflusst, wurde die H_2O_2-Produktion in Reaktion auf Dunkelheit gemessen. Diese war jedoch in *ahk5*-Schließzellen nicht beeinträchtigt. Demnach ist AHK5, obwohl es zum Schließen der Stomata im Dunkeln nötig ist, nicht an der dunkelinduzierten H_2O_2-Produktion beteiligt. Im Gegensatz dazu produzierte die *atrbohD/F* Doppelmutante im Dunkeln weder H_2O_2 noch schloss sie ihre Stomata, was bedeutet, dass diese beiden Proteine die Bildung von H_2O_2 im Dunkeln regulieren.

Obwohl die Stomata der *ahk5*-Mutanten nicht auf H_2O_2 reagierten, konnte die H_2O_2-Bildung durch die Gabe von ABA wie im Wildtyp induziert werden. Allerdings war die ethyleninduzierte H_2O_2-Produktion in Stomata von *ahk5-1* beeinträchtigt, was zeigt, dass AHK5 im Ethylensignalweg eine entscheidende Rolle spielt, möglicherweise durch eine funktionale oder physische Interaktion mit dem Ethylenrezeptor ETR1.

Stomata sind des Weiteren auch Eintrittsstellen für Pathogene, wobei Bakterien und bakterielle PAMPs (*pathogen associated molecular pattern*) als erste Abwehrreaktion das Schließen der Stomata hervorrufen (Melotto *et al.* 2006). Bei Experimenten mit zwei *Pseudomonas syringae* Stämmen konnte gezeigt werden, dass die *ahk5-1* Mutante nicht mehr mit Schließen der Stomata auf diese Pathogene reagiert. Die fehlende Reaktion lässt vermuten, dass AHK5 an der basalen Abwehr beteiligt ist, die durch PAMPs wie flg22 und elf26 (Zipfel *et al.* 2006) vermittelt wird. Tatsächlich reagierten die Stomata von *ahk5-1* nicht auf flg22. Sie zeigten jedoch interessanterweise eine Reaktion auf elf26, was darauf hindeutet, dass AHK5 speziell im Flagellinsignalweg in Schließzellen eine Rolle spielt. Das ist überraschend, da die Signalwege von flg22 und elf26 in anderen Geweben beträchtlich überlappen, könnte aber auf Unterschiede zwischen Schließ- und Mesophyllzellen bei der prä- und postinvasiven Immunität (Bittel & Robatzek 2007) zurückzuführen sein. Eine Möglichkeit wie AHK5 mit dem flg22-Signalweg wechselwirken könnte ist die Interaktion mit dem flg22-Rezeptor FLS2, welcher ebenfalls in Schließzellen exprimiert ist (Robatzek *et al.* 2006).

Von Bakterien stammende PAMPs induzieren die Ethylensynthese (Felix *et al.* 1999) und einen oxidativen *Burst* in *Arabidopsis* Blättern, welcher durch ATRBOHD vermittelt wird (Zhang *et al.* 2007). Um die Rolle von AHK5 an der Redoxhomöostase weiter aufzuklären, wurde die PAMP-induzierte H_2O_2-Produktion in

den *ahk5*-Mutanten untersucht. Elf26 führte in Stomata von Wildtyp- und *ahk5*-Pflanzen zu einer vermehrten H_2O_2-Produktion, wohingegen flg22 in den Stomata der Mutante keinen Effekt hatte. Daher scheint AHK5 spezifisch in der flg22-regulierten H_2O_2-Produktion sowie beim Schließen der Stomata durch flg22 eine Rolle zu spielen.
Genau wie ETR1 (Desikan *et al.* 2006) hat AHK5 offensichtlich mehrere Funktionen in Schließzellen: Erstens die Regulation der flagellin- und ethyleninduzierten H_2O_2-Akkumulation und zweitens die Perzeption jenes H_2O_2, welches auf Ethylen, NO, flg22 und Dunkelheit in den Stomata gebildet wird. AHK5 verknüpft demnach unterschiedliche H_2O_2-abhängige Vorgänge auf diversen molekularen Ebenen.

Experimente mit TCSA, einem Inhibitor für Histidinkinaseaktivität (Papon *et al.* 2003), haben gezeigt, dass diese für das Schließen der Stomata durch H_2O_2, NO, Dunkelheit, Ethylen und flg22 erforderlich ist. Es kann daher vermutet werden, dass die von AHK5 abhängige Signaltransduktion über ein *Multi-Step* TCS abläuft. Um Elemente des TCS *downstream* von AHK5 zu identifizieren, wurden Interaktionsstudien mit den AHPs durchgeführt, die durch Hybrid-Histidinkinasen wie AHK5 phosphoryliert werden. Mittels *in planta* BiFC-Analysen konnte eine Interaktion von AHK5 mit AHP1, 2 und 5 nachgewiesen werden. Um zu untersuchen, ob diese Interaktionen von physiologischer Relevanz sind, wurde das Schließen der Stomata verschiedener *ahp*-Mutanten (Hutchison *et al.* 2006) in Reaktion auf Ethylen untersucht. Die Stomata der *ahp1*- und der *ahp2*-Mutante waren ethyleninsensitiv, ebenso die der *ahp1,5*- und *ahp1,2*-Doppelmutanten sowie die der *ahp1,2,5*-Tripelmutante. Die Stomata der *ahp5*-Mutante sowie der *ahp2,5*-Doppelmutante reagierten hingegen schwach auf Ethylen. Aus den Ergebnissen der Einzelmutanten lässt sich schließen, dass AHP1 und AHP2 für das Schließen der Stomata auf Ethylen erforderlich sind, nicht jedoch AHP5. Da die *ahp2,5*-Doppelmutante jedoch auf Ethylen reagierte, scheint AHP5 zumindest in diesem Signalweg epistatisch über AHP2 zu sein. In der Tripelmutante ist dieser Effekt vermutlich durch das Fehlen von AHP1 maskiert, was bedeuten könnte, dass der AHK5-Signalweg in Reaktion auf Ethylen hauptsächlich über AHP1 abläuft.
Des Weiteren wurde die Reaktion der verschiedenen *ahp*-Mutanten auf H_2O_2 untersucht. Die *ahp1*- sowie die *ahp5*-Mutante zeigten eine wildtypische Reaktion. Dagegen war die *ahp2*-Mutante H_2O_2-insensitiv. Die *ahp1,5*-Doppelmutante verhielt sich wie *ahp5* und die *ahp1,2*- und *ahp2,5*-Doppelmutanten wie *ahp2*. Die Stomata der Tripelmutante reagierten ebenfalls nicht auf H_2O_2. AHP1 und AHP5 sind daher offensichtlich nicht in den Signalweg involviert, wohingegen AHP2 für die Reaktion der Stomata auf H_2O_2 essentiell ist. Das lässt den Schluss zu, dass die AHK5- und AHP-abhängigen Signalwege in Stomata je nach Eingangssignal unterschiedlich sind.
Zur Vervollständigung des AHK5-Signalwegs, wurden des Weiteren die *Output*-Elemente des TCS, die ARRs, analysiert. Um *downstream* von AHK5-AHP zu stehen, müsste der entsprechende Responseregulator mit AHP1 und/oder AHP2 interagieren können. Dies ist bei zehn ARRs der Fall (Dortay *et al.* 2006), von denen allerdings nur ARR1, 2, 4 und 7 in Schließzellen exprimiert sind (Leonhardt *et al.* 2004). Die Tatsache, dass ARR4 mit AHP1 interagiert und auch von diesem phosphoryliert werden kann (Mira-Rodado *et al.* 2007), macht ARR4 zu einem vielversprechenden Kandidaten *downstream* von AHK5-AHP1.

In *Yeast-Two-Hybrid-* und BiFC-Analysen konnte außerdem gezeigt werden, dass ARR4 mit AHP1, 2, 3, 5 und 6 interagiert. Es besteht daher die Möglichkeit, dass AHK5 mit AHP1 oder AHP2 und ARR4 einen Signalweg bildet, der die Reaktion der Schließzellen auf H_2O_2 und Ethylen reguliert.

Um die Bedeutung von ARR4 beim Schließen der Stomata näher zu beleuchten, wurde die Reaktion der *arr4*-Mutante (To *et al.* 2004; Mira-Rodado *et al.* 2007) auf Ethylen und H_2O_2 untersucht. Die *arr4*-Stomata wurden weder durch Ethylenbehandlung noch durch H_2O_2 geschlossen, was bedeutet dass ARR4 als positiver Regulator dieser beiden Signalwege fungiert. Da das TCS auf einem *Phosphorelay* basiert, wurde des Weiteren untersucht, ob das Schließen der Stomata auf Ethylen und H_2O_2 vom Phosphorylierungszustand von ARR4 abhängt. Es wurde dafür eine transgene Linie herangezogen, die eine nicht phosphorylierbare Variante von ARR4 ($ARR4^{D95N}$) überexprimiert (Mira-Rodado *et al.* 2007). Die Stomata dieser Linie zeigten ein wildtypisches Verhalten auf Ethylen, wurden jedoch in Reaktion auf H_2O_2 nicht geschlossen. Da der Ethylensignalweg nicht vom Phosphorylierungszustand von ARR4 abzuhängen scheint, müsste der H_2O_2-Weg demnach als Antwort auf andere Stimuli als Ethylen ablaufen. Das bedeutet, dass es einen bisher unbekannten Ethylensignalweg gibt, der nicht über die Bildung von H_2O_2 abläuft.

Für ARR2 ist bekannt, dass es *downstream* von ETR1 im Ethylen- und H_2O_2-Signalweg in Schließzellen steht (Desikan *et al.* 2006). Es wurde ebenfalls ein *Phosphorelay downstream* von ETR1 gezeigt, der über ARR2 läuft (Hass *et al.* 2004). Außerdem interagieren ETR1 und ARR2 mit AHP1 und AHP2 *in vitro* (Dortay *et al.* 2008; Scharein *et al.* 2008). Der Ethylensignalweg könnte daher über AHP1, AHP2 und ARR2 ablaufen, wobei ARR2 von AHP1 oder AHP2 phosphoryliert und damit aktiviert würde und die *ARR4*-Genexpression induzierte. Die erhöhte ARR4-Proteinmenge könnte dann die Ethylenantwort in Stomata phosphorylierungsunabhängig vermitteln.

Die gezeigten Daten eröffnen neue Perspektiven und lassen einen *cross-talk* zwischen den Histidinkinasen AHK5 und ETR1 im Ethylensignalweg in Schließzellen vermuten. Die Beteiligung untergeordneter Elemente des Zweikomponentensystems und die Tatsache, dass auch deren Phosphorylierungszustand von Bedeutung ist, unterstreichen die Wichtigkeit einer präzisen Feinregulierung der Stomatabewegung.

5 LITERATUR

ALTMANN, T. (1999). Molecular physiology of brassinosteroids revealed by the analysis of mutants. *Planta* **208**(1): 1-11.

APEL, K. and HIRT, H. (2004). Reactive oxygen species: metabolism, oxidative stress, and signal transduction. *Annu Rev Plant Biol* **55**: 373-399.

ARGYROS, R.D., MATHEWS, D.E., CHIANG, Y.H., PALMER, C.M., THIBAULT, D.M., ETHERIDGE, N., ARGYROS, D.A., MASON, M.G.*, et al.* (2008). Type B response regulators of Arabidopsis play key roles in cytokinin signaling and plant development. *Plant Cell* **20**(8): 2102-2116.

BISHOP, G.J. (2003). Brassinosteroid Mutants of Crops. *J Plant Growth Regul* **22**(4): 325-335.

BITTEL, P. and ROBATZEK, S. (2007). Microbe-associated molecular patterns (MAMPs) probe plant immunity. *Curr Opin Plant Biol* **10**(4): 335-341.

BOBIK, K., BOUTRY, M. and DUBY, G. (2010). Activation of the plasma membrane H^+-ATPase by acid stress: antibodies as a tool to follow the phosphorylation status of the penultimate activating Thr. *Plant Signal Behav* **5**(6): 681-683.

BRANDSTATTER, I. and KIEBER, J.J. (1998). Two genes with similarity to bacterial response regulators are rapidly and specifically induced by cytokinin in Arabidopsis. *Plant Cell* **10**(6): 1009-1019.

BRIGHT, J., DESIKAN, R., HANCOCK, J.T., WEIR, I.S. and NEILL, S.J. (2006). ABA-induced NO generation and stomatal closure in Arabidopsis are dependent on H_2O_2 synthesis. *Plant J* **45**(1): 113-122.

BUCK, V., QUINN, J., SOTO PINO, T., MARTIN, H., SALDANHA, J., MAKINO, K., MORGAN, B.A. and MILLAR, J.B. (2001). Peroxide sensors for the fission yeast stress-activated mitogen-activated protein kinase pathway. *Mol Biol Cell* **12**(2): 407-419.

BURKLE, L., CEDZICH, A., DOPKE, C., STRANSKY, H., OKUMOTO, S., GILLISSEN, B., KUHN, C. and FROMMER, W.B. (2003). Transport of cytokinins mediated by purine transporters of the PUP family expressed in phloem, hydathodes, and pollen of Arabidopsis. *Plant J* **34**(1): 13-26.

CEDZICH, A., STRANSKY, H., SCHULZ, B. and FROMMER, W.B. (2008). Characterization of cytokinin and adenine transport in Arabidopsis cell cultures. *Plant Physiol* **148**(4): 1857-1867.

CERANA, R., SPELTA, M., BONETTI, A. and LADO, P. (1985). On the effects of cholesterol on H^+ extrusion and on groth in maize root segments: Comparison with brassinosteroid. *Plant Sci* **38**: 99-105.

CHANG, C., KWOK, S.F., BLEECKER, A.B. and MEYEROWITZ, E.M. (1993). Arabidopsis ethylene-response gene ETR1: similarity of product to two-component regulators. *Science* **262**(5133): 539-544.

CHO, H.T. and COSGROVE, D.J. (2004). Expansins as agents in hormone action. *Plant Hormones, Biosynthesis, Signal Transduction, Action.* P. J. Davies. Dordrecht/Boston/London, Kluwer Academics Publisher**:** 262-281.

CLELAND, R.E. (2004). Auxin and cell elongation. *Plant Hormones, Biosynthesis, Signal Transduction, Action.* P. J. Davies. Dordrecht, Kluwer Academic Publishers**:** 204-220.

CLELAND, R.E., BUCKLEY, G., NOWBAR, S., LEW, N.M., STINEMETZ, C., EVANS, M.L. and RAYLE, D.L. (1991). The pH profile for acid-induced elongation of coleoptile and epicotyl sections is consistent with the acid-growth theory. *Planta* **186**: 70-74.

CLOUSE, S.D. (2011). Brassinosteroid signal transduction: from receptor kinase activation to transcriptional networks regulating plant development. *Plant Cell* **23**(4): 1219-1230.

CLOUSE, S.D., LANGFORD, M. and MCMORRIS, T.C. (1996). A brassinosteroid-insensitive mutant in *Arabidopsis thaliana* exhibits multiple defects in growth and development. *Plant Physiol* **111**(3): 671-678.

CLOUSE, S.D. and SASSE, J.M. (1998). Brassinosteroids: Essential Regulators of Plant Growth and Development. *Annu Rev Plant Physiol Plant Mol Biol* **49**: 427-451.

COOPER, C.E., PATEL, R.P., BROOKES, P.S. and DARLEY-USMAR, V.M. (2002). Nanotransducers in cellular redox signaling: modification of thiols by reactive oxygen and nitrogen species. *Trends Biochem Sci* **27**(10): 489-492.

COSTACURTA, A. and VANDERLEYDEN, J. (1995). Synthesis of phytohormones by plant-associated bacteria. *Crit Rev Microbiol* **21**(1): 1-18.

CUTLER, S.R., EHRHARDT, D.W., GRIFFITTS, J.S. and SOMERVILLE, C.R. (2000). Random GFP::cDNA fusions enable visualization of subcellular structures in cells of Arabidopsis at a high frequency. *PNAS* **97**(7): 3718-3723.

D'AGOSTINO, I.B., DERUERE, J. and KIEBER, J.J. (2000). Characterization of the response of the Arabidopsis response regulator gene family to cytokinin. *Plant Physiol* **124**(4): 1706-1717.

DANG, C.V. and LEE, W.M. (1988). Identification of the human c-myc protein nuclear translocation signal. *Mol Cell Biol* **8**(10): 4048-4054.

DESIKAN, R., CHEUNG, M., CLARKE, A., GOLDING, S., SAGI, M., FLUHR, R., ROCK, C., HANCOCK, J., *et al.* (2004). Hydrogen peroxide is a common signal for darkness- and ABA-induced stomatal closure in *Pisum sativum*. *Func Plant Biol* **31**: 913-920.

DESIKAN, R., HANCOCK, J.T., BRIGHT, J., HARRISON, J., WEIR, I., HOOLEY, R. and NEILL, S.J. (2005). A role for ETR1 in hydrogen peroxide signaling in stomatal guard cells. *Plant Physiol* **137**(3): 831-834.

DESIKAN, R., LAST, K., HARRETT-WILLIAMS, R., TAGLIAVIA, C., HARTER, K., HOOLEY, R., HANCOCK, J.T. and NEILL, S.J. (2006). Ethylene-induced stomatal closure in Arabidopsis occurs via AtrbohF-mediated hydrogen peroxide synthesis. *Plant J* **47**(6): 907-916.

DIXIT, R., CYR, R. and GILROY, S. (2006). Using intrinsically fluorescent proteins for plant cell imaging. *Plant J* **45**(4): 599-615.

DORTAY, H., GRUHN, N., PFEIFER, A., SCHWERDTNER, M., SCHMÜLLING, T. and HEYL, A. (2008). Toward an Interaction Map of the Two-Component Signaling Pathway of *Arabidopsis thaliana*. *J Proteome Res* **7**(9): 3649-3660.

DORTAY, H., MEHNERT, N., BURKLE, L., SCHMULLING, T. and HEYL, A. (2006). Analysis of protein interactions within the cytokinin-signaling pathway of *Arabidopsis thaliana*. *FEBS J* **273**(20): 4631-4644.

DUPRÉ, E. and SCHAAF, G. (1996). Influence of Ions on the Unfolding of the Spermatozoa of the Rock Shrimp, *Rhynchocinetes typus*. *J Exp Zool* **274**: 358-364.

ELGASS, K., CAESAR, K., SCHLEIFENBAUM, F., MEIXNER, A.J. and HARTER, K. (2010a). The fluorescence lifetime of BRI1-GFP as probe for the noninvasive determination of the membrane potential in living cells *Proc. SPIE* **7568**: 756804.

ELGASS, K., CAESAR, K., SCHLEIFENBAUM, F., STIERHOF, Y.D., MEIXNER, A.J. and HARTER, K. (2009). Novel application of fluorescence lifetime and fluorescence microscopy enables quantitative access to subcellular dynamics in plant cells. *PloS One* **4**(5): e5716.

ELGASS, K., CAESAR, K., WANKE, D., HARTER, K., MEIXNER, A.J. and SCHLEIFENBAUM, F. (2010b). Application of FLIM-FIDSAM for the in vivo analysis of hormone competence of different cell types. *Anal Bioanal Chem* **398**(5): 1919-1925.

FELIX, G., DURAN, J.D., VOLKO, S. and BOLLER, T. (1999). Plants have a sensitive perception system for the most conserved domain of bacterial flagellin. *Plant J* **18**(3): 265-276.

FRANCO-ZORRILLA, J.M., MARTIN, A.C., LEYVA, A. and PAZ-ARES, J. (2005). Interaction between phosphate-starvation, sugar, and cytokinin signaling in Arabidopsis and the roles of cytokinin receptors CRE1/AHK4 and AHK3. *Plant Physiol* **138**(2): 847-857.

FRANCO-ZORRILLA, J.M., MARTIN, A.C., SOLANO, R., RUBIO, V., LEYVA, A. and PAZ-ARES, J. (2002). Mutations at CRE1 impair cytokinin-induced repression of phosphate starvation responses in Arabidopsis. *Plant J* **32**(3): 353-360.

FRIEDRICHSEN, D. and CHORY, J. (2001). Steroid signaling in plants: from the cell surface to the nucleus. *BioEssays* **23**(11): 1028-1036.

FRIEDRICHSEN, D.M., JOAZEIRO, C.A., LI, J., HUNTER, T. and CHORY, J. (2000). Brassinosteroid-insensitive-1 is a ubiquitously expressed leucine-rich repeat receptor serine/threonine kinase. *Plant Physiol* **123**(4): 1247-1256.

FRIML, J. and JONES, A.R. (2010). Endoplasmic reticulum: the rising compartment in auxin biology. *Plant Physiol* **154**(2): 458-462.

GAN, S. and AMASINO, R.M. (1995). Inhibition of leaf senescence by autoregulated production of cytokinin. *Science* **270**(5244): 1986-1988.

GAO, Z., CHEN, Y.F., RANDLETT, M.D., ZHAO, X.C., FINDELL, J.L., KIEBER, J.J. and SCHALLER, G.E. (2003). Localization of the Raf-like kinase CTR1 to the endoplasmic reticulum of Arabidopsis through participation in ethylene receptor signaling complexes. *J Biol Chem* **278**(36): 34725-34732.

GATTOLIN, S., ALANDETE-SAEZ, M., ELLIOTT, K., GONZALEZ-CARRANZA, Z., NAOMAB, E., POWELL, C. and ROBERTS, J.A. (2006). Spatial and temporal expression of the response regulators ARR22 and ARR24 in *Arabidopsis thaliana*. *J Exp Bot* **57**(15): 4225-4233.

GIEPMANS, B.N., ADAMS, S.R., ELLISMAN, M.H. and TSIEN, R.Y. (2006). The fluorescent toolbox for assessing protein location and function. *Science* **312**(5771): 217-224.

GODA, H., SASAKI, E., AKIYAMA, K., MARUYAMA-NAKASHITA, A., NAKABAYASHI, K., LI, W., OGAWA, M., YAMAUCHI, Y.*, et al.* (2008). The AtGenExpress hormone and chemical treatment data set: experimental design, data evaluation, model data analysis and data access. *Plant J* **55**(3): 526-542.

GRAINGER, J.L., WINKLER, M.M., SHEN, S.S. and STEINHARDT, R.A. (1979). Intracellular pH controls protein synthesis rate in the sea urchine egg and early embryo. *Dev Biol* **68**(2): 396-406.

GREFEN, C. and HARTER, K. (2004). Plant two-component systems: principles, functions, complexity and cross talk. *Planta* **219**(5): 733-742.

GREFEN, C., OBRDLIK, P. and HARTER, K. (2009). The determination of protein-protein interactions by the mating-based split-ubiquitin system (mbSUS). *Meth Mol Biology* **479**: 217-233.

GROVE, M.D., SPENCER, G.F., ROHWEDDER, W.K., MANDAVA, N.B., WORLEY, J.F., WARTHEN, J.D., STEFFENS, G.L., FLIPPEN-ANDERSEN, J.L.*, et al.* (1979). Brassinolide, a plant growth-promoting steroid isolated from *Brassica napus* pollen. *Nature* **281**: 216-217.

GUO, H. and ECKER, J.R. (2004). The ethylene signaling pathway: new insights. *Curr Opin Plant Biol* **7**(1): 40-49.

HAHN, A. and HARTER, K. (2009). Mitogen-activated protein kinase cascades and ethylene: signaling, biosynthesis, or both? *Plant Physiol* **149**(3): 1207-1210.

HALL, A.E. and BLEECKER, A.B. (2003). Analysis of combinatorial loss-of-function mutants in the *Arabidopsis* ethylene receptors reveals that the *ers1etr1* double mutant has severe developmental defects that are EIN2 dependent. *Plant Cell* **15**(9): 2032-2041.

HALLIDAY, K.J. (2004). Plant hormones: the interplay of brassinosteroids and auxin. *Curr Biol* **14**(23): R1008-1010.

HARTER, K., MEIXNER, A.J. and SCHLEIFENBAUM, F. (2011). Spectro-Microscopy of Living Plant Cells. *Mol Plant*.

HASS, C., LOHRMANN, J., ALBRECHT, V., SWEERE, U., HUMMEL, F., YOO, S.D., HWANG, I., ZHU, T.*, et al.* (2004). The response regulator 2 mediates ethylene signalling and hormone signal integration in Arabidopsis. *EMBO J* **23**(16): 3290-3302.

HAUBRICK, L.L. and ASSMANN, S.M. (2006). Brassinosteroids and plant function: some clues, more puzzles. *Plant Cell Environ* **29**(3): 446-457.

HE, J.X., GENDRON, J.M., SUN, Y., GAMPALA, S.S., GENDRON, N., SUN, C.Q. and WANG, Z.Y. (2005). BZR1 is a transcriptional repressor with dual roles in brassinosteroid homeostasis and growth responses. *Science* **307**(5715): 1634-1638.

HE, J.X., GENDRON, J.M., YANG, Y., LI, J. and WANG, Z.Y. (2002). The GSK3-like kinase BIN2 phosphorylates and destabilizes BZR1, a positive regulator of the brassinosteroid signaling pathway in Arabidopsis. *PNAS* **99**(15): 10185-10190.

HECHT, V., VIELLE-CALZADA, J.P., HARTOG, M.V., SCHMIDT, E.D., BOUTILIER, K., GROSSNIKLAUS, U. and DE VRIES, S.C. (2001). The Arabidopsis SOMATIC EMBRYOGENESIS RECEPTOR KINASE 1 gene is expressed in developing ovules and embryos and enhances embryogenic competence in culture. *Plant Physiol* **127**(3): 803-816.

HEJATKO, J., PERNISOVA, M., ENEVA, T., PALME, K. and BRZOBOHATY, B. (2003). The putative sensor histidine kinase CKI1 is involved in female gametophyte development in Arabidopsis. *Mol Genet Genom* **269**(4): 443-453.

HICKS, G.R., SMITH, H.M., SHIEH, M. and RAIKHEL, N.V. (1995). Three classes of nuclear import signals bind to plant nuclei. *Plant Physiol* **107**(4): 1055-1058.

HIGUCHI, M., PISCHKE, M.S., MAHONEN, A.P., MIYAWAKI, K., HASHIMOTO, Y., SEKI, M., KOBAYASHI, M., SHINOZAKI, K.*, et al.* (2004). In planta functions of the Arabidopsis cytokinin receptor family. *PNAS* **101**(23): 8821-8826.

HIROSE, N., MAKITA, N., YAMAYA, T. and SAKAKIBARA, H. (2005). Functional characterization and expression analysis of a gene, OsENT2, encoding an equilibrative nucleoside transporter in rice suggest a function in cytokinin transport. *Plant Physiol* **138**(1): 196-206.

HONG, Z., JIN, H., TZFIRA, T. and LI, J. (2008). Multiple mechanism-mediated retention of a defective brassinosteroid receptor in the endoplasmic reticulum of Arabidopsis. *Plant Cell* **20**(12): 3418-3429.

HORÁK, J., GREFEN, C., BERENDZEN, K.W., HAHN, A., STIERHOF, Y.D., STADELHOFER, B., STAHL, M., KONCZ, C.*, et al.* (2008). The *Arabidopsis thaliana* response regulator ARR22 is a

putative AHP phospho-histidine phosphatase expressed in the chalaza of developing seeds. *BMC Plant Biol* **8**: 77.

HORAK, J., JANDA, L., PEKAROVA, B. and HEJATKO, J. (2011). Molecular mechanisms of signalling specificity via phosphorelay pathways in Arabidopsis. *Curr Protein Pept Sci* **12**(2): 126-136.

HOTHORN, M., BELKHADIR, Y., DREUX, M., DABI, T., NOEL, J.P., WILSON, I.A. and CHORY, J. (2011). Structural basis of steroid hormone perception by the receptor kinase BRI1. *Nature* **474**(7352): 467-471.

HUTCHISON, C.E., LI, J., ARGUESO, C., GONZALEZ, M., LEE, E., LEWIS, M.W., MAXWELL, B.B., PERDUE, T.D.*, et al.* (2006). The Arabidopsis histidine phosphotransfer proteins are redundant positive regulators of cytokinin signaling. *Plant Cell* **18**(11): 3073-3087.

HWANG, I., CHEN, H.C. and SHEEN, J. (2002). Two-component signal transduction pathways in Arabidopsis. *Plant Physiol* **129**(2): 500-515.

HWANG, I. and SHEEN, J. (2001). Two-component circuitry in Arabidopsis cytokinin signal transduction. *Nature* **413**(6854): 383-389.

IMAMURA, A., HANAKI, N., NAKAMURA, A., SUZUKI, T., TANIGUCHI, M., KIBA, T., UEGUCHI, C., SUGIYAMA, T.*, et al.* (1999). Compilation and characterization of *Arabidopsis thaliana* response regulators implicated in His-Asp phosphorelay signal transduction. *Plant Cell Physiol* **40**(7): 733-742.

IMAMURA, A., KIBA, T., TAJIMA, Y., YAMASHINO, T. and MIZUNO, T. (2003). *In vivo* and *in vitro* characterization of the ARR11 response regulator implicated in the His-to-Asp phosphorelay signal transduction in *Arabidopsis thaliana*. *Plant Cell Physiol* **44**(2): 122-131.

IMAMURA, A., YOSHINO, Y. and MIZUNO, T. (2001). Cellular localization of the signaling components of Arabidopsis His-to-Asp phosphorelay. *Biosci Biotech Biochem* **65**(9): 2113-2117.

INOUE, T., HIGUCHI, M., HASHIMOTO, Y., SEKI, M., KOBAYASHI, M., KATO, T., TABATA, S., SHINOZAKI, K.*, et al.* (2001). Identification of CRE1 as a cytokinin receptor from Arabidopsis. *Nature* **409**(6823): 1060-1063.

ISHIDA, K., YAMASHINO, T. and MIZUNO, T. (2008). Expression of the cytokinin-induced type-A response regulator gene ARR9 is regulated by the circadian clock in *Arabidopsis thaliana*. *Biosci Biotech Biochem* **72**(11): 3025-3029.

IWAMA, A., YAMASHINO, T., TANAKA, Y., SAKAKIBARA, H., KAKIMOTO, T., SATO, S., KATO, T., TABATA, S.*, et al.* (2007). AHK5 histidine kinase regulates root elongation through an ETR1-dependent abscisic acid and ethylene signaling pathway in *Arabidopsis thaliana*. *Plant Cell Physiol* **48**(2): 375-380.

JAILLAIS, Y., BELKHADIR, Y., BALSEMAO-PIRES, E., DANGL, J.L. and CHORY, J. (2011a). Extracellular leucine-rich repeats as a platform for receptor/coreceptor complex formation. *PNAS* **108**(20): 8503-8507.

JAILLAIS, Y., HOTHORN, M., BELKHADIR, Y., DABI, T., NIMCHUK, Z.L., MEYEROWITZ, E.M. and CHORY, J. (2011b). Tyrosine phosphorylation controls brassinosteroid receptor activation by triggering membrane release of its kinase inhibitor. *Genes Dev* **25**(3): 232-237.

JEON, J., KIM, N.Y., KIM, S., KANG, N.Y., NOVAK, O., KU, S.J., CHO, C., LEE, D.J.*, et al.* (2010). A subset of cytokinin two-component signaling system plays a role in cold temperature stress response in Arabidopsis. *J Biol Chem* **285**(30): 23371-23386.

JOHNSON, C.H. and EPEL, D. (1981). Intracellular pH of sea urchin eggs measured by the dimethyloxazolidinedione (DMO) method. *J Cell Biol* **89**(2): 284-291.

KALDERON, D., ROBERTS, B.L., RICHARDSON, W.D. and SMITH, A.E. (1984). A short amino acid sequence able to specify nuclear location. *Cell* **39**(3 Pt 2): 499-509.

KIBA, T., AOKI, K., SAKAKIBARA, H. and MIZUNO, T. (2004). Arabidopsis response regulator, ARR22, ectopic expression of which results in phenotypes similar to the wol cytokinin-receptor mutant. *Plant Cell Physiol* **45**(8): 1063-1077.

KIBA, T., YAMADA, H. and MIZUNO, T. (2002). Characterization of the ARR15 and ARR16 response regulators with special reference to the cytokinin signaling pathway mediated by the AHK4 histidine kinase in roots of Arabidopsis thaliana. *Plant Cell Physiol* **43**(9): 1059-1066.

KIEBER, J.J. and SCHALLER, G.E. (2010). The perception of cytokinin: a story 50 years in the making. *Plant Physiol* **154**(2): 487-492.

KIM, H.J., RYU, H., HONG, S.H., WOO, H.R., LIM, P.O., LEE, I.C., SHEEN, J., NAM, H.G.*, et al.* (2006). Cytokinin-mediated control of leaf longevity by AHK3 through phosphorylation of ARR2 in Arabidopsis. *PNAS* **103**(3): 814-819.

KIM, J.H., JOHANNES, L., GOUD, B., ANTONY, C., LINGWOOD, C.A., DANEMAN, R. and GRINSTEIN, S. (1998). Noninvasive measurement of the pH of the endoplasmic reticulum at rest and during calcium release. *PNAS* **95**(6): 2997-3002.

KIM, T.W., GUAN, S., SUN, Y., DENG, Z., TANG, W., SHANG, J.X., BURLINGAME, A.L. and WANG, Z.Y. (2009). Brassinosteroid signal transduction from cell-surface receptor kinases to nuclear transcription factors. *Nature Cell Biol* **11**(10): 1254-1260.

KIM, T.W. and WANG, Z.Y. (2010). Brassinosteroid signal transduction from receptor kinases to transcription factors. *Annu Rev Plant Biol* **61**: 681-704.

KOSUGI, S., HASEBE, M., TOMITA, M. and YANAGAWA, H. (2009). Systematic identification of cell cycle-dependent yeast nucleocytoplasmic shuttling proteins by prediction of composite motifs. *PNAS* **106**(25): 10171-10176.

KWAK, J.M., MORI, I.C., PEI, Z.M., LEONHARDT, N., TORRES, M.A., DANGL, J.L., BLOOM, R.E., BODDE, S.*, et al.* (2003). NADPH oxidase AtrbohD and AtrbohF genes function in ROS-dependent ABA signaling in Arabidopsis. *EMBO J* **22**(11): 2623-2633.

LANGE, A., MILLS, R.E., LANGE, C.J., STEWART, M., DEVINE, S.E. and CORBETT, A.H. (2007). Classical nuclear localization signals: definition, function, and interaction with importin alpha. *J Biol Chem* **282**(8): 5101-5105.

LAPLAZE, L., BENKOVA, E., CASIMIRO, I., MAES, L., VANNESTE, S., SWARUP, R., WEIJERS, D., CALVO, V.*, et al.* (2007). Cytokinins act directly on lateral root founder cells to inhibit root initiation. *Plant Cell* **19**(12): 3889-3900.

LEIBFRIED, A., TO, J.P., BUSCH, W., STEHLING, S., KEHLE, A., DEMAR, M., KIEBER, J.J. and LOHMANN, J.U. (2005). WUSCHEL controls meristem function by direct regulation of cytokinin-inducible response regulators. *Nature* **438**(7071): 1172-1175.

LEONHARDT, N., KWAK, J.M., ROBERT, N., WANER, D., LEONHARDT, G. and SCHROEDER, J.I. (2004). Microarray expression analyses of Arabidopsis guard cells and isolation of a recessive abscisic acid hypersensitive protein phosphatase 2C mutant. *Plant Cell* **16**(3): 596-615.

LI, J. and CHORY, J. (1997). A putative leucine-rich repeat receptor kinase involved in brassinosteroid signal transduction. *Cell* **90**(5): 929-938.

LI, J., WEN, J., LEASE, K.A., DOKE, J.T., TAX, F.E. and WALKER, J.C. (2002). BAK1, an Arabidopsis LRR receptor-like protein kinase, interacts with BRI1 and modulates brassinosteroid signaling. *Cell* **110**(2): 213-222.

LI, J., YANG, H., PEER, W.A., RICHTER, G., BLAKESLEE, J., BANDYOPADHYAY, A., TITAPIWANTAKUN, B., UNDURRAGA, S.*, et al.* (2005). Arabidopsis H^+-PPase AVP1 regulates auxin-mediated organ development. *Science* **310**(5745): 121-125.

LI, X., MO, X., SHOU, H. and WU, P. (2006). Cytokinin-mediated cell cycling arrest of pericycle founder cells in lateral root initiation of Arabidopsis. *Plant Cell Physiol* **47**(8): 1112-1123.

LOHRMANN, J., BUCHHOLZ, G., KEITEL, C., SWEERE, U., KIRCHER, S., BÄURLE, I., KUDIA, J., SCHÄFER, E.*, et al.* (1999). Differential Expression and Nuclear Localization of Response Regulator-Like Proteins from *Arabidopsis thaliana*. *Plant Biol* **1**: 495-505.

LOHRMANN, J., SWEERE, U., ZABALETA, E., BÄURLE, I., KEITEL, C., KOZMA-BOGNAR, L., BRENNICKE, A., SCHÄFER, E.*, et al.* (2001). The response regulator ARR2: a pollen-specific transcription factor involved in the expression of nuclear genes for components of mitochondrial complex I in *Arabidopsis*. *Mol Genet Genom* **265**: 2-13.

LOMIN, S.N., YONEKURA-SAKAKIBARA, K., ROMANOV, G.A. and SAKAKIBARA, H. (2011). Ligand-binding properties and subcellular localization of maize cytokinin receptors. *Journal of experimental botany*.

LUMMER, M., HUMPERT, F., STEUWE, C., CAESAR, K., SCHUTTPELZ, M., SAUER, M. and STAIGER, D. (2011). Reversible Photoswitchable DRONPA-s Monitors Nucleocytoplasmic Transport of an RNA-Binding Protein in Transgenic Plants. *Traffic* **12**(6): 693-702.

MACARA, I.G. (2001). Transport into and out of the nucleus. *Microbiol Mol Biol Rev* **65**(4): 570-594, table of contents.

MACLENNAN, D.H., RICE, W.J. and GREEN, N.M. (1997). The mechanism of Ca^{2+} transport by sarco(endo)plasmic reticulum Ca^{2+}-ATPases. *J Biol Chem* **272**(46): 28815-28818.

MAEDA, T., WURGLER-MURPHY, S.M. and SAITO, H. (1994). A two-component system that regulates an osmosensing MAP kinase cascade in yeast. *Nature* **369**(6477): 242-245.

MÄHÖNEN, A.P., BISHOPP, A., HIGUCHI, M., NIEMINEN, K.M., KINOSHITA, K., TÖRMÄKANGAS, K., IKEDA, Y., OKA, A.*, et al.* (2006a). Cytokinin signaling and its inhibitor AHP6 regulate cell fate during vascular development. *Science* **311**(5757): 94-98.

MÄHÖNEN, A.P., HIGUCHI, M., TORMAKANGAS, K., MIYAWAKI, K., PISCHKE, M.S., SUSSMAN, M.R., HELARIUTTA, Y. and KAKIMOTO, T. (2006b). Cytokinins regulate a bidirectional phosphorelay network in Arabidopsis. *Curr Biol* **16**(11): 1116-1122.

MALEY, F., TRIMBLE, R.B., TARENTINO, A.L. and PLUMMER, T.H., JR. (1989). Characterization of glycoproteins and their associated oligosaccharides through the use of endoglycosidases. *Anal Biochem* **180**(2): 195-204.

MANDAVA, N.B. (1988). Plant Growth-Promoting Brassinosteroids. *Annu Rev Plant Physiol Plant Mol Biol* **39**: 23-52.

MASON, M.G., MATHEWS, D.E., ARGYROS, D.A., MAXWELL, B.B., KIEBER, J.J., ALONSO, J.M., ECKER, J.R. and SCHALLER, G.E. (2005). Multiple type-B response regulators mediate cytokinin signal transduction in Arabidopsis. *Plant Cell* **17**(11): 3007-3018.

MATTAJ, I.W. and ENGLMEIER, L. (1998). NUCLEOCYTOPLASMIC TRANSPORT: The Soluble Phase. *Annu Rev Biochem* **67**: 265-306.

MCCLUNG, C.R. (2006). Plant circadian rhythms. *Plant Cell* **18**(4): 792-803.

MELOTTO, M., UNDERWOOD, W., KOCZAN, J., NOMURA, K. and HE, S.Y. (2006). Plant stomata function in innate immunity against bacterial invasion. *Cell* **126**(5): 969-980.

MILLER, C.O., SKOOG, F., VON SALTZA, M.H. and STRONG, F.M. (1955). Kinetin, a cell division factor from desoxyribonucleic acid. *J. Amer. Chem. Soc.* **77**(1392).

MIRA-RODADO, V., SWEERE, U., GREFEN, C., KUNKEL, T., FEJES, E., NAGY, F., SCHAFER, E. and HARTER, K. (2007). Functional cross-talk between two-component and phytochrome B signal transduction in Arabidopsis. *J Exp Bot* **58**(10): 2595-2607.

MOORE, M.S. (1998). Ran and Nuclear Transport. *J Biol Chem* **273**: 22857-22860.

MORA-GARCIA, S., VERT, G., YIN, Y., CANO-DELGADO, A., CHEONG, H. and CHORY, J. (2004). Nuclear protein phosphatases with Kelch-repeat domains modulate the response to brassinosteroids in Arabidopsis. *Genes Dev* **18**(4): 448-460.

MÜLLER, B. (2011). Generic signal-specific responses: cytokinin and context-dependent cellular responses. *J Exp Bot* **62**(10): 3273-3288.

MÜLLER, B. and SHEEN, J. (2007). Arabidopsis cytokinin signaling pathway. *Sci. STKE* **2007**(407): cm5.

MÜLLER, B. and SHEEN, J. (2008). Cytokinin and auxin interaction in root stem-cell specification during early embryogenesis. *Nature* **453**(7198): 1094-1097.

MUNOZ-FONTELA, C., RODRIGUEZ, E., NOMBELA, C., ARROYO, J. and RIVAS, C. (2003). Characterization of the bipartite nuclear localization signal of protein LANA2 from Kaposi's sarcoma-associated herpesvirus. *Biochem J* **374**(Pt 2): 545-550.

NAM, K.H. and LI, J. (2002). BRI1/BAK1, a receptor kinase pair mediating brassinosteroid signaling. *Cell* **110**(2): 203-212.

NEILL, S., DESIKAN, R. and HANCOCK, J. (2002). Hydrogen peroxide signalling. *Curr Opin Plant Biol* **5**(5): 388-395.

NEMHAUSER, J.L., MOCKLER, T.C. and CHORY, J. (2004). Interdependency of brassinosteroid and auxin signaling in Arabidopsis. *PLoS Biology* **2**(9): E258.

NISHIMURA, C., OHASHI, Y., SATO, S., KATO, T., TABATA, S. and UEGUCHI, C. (2004). Histidine kinase homologs that act as cytokinin receptors possess overlapping functions in the regulation of shoot and root growth in Arabidopsis. *Plant Cell* **16**(6): 1365-1377.

OH, M.H., RAY, W.K., HUBER, S.C., ASARA, J.M., GAGE, D.A. and CLOUSE, S.D. (2000). Recombinant brassinosteroid insensitive 1 receptor-like kinase autophosphorylates on serine and threonine residues and phosphorylates a conserved peptide motif in vitro. *Plant Physiol* **124**(2): 751-766.

OHTA, N., NAKABAYASHI, T., OSHITA, S. and KINJO, M. (2010). Fluorescence lifetime imaging spectroscopy in living cells with particular regards to pH dependence and electric field effect. *Proc. SPIE* **7576**: 75760G.

OTA, I.M. and VARSHAVSKY, A. (1993). A yeast protein similar to bacterial two-component regulators. *Science* **262**(5133): 566-569.

PAPON, N., CLASTRE, M., GANTET, P., RIDEAU, M., CHENIEUX, J.C. and CRECHE, J. (2003). Inhibition of the plant cytokinin transduction pathway by bacterial histidine kinase inhibitors in *Catharanthus roseus* cell cultures. *FEBS Letters* **537**(1-3): 101-105.

PAWLOWSKI, R., RAJAKYLA, E.K., VARTIAINEN, M.K. and TREISMAN, R. (2010). An actin-regulated importin alpha/beta-dependent extended bipartite NLS directs nuclear import of MRTF-A. *EMBO J* **29**(20): 3448-3458.

PEI, Z.M., MURATA, Y., BENNING, G., THOMINE, S., KLUSENER, B., ALLEN, G.J., GRILL, E. and SCHROEDER, J.I. (2000). Calcium channels activated by hydrogen peroxide mediate abscisic acid signalling in guard cells. *Nature* **406**(6797): 731-734.

PENG, P., YAN, Z., ZHU, Y. and LI, J. (2008). Regulation of the Arabidopsis GSK3-like kinase BRASSINOSTEROID-INSENSITIVE 2 through proteasome-mediated protein degradation. *Mol Plant* **1**(2): 338-346.

PETERS, R. (2009). Translocation through the nuclear pore: Kaps pave the way. *BioEssays* **31**(4): 466-477.

PISCHKE, M.S., JONES, L.G., OTSUGA, D., FERNANDEZ, D.E., DREWS, G.N. and SUSSMAN, M.R. (2002). An Arabidopsis histidine kinase is essential for megagametogenesis. *PNAS* **99**(24): 15800-15805.

POSAS, F., WURGLER-MURPHY, S.M., MAEDA, T., WITTEN, E.A., THAI, T.C. and SAITO, H. (1996). Yeast HOG1 MAP kinase cascade is regulated by a multistep phosphorelay mechanism in the SLN1-YPD1-SSK1 "two-component" osmosensor. *Cell* **86**(6): 865-875.

PUNWANI, J.A., HUTCHISON, C.E., SCHALLER, G.E. and KIEBER, J.J. (2010). The subcellular distribution of the Arabidopsis histidine phosphotransfer proteins is independent of cytokinin signaling. *Plant J* **62**(3): 473-482.

RAIKHEL, N. (1992). Nuclear targeting in plants. *Plant Physiol* **100**(4): 1627-1632.

RAYLE, D.L. and CLELAND, R. (1970). Enhancement of wall loosening and elongation by Acid solutions. *Plant Physiol* **46**(2): 250-253.

RAYLE, D.L. and CLELAND, R. (1977). Control of plant cell enlargement by hydrogen ions. *Curr Top Dev Biol* **11**: 187-214.

RAYLE, D.L. and CLELAND, R.E. (1992). The Acid Growth Theory of auxin-induced cell elongation is alive and well. *Plant Physiol* **99**(4): 1271-1274.

RICHMOND, A.E. and LANG, A. (1957). Effect of Kinetin on Protein Content and Survival of Detached *Xanthium* Leaves *Science* **125**: 650-651.

RIECHMANN, J.L., HEARD, J., MARTIN, G., REUBER, L., JIANG, C., KEDDIE, J., ADAM, L., PINEDA, O.*, et al.* (2000). Arabidopsis transcription factors: genome-wide comparative analysis among eukaryotes. *Science* **290**(5499): 2105-2110.

RIEFLER, M., NOVAK, O., STRNAD, M. and SCHMULLING, T. (2006). Arabidopsis cytokinin receptor mutants reveal functions in shoot growth, leaf senescence, seed size, germination, root development, and cytokinin metabolism. *Plant Cell* **18**(1): 40-54.

ROBATZEK, S., CHINCHILLA, D. and BOLLER, T. (2006). Ligand-induced endocytosis of the pattern recognition receptor FLS2 in Arabidopsis. *Genes Dev* **20**(5): 537-542.

ROBBINS, J., DILWORTH, S.M., LASKEY, R.A. and DINGWALL, C. (1991). Two interdependent basic domains in nucleoplasmin nuclear targeting sequence: identification of a class of bipartite nuclear targeting sequence. *Cell* **64**(3): 615-623.

ROMANI, G., MARRÈ, M.T., BONETTI, A., CERANA, R., LADO, P. and MARRÈ, E. (1983). Effects of a brassinosteroid on growth and electrogenic proton extrusion in maize root segments. *Physiol Plant* **59**: 528-532.

ROMANOV, G.A., LOMIN, S.N. and SCHMULLING, T. (2006). Biochemical characteristics and ligand-binding properties of Arabidopsis cytokinin receptor AHK3 compared to CRE1/AHK4 as revealed by a direct binding assay. *J Exp Bot* **57**(15): 4051-4058.

RUSSINOVA, E., BORST, J.W., KWAAITAAL, M., CANO-DELGADO, A., YIN, Y., CHORY, J. and DE VRIES, S.C. (2004). Heterodimerization and endocytosis of Arabidopsis brassinosteroid receptors BRI1 and AtSERK3 (BAK1). *Plant Cell* **16**(12): 3216-3229.

SAKAI, H., AOYAMA, T. and OKA, A. (2000). Arabidopsis ARR1 and ARR2 response regulators operate as transcriptional activators. *Plant J* **24**(6): 703-711.

SAKAI, H., HONMA, T., AOYAMA, T., SATO, S., KATO, T., TABATA, S. and OKA, A. (2001). ARR1, a transcription factor for genes immediately responsive to cytokinins. *Science* **294**(5546): 1519-1521.

SAKAKIBARA, H. (2006). Cytokinins: Activity, Biosynthesis, and Translocation. *Annu Rev Plant Biol* **57**: 431-449.

SALOME, P.A., TO, J.P., KIEBER, J.J. and MCCLUNG, C.R. (2006). Arabidopsis response regulators ARR3 and ARR4 play cytokinin-independent roles in the control of circadian period. *Plant Cell* **18**(1): 55-69.

SAMSON, F., BRUNAUD, V., BALZERGUE, S., DUBREUCQ, B., LEPINIEC, L., PELLETIER, G., CABOCHE, M. and LECHARNY, A. (2002). FLAGdb/FST: a database of mapped flanking insertion sites (FSTs) of *Arabidopsis thaliana* T-DNA transformants. *Nucleic Acids Res* **30**(1): 94-97.

SANCHEZ-RODRIGUEZ, C., RUBIO-SOMOZA, I., SIBOUT, R. and PERSSON, S. (2010). Phytohormones and the cell wall in Arabidopsis during seedling growth. *Trends Plant Sci* **15**(5): 291-301.

SCHALLER, A. and OECKING, C. (1999). Modulation of plasma membrane H^+-ATPase activity differentially activates wound and pathogen defense responses in tomato plants. *Plant Cell* **11**(2): 263-272.

SCHAREIN, B., VOET-VAN-VORMIZEELE, J., HARTER, K. and GROTH, G. (2008). Ethylene signaling: identification of a putative ETR1-AHP1 phosphorelay complex by fluorescence spectroscopy. *Anal Biochem* **377**(1): 72-76.

SCHMIDT, E.D., GUZZO, F., TOONEN, M.A. and DE VRIES, S.C. (1997). A leucine-rich repeat containing receptor-like kinase marks somatic plant cells competent to form embryos. *Development* **124**(10): 2049-2062.

SESSIONS, A., BURKE, E., PRESTING, G., AUX, G., MCELVER, J., PATTON, D., DIETRICH, B., HO, P.*, et al.* (2002). A high-throughput Arabidopsis reverse genetics system. *Plant Cell* **14**(12): 2985-2994.

SHIMIZU-SATO, S., TANAKA, M. and MORI, H. (2009). Auxin-cytokinin interactions in the control of shoot branching. *Plant Mol Biol* **69**(4): 429-435.

SINGH, K.K. (2000). The *Saccharomyces cerevisiae* Sln1p-Ssk1p two-component system mediates response to oxidative stress and in an oxidant-specific fashion. *Free Radic Biol Med* **29**(10): 1043-1050.

SKOOG, F. and MILLER, C.O. (1957). Chemical regulation of growth and organ formation in plant tissues cultured in vitro. *Symp Soc Exp Biol* **11**: 118-130.

SPETH, C., JASPERT, N., MARCON, C. and OECKING, C. (2010). Regulation of the plant plasma membrane H^+-ATPase by its C-terminal domain: what do we know for sure? *Eur J Cell Biol* **89**(2-3): 145-151.

SUN, Y., FAN, X.Y., CAO, D.M., TANG, W., HE, K., ZHU, J.Y., HE, J.X., BAI, M.Y.*, et al.* (2010). Integration of brassinosteroid signal transduction with the transcription network for plant growth regulation in Arabidopsis. *Dev Cell* **19**(5): 765-777.

SUZUKI, T., MATSUZAKI, T., HAGIWARA, H., AOKI, T. and TAKATA, K. (2007). Recent advances in fluorescent labeling techniques for fluorescence microscopy. *Acta Histochem Cytochem* **40**(5): 131-137.

SUZUKI, T., MIWA, K., ISHIKAWA, K., YAMADA, H., AIBA, H. and MIZUNO, T. (2001). The Arabidopsis sensor His-kinase, AHk4, can respond to cytokinins. *Plant Cell Physiol* **42**(2): 107-113.

SWEERE, U., EICHENBERG, K., LOHRMANN, J., MIRA-RODADO, V., BAURLE, I., KUDLA, J., NAGY, F., SCHAFER, E.*, et al.* (2001). Interaction of the response regulator ARR4 with phytochrome B in modulating red light signaling. *Science* **294**(5544): 1108-1111.

TANAKA, M., TAKEI, K., KOJIMA, M., SAKAKIBARA, H. and MORI, H. (2006). Auxin controls local cytokinin biosynthesis in the nodal stem in apical dominance. *Plant J* **45**(6): 1028-1036.

TANG, W., KIM, T.W., OSES-PRIETO, J.A., SUN, Y., DENG, Z., ZHU, S., WANG, R., BURLINGAME, A.L.*, et al.* (2008). BSKs mediate signal transduction from the receptor kinase BRI1 in Arabidopsis. *Science* **321**(5888): 557-560.

TO, J.P., DERUERE, J., MAXWELL, B.B., MORRIS, V.F., HUTCHISON, C.E., FERREIRA, F.J., SCHALLER, G.E. and KIEBER, J.J. (2007). Cytokinin regulates type-A Arabidopsis Response Regulator activity and protein stability via two-component phosphorelay. *Plant Cell* **19**(12): 3901-3914.

TO, J.P., HABERER, G., FERREIRA, F.J., DERUERE, J., MASON, M.G., SCHALLER, G.E., ALONSO, J.M., ECKER, J.R.*, et al.* (2004). Type-A Arabidopsis response regulators are partially redundant negative regulators of cytokinin signaling. *Plant Cell* **16**(3): 658-671.

TO, J.P. and KIEBER, J.J. (2008). Cytokinin signaling: two-components and more. *Trends Plant Sci* **13**(2): 85-92.

TRAN, L.S., SHINOZAKI, K. and YAMAGUCHI-SHINOZAKI, K. (2010). Role of cytokinin responsive two-component system in ABA and osmotic stress signalings. *Plant Signal Behav* **5**(2): 148-150.

TRAN, L.S., URAO, T., QIN, F., MARUYAMA, K., KAKIMOTO, T., SHINOZAKI, K. and YAMAGUCHI-SHINOZAKI, K. (2007). Functional analysis of AHK1/ATHK1 and cytokinin receptor histidine

kinases in response to abscisic acid, drought, and salt stress in Arabidopsis. *PNAS* **104**(51): 20623-20628.

UEGUCHI, C., SATO, S., KATO, T. and TABATA, S. (2001). The AHK4 gene involved in the cytokinin-signaling pathway as a direct receptor molecule in *Arabidopsis thaliana*. *Plant Cell Physiol* **42**(7): 751-755.

URAO, T., YAKUBOV, B., SATOH, R., YAMAGUCHI-SHINOZAKI, K., SEKI, M., HIRAYAMA, T. and SHINOZAKI, K. (1999). A transmembrane hybrid-type histidine kinase in Arabidopsis functions as an osmosensor. *Plant Cell* **11**(9): 1743-1754.

VARAGONA, M.J., SCHMIDT, R.J. and RAIKHEL, N.V. (1992). Nuclear localization signal(s) required for nuclear targeting of the maize regulatory protein Opaque-2. *Plant Cell* **4**(10): 1213-1227.

VERT, G. and CHORY, J. (2006). Downstream nuclear events in brassinosteroid signalling. *Nature* **441**(7089): 96-100.

WANG, X. and CHORY, J. (2006). Brassinosteroids regulate dissociation of BKI1, a negative regulator of BRI1 signaling, from the plasma membrane. *Science* **313**(5790): 1118-1122.

WANG, X., GOSHE, M.B., SODERBLOM, E.J., PHINNEY, B.S., KUCHAR, J.A., LI, J., ASAMI, T., YOSHIDA, S.*, et al.* (2005). Identification and functional analysis of in vivo phosphorylation sites of the Arabidopsis BRASSINOSTEROID-INSENSITIVE1 receptor kinase. *Plant Cell* **17**(6): 1685-1703.

WANG, X., KOTA, U., HE, K., BLACKBURN, K., LI, J., GOSHE, M.B., HUBER, S.C. and CLOUSE, S.D. (2008). Sequential transphosphorylation of the BRI1/BAK1 receptor kinase complex impacts early events in brassinosteroid signaling. *Dev Cell* **15**(2): 220-235.

WANG, Z.Y., NAKANO, T., GENDRON, J., HE, J., CHEN, M., VAFEADOS, D., YANG, Y., FUJIOKA, S.*, et al.* (2002). Nuclear-localized BZR1 mediates brassinosteroid-induced growth and feedback suppression of brassinosteroid biosynthesis. *Dev Cell* **2**(4): 505-513.

WERNER, T., MOTYKA, V., LAUCOU, V., SMETS, R., VAN ONCKELEN, H. and SCHMULLING, T. (2003). Cytokinin-deficient transgenic Arabidopsis plants show multiple developmental alterations indicating opposite functions of cytokinins in the regulation of shoot and root meristem activity. *Plant Cell* **15**(11): 2532-2550.

WERNER, T. and SCHMÜLLING, T. (2009). Cytokinin action in plant development. *Curr Opin Plant Biol* **12**(5): 527-538.

WOHLBACH, D.J., QUIRINO, B.F. and SUSSMAN, M.R. (2008). Analysis of the Arabidopsis histidine kinase ATHK1 reveals a connection between vegetative osmotic stress sensing and seed maturation. *Plant Cell* **20**(4): 1101-1117.

WORMIT, A., TRAUB, M., FLORCHINGER, M., NEUHAUS, H.E. and MOHLMANN, T. (2004). Characterization of three novel members of the *Arabidopsis thaliana* equilibrative nucleoside transporter (ENT) family. *Biochem J* **383**(Pt 1): 19-26.

WULFETANGE, K., LOMIN, S.N., ROMANOV, G.A., STOLZ, A., HEYL, A. and SCHMULLING, T. (2011a). The cytokinin receptors of Arabidopsis are located mainly to the endoplasmic reticulum. *Plant physiology* **156**(4): 1808-1818.

WULFETANGE, K., SAENGER, W., SCHMÜLLING, T. and HEYL, A. (2011b). E. coli-based cell-free expression, purification and characterization of the membrane-bound ligand-binding CHASE-TM domain of the cytokinin receptor CRE1/AHK4 of *Arabidopsis thaliana*. *Mol Biotech* **47**(3): 211-219.

WURTELE, M., JELICH-OTTMANN, C., WITTINGHOFER, A. and OECKING, C. (2003). Structural view of a fungal toxin acting on a 14-3-3 regulatory complex. *EMBO J* **22**(5): 987-994.

YAMADA, H., SUZUKI, T., TERADA, K., TAKEI, K., ISHIKAWA, K., MIWA, K., YAMASHINO, T. and MIZUNO, T. (2001). The Arabidopsis AHK4 histidine kinase is a cytokinin-binding receptor that transduces cytokinin signals across the membrane. *Plant Cell Physiol* **42**(9): 1017-1023.

YANG, C.J., ZHANG, C., LU, Y.N., JIN, J.Q. and WANG, X.L. (2011). The mechanisms of brassinosteroids' action: from signal transduction to plant development. *Mol Plant* **4**(4): 588-600.

YIN, Y., VAFEADOS, D., TAO, Y., YOSHIDA, S., ASAMI, T. and CHORY, J. (2005). A new class of transcription factors mediates brassinosteroid-regulated gene expression in Arabidopsis. *Cell* **120**(2): 249-259.

YIN, Y., WANG, Z.Y., MORA-GARCIA, S., LI, J., YOSHIDA, S., ASAMI, T. and CHORY, J. (2002). BES1 accumulates in the nucleus in response to brassinosteroids to regulate gene expression and promote stem elongation. *Cell* **109**(2): 181-191.

ZHANG, J., SHAO, F., LI, Y., CUI, H., CHEN, L., LI, H., ZOU, Y., LONG, C.*, et al.* (2007). A Pseudomonas syringae effector inactivates MAPKs to suppress PAMP-induced immunity in plants. *Cell Host Microbe* **1**(3): 175-185.

ZHANG, X., ZHANG, L., DONG, F., GAO, J., GALBRAITH, D.W. and SONG, C.P. (2001). Hydrogen peroxide is involved in abscisic acid-induced stomatal closure in *Vicia faba*. *Plant Physiol* **126**(4): 1438-1448.

ZHANG, Z., RAMIREZ, J., REBOUTIER, D., BRAULT, M., TROUVERIE, J., PENNARUN, A.M., AMIAR, Z., BILIGUI, B.*, et al.* (2005). Brassinosteroids regulate plasma membrane anion channels in addition to proton pumps during expansion of *Arabidopsis thaliana* cells. *Plant Cell Physiol* **46**(9): 1494-1504.

ZHAO, J., PENG, P., SCHMITZ, R.J., DECKER, A.D., TAX, F.E. and LI, J. (2002). Two putative BIN2 substrates are nuclear components of brassinosteroid signaling. *Plant Physiol* **130**(3): 1221-1229.

ZHAO, Z., ANDERSEN, S.U., LJUNG, K., DOLEZAL, K., MIOTK, A., SCHULTHEISS, S.J. and LOHMANN, J.U. (2010). Hormonal control of the shoot stem-cell niche. *Nature* **465**(7301): 1089-1092.

ZHENG, B., DENG, Y., MU, J., JI, Z., XIANG, T., NIU, Q.-W., CHUA, N.-H. and ZUO, J. (2006). Cytokinin affects circadian-clock oscillation in a phytochrome B- and Arabidopsis response regulator 4-dependent manner. *Physiol Plant* **127**(2): 277-292.

ZIPFEL, C., KUNZE, G., CHINCHILLA, D., CANIARD, A., JONES, J.D., BOLLER, T. and FELIX, G. (2006). Perception of the bacterial PAMP EF-Tu by the receptor EFR restricts Agrobacterium-mediated transformation. *Cell* **125**(4): 749-760.

DANKE

Hier möchte ich die Gelegenheit nutzen, allen zu danken, die direkt oder indirekt zum Gelingen meiner Doktorarbeit beigetragen haben.

Mein besonderer Dank gilt **KLAUS HARTER**, in dessen Arbeitsgruppe ich meine Doktorarbeit durchführen konnte und der, im Gegensatz zu mir, immer daran geglaubt hat, dass es am Ende doch noch was wird mit dem „Dr". Danke für deine Unterstützung, deine unkomplizierte Art und deinen Optimismus!

Bei **CLAUDIA OECKING** möchte ich mich für die Erstellung des zweiten Gutachtens bedanken.

Danke auch an **VIRTUDES MIRA-RODADO** für die Betreuung der Doktorarbeit und die Korrektur der schriftlichen Fassung. Danke Virtudes, dass du mir deinen Hiwi vererbt hast!

Als nächstes wäre deshalb mein Hiwi, Lieblingsdiplomand und Laborbankkollege **MICHAEL HEUNEMANN** zu nennen, der durch seine Arbeit in Labor 226 sehr zum Gelingen meiner Doktorarbeit beigetragen hat. Danke für alles im Labor, die Abende in der Kletterhalle und die Wochenenden am Fels!

Ein großes Dankeschön geht außerdem an **KATHARINA CAESAR**, die – obwohl nicht mehr am ZMBP – meine Doktorarbeit Korrektur gelesen hat. Danke auch für die tolle gemeinsame Zeit in Labor 226 und für seelische und moralische Unterstützung in allen Lebenslagen. DANKE KATHA!

Vielen Dank auch an **ANNE MOHRHOLZ** für die nervliche Unterstützung beim Formatieren und dafür, dass ich ab und zu an ihrem Rechner mit dem großen Bildschirm arbeiten durfte.

Ein besonderer Dank gilt auch dem **GEWÄCHSHAUSTEAM**, das sich immer sehr fürsorglich um meine Unmengen an Pflanzen gekümmert hat. Der manchmal fast tägliche Gang ins Gewächshaus war immer eine willkommene Abwechslung! Danke **SOFIA** für die netten Schwätzchen!

Danke auch an alle aktuellen und ehemaligen Laborkollegen, die bei Fragen und Problemen immer für mich da waren und sind und mit denen ich auch viele schöne Momente außerhalb von Morgenstelle 1 verbracht habe: **ACHIM HAHN**, **CHRISTOPHER GREFEN**, **JAKUB HORAK**, **MANIKANDAN VEERABAGU**, **MELANIE KEINATH**, **PETER HUPPENBERGER**, und **ULI BLOSS**.

Vielen Dank **ANJA**, **BETTINA** und **SABINE** für die vielen leckeren Mittagessen und gemeinsamen Mittagspausen!

Zum Schluss möchte ich noch von Herzen meiner **FAMILIE** für ihre Unterstützung und ihr Interesse an meiner Arbeit bedanken, obwohl diese für Nicht-Biologen doch recht kompliziert erscheinen mag. Danke, dass ihr immer für mich da seid!

Und ganz zum Schluss: Danke lieber **FLO** für dich und alles und überhaupt und irgendwie ist hier zu wenig Platz dafür!

…und hoffentlich habe ich niemanden vergessen!

PUBLIKATIONEN UND MANUSKRIPTE

Caesar, K., Thamm, A. M. K., Witthöft, J., Elgass, K., Huppenberger, P., Grefen, C., Horák, J., Harter, K. (2011) Evidence for the Localization of the *Arabidopsis* Cytokinin Receptors AHK3 and AHK4 at the Endoplasmic Reticulum. *Journal of Experimental Botany*. DOI:10.1093/jxb/err238.

Caesar, K., Elgass, K., Chen, Z., Huppenberger, P., Witthöft, J., Schleifenbaum, F., Blatt, M. R., Oecking, C., Harter, K. (2011) A fast brassinolide-regulated response pathway in the plasma membrane of *Arabidopsis thaliana*. *The Plant Journal* 66, 528-540. DOI: 10.1111/j.1365-313X.2011.04510.x.

Witthöft, J., Caesar, K., Elgass, K., Huppenberger, P., Kilian, J., Schleifenbaum, F., Oecking, C., Harter, K. (2011) The activation of the *Arabidopsis* P-ATPase 1 by the brassinosteroid receptor BRI1 is independent of threonine 948 phosphorylation. *Plant Signaling & Behavior* 6, 1-4.

Witthöft, J. and Harter, K. (2011) Latest news on *Arabidopsis* brassinosteroid perception and signaling. *Front. Plant Sci.* 2:58. doi: 10.3389/fpls.2011.00058.

Heunemann, M., Mira-Rodado, V., Harter, K., Witthöft, J. (2011) Nuclear localization signals in A-type response regulators. In Preparation.

Desikan, R., Horák, J., Chaban, C., Mira-Rodado, V., Witthöft, J., Elgass, K., Grefen, C., Cheung, M.-K., Meixner, A. J., Hooley, R., Neill, S. J., Hancock, J. T., Harter, K. (2008) The Histidine Kinase AHK5 Integrates Endogenous and Environmental Signals in *Arabidopsis* Guard Cells. *PLoS One* 3, e2491.

Mira-Rodado, V., Veerabagu, M., Witthöft, J., Teply, J., Harter, K., Desikan, R. (2011) Identification of two-component system elements downstream of AHK5 in the stomatal closure response. In Revision.

Journal of Experimental Botany, Page 1 of 10
doi:10.1093/jxb/err238
This paper is available online free of all access charges (see http://jxb.oxfordjournals.org/open_access.html for further details)

Journal of Experimental Botany
www.jxb.oxfordjournals.org

RESEARCH PAPER

Evidence for the localization of the *Arabidopsis* cytokinin receptors AHK3 and AHK4 in the endoplasmic reticulum

Katharina Caesar[1,*], Antje M. K. Thamm[1,*], Janika Witthöft[1,*], Kirstin Elgass[1], Peter Huppenberger[1], Christopher Grefen[2], Jakub Horak[3] and Klaus Harter[1,†]

[1] Center for Plant Molecular Biology, Department of Plant Physiology, University of Tübingen, Auf der Morgenstelle 1, D-72076 Tübingen, Germany
[2] Institute of Molecular Cell and Systems Biology, University of Glasgow, Glasgow G12 8QQ, UK
[3] Faculty of Science, Masaryk University, Kamenice 5, 625 00 Brno, Czech Republic

* These authors contributed equally to this work.
† To whom correspondence should be addressed. E-mail: klaus.harter@zmbp.uni-tuebingen.de

Received 21 December 2010; Revised 8 July 2011; Accepted 12 July 2011

Abstract

Cytokinins are hormones that are involved in various processes of plant growth and development. The model of cytokinin signalling starts with hormone perception through membrane-localized histidine kinase receptors. Although the biochemical properties and functions of these receptors have been extensively studied, there is no solid proof of their subcellular localization. Here, cell biological and biochemical evidence for the localization of functional fluorophor-tagged fusions of *Arabidopsis* histidine kinase 3 (AHK3) and 4 (AHK4), members of the cytokinin receptor family, in the endoplasmic reticulum (ER) is provided. Furthermore, membrane-bound AHK3 interacts with AHK4 *in vivo*. The ER localization and putative function of cytokinin receptors from the ER have major impacts on the concept of cytokinin perception and signalling, and hormonal cross-talk in plants.

Key words: AHK3, cytokinin perception, endoplasmic reticulum, FIDSAM.

Introduction

Cytokinins, a class of adenine-derived plant hormones, have been implicated in almost every aspect of plant growth and development, including root and shoot growth, vasculature differentiation, photomorphogenesis, senescence, fertility, and seed development (Muller and Sheen, 2007*a*; Werner and Schmulling, 2009) as well as in responses to cold and osmotic stress (Tran *et al.*, 2007; Jeon *et al.*, 2010). It is well established that cytokinin perception and signalling is mediated by a multistep two-component circuitry. In *Arabidopsis thaliana* three transmembrane histidine kinases, namely AHK2, AHK3, and AHK4, serve as cytokinin receptors (Inoue *et al.*, 2001; Suzuki *et al.*, 2001; Ueguchi *et al.*, 2001). Cytokinin binding to their CHASE domain is proposed to initiate autophosphorylation of the receptors at a conserved histidine residue in the transmitter domain (Pas *et al.*, 2004; Muller and Sheen, 2007*b*). The phosphoryl group is then transferred to a conserved aspartate residue in the receptor's receiver domain. Histidine phosphotransfer proteins (AHPs) finally transmit the signal to response regulators (ARRs), which then regulate the cellular responses (Muller and Sheen, 2007*b*; Werner and Schmulling, 2009; Kieber and Schaller, 2010).

Although the cytokinin receptors have been extensively studied regarding their specific functions, biochemical properties, and expression patterns (Higuchi *et al.*, 2004; Nishimura *et al.*, 2004; Riefler *et al.*, 2006; Romanov *et al.*, 2006), their subcellular localization and molecular function are still not fully determined. It has been assumed that they reside in the plasma membrane, and a green fluorescent protein (GFP) fusion of AHK3 appears to localize to the plasma membrane of protoplasts (Kim *et al.*, 2006). However, further attempts to ascertain this localization led to the observation that they show a more diverse localization pattern (Dortay *et al.*, 2008).

In this report, cell biological and biochemical evidence for the localization of functional fluorescent protein fusions of AHK3—a representative of the cytokinin receptor family—in the endoplasmic reticulum (ER) is provided. This localization is detected not only in transiently transformed tobacco (*Nicotiana benthamiana*) and *Arabidopsis* cells but also in stably transgenic *Arabidopsis* plants. The present observation entails a reconsideration of the current model of cytokinin signal perception and, as other hormone receptors are also located in the ER, opens new perspectives for hormonal cross-talk at this cellular compartment in plant cells.

Materials and methods

Construction of cDNA fusions

To generate the fusion proteins, attB sites were added via PCR-mediated ligation to the coding regions of *AHK1* (AT2G17820), *AHK3* (AT1G27320), *AHK4* (AT2G01830), *ERS1* (AT2G40940), and *NHL3* (AT5G06320) with or without a STOP codon and recombined into pDONR™201 according to the manufacturer's protocol (Invitrogen). The cDNA was then transferred via LR reaction (Invitrogen) into the destination vectors pH7WGF2, pH7FWG2, or pB7WGR2 (Karimi *et al.*, 2002) and pABindmCherry (Bleckmann *et al.*, 2010).

For constructs under the control of the *ubiquitin 10* (*UBQ10*) promoter, a gateway cassette (reading frame A) was inserted into the vectors pUGT1kan+ and pUGT2kan+ (Karin Schumacher, unpublished) at the *Sma*I site in the multiple cloning site. The *AHK3* coding sequence was then inserted in the destination vectors by LR reaction.

For the fusion construct with internal GFP (*AHK3intGFP*), linker sequences (coding for GGGGS/T) were added via PCR to the coding sequence of GFP using the primers GFP-BcuI-S and GFP-BcuI-A (Supplementary Table S1 available at *JXB* online). For ligation into the AHK3 entry clone an appropriate restriction site was produced via site-directed mutagenesis in the AHK3 coding sequence at position 123 (corresponding to amino acid 41) where the linker–GFP–linker sequence was introduced. The *AHK3intGFP* cDNA was then recombined into pMDC32 (Curtis and Grossniklaus, 2003) by LR reaction. For mating-based split-ubiquitin system (mbSUS) assay, the *AHK4* cDNA was transferred

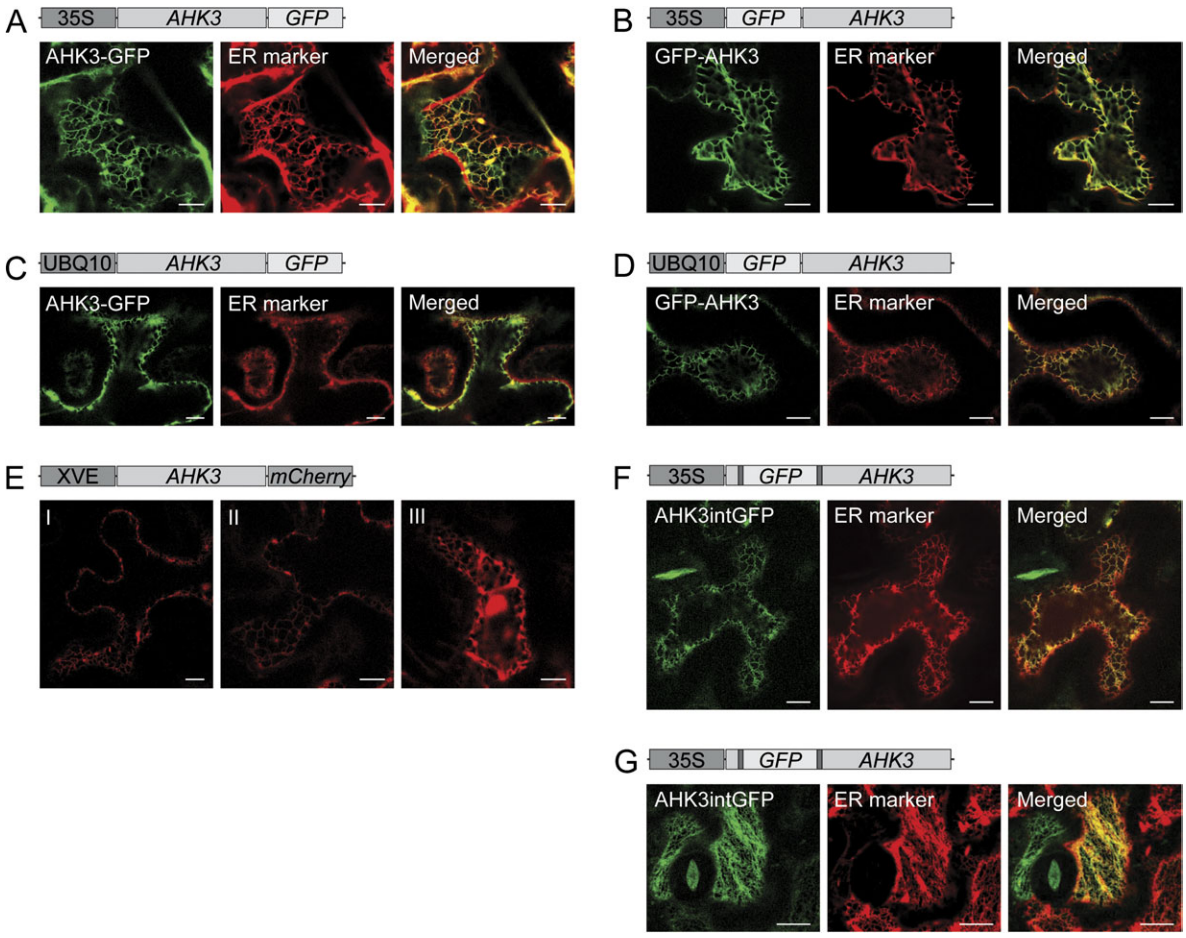

Fig. 1. The *Arabidopsis* cytokinin receptor AHK3 localizes to the ER in transiently transformed tobacco leaf cells and *Arabidopsis* seedlings. (A–D) and (F) Confocal images of transiently transformed tobacco epidermal leaf cells co-expressing the indicated AHK3 fusion protein under the control of the *35S* promoter or the *UBQ10* promoter with the ER marker ER-rk CD3-959. (E) Confocal images of transiently transformed tobacco epidermal leaf cells expressing an AHK3–mCherry fusion protein under the control of the estradiol-inducible promoter (XVE). Images were recorded 2 h (I), 4 h (II), and 24 h (III) after application of 20 μM β-estradiol. Images (I) and (II) were recorded at the highest sensitivity settings of the microscope at which the mCherry fluorescence was just detectable. (G) Confocal images of transiently transformed *Arabidopsis* cotyledon cells co-expressing the indicated AHK3 fusion protein with the ER marker ER-rk CD3-959. Bars represent 10 μm.

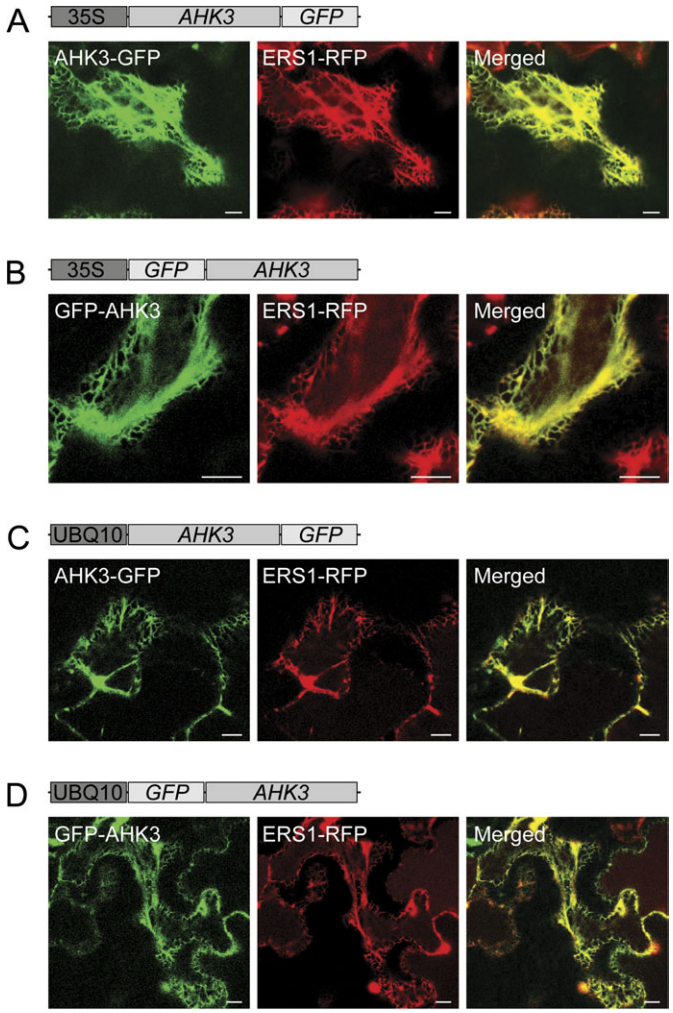

Fig. 2. AHK3–GFP and GFP–AHK3 fusion proteins co-localize with ERS1–RFP. (A–D) Confocal images of transiently transformed tobacco epidermal leaf cells co-expressing the indicated AHK3 fusion protein under the control of the *35S* or the *UBQ10* promoter and an RFP fusion of the ethylene receptor ERS1 (ERS1–RFP). Bars represent 10 μm.

by LR reaction to pMetYC-Dest and the *AHK3* and *ERS1* cDNAs to pXNubA22 (Grefen *et al.*, 2009).

Transient gene expression in Nicotiana benthamiana *leaves and* Arabidopsis *seedlings*

Transient transformations of *N. benthamiana* leaves with the *Agrobacterium tumefaciens* strain GV3101 pMP90 containing the expression constructs were carried out as described in Schutze *et al.* (2009). The transformed leaves were assayed for fluorescence by confocal laser scanning microscopy (CLSM) 2–3 d post-infiltration. The transgene expression from the estradiol-inducible promoter was induced 2–3 d after infiltration with 20 μM β-estradiol supplemented with 0.1% Tween-20. For transient expression in *Arabidopsis* seedlings, the *Agrobacterium* strains containing the fusion constructs and the marker constructs used were grown as described (Marion *et al.*, 2008), prior to infiltration diluted in 5% sucrose, 200 μM acetosyringone to an OD_{600} of 2.0, and mixed 1:1. 3–4 d old *Arabidopsis efr1* seedlings (Zipfel *et al.*, 2006) were transformed via vacuum infiltration as described by Marion *et al.* (2008) and the seedlings were examined for fluorescence 3 d post-infiltration.

CLSM and fluorescence intensity decay shape analysis microscopy (FIDSAM)

CLSM and FIDSAM as well as the used spectromicroscopic systems and measurement protocols have been described previously (Elgass *et al.*, 2009; Schleifenbaum *et al.*, 2010).

Construction of transgenic Arabidopsis *lines*

The transgenes were transformed into *Arabidopsis ahk2-2ahk3-3* plants (*ahk2ahk3*, Higuchi *et al.*, 2004) via the floral dip method and selected by phenotype (complemented dwarf phenotype of the *ahk2ahk3* mutant background). Twenty independent *ahk2-2ahk3-3* lines complemented by *AHK3-GFP* and 10 independent lines complemented by *GFP-AHK3* were isolated. After verification of the transgene integration, the lines were analysed for the GFP fluorescence signal using CLSM and FIDSAM. The line with the most intense GFP signal was used for imaging and endogylcosidase H (EndoH) assays.

EndoH assay

The EndoH assay was performed according to the manufacturer's manual (New England BioLabs) by using crude protein extracts of transiently transformed tobacco or *Arabidopsis* leaves. The proteins were analysed by SDS–PAGE and western blot using a GFP antibody.

Root growth and yeast mbSUS assays

For the root elongation assay, seedlings were grown vertically on 0.5× MS plates supplemented with different concentrations of kinetin. The root length was measured 6 d post-germination. The yeast mbSUS assays using *AHK4-Cub-PLV* and the *NubA* fusions of *AHK3* and *ERS1* as constructs were carried out as described previously (Grefen *et al.*, 2009; Caesar *et al.*, 2011).

Results and Discussion

FP fusions of AHK3 localize to the ER

In order to examine the subcellular localization of AHK3, C- and N-terminal GFP fusions of the receptor were transiently expressed in leaf epidermal cells of *N. benthamiana* and in cotyledon cells of *Arabidopsis* seedlings under the control of either the 35S *Cauliflower mosaic virus* (*35S*) or the *Arabidopsis UBQ10* promoter. Both AHK3–GFP and GFP–AHK3 showed an ER-like localization pattern in tobacco and *Arabidopsis* independent of the promoter used (Fig. 1A–D, Supplementary Fig. S1 at *JXB* online). The identity of the endomembrane system as ER was verified by the co-localization of the GFP fusions of AHK3 with the mCherry-tagged ER marker ER-rk CD3-959 (Nelson *et al.*, 2007; Fig. 1A–D, Supplementary Fig. S1B, C). In addition, there was a co-localization of the GFP fusion proteins of AHK3 with the ER-localized red fluorescent protein (RFP) fusion of the ethylene receptor ERS1 (Grefen *et al.*, 2008; Fig. 2). In contrast, no co-localization of these AHK3 fusion proteins was found with the mCherry-tagged Golgi marker G-rk CD2-967 (Nelson *et al.*, 2007; Supplementary Fig. S2) and the RFP fusion of the plasma membrane protein NHL3 (Varet *et al.*, 2003; Fig. 3). Furthermore, the GFP fusion of the plasma membrane-bound AHK1, which is a positive regulator of drought and salt stress response and functions as an osmosensor in yeast (Urao *et al.*, 1999; Tran *et al.*, 2007;

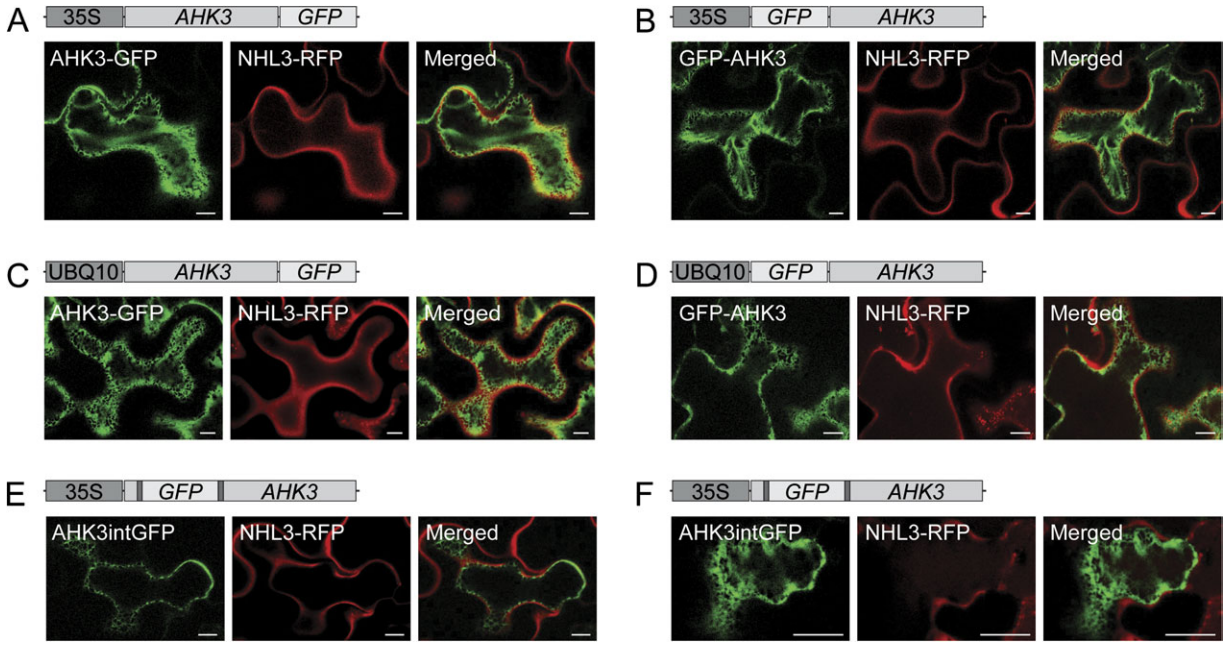

Fig. 3. AHK3–GFP and GFP–AHK3 fusion proteins do not co-localize with the plasma membrane-localized fusion protein NHL3–RFP. (A–E) Confocal images of transiently transformed tobacco epidermal leaf cells co-expressing the indicated AHK3 fusion protein under the control of the *35S* promoter or the *UBQ10* promoter and the plasma membrane-localized fusion protein NHL3–RFP. (F) Confocal images of transiently transformed *Arabidopsis* cotyledon cells co-expressing the indicated AHK3 fusion protein and the plasmalemma-localized fusion protein NHL3–RFP. Bars represent 10 μm.

Wohlbach *et al.*, 2008), also did not co-localize with an mCherry fusion of AHK3 (Fig. 4). The yellow colour, partially visible in the merged images of Supplementary Fig. S2D, and Figs 3A, C, 4, results from the very strong GFP signal in this area and the physically restricted resolution of light microscopy below Abbe's diffraction limit (250 nm). However, the magnified images of these yellow domains showed an incomplete overlap of the GFP and RFP or mCherry fluorescence (Fig. 4; Supplementary Fig. S3), indicating that the fusion proteins localize to different membrane compartments.

It has been reported that strong expression of fusion proteins under the control of promoters such as *35S* or *UBQ10* might lead to mislocalization artefacts (Bleckmann *et al.*, 2010). A C-terminal mCherry fusion of AHK3 (AHK3–mCherry) expressed from an estradiol-controlled promoter system was therefore used to trigger the expression level of the histidine kinase (Bleckmann *et al.*, 2010). After transformation of the construct into *N. benthamiana* leaves, the expression was induced by brushing the leaves with β-estradiol. AHK3–mCherry fluorescence was detectable 2 h after β-estradiol application at the earliest (Fig. 1E). Already at this early time point the AHK3–mCherry fluorescence displayed a net-like ER localization pattern, which did not change within the next 22 h (Fig. 1E). The localization of β-estradiol-induced AHK3–mCherry was never observed in the plasma membrane.

The amino acid sequence of AHK3 contains potential signals for the secretory pathway and ER export, respectively [Fig. 6A; iPsort Prediction, http://ipsort.hgc.jp/ (Bendtsen *et al.*, 2004); YLoc Prediction, www.multiloc.org/YLoc (Hanton *et al.*, 2005; Langhans *et al.*, 2008; Briesemeister *et al.*, 2010)]. To exclude a possible mislocalization of the fusion proteins due to masking of potential sorting signals, a construct was generated where GFP is inserted between the first and the second predicted transmembrane domain of AHK3 (AHK3intGFP; see Fig. 6A for the details of the insertion site). AHK3intGFP showed the identical ER localization pattern to AHK3–GFP and GFP–AHK3 when transiently expressed in tobacco leaves as well as in *Arabidopsis* seedlings, and co-localized with the mCherry-tagged ER marker (Fig. 1F, G) but not with the plasma membrane marker NHL3–RFP (Fig. 3E, F).

Signal-induced translocation of receptors to the plasma membrane is reported for animal systems (Shuster *et al.*, 1999; Song *et al.*, 2004). Therefore, assays were carried out to determine whether the application of kinetin, a synthetic cytokinin, has an influence on the subcellular localization of the N- and C-terminal GFP fusions of AHK3. However, 4 h of kinetin treatment did not alter the ER localization of AHK3–GFP and GFP–AHK3 (Supplementary Fig. S4 at *JXB* online).

Furthermore, it was tested whether the intracellular location of AHK3 changed when it was co-expressed with an RFP fusion of its sister receptor, AHK4. As shown in Fig. 5A, both fusion proteins co-localized in the ER. To determine whether AHK3 is able to interact with AHK4 in the membrane, *in vivo* interaction studies were performed using the yeast mbSUS (Grefen *et al.*, 2009). The mbSUS experiments revealed that AHK3 not only forms homo-oligomers (data not shown) but also interacts with AHK4 *in vivo* (Fig. 5B). No interaction was observed with ERS1 (Fig. 5B), which also localized to the ER (Fig. 2; Grefen *et al.*, 2008). These

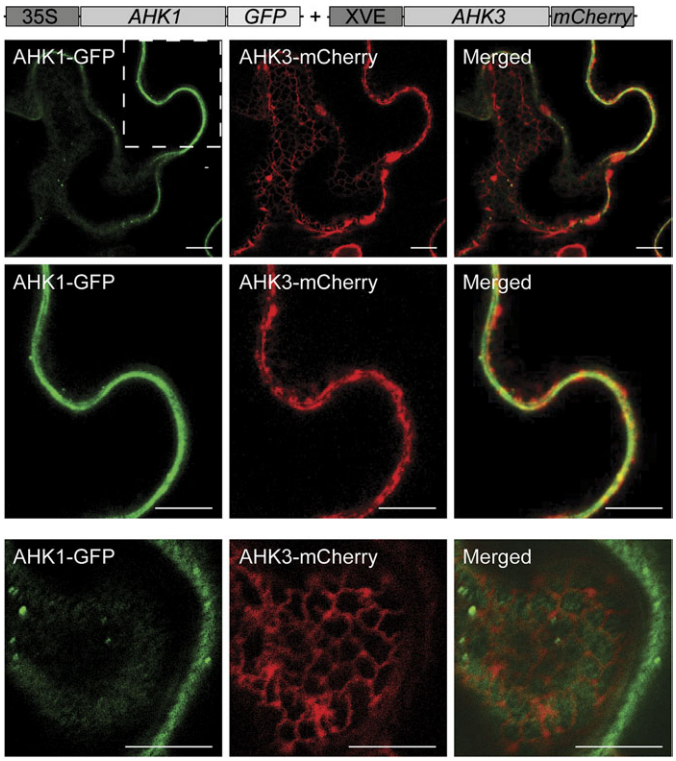

Fig. 4. AHK3–mCherry does not co-localize with a GFP fusion of the plasma membrane-bound *Arabidopsis* histidine kinase 1 (AHK1–GFP). Confocal images of different magnification of transiently transformed tobacco epidermal leaf cells co-expressing AHK3–mCherry under the control of the estradiol-inducible promoter (XVE) and AHK1–GFP under control of the *35S* promoter. The image series of the second row represents a magnified detail of the images of the first row. The image series of the third row derives from an independent cell. Images were recorded 4 h after application of 20 μM β-estradiol. Bars represent 10 μm.

data suggest that the cytokinin receptors are able specifically to homo- and heterodimerize in the ER and that their interaction has no influence on their subcellular localization.

In conclusion, all tested fluorescent protein fusions of AHK3—no matter whether GFP is tagged to the C-terminus, N-terminus, or internally—show an ER localization. A mislocalization of the fusion proteins due to overexpression or masking of potential sorting signals is unlikely. Furthermore, neither cytokinin application nor the co-expression of AHK3 and 4 or their potential *in planta* interaction are capable of altering the ER localization of AHK3.

The AHK3 protein is EndoH sensitive

To substantiate the ER localization of the AHK3 fusion proteins, a biochemical survey was conducted applying an EndoH assay. EndoH is a glycosidase which cleaves asparagine-linked oligomannose and hybrid, but not complex oligosaccharides from glycoproteins (Maley *et al.*, 1989). EndoH, therefore, enables, by electrophoretic mobility shift, the differentiation of ER-localized glycoproteins from glycoproteins in the plasma membrane, whose asparagine-linked glycans are further modified in the secretory pathway and are no longer substrates for the glycolytic enzyme (Hong *et al.*, 2008). In the AHK3 amino acid sequence, five potential N-X-S/T glycosylation sites were identified; one N-terminally of and three within the CHASE domain, and one in the receiver domain close to the C-terminus (Fig. 6A, B). Therefore, a mobility shift of EndoH-treated AHK3 would be expected on condition that AHK3 is located in the ER. As controls, AHK1–GFP, which is a plasma membrane-localized protein (Fig. 4) and has nine potential N-X-S/T glycosylation sites (Fig. 6B), and ERS1–GFP, which is, like ERS1–RFP, bound to the ER (Grefen *et al.*, 2008), were used. The ERS1 single N-X-S/T site is predicted not to be glycosylated due to its C-terminal location (Fig. 6B; Gavel and von Heijne, 1990). Total crude protein extracts of tobacco leaves expressing the GFP fusion proteins were exposed to EndoH or mock treated. After SDS–PAGE and western blot using a GFP-specific antibody, the fusion proteins were analysed for changes in their electrophoretic mobility. There was no mobility shift and, thus, no EndoH sensitivity of plasma membrane-bound AHK1–GFP or of ER-bound ERS1–GFP detected, indicating that AHK1–GFP is not retained in the ER and ERS1 is not glycosylated in tobacco cells (Fig. 6C). The unaltered pattern of AHK1–GFP in particular also proves that the reaction mixture conditions *per se* have no influence on the electrophoretic mobility of the fusion proteins. In contrast, the EndoH-treated AHK3 fusion proteins showed a significant mobility shift compared with the non-treated control (Fig. 6C). Most importantly, there was no high mobility band in the non-treated AHK3 preparations.

The results of the EndoH assays thus support the cell biological observations that the GFP fusions of AHK3 localize to the ER. Furthermore, there appears to be no subfraction of AHK3 in the plasmalemma because the entire population of the cytokinin receptor carries EndoH-sensitive mannose structures typical for ER-resident glycoproteins.

AHK3–GFP and GFP–AHK3 rescue the cytokinin-insensitive phenotype of the ahk2ahk3 *receptor mutant*

To determine the functionality of the GFP fusions of AHK3, their capability to complement the dwarf and cytokinin-insensitive root growth phenotype of the *ahk2-2ahk3-3* (*ahk2ahk3*) mutant was analysed. The *ahk2-2* or the *ahk3-3* single mutants were not used for the complementation analysis as they show the wild-type phenotype (Higuchi *et al.*, 2004). Those *ahk2ahk3* plants were selected whose dwarf and cytokinin-insensitive root growth phenotypes were complemented by *UBQ10*-driven expression of *AHK3-GFP* or *GFP-AHK3* demonstrating that both fusion proteins are functional receptors (Fig. 7A–C). Next the *AHK3-GFP*-complemented transgenic line was studied for the accumulation and subcellular localization of the fusion protein using standard CLSM. Weak fluorescence signals were detected in epidermal and stomatal cotyledon cells. The fluorescence signal appeared in a net-like and discontinuous pattern as well as in the perinuclear space (Fig. 7D). This observation suggests that AHK3–GFP is predominantly localized in the ER. To

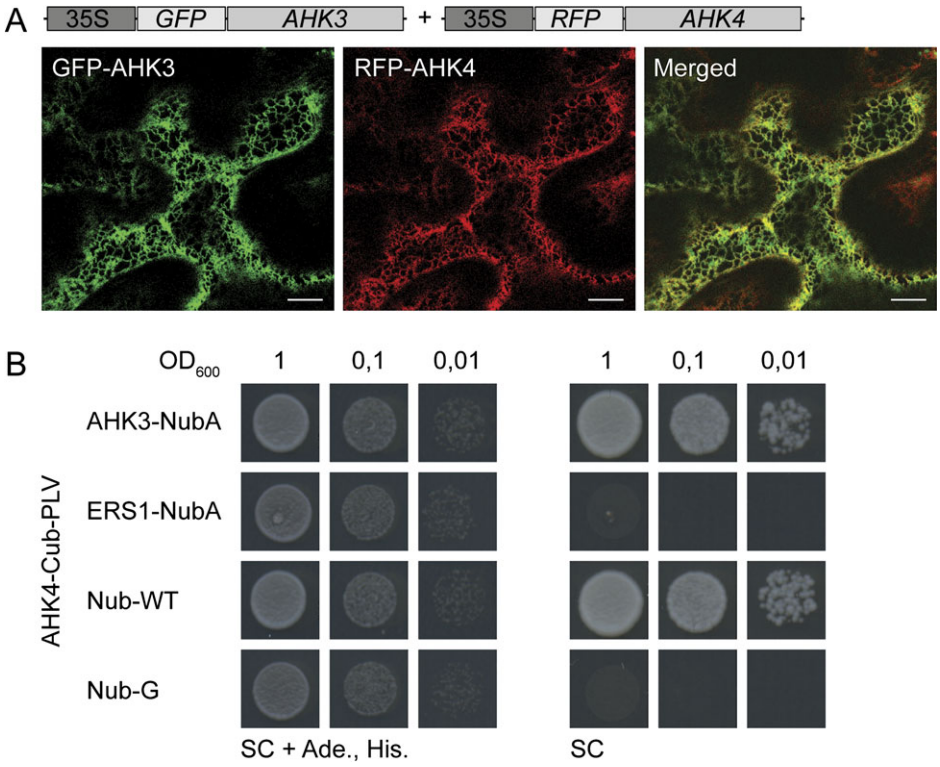

Fig. 5. The cytokinin receptor AHK4 co-localizes with AHK3 in the ER and interacts with AHK3 *in vivo* (yeast). (A) Confocal images of transiently transformed tobacco epidermal leaf cells co-expressing RFP–AHK4 and GFP–AHK3 under control of the *35S* promoter. Bars represent 10 μm. (B) Yeast mbSUS protein–protein interaction analysis. The *AHK4-Cub-PLV* construct was transformed in yeast strain THY.AP4 (MATa), and the Nub constructs of AHK3 and ERS1 were transformed in yeast strain THY.AP5 (MATα). After mating, activation of the reporter gene was determined by growth of the transformants in a dilution series (OD_{600nm} from 1 to 0.01) on SC medium (SC). The presence of the plasmid was assayed by growth on SC medium supplemented with adenine and histidine (SC+Ade., His.). Co-transformations of the AHK4–Cub-PLV fusion with NubG served as negative control and co-transformation with NubWT served as positive control.

be sure that background autofluorescence was not recorded, FIDSAM was applied. FIDSAM enhances the contrast of fluorescence images due to efficient background fluorescence repression (Schleifenbaum *et al.*, 2010). In the FIDSAM images, AHK3–GFP again became visible as a discontinuous fluorescence pattern with a net-like structure that is typical for ER-localized fusion proteins (Supplementary Fig. S5 at *JXB* online) but atypical for plasma membrane proteins (Grefen *et al.*, 2008). These data demonstrate that the observed fluorescence actually derives from the GFP of AHK3–GFP. The low accumulation of AHK3–GFP fusion protein was surprising as the *AHK3* fusion constructs were under the control of the constitutive *UBQ10* promoter, which usually provides for a high level of accumulation of the corresponding fusion protein. This suggests that the transgenic plants must keep the AHK3 protein amount at a level which is similarly low as that of wild-type *Arabidopsis*.

To substantiate the ER localization, EndoH assays were performed, using extracts from the AHK3–GFP line, the ERS1–GFP line, and the *ahk2ahk3* mutant. Again, an EndoH-caused mobility shift of the AHK3 fusion protein was observed, but not a clear shift of ERS1–GFP (Fig. 7E). Again, there was no high mobility band in the mock-treated AHK3 preparations (Fig. 7E) and no free GFP (data not shown). Thus, the observed complementation of the *ahk2ahk3* mutant phenotype was not due to post-translational cleavage of the GFP and release of non-tagged AHK3 or a translocation of an AHK3 subpopulation to the plasma membrane.

Summarizing, the results of the EndoH assay and the CLSM/FIDSAM analysis suggest that AHK3–GFP localizes to the ER not only in transiently transformed tobacco and *Arabidopsis* cells but also in transgenic plants. As AHK3–GFP complements the cytokinin-insensitive phenotype of the *ahk2ahk3* mutant and as there is no indication that a subpopulation of AHK3 targets to the plasma membrane, the receptor appears to function from the ER. However, the possibility that minuscule amounts of AHK3 are transferred to the plasma membrane, which are detectable neither by CLSM nor by western blot after EndoH treatment, cannot be entirely excluded.

Conclusion

The ER localization of AHK3 (and AHK4) has major consequences for the concept of cytokinin perception and signalling in plants. The present data indicate that the cytokinin-binding CHASE domain is not oriented to the apoplast, as previously assumed, but exposed to the ER lumen, whereas the C-terminal kinase domain, that, upon activation, transfers the phosphoryl residues to the nucleocytoplasmic histidine phosphotransfer proteins, is exposed to

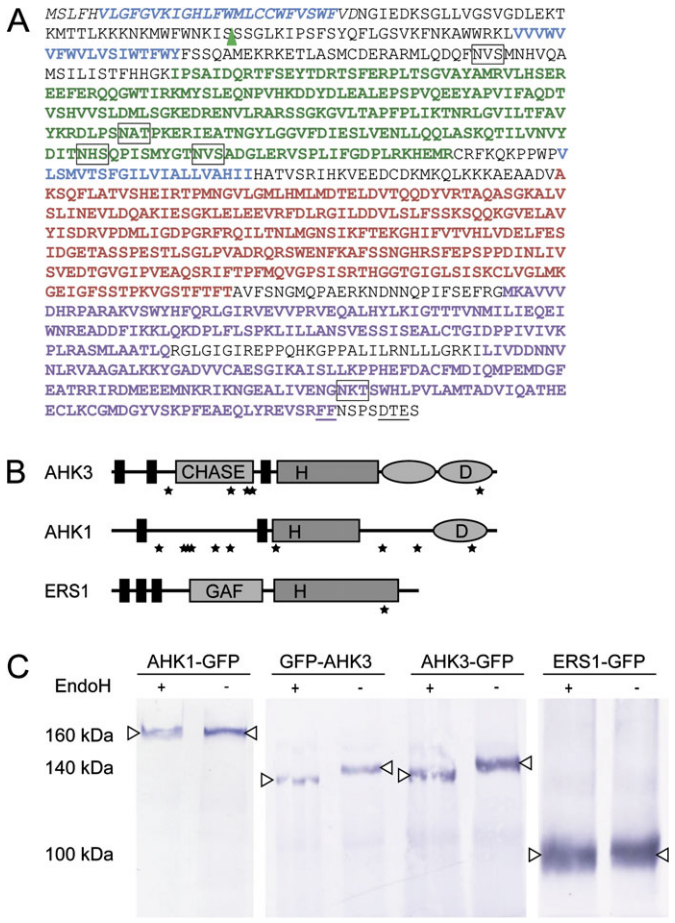

Fig. 6. The GFP fusion proteins of AHK3 show EndoH sensitivity and are glycosylated in vivo. (A) Amino acid sequence of AHK3. The transmembrane domains are shown in blue, the histidine kinase domain in red, and the pseudo receiver domain and the receiver domain in purple. N-X-S/T sequons are framed. The predicted signal peptide is italicized, and the putative ER export signals are underlined. The green triangle marks the site where GFP was inserted into AHK3intGFP. (B) Representations of AHK3, AHK1, and the ethylene receptor ERS1. Putative glycosylation sites are indicated with asterisks. (C) The electrophoretic mobility of AHK3 is endoglycosidase H (EndoH) sensitive. Equal volumes of protein extracts from transiently transformed tobacco leaves expressing the indicated fusion proteins were treated with EndoH (+) or mock treated (–), followed by western blot analysis and immunodetection using an anti-GFP antibody. The fusion proteins are indicated by arrowheads.

the cytoplasm. This topology of the receptor is in agreement with the observation that the binding of the cytokinin zeatin to AHK3 and AHK4 has a pH optimum of ~6.5 (Romanov *et al.*, 2006)—a pH found in the ER lumen (Kim *et al.*, 1998). At pH values of ~5.5—as reported for the apoplast (Li *et al.*, 2005)—the binding of zeatin to AHK3 is almost abolished (Romanov *et al.*, 2006). Thus, when the cytokinin receptors are located in the ER and expose the CHASE domain to the lumen, they bind their ligand with much higher affinity. Furthermore, although the subcellular distribution of active cytokinins and their ability to permeate the cell membrane (Laloue *et al.*, 1981) have not yet been examined in detail, many enzymes involved in cytokinin biosynthesis, such as the isopentenyl transferases (IPTs) and lonely guys (LOGs), and in catabolism, such as cytokinin oxidases (CKXs), are not only found in plastids (IPTs; Kasahara *et al.*, 2004) but also in the cytoplasm and nucleus (LOGs; Kuroha *et al.*, 2009) and other organelles such as the vacuole and the ER (CKXs; Werner *et al.*, 2003). These observations suggest intracellular mechanisms which distribute the hormone and its derivates within the cell. In addition, several plasma membrane-bound carriers have been identified which are able to transport cytokinin into the cell (Burkle *et al.*, 2003; Wormit *et al.*, 2004; Hirose *et al.*, 2005; Cedzich *et al.*, 2008) where it could be distributed further. So apparently the current model of cytokinin signal perception at the plasma membrane needs to be reconsidered.

Recent analyses showed that other hormone perception, signalling, and distribution compounds as well as hormone metabolic enzymes are also found at the ER (Friml and Jones, 2010). For instance, ethylene perception by the five ethylene receptors and their interaction with central downstream signalling elements such as constitutive triple response 1 (CTR1) and ethylene insensitive 2 (EIN2) occur at the ER (Chen *et al.*, 2002; Gao *et al.*, 2003; Grefen *et al.*, 2008; Bisson *et al.*, 2009; Bisson and Groth, 2010). Furthermore, the auxin-binding protein 1 (ABP1) and the PIN-formed 5 (PIN5) auxin efflux carrier localize to the ER (Tian *et al.*, 1995; Chen *et al.*, 2006; Mravec *et al.*, 2009), where they are discussed to be involved not only in auxin homeostasis and metabolism but also in auxin signalling (Friml and Jones, 2010). Hormonal cross-talk decisively contributes to the final physiological and developmental output of hormone action (Benkova and Hejatko, 2009). It is, therefore, intriguing to speculate that the ER might represent the intracellular site for hormonal cross-talk.

Supplementary data

Supplementary data are available at *JXB* online.

Figure S1. AHK3GFP fusion proteins localize to the ER in transiently transformed *Arabidopsis* cotyledon cells.

Figure S2. GFP fusion proteins of AHK3 do not co-localize with the Golgi marker G-rk CD3-967.

Figure S3. AHK3–GFP fusion proteins do not co-localize with the plasma membrane-localized fusion protein NHL3–RFP.

Figure S4. The ER localization of AHK3–GFP and GFP–AHK3 does not change upon cytokinin treatment.

Figure S5. AHK3–GFP fluorescence is detectable in the ER of the AHK3–GFP-expressing *Arabidopsis* line.

Table S1. Oligonucleotides used in the study.

Acknowledgements

We thank G. Felix for the *efr1* seeds, A. Kakimoto for the *ahk2-2ahk3-3* seeds, and K. Schumacher for vectors. We are also grateful to F. de-Courcy for proofreading the manuscript. This work was supported by a DFG grant to KH (HA 2146/10-1) and PhD fellowships of the University of Tübingen to KC and KE.

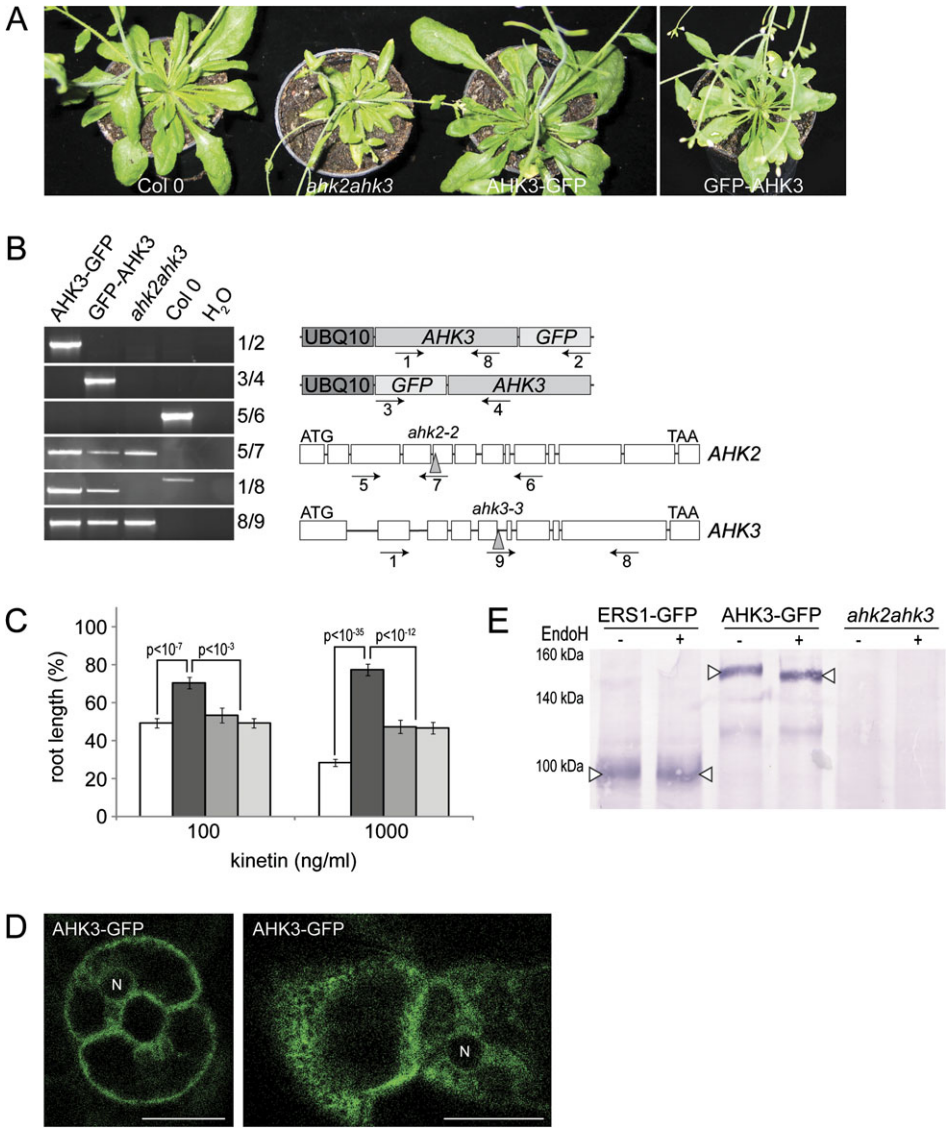

Fig. 7. The GFP fusions of AHK3 are able to complement the mutant phenotype of the *ahk2ahk3* receptor mutant and locate to the ER in the complemented lines. (A) Adult plants of the wild type (Col 0), the *ahk2ahk3* mutant, and plants expressing AHK3–GFP or GFP–AHK3 from the *UBQ10* promoter in the *ahk2ahk3* background (AHK3–GFP and GFP–AHK3). (B) Genotypic analysis of AHK3–GFP and GFP–AHK3 lines by PCR using the indicated primer pairs. (C) Inhibition of root elongation by increasing amounts of exogenously applied cytokinin (kinetin). Seedlings of the wild type (Col 0, white columns), the *ahk2ahk3* mutant (black columns), and the complemented, heterozygous AHK3–GFP and GFP–AHK3 lines (dark and light grey columns) were grown on 0.5× MS agar plates supplemented with the indicated concentrations of kinetin. Mean values (n=18; standard errors) relative to the root length of non-treated controls and P-values for statistical significance are given. (D) AHK3–GFP fluorescence is detectable in the ER of the *AHK3-GFP*-complemented *Arabidopsis* line. CLSM images of epidermis and stomatal cells from cotyledons of etiolated seedlings are shown. N indicates the nucleus. Bars represent 10 μm. (E) EndoH sensitivity of the AHK3–GFP fusion protein in the *AHK3-GFP*-complemented line. Equal amounts of protein extract from seedlings of the indicated lines were treated or not with endoglycosidase H (EndoH), followed by western blot analysis and immunodetection with an anti-GFP antibody. The fusion proteins are indicated by arrowheads.

References

Bendtsen JD, Nielsen H, von Heijne G, Brunak S. 2004. Improved prediction of signal peptides: SignalP 3.0. *Journal of Molecular Biology* **340,** 783–795.

Benkova E, Hejatko J. 2009. Hormone interactions at the root apical meristem. *Plant Molecular Biology* **69,** 383–396.

Bisson MM, Bleckmann A, Allekotte S, Groth G. 2009. EIN2, the central regulator of ethylene signalling, is localized at the ER membrane where it interacts with the ethylene receptor ETR1. *Biochemical Journal* **424,** 1–6.

Bisson MM, Groth G. 2010. New insight in ethylene signaling: autokinase activity of ETR1 modulates the interaction of receptors and EIN2. *Molecular Plant* **3,** 882–889.

Bleckmann A, Weidtkamp-Peters S, Seidel CA, Simon R. 2010. Stem cell signaling in Arabidopsis requires CRN to localize CLV2 to the plasma membrane. *Plant Physiology* **152,** 166–176.

Briesemeister S, Rahnenfuhrer J, Kohlbacher O. 2010. Going from where to why—interpretable prediction of protein subcellular localization. *Bioinformatics* **26,** 1232–1238.

Burkle L, Cedzich A, Dopke C, Stransky H, Okumoto S, Gillissen B, Kuhn C, Frommer WB. 2003. Transport of cytokinins mediated by purine transporters of the PUP family expressed in phloem, hydathodes, and pollen of Arabidopsis. *The Plant Journal* **34,** 13–26.

Caesar K, Elgass K, Chen Z, Huppenberger P, Witthöft J, Schleifenbaum F, Blatt MR, Oecking C, Harter K. 2011. A fast brassinolide-regulated response pathway in the plasma membrane of Arabidopsis thaliana. *The Plant Journal* **66,** 528–540.

Cedzich A, Stransky H, Schulz B, Frommer WB. 2008. Characterization of cytokinin and adenine transport in Arabidopsis cell cultures. *Plant Physiology* **148,** 1857–1867.

Chen JG, Wang SC, Lazarus CM, Napier RM, Jones AM. 2006. Altered expression of auxin-binding protein 1 affects cell expansion and auxin pool size in tobacco cells. *Journal of Plant Growth Regulation* **25,** 69–78.

Chen YF, Randlett MD, Findell JL, Schaller GE. 2002. Localization of the ethylene receptor ETR1 to the endoplasmic reticulum of Arabidopsis. *Journal of Biological Chemistry* **277,** 19861–19866.

Curtis MD, Grossniklaus U. 2003. A gateway cloning vector set for high-throughput functional analysis of genes in planta. *Plant Physiology* **133,** 462–469.

Dortay H, Gruhn N, Pfeifer A, Schwerdtner M, Schmulling T, Heyl A. 2008. Toward an interaction map of the two-component signaling pathway of Arabidopsis thaliana. *Journal of Proteomic Research* **7,** 3649–3660.

Elgass K, Caesar K, Schleifenbaum F, Stierhof Y-D, Meixner AJ, Harter K. 2009. Novel application of fluorescence lifetime and fluorescence microscopy enables quantitative access to subcellular dynamics in plant cells. *PLoS One* **4,** e5716.

Friml J, Jones AR. 2010. Endoplasmic reticulum: the rising compartment in auxin biology. *Plant Physiology* **154,** 458–462.

Gao Z, Chen YF, Randlett MD, Zhao XC, Findell JL, Kieber JJ, Schaller GE. 2003. Localization of the Raf-like kinase CTR1 to the endoplasmic reticulum of Arabidopsis through participation in ethylene receptor signaling complexes. *Journal of Biological Chemistry* **278,** 34725–34732.

Gavel Y, von Heijne G. 1990. Sequence differences between glycosylated and non-glycosylated Asn-X-Thr/Ser acceptor sites: implications for protein engineering. *Protein Engineering* **3,** 433–442.

Grefen C, Obrdlik P, Harter K. 2009. The determination of protein–protein interactions by the mating-based split-ubiquitin system (mbSUS). *Methods in Molecular Biology* **479,** 217–233.

Grefen C, Stadele K, Ruzicka K, Obrdlik P, Harter K, Horak J. 2008. Subcellular localization and *in vivo* interactions of the Arabidopsis thaliana ethylene receptor family members. *Molecular Plant* **1,** 308–320.

Hanton SL, Renna L, Bortolotti LE, Chatre L, Stefano G, Brandizzi F. 2005. Diacidic motifs influence the export of transmembrane proteins from the endoplasmic reticulum in plant cells. *The Plant Cell* **17,** 3081–3093.

Higuchi M, Pischke MS, Mahonen AP, *et al*. 2004. In planta functions of the Arabidopsis cytokinin receptor family. *Proceedings of the National Academy of Sciences, USA* **101,** 8821–8826.

Hirose N, Makita N, Yamaya T, Sakakibara H. 2005. Functional characterization and expression analysis of a gene, OsENT2, encoding an equilibrative nucleoside transporter in rice suggest a function in cytokinin transport. *Plant Physiology* **138,** 196–206.

Hong Z, Jin H, Tzfira T, Li J. 2008. Multiple mechanism-mediated retention of a defective brassinosteroid receptor in the endoplasmic reticulum of Arabidopsis. *The Plant Cell* **20,** 3418–3429.

Inoue T, Higuchi M, Hashimoto Y, Seki M, Kobayashi M, Kato T, Tabata S, Shinozaki K, Kakimoto T. 2001. Identification of CRE1 as a cytokinin receptor from Arabidopsis. *Nature* **409,** 1060–1063.

Jeon J, Kim NY, Kim S, *et al*. 2010. A subset of cytokinin two-component signaling system plays a role in cold temperature stress response in Arabidopsis. *Journal of Biological Chemistry* **285,** 23371–23386.

Karimi M, Inze D, Depicker A. 2002. GATEWAY vectors for Agrobacterium-mediated plant transformation. *Trends in Plant Science* **7,** 193–195.

Kasahara H, Takei K, Ueda N, Hishiyama S, Yamaya T, Kamiya Y, Yamaguchi S, Sakakibara H. 2004. Distinct isoprenoid origins of cis- and trans-zeatin biosyntheses in Arabidopsis. *Journal of Biological Chemistry* **279,** 14049–14054.

Kieber JJ, Schaller GE. 2010. The perception of cytokinin: a story 50 years in the making. *Plant Physiology* **154,** 487–492.

Kim HJ, Ryu H, Hong SH, Woo HR, Lim PO, Lee IC, Sheen J, Nam HG, Hwang I. 2006. Cytokinin-mediated control of leaf longevity by AHK3 through phosphorylation of ARR2 in Arabidopsis. *Proceedings of the National Academy of Sciences, USA* **103,** 814–819.

Kim JH, Johannes L, Goud B, Antony C, Lingwood CA, Daneman R, Grinstein S. 1998. Noninvasive measurement of the pH of the endoplasmic reticulum at rest and during calcium release. *Proceedings of the National Academy of Sciences, USA* **95,** 2997–3002.

Kuroha T, Tokunaga H, Kojima M, Ueda N, Ishida T, Nagawa S, Fukuda H, Sugimoto K, Sakakibara H. 2009. Functional analyses of LONELY GUY cytokinin-activating enzymes reveal the importance of the direct activation pathway in Arabidopsis. *The Plant Cell* **21,** 3152–3169.

Laloue M, Pethe-Terrine C, Gruen J. 1981. Uptake and metabolism of cytokinins in tobacco cells: studies in relation to the expression of their biological activities. In: Guern J, Peaud-Lenoel C, eds. *Metabolism and molecular activities of cytokinins*. Berlin: Springer, 80–96.

Langhans M, Marcote MJ, Pimpl P, Virgili-Lopez G, Robinson DG, Aniento F. 2008. *In vivo* trafficking and localization of p24 proteins in plant cells. *Traffic* **9,** 770–785.

Li J, Yang H, Peer WA, *et al*. 2005. Arabidopsis H+-PPase AVP1 regulates auxin-mediated organ development. *Science* **310,** 121–125.

Maley F, Trimble RB, Tarentino AL, Plummer TH Jr. 1989. Characterization of glycoproteins and their associated oligosaccharides through the use of endoglycosidases. *Analytical Biochemistry* **180,** 195–204.

Marion J, Bach L, Bellec Y, Meyer C, Gissot L, Faure JD. 2008. Systematic analysis of protein subcellular localization and interaction using high-throughput transient transformation of Arabidopsis seedlings. *The Plant Journal* **56,** 169–179.

Mravec J, Skupa P, Bailly A, *et al*. 2009. Subcellular homeostasis of phytohormone auxin is mediated by the ER-localized PIN5 transporter. *Nature* **459,** 1136–1140.

Muller B, Sheen J. 2007 *a*. Arabidopsis cytokinin signaling pathway. *Science Signaling STKE* **2007**, cm5.

Muller B, Sheen J. 2007 *b*. Cytokinin signaling pathway. *Science Signaling STKE* **2007**, cm4.

Nelson BK, Cai X, Nebenfuhr A. 2007. A multicolored set of *in vivo* organelle markers for co-localization studies in Arabidopsis and other plants. *The Plant Journal* **51,** 1126–1136.

Nishimura C, Ohashi Y, Sato S, Kato T, Tabata S, Ueguchi C. 2004. Histidine kinase homologs that act as cytokinin receptors possess overlapping functions in the regulation of shoot and root growth in Arabidopsis. *The Plant Cell* **16,** 1365–1377.

Pas J, von Grotthuss M, Wyrwicz LS, Rychlewski L, Barciszewski J. 2004. Structure prediction, evolution and ligand interaction of CHASE domain. *FEBS Letters* **576,** 287–290.

Riefler M, Novak O, Strnad M, Schmulling T. 2006. Arabidopsis cytokinin receptor mutants reveal functions in shoot growth, leaf senescence, seed size, germination, root development, and cytokinin metabolism. *The Plant Cell* **18,** 40–54.

Romanov GA, Lomin SN, Schmülling T. 2006. Biochemical characteristics and ligand-binding properties of Arabidopsis cytokinin receptor AHK3 compared to CRE1/AHK4 as revealed by a direct binding assay. *Journal of Experimental Botany* **57,** 4051–4058.

Schleifenbaum F, Elgass K, Sackrow M, Caesar K, Berendzen K, Meixner AJ, Harter K. 2010. Fluorescence intensity decay shape analysis microscopy (FIDSAM) for quantitative and sensitive live-cell imaging: a novel technique for fluorescence microscopy of endogenously expressed fusion-proteins. *Molecular Plant* **3,** 555–562.

Schütze K, Harter K, Chaban C. 2009. Bimolecular fluorescence complementation (BiFC) to study protein–protein interactions in living plant cells. *Methods in Molecular Biology* **479,** 189–202.

Shuster SJ, Riedl M, Li X, Vulchanova L, Elde R. 1999. Stimulus-dependent translocation of kappa opioid receptors to the plasma membrane. *Journal of Neuroscience* **19,** 2658–2664.

Song RX, Barnes CJ, Zhang Z, Bao Y, Kumar R, Santen RJ. 2004. The role of Shc and insulin-like growth factor 1 receptor in mediating the translocation of estrogen receptor alpha to the plasma membrane. *Proceedings of the National Academy of Sciences, USA* **101,** 2076–2081.

Suzuki T, Miwa K, Ishikawa K, Yamada H, Aiba H, Mizuno T. 2001. The Arabidopsis sensor His-kinase, AHK4, can respond to cytokinins. *Plant and Cell Physiology* **42,** 107–113.

Tian H, Klambt D, Jones AM. 1995. Auxin-binding protein 1 does not bind auxin within the endoplasmic reticulum despite this being the predominant subcellular location for this hormone receptor. *Journal of Biological Chemistry* **270,** 26962–26969.

Tran LS, Urao T, Qin F, Maruyama K, Kakimoto T, Shinozaki K, Yamaguchi-Shinozaki K. 2007. Functional analysis of AHK1/ATHK1 and cytokinin receptor histidine kinases in response to abscisic acid, drought, and salt stress in Arabidopsis. *Proceedings of the National Academy of Sciences, USA* **104,** 20623–20628.

Ueguchi C, Koizumi H, Suzuki T, Mizuno T. 2001. Novel family of sensor histidine kinase genes in Arabidopsis thaliana. *Plant and Cell Physiology* **42,** 231–235.

Urao T, Yakubov B, Satoh R, Yamaguchi-Shinozaki K, Seki M, Hirayama T, Shinozaki K. 1999. A transmembrane hybrid-type histidine kinase in Arabidopsis functions as an osmosensor. *The Plant Cell* **11,** 1743–1754.

Varet A, Hause B, Hause G, Scheel D, Lee J. 2003. The Arabidopsis NHL3 gene encodes a plasma membrane protein and its overexpression correlates with increased resistance to Pseudomonas syringae pv. tomato DC3000. *Plant Physiology* **132,** 2023–2033.

Werner T, Motyka V, Laucou V, Smets R, Van Onckelen H, Schmulling T. 2003. Cytokinin-deficient transgenic Arabidopsis plants show multiple developmental alterations indicating opposite functions of cytokinins in the regulation of shoot and root meristem activity. *The Plant Cell* **15,** 2532–2550.

Werner T, Schmulling T. 2009. Cytokinin action in plant development. *Current Opinion in Plant Biology* **12,** 527–538.

Wohlbach DJ, Quirino BF, Sussman MR. 2008. Analysis of the Arabidopsis histidine kinase ATHK1 reveals a connection between vegetative osmotic stress sensing and seed maturation. *The Plant Cell* **20,** 1101–1117.

Wormit A, Traub M, Florchinger M, Neuhaus HE, Mohlmann T. 2004. Characterization of three novel members of the Arabidopsis thaliana equilibrative nucleoside transporter (ENT) family. *Biochemical Journal* **383,** 19–26.

Zipfel C, Kunze G, Chinchilla D, Caniard A, Jones JD, Boller T, Felix G. 2006. Perception of the bacterial PAMP EF-Tu by the receptor EFR restricts Agrobacterium-mediated transformation. *Cell* **125,** 749–760.

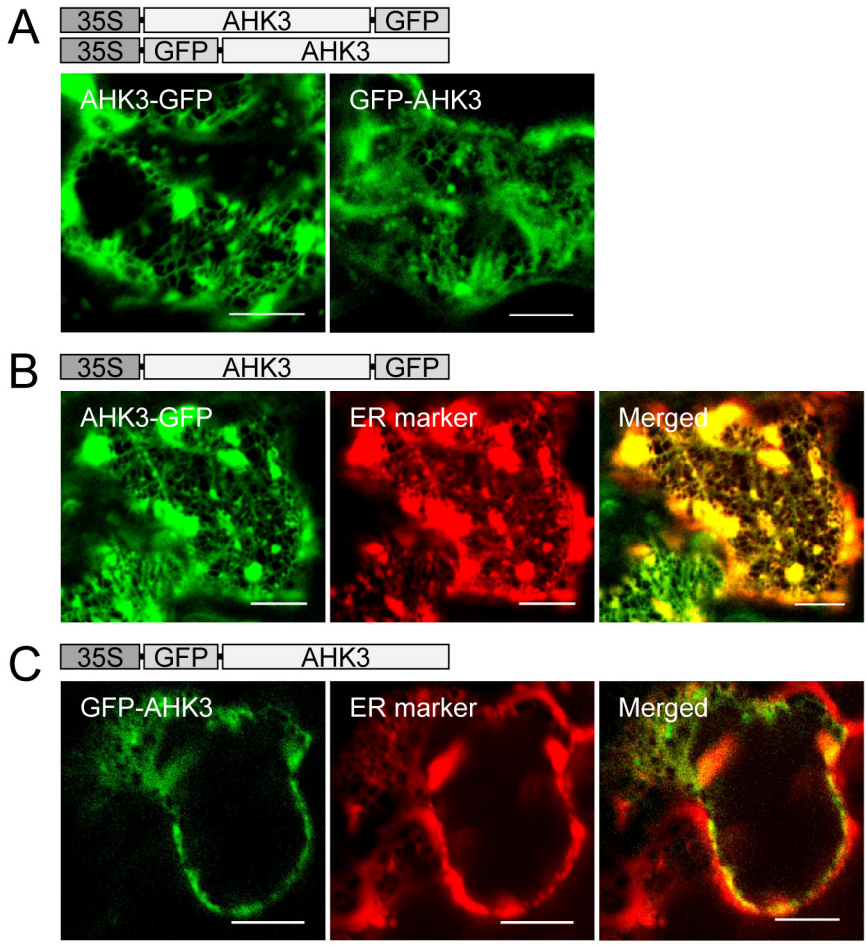

Supplementary Fig. S1. AHK3 GFP fusion proteins localize to the ER in transiently transformed *Arabidopsis* cotyledon cells. (A) Transiently transformed *Arabidopsis* cotyledon cells expressing the indicated AHK3 fusion proteins under the control of the *35S* promoter. (B) and (C) Transiently transformed *Arabidopsis* cotyledon cells coexpressing the indicated AHK3 fusion proteins under the control of the *35S* promoter with the ER marker ER-rk CD3-959. Bars represent 10 µm.

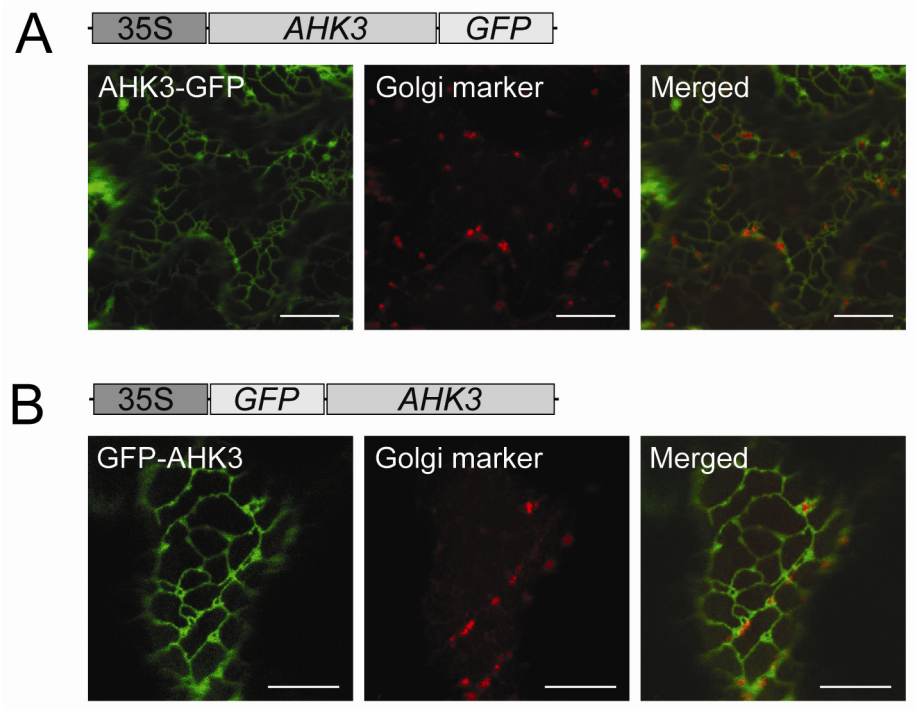

Supplementary Fig. S2. GFP fusion proteins of AHK3 do not colocalize with the Golgi marker G-rk CD3-967. (A, B) Confocal images of transiently transformed tobacco epidermal leaf cells co-expressing the indicated AHK3 fusion proteins under the control of the *35S* promoter and the Golgi marker G-rk CD3-967. Bars represent 10 µm.

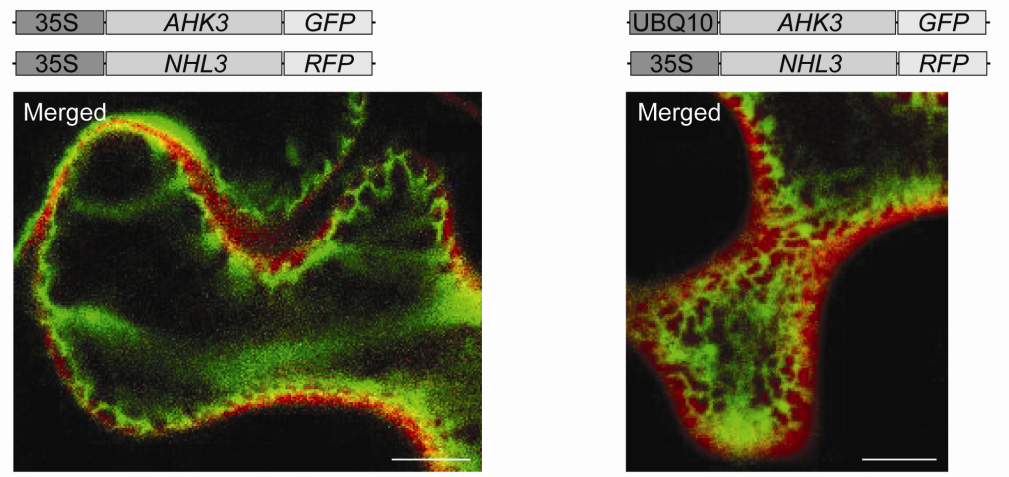

Supplementary Fig. S3. AHK3 GFP fusion proteins do not colocalize with the plasma membrane localized fusion protein NHL3-RFP. Magnified confocal images of transiently transformed tobacco epidermal leaf cells (see Fig. 3A, C) co-expressing the indicated AHK3 fusion protein under the control of the *35S* promoter or the *UBQ10* promoter and the plasma membrane localized fusion protein NHL3-RFP. Bars represent 10 µm.

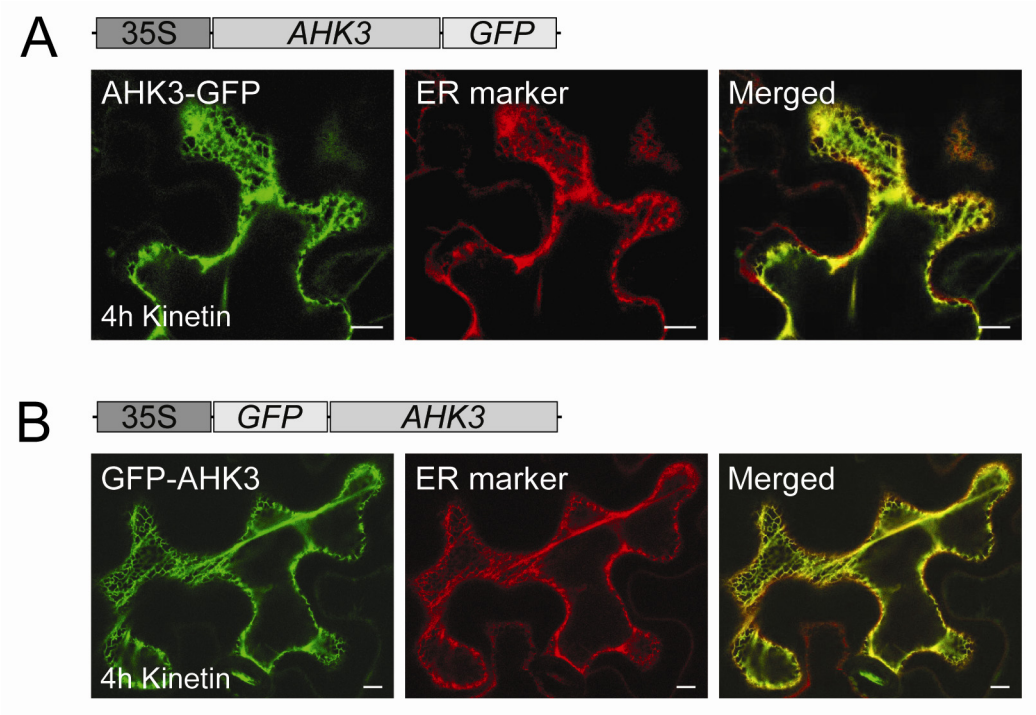

Supplementary Fig. S4. The ER localization of AHK3-GFP and GFPAHK3 does not change upon cytokinin treatment. (A, B) Confocal images of transiently transformed tobacco epidermal cells co-expressing the indicated AHK3 fusion protein with the ER marker ER-rk CD3-959. The images were taken 4 h after application of 1 µM kinetin to the leaves. Bars represent 10 µm.

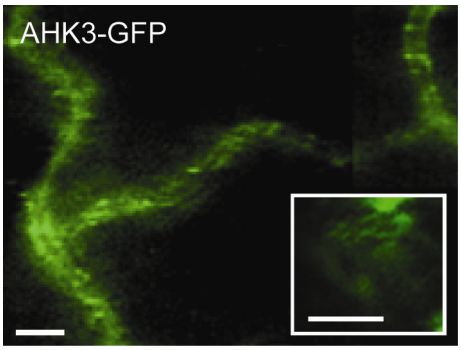

Supplementary Fig. S5. AHK3-GFP fluorescence is detectable in the ER of the AHK3-GFP-expressing *Arabidopsis* line. FIDSAM image after a 3-fold decay shape analysis correction of the raw image. Bars represent 4 µm.
Due to the FIDSAM analysis the recorded fluorescent signal can be unequivocally attributed to GFP fluorescence.

Supplementary Table 1. Oligonucleotides used in the study

1	gaagagttcgagaggcaaca
2	tttgtatagttcatccatgccatgtg
3	atgagtaaaggagaagaacttttcac
4	cgcatctcatgctttctcaatg
5	tggtggtgtctaatccttggtgtg
6	gcatagtccatctgcttcgca
7	ataacgctgcggacatctac
8	gaccatccatatccaggacgcatg
9	tggttcacgtagtgggccatcg
GFP-BcuI-S	**actagt***gggaggtggaagc*atggtgagcaagggc
GFP-BcuI-A	**actagt***gttccacctcc*cttgtacagctcgtc

the plant journal

SEB Society for Experimental Biology

The Plant Journal (2011) doi: 10.1111/j.1365-313X.2011.04510.x

A fast brassinolide-regulated response pathway in the plasma membrane of *Arabidopsis thaliana*

Katharina Caesar[1,†], Kirstin Elgass[1,†], Zhonghua Chen[2], Peter Huppenberger[1], Janika Witthöft[1], Frank Schleifenbaum[1], Michael R. Blatt[2], Claudia Oecking[1] and Klaus Harter[1,*]

[1]*Center for Plant Molecular Biology, Department of Plant Physiology, University of Tübingen, Auf der Morgenstelle 1, 72076 Tübingen, Germany, and*

[2]*Laboratory of Plant Physiology and Biophysics, Faculty of Biomedical and Life Sciences – Bower Building, University of Glasgow, Glasgow G12 8QQ, UK*

Received 21 April 2010; revised 17 January 2011; accepted 19 January 2011.

[*]For correspondence (fax +49 7071 29 3287; e-mail klaus.harter@zmbp.uni-tuebingen.de).

[†]These authors contributed equally to this work.

SUMMARY

To understand molecular processes in living plant cells, quantitative spectro-microscopic technologies are required. By combining fluorescence lifetime spectroscopy with confocal microscopy, we studied the subcellular properties and function of a GFP-tagged variant of the plasma membrane-bound brassinosteroid receptor BRI1 (BRI1–GFP) in living cells of Arabidopsis seedlings. Shortly after adding brassinolide, we observed BRI1-dependent cell-wall expansion, preceding cell elongation. In parallel, the fluorescence lifetime of BRI1–GFP decreased, indicating an alteration in the receptor's physico-chemical environment. The parameter modulating the fluorescence lifetime of BRI1–GFP was found to be BL-induced hyperpolarization of the plasma membrane. Furthermore, for induction of hyperpolarization and cell-wall expansion, activation of the plasma membrane P-ATPase was necessary. This activation required BRI1 kinase activity, and was mediated by BL-modulated interaction of BRI1 with the P-ATPase. Our results were used to develop a model suggesting that there is a fast BL-regulated signal response pathway within the plasma membrane that links BRI1 with P-ATPase for the regulation of cell-wall expansion.

Keywords: brassinolide, brassinosteroid-insensitive 1 (BRI1), fluorescence lifetime, membrane potential, P-ATPase, cell wall.

INTRODUCTION

For quantitative analysis of molecular processes in living (plant) cells, such as perception and processing of environmental and endogenous signals, new combinatorial approaches in optical and spectroscopic technologies are needed. The use of green fluorescent protein (GFP) and its variants to create fluorescing fusion proteins, and of dyes labelling specific compartments, has revolutionized *in vivo* analysis of cell biological processes (Dixit *et al.*, 2006; Giepmans *et al.*, 2006; Suzuki *et al.*, 2007). However, fluorescence intensity measurements provide images but do not usually provide information on changes in the physico-chemical parameters in the immediate environment of the fluorophor-tagged protein. Progress has been made in generating mutant versions of GFP that show a spectral shift in response to changes in the intracellular pH or redox state (Moseyko and Feldman, 2001; Ashby *et al.*, 2004; Meyer and Brach, 2009; Orij *et al.*, 2009). Although this has opened new field for intracellular studies, their use has intrinsic limitations. For instance, background fluorescence, with broad spectral emission of wavelength-specific intensity, such as that of plant cell walls, interferes with the quantitative analysis of GFP fluorescence shifts (Elgass *et al.*, 2009). The fluorescence lifetime (FLT) of a fluorophor-tagged protein can be recorded without the intrinsic limitations of the exclusively spectral approach (Wang *et al.*, 2008). The lifetime of fluorescent proteins, such as GFP, changes with the pH, refractive index and electric field (Ohta *et al.*, 2010). Therefore, alterations in the FLT of GFP have been used to measure these physico-chemical parameters in human cells (van Manen *et al.*, 2008; Nakabayashi *et al.*, 2008).

We have recently commenced quantitative analysis of the properties and subcellular function of GFP fusions of the plasma membrane-localized brassinosteroid (BR) receptor,

BRI1, in living plant cells of *Arabidopsis thaliana*, using spectro-microscopic technologies (Elgass *et al.*, 2009). BRs, such as brassinolide (BL), are involved in responses to biotic and abiotic stresses and developmental processes, including cell elongation (Clouse and Sasse, 1998; Clouse, 2004). The present model of the BR response pathway includes binding of BRs to BRI1, resulting in autophosphorylation of the receptor and subsequent recruitment of the co-receptor BRI1-associated receptor kinase 1 (BAK1). The association is followed by trans-phosphorylation between BRI1 and BAK1, and results in activation of BR signalling, leading to differential gene expression and execution of the specific responses (Clouse, 2004; Vert *et al.*, 2005; Li and Jin, 2007; Chinchilla *et al.*, 2009). However, the molecular events that occur immediately after perception of BL in the plasma membrane and are required for initiation of cell elongation, for example, have yet to be included in this model (Szymanski and Cosgrove, 2009; Sanchez-Rodriguez *et al.*, 2010). Previous physiological studies reported electrogenic proton extrusion into the apoplastic space and hyperpolarization of the plasmalemma in response to BR treatment before onset of cell elongation (Romani *et al.*, 1983; Cerana *et al.*, 1985; Mandava, 1988).

By combining FLT spectroscopy and confocal sample scanning microscopy (CSSM), we observed a dynamic cell-wall expansion a few minutes after application of BL in cells of Arabidopsis seedlings, and found that this expansion was dependent on the amount of BRI1–GFP (Elgass *et al.*, 2009, 2010). This phenomenon is attributed to the wall loosening, apoplastic water uptake and wall swelling that precede cell elongation (Clouse and Sasse, 1998; Clouse, 2004; Haubrick and Assmann, 2006; Elgass *et al.*, 2009). The expansion response was accompanied by a change in the FLT of BRI1–GFP, reflecting an alteration in the physico-chemical environment of BRI1–GFP (Elgass *et al.*, 2009). Changes in the refractive index, pH, hydrostatic pressure and temperature were not responsible for the alteration in the FLT of BRI1–GFP (Appendix S1) (Elgass *et al.*, 2010). Our initial data suggest that an alteration in the plasma membrane potential (E_m) could cause the change in the FLT of BRI1–GFP (Elgass *et al.*, 2010).

Here we show that the physico-chemical parameter causing BL-regulated alteration of the FLT of BRI1–GFP is hyperpolarization of the E_m, thus altering the electric field in the immediate environment of the GFP tag. In agreement with this, BL induces E_m hyperpolarization in wild-type and BRI1–GFP-expressing cells, as demonstrated by electrophysiological experiments. Furthermore, activation of the plasma membrane P-ATPase is required for both the change in the FLT of BRI1–GFP and cell-wall expansion in response to BL application. Our data provide evidence for a fast BRI1-dependent response pathway in the plasma membrane, which links BL perception via P-ATPase activation and E_m hyperpolarization to cell-wall expansion.

RESULTS

The E_m is the physico-chemical parameter that modulates the FLT of BRI1–GFP

For our spectro-microscopic studies, we used a transgenic *Arabidopsis thaliana* line expressing a C-terminal GFP fusion of BRI1 (Friedrichsen *et al.*, 2000) and two control lines expressing the plasma membrane-localized fusion proteins GFP–LTI6b (Cutler *et al.*, 2000) or PMA4–GFP (Lefebvre *et al.*, 2004). The fluorophore of these fusion proteins is exposed to the cytoplasm. To determine cell-wall expansion, the full width at half maximum (FWHM) for Gaussian fits (see Experimental procedures) of fluorescence intensity profiles of plasma membrane-cell wall sections was recorded (Elgass *et al.*, 2009). The *in planta* FLT of the GFP fusion proteins was measured by one-chromophore fluorescence lifetime microscopy at the whole-cell level (ocFLM) (Elgass *et al.*, 2009).

Our previous studies indicated that the E_m of the plasma membrane might influence the FLT of BRI1–GFP (Elgass *et al.*, 2010). To confirm this observation, we applied 10 mM sodium acetate (pH 6.0) to BRI1–GFP-expressing seedlings, as weak organic acids have been shown to permeate the membrane in their protonated form, resulting in equilibration of the pH gradient between the extracellular space and the protoplast (Grainger *et al.*, 1979; Johnson and Epel, 1981; Dupre and Schaaf, 1996; Bobik *et al.*, 2010). Sodium acetate treatment did not significantly alter the FLT of BRI1–GFP *per se* (Figure 1a), nor was cell-wall expansion observed (Figure 1b). However, BL was no longer able to induce cell-wall expansion and FLT changes in the presence of sodium acetate (Figure 1c,d and Table S1). This loss of BL responsiveness suggests that a proton electrochemical force or an electric field across the plasma membrane is required for both cell physiological processes.

To support the hypothesis that the FLT of BRI1–GFP responds to changes in the E_m, we incubated seedlings expressing various membrane-bound GFP fusion proteins for 30 min in HVS and LVS, with either high-voltage (hyperpolarization) or low-voltage (depolarization) conditions across the plasma membrane (Grabov and Blatt, 1998; Allen *et al.*, 2001). In the presence of high-voltage solution (HVS), the FLT of BRI1–GFP, but not of the membrane-bound GFP–LTI6b and PMA4–GFP fusion proteins, was shifted to values lower than those achieved with low-voltage solution (LVS) (Figure 2a and Table S2). This HVS-induced change in FLT was very rapid and detectable within 5 min after exposure of LVS-treated cells to HVS (Figure 2d). In BRI1–GFP-expressing seedlings incubated in LVS and then exposed to HVS, a weak but significant cell-wall expansion was detected (Figure 2b,c). No differences in wall dimension and FLT were detected when GFP–LTI6b-expressing cells were exposed to HVS (Figure S1).

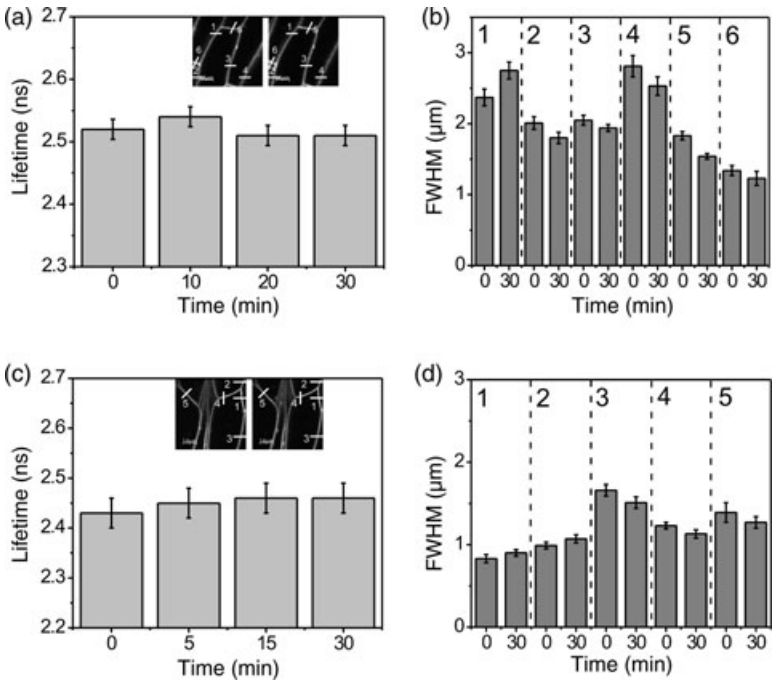

Figure 1. Sodium acetate inhibits BL-regulated cell-wall expansion and changes in the FLT of BRI1–GFP in Arabidopsis hypocotyl cells.
(a, b) FLT of BRI1–GFP (a) and FWHM values (b) of cells before (0 min) and at the indicated time points after addition of 10 mM sodium acetate (pH 6.0). The FWHM values were recorded over plasma membrane/cell wall sections at the positions indicated by the white lines (1–6) in the confocal image insets in (a).
(c, d) FLT of BRI1–GFP (c) and FWHM values (d) of cells before (0 min) and at the indicated time points after addition of 10 mM sodium acetate (pH 6.0) plus 10 nM BL. The FWHM values were recorded over the plasma membrane/cell wall sections indicated by the white lines (1–5) in the confocal image insets in (c).
For statistical analysis of FLT values, see Table S1.

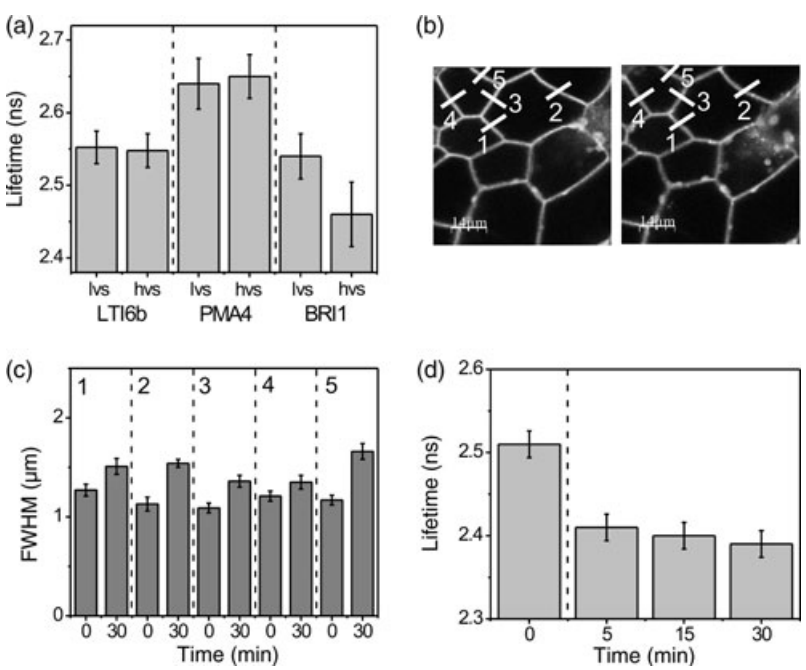

Figure 2. The FLT of BRI1–GFP, but not of other integral GFP fusion proteins, is modulated by the plasma membrane potential (E_m) in Arabidopsis hypocotyl cells.
(a) FLT of GFP in cells expressing GFP–LTI6b (LTI6b), PMA4–GFP (PMA4) and BRI1–GFP (BRI1). Cells were treated with either low-voltage solution (lvs; depolarization of E_m) or high-voltage solution (HVS; hyperpolarization of E_m).
(b) Confocal images of BRI1–GFP-expressing cells pre-treated for 1 h with low-voltage solution (left) and subsequent incubation for 30 min in high-voltage solution (right).
(c) FWHM values of the plasma membrane/cell wall sections indicated by the white lines in the confocal images (b), in BRI1–GFP-expressing cells pre-treated for 1 h in low-voltage solution before (0 min) and 30 min after addition of high-voltage solution. The cell-wall expansion after addition of high-voltage solution is statistically significant ($n = 17$, $P = 10^{-7}$).
(d) FLT of BRI1–GFP recorded before (0 min) and at the indicated time points after addition of high-voltage solution.
For the statistical analysis of the FLT values, see Table S2.

We also applied the phytohormone auxin, in the form of 2,4-dichlorophenoxyacetic acid (2,4-D), to BRI1–GFP-expressing seedlings. Auxin is known to regulate cell elongation and wall expansibility, accompanied by hyperpolarization of the plasma membrane (Cleland, 2004). In the presence of 20 nM 2,4-D, we also observed wall expansion and a decrease in the FLT of BRI1–GFP (Figure 3 and Table S1). These data indicate that the physico-chemical parameter 'sensed' by the FLT of BRI1–GFP is the E_m.

BL-induced changes in the E_m and wall expansion depend on P-ATPase activity

Our data favour the hypothesis that BL induces changes in the FLT of BRI1–GFP by modulating the E_m. We therefore performed electrophysiological E_m measurements in root epidermal cells of both wild-type and BRI1–GFP-expressing Arabidopsis lines. The E_m of these cells in the resting condition followed a Gaussian distribution centred on a mean

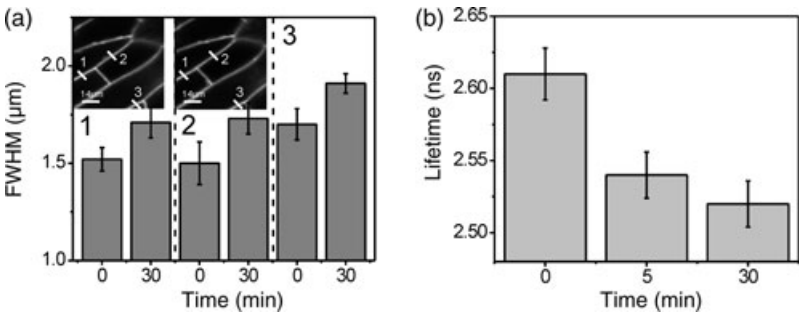

Figure 3. Auxin induces cell-wall expansion and a change in the FLT of BRI1–GFP.
FWHM values (a) and the FLT of BRI1–GFP (b) in cells expressing BRI1–GFP before (0 min) and 5 and 30 min after addition of 20 nM 2,4-D. The FWHM values were recorded over the plasma membrane/cell wall sections indicated by the white lines in the confocal image insets.
For the statistical analysis of the FLT values, see Table S1.

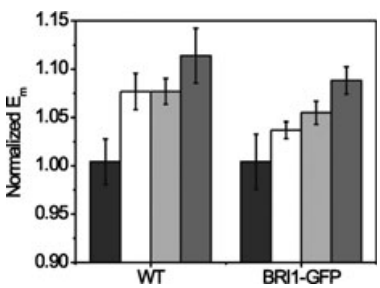

Figure 4. Brassinolide induces membrane hyperpolarization of root epidermal cells in Col-0 wild-type and BRI1–GFP-expressing plants.
Membrane potentials (E_m) of root epidermal cells after treatment with BL at 10 nM (white bars), 50 nM (grey bars) or 100 nM (dark grey bars) normalized to that in the control (0 nM BL, black bars). All measurements were performed in 5 mM Ca^{2+}/MES buffer with 1 mM KCl with or without BL. Values are means ± SE (n = 4–14 for each treatment).

Table 1 Brassinolide induces membrane hyperpolarization of root epidermal cells in wild-type and BRI1–GFP plants

	ΔE_m (mV)	
Concentration of brassinolide used (nM)	Col-0	BRI1–GFP-expressing cells
10	−7.2 ± 2.0	−3.1 ± 0.9
50	−7.1 ± 1.2	−4.8 ± 1.1
100	−10.8 ± 2.6	−8.2 ± 1.2

Concentration-dependent changes in E_m before and after 20 min of BL application. All measurements were performed in 5 mM Ca^{2+}/MES buffer with 1 mM KCl. Values are means ± SE (n = 4–14 for each treatment).

value of −121 ± 2 mV (Figure S2). BL was able to hyperpolarize the plasma membrane of all root cells analysed (Figure 4, Table 1 and Figure S3). There was no significant difference in the BL-induced E_m hyperpolarization between BRI1–GFP-expressing and wild-type cells grown under the identical physiological conditions (Figure 4, Table 1 and Figure S3). These results demonstrate a role for BRI1 in regulating BL-induced plasma membrane transport activities and hence the E_m.

The BL-induced E_m hyperpolarization could be due to enhanced proton secretion, caused by BL-enhanced activity of the plasma membrane-bound P-ATPase (Friedrichsen and Chory, 2001; Clouse, 2004). We therefore recorded the FLT of BRI1–GFP and the wall expansion in Arabidopsis seedlings pre-treated for 1 h with 2 μM fusicoccin (Fc), an activator of P-ATPase activity (Marre, 1979; Wurtele *et al.*, 2003), or 50 μM *ortho*-vanadate (*o*V), an inhibitor of P-ATPase activity (MacLennan *et al.*, 1997; Schaller and Oecking, 1999), before addition of BL. After pre-treatment with *o*V, the BL-induced wall expansion and change in the FLT of BRI1–GFP were no longer observed (Figure 5a). However, when the *o*V was washed out before BL treatment, both processes were observed again (Figure 5b). In the presence of Fc, we observed a weak positive effect of BL on wall expansion and the FLT of BRI1–GFP (Figure 5c). This indicates that Fc up-regulated the P-ATPase activity in the absence of BL, and this up-regulation was only slightly enhanced by the hormone. In contrast to BRI1–GFP (Figure 5e and Table S3), no change was observed in the FLT of GFP–LTI6b in response to *o*V or Fc (Figure 5d and Table S3).

If P-ATPase activity is required for BL-induced cell-wall expansion and the change in the FLT of BRI1–GFP, Fc should be able to induce the responses in the absence of BL. As shown in Figure 6(a–c), treatment of seedlings for 30 min with Fc resulted in wall expansion not only in BRI1–GFP-expressing cells but also in GFP–LTI6b-expressing and wild-type cells. Treatment with Fc also resulted in changes in the FLT of BRI1–GFP but not that of GFP–LTI6b (Figure 6a,b). Furthermore, Fc reversed the inhibiting effect of *o*V on the FLT of BRI1–GFP (Figure S4). The importance of the P-ATPase activity for controlling wall expansion and changes in the FLT of BRI1–GFP was further substantiated by the observation that, after pre-incubated *o*V was washed out, both processes recovered within 40 min and were again inducible by BL (Figure 6d). These data indicate that up-regulation of P-ATPase activity is required for cell-wall expansion and changes in the FLT of BRI1–GFP.

The degree of cell-wall expansion in response to various conditions can be captured quantitatively as the ratio of the FWHM values to the corresponding intensity profiles under various conditions (Elgass *et al.*, 2009). As shown in Figure 7, acidification of the extracellular environment to pH 5.5 had no significant effect on wall expansion, but hyperpolarization of the plasma membrane by addition of

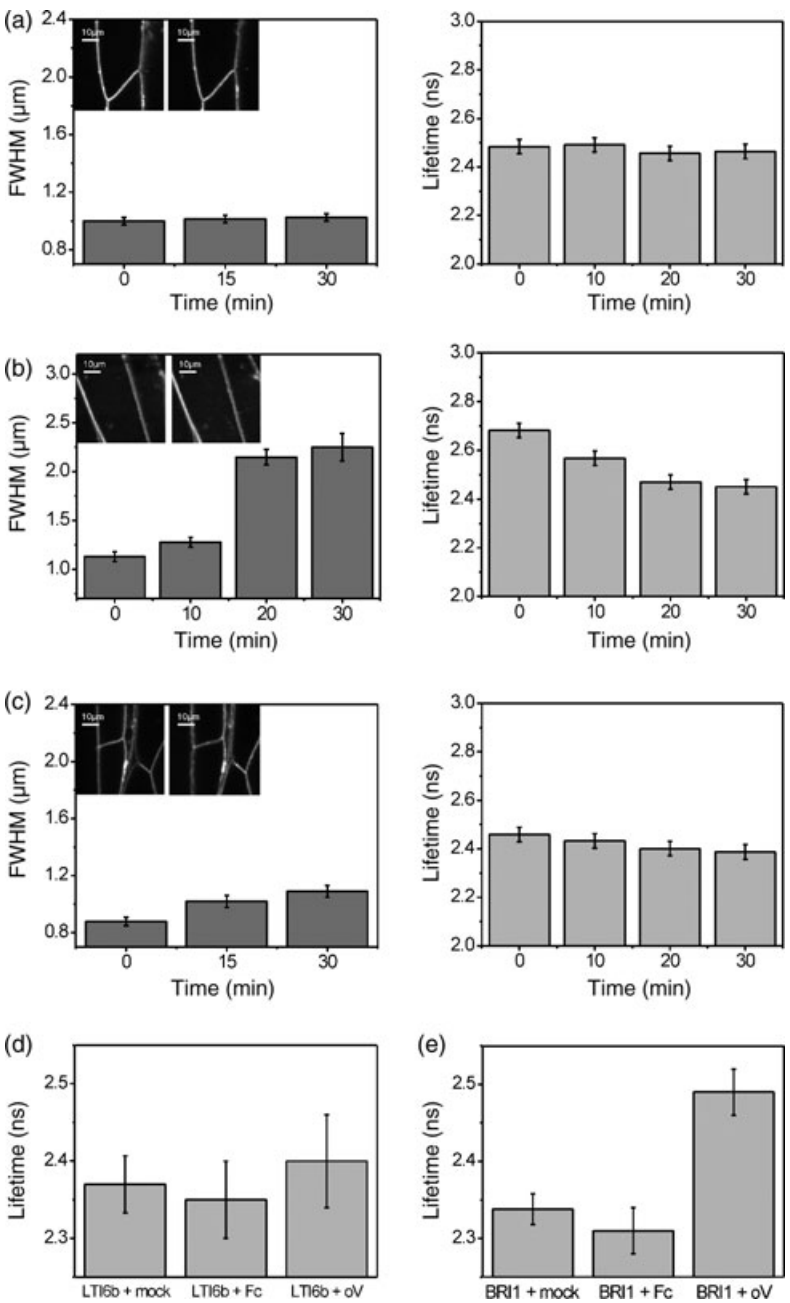

Figure 5. BL-regulated cell-wall expansion and changes in the FLT of BRI1–GFP depend on P-ATPase activity.
(a) FWHM (left) and FLT kinetics (right) over a plasma membrane/cell wall section in BRI1–GFP-expressing cells pre-treated for 1 h with 50 μM *o*V before addition of 10 nM BL. The insets show corresponding confocal images recorded before (0 min, left) and 30 min after hormone application (right).
(b) Equivalent experiment to (a) but *o*V was washed out before addition of 10 nM BL.
(c) Equivalent experiment to (a) but cells were pre-treated with 2 μM Fc before addition of 10 nM BL.
(d) FLT of GFP–LTI6b in hypocotyl cells either mock-treated (LTI6b + mock) or treated for 30 min with either 2 μM Fc (LTI6b + Fc) or 50 μM *o*V (LTI6b + *o*V).
(e) FLT of BRI1–GFP in hypocotyl cells either mock-treated (BRI1 + mock) or treated for 30 min with either 2 μM Fc (BRI1 + Fc) or 50 μM *o*V (BRI1 + *o*V).
For the statistical analysis of FLT values, see Table S3.

HVS resulted in a significant response. Combined application of HVS and acidification of the apoplast acted synergistically in induction of wall expansion (Figure 7). However, the most significant effect was observed in the presence of BL (Figure 7). These data suggest that several factors may act together to achieve maximum cell-wall expansion *in vivo*.

Kinase activity of BRI1 is required for P-ATPase activity

For induction of BL-regulated gene expression, BRI1 phosphorylation activity is required (Wang *et al.*, 2005). We therefore addressed the question of whether BRI1 kinase activity is also necessary for regulating P-ATPase activity and E_m hyperpolarization. We generated a variant of the BRI1–GFP fusion without kinase activity (BRI1^{KE}–GFP), which has a point mutation in the kinase subdomain II of BRI1 (Oh *et al.*, 2000; Wang *et al.*, 2005). In addition, we reconstituted the BL response pathway in transiently transformed tobacco (*Nicotiana benthamiana*) leaf cells. The BRI1–GFP fusions were co-expressed with a non-tagged version of Arabidopsis P-ATPase 1 (AHA1). AHA1 (together with AHA2) is essential for apoplastic proton extrusion and plant development (Haruta *et al.*, 2010). As shown in Figure 8(a), BRI1–GFP and BRI1^{KE}–GFP accumulated to similar levels

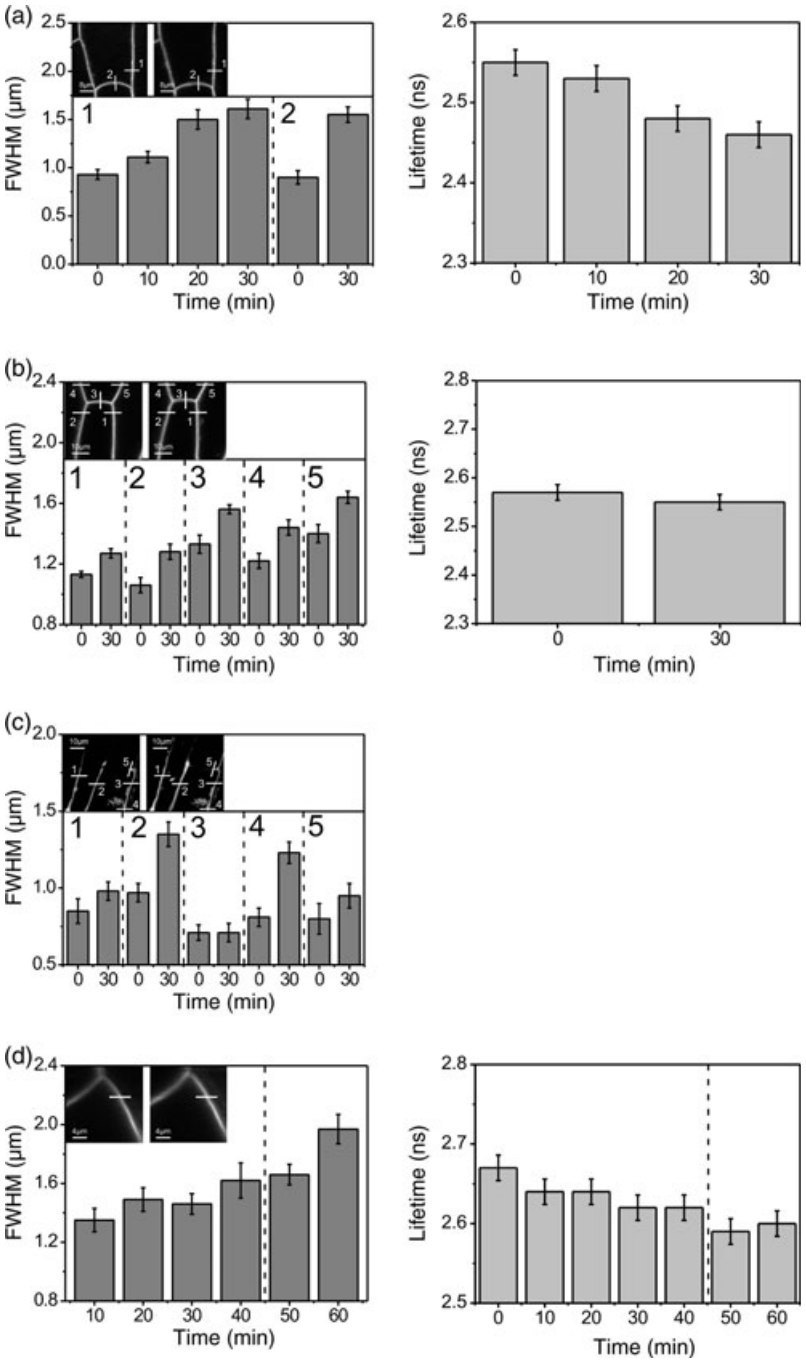

Figure 6. P-ATPase activity is required for wall expansion and FLT changes in hypocotyl cells.
(a) FWHM values (left) and FLT kinetics (right) over a plasma membrane/cell wall section in BRI1–GFP-expressing cells treated with 2 µM Fc. The insets show the corresponding confocal images recorded before (0 min, left) and 30 min after hormone application (right).
(b) Equivalent experiment to (a) but using seedlings expressing GFP–LTI6b.
(c) Equivalent experiment to (a) but the autofluorescence of the cell walls of wild-type seedlings was used to assess wall expansion.
(d) FWHM (left) and FLT kinetics (right) over a plasma membrane/cell wall section in BRI1–GFP-expressing cells pre-treated for 1 h with 50 µM *o*V. Afterwards *o*V was washed out and the cells were incubated in water for 40 min. Then 10 nM BL was applied and the cells were incubated for further 20 min. The recorded section is indicated by the white line in the confocal image insets before (left) and 60 min after onset of treatment (right).

in tobacco cells. When wild-type BRI1–GFP or BRI1^{KE}–GFP were expressed alone in tobacco cells, no significant decrease in FLT was observed in response to BL (Figure 8c). In contrast, co-expression of AHA1 together with BRI1–GFP resulted in a BL-dependent decrease in the FLT, reflecting strong E_m hyperpolarization (Figure 8b). This BL-induced change was not observed when BRI1^{KE}–GFP was co-expressed with AHA1 (Figure 8b). The differential FLT decrease was not due to differential expression of *AHA1* in the leaf cells, as demonstrated by RT-PCR (Figure 8c).

These data indicate that the BL- and BRI1-dependent response pathway that regulates AHA1 activity in *Arabidopsis thaliana* can be reconstituted in tobacco cells. Furthermore, BRI1 kinase activity is required for the regulation of AHA1.

BRI1–GFP interacts with the P-ATPase in the plasma membrane

One hypothesis as to how BRI1 activates P-ATPase activity could be by physical interaction and initiation of phosphor-

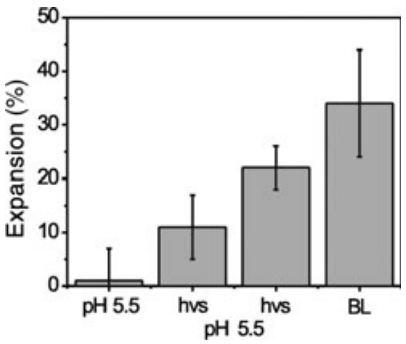

Figure 7. Quantitative comparison of cell-wall expansion in BRI1–GFP-expressing Arabidopsis cells treated with various agents.
The wall expansion, as determined by analysis of the FWHM values of Gaussian fits, was normalized to the GFP intensity profiles at plasma membrane/cell wall sections before (control) and 30 min after application of the indicated agent. The relative expansion was calculated, setting the control value to one. At least 15 measurements were performed per treatment. The differences in the mean values between all treatments are statistically significant ($n > 15$, $P < 5.7 \times 10^{-4}$).

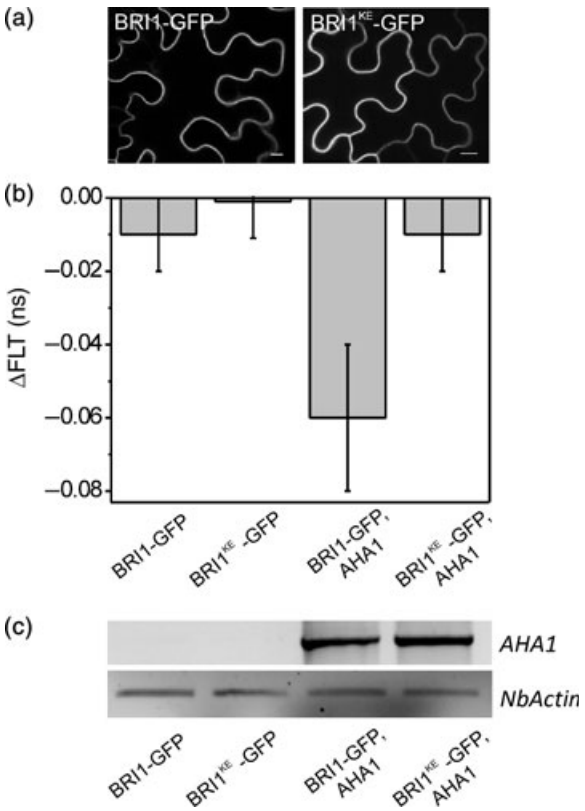

Figure 8. Activation of P-ATPase requires BRI1 kinase activity.
(a) Expression of BRI1–GFP or BRI1^{KE}–GFP in transiently transformed tobacco (*Nicotiana benthamiana*) epidermal leaf cells. Images were recorded 3 days after transformation. Scale bars = 10 μm.
(b) Change in the FLT of BRI1–GFP and BRI1^{KE}–GFP in response to BL treatment in transiently transformed tobacco epidermal leaf cells. The cells were transformed using the indicated constructs, and 3 days after transformation, the FLT was recorded before (0 min) and 30 min after application of 10 nM BL. Values are means ± standard deviations for three independent measurements.
(c) Amount of Arabidopsis *P-ATPase 1* (*AHA1*) transcript in transiently transformed tobacco epidermal leaf cells. RT-PCR analysis for the presence of *AHA1* and *NbActin* (loading control) was performed using RNA from leaf discs transformed with the indicated constructs. Before extraction, the presence of the BRI1–GFP or BRI1^{KE}–GFP in the leaf tissue was confirmed by fluorescence microscopy.

ylation. We therefore performed interaction studies using the yeast mating-based split-ubiquitin system (mbSUS) (Grefen *et al.*, 2009). Full-length AHA1 and BAK1 were expressed as Cub-PLV fusions in the THY.AP4 strain (MATa), and BRI1, LTI6b and AHA1 as NubA fusions as well as free NubG and NubWT in the THY.AP5 strain (MATα). BAK1 was chosen as a positive heterotypic interaction partner for BRI1, because its association with this receptor has been reported using Förster resonance energy transfer (FRET) in plant protoplasts (Russinova *et al.*, 2004). After mating, the presence of the plasmids was tested by the growth of yeast cells on synthetic complete medium supplemented with adenin and histidin (SC+Ade,His) medium, whereas the putative interaction of the Cub-PLV and NubA fusion proteins was assayed by growth on SC medium. AHA1 and BAK1 showed a homotypic interaction, indicating that the corresponding Cub-PLV and NubA fusion proteins were correctly expressed (Figure 9a and Figure S5). The integrity of the Cub-PLV fusion proteins was further substantiated by their strong interaction with NubWT (Figure 9a and Figure S5) and the heterotypic interaction of BAK1 with BRI1 (Figure S5). We also observed AHA1 interaction with BRI1 but not with the control protein LTI6b (Figure 9a). Application of BL (10 nM) or epi-BL (100 nM) to the yeast growth medium did not alter this interaction pattern (data not shown).

To confirm the results of the mbSUS study, we used CSSM, combined with a FRET approach based on fluorescence intensity decay shape analysis microscopy (FRET-FIDSAM) (Schleifenbaum *et al.*, 2009) and coupled FRET-fluorescence lifetime imaging microscopy analysis (FRET-FLIM) in transiently transformed *Nicotiana benthamiana* leaf cells. In FRET-FIDSAM, the donor intensity decay in the presence of a FRET acceptor is fitted to a mono-exponential decay function. Deviation from the mono-exponential decay increases for enhanced FRET rates, and this can be quantified by the fitting error value (chi-square). Accordingly, chi-square can be used directly as a measure for FRET (see Experimental procedures). The FRET-FIDSAM approach is sensitive, reliable, independent of the cellular environment, and therefore highly suitable for interaction studies in living plant cells (Schleifenbaum *et al.*, 2009). For expression of fusion proteins, we used oestradiol-inducible mCherry and GFP constructs (Bleckmann *et al.*, 2010) of AHA1, LTI6b, BAK1 and BRI1. To determine the maximal FRET-FIDSAM and FRET-FLIM values, C-terminal GFP–mCherry fusion constructs of BRI1 and LTI6b were used as positive controls (FRET controls) (Bleckmann *et al.*, 2010).

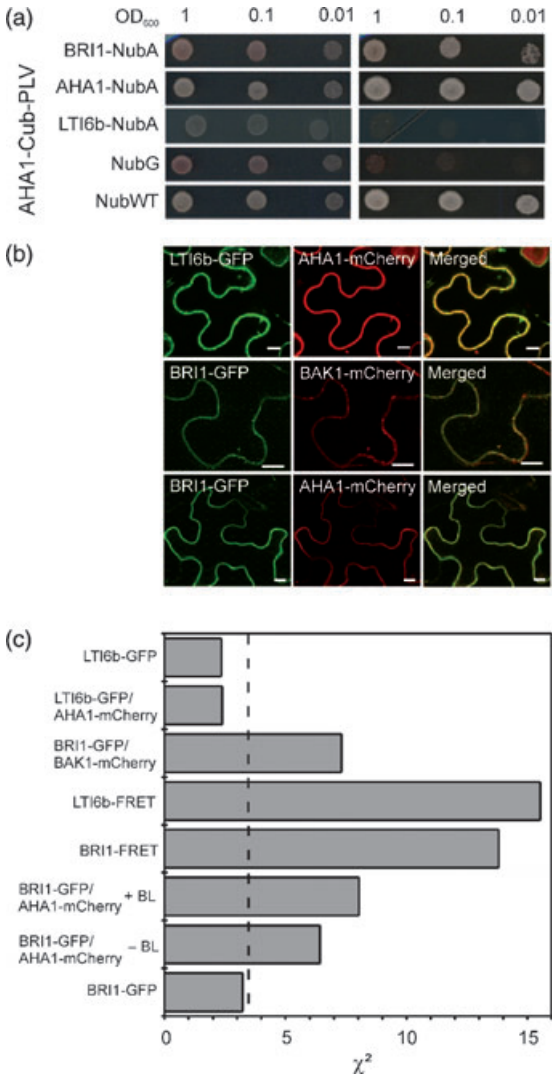

Figure 9. BRI1 interacts with the P-ATPase *in vivo*.
(a) Yeast mbSUS protein–protein interaction analysis. Cub-PLV constructs were transformed in yeast strain THY.AP4 (MATa) and Nub constructs were transformed in the yeast strain THY.AP5 (MATα). After mating, activation of the reporter gene was determined by growth of the transformants in a dilution series (of OD 600 nm from 1 to 0.01) on SC medium. The presence of the plasmids was tested by growth on SC+Ade,His medium. Co-transformations of the AHA1–Cub-PLV fusion with NubG served as a negative control and co-transformations with NubWT served as a positive control.
(b) CSSM images of transiently transformed tobacco epidermal leaf cells co-expressing the indicated GFP and mCherry fusion proteins.
(c) FRET-FIDSAM protein–protein interaction analysis. The fusion proteins were expressed in tobacco cells as indicated, and the fitting error values (chi-square) were recorded as described in Experimental procedures. The higher the chi-square value, the better the FRET efficiency. Individually transformed FRET fusions of BRI1 and LTI6b served as positive controls. Single transformed GFP fusions of BRI1 and LTI6b were used to determine the background chi-square value (dashed line). Values are means of at least 14 independent measurements. Detailed statistics of the FRET-FIDSAM data are given in the text.

The C-terminal GFP fusions of BRI1 and LTI6b served as background chi-square references. On the basis of fluorescence intensity measurements, the fusion constructs were expressed to very similar levels in the cells (Figure 9b). The FRET control fusions of BRI1 (BRI1-FRET) and LTI6b (LTI6b-FRET) resulted in strong FRET-FIDSAM and FRET-FLIM values compared to the BRI1–GFP and LTI6b–GFP background references [BRI1-FRET: $n = 28$, $P = 4.7 \times 10^{-16}$ (Figures 9c, S6); LTI6b-FRET: $n = 15$, $P = 5.0 \times 10^{-7}$ (Figures 9c, S6)]. When BRI1–GFP was co-expressed with BAK1–mCherry, the interaction was detectable by both FRET approaches as indicated by a significantly increased chi-square value and a reduced FLT value compared to the BRI1–GFP reference ($n = 16$, $P = 9.9 \times 10^{-3}$; Figure 9c and Figure S6). The FLT and chi-square values also revealed a significant interaction of BRI1–GFP with AHA1–mCherry, even in the absence of exogenous BL ($n = 77$, $P = 8.5 \times 10^{-9}$; Figure 9c and Figure S6). External application of BL modified the BRI1–GFP/AHA1–mCherry association as indicated by enhanced chi-square and FLT values ($n = 59$, $P = 0.01$; Figure 9c and Figure S6). In contrast, there was no significant interaction of LTI6b–GFP with AHA1–mCherry ($n = 14$, $P = 0.38$; Figure 9c and Figure S6).

These data suggest that there is a specific BRI1 interaction with the P-ATPase in yeast and *in planta*. In plant cells, this interaction is altered by BL application.

DISCUSSION

BRI1–GFP is a specific *in vivo* probe for E_m hyperpolarization

Our progress in using *in vivo* FLT spectroscopy, in combination with CSSM, to analyse subcellular processes allowed us to unravel the kinetics and properties of BL-regulated and BRI1-dependent cell-wall expansion at subcellular resolution (Elgass *et al.*, 2009). In parallel, we also observed a BL-induced change in the FLT of BRI1–GFP (Elgass *et al.*, 2009, 2010). The results presented here support our previous observations (Elgass *et al.*, 2010) that the physico-chemical parameter responsible for the FLT status of BRI1–GFP is the plasma membrane potential (E_m). This is substantiated by the observation that application of E_m-modifying salt solutions or auxin (2,4-D) and the modification of P-ATPase activity are reflected in a reversible change in the FLT of BRI1–GFP. Thus, by recording its FLT, BRI1–GFP can be used as highly sensitive, non-invasive, molecular probe for measurement of the E_m in living plant cells at high spatio-temporal resolution. Interestingly, the FLT of other plasma membrane-bound GFP fusion proteins does not significantly react to E_m changes. The fact that the electric field strength of the E_m decreases strongly with the distance to the plasma membrane is important in this context. Thus, when the GFP tag reaches far into the cytoplasm, as is predicted for PMA4–GFP, the FLT of the fluorophore is less sensitive or insensitive to the E_m and thus to changes in the E_m. In contrast, the FLT is sensitive to the E_m when the GFP tag is located very close to the surface of the plasma membrane, which we assume to be the case for BRI1–GFP. However, without

knowing the exact structure of BRI1, and in particular the distance of the GFP tag to the inner plasma membrane surface, the exact molecular basis for the specific sensitivity of BRI1–GFP to the E_m remains an open question. Alternatively, as BRI1–GFP is associated with the P-ATPase, the change in the FLT could also result from the close proximity of the GFP tag to the BL-activated proton pump. Due to its association with P-ATPase, the FLT of BRI1–GFP shows the most dramatic local changes in the E_m.

P-ATPase activity is required for BL-regulated cell-wall expansion and changes in the FLT of BRI1–GFP

Sodium acetate, which equilibrates the pH gradient over the plasma membrane, represses the BL-controlled cell-wall expansion and the change in the FLT of BRI1–GFP. Interestingly, we did not detect the organic acid stress-induced activation of P-ATPase reported for the tobacco P-ATPase PMA2 in tobacco BY2 cells (Bobik *et al.*, 2010). PMA2 has been suggested to be responsible for the maintenance of cytoplasmic proton homeostasis (Bobik *et al.*, 2010). This indicates that other proton pumps such as the vacuolar H^+-ATPase and H^+-pyrophosphatase contribute efficiently to regulation of the cytoplasmic pH in Arabidopsis seedlings under organic acid stress.

*o*V, an inhibitor of the P-ATPase that controls the E_m in the plasma membrane (Schaller and Oecking, 1999), abolishes the BL-induced change in the FLT of BRI1–GFP and cell-wall expansion. Both responses recurred when *o*V was washed out before application of the hormone. In addition, application of Fc, an activator of the P-ATPase, is sufficient to induce changes in the FLT of BRI1–GFP in BRI1–GFP-expressing cells and cell-wall expansion in all tested Arabidopsis lines, and was able to reverse the inhibiting effect of *o*V. These observations suggest that plasma membrane hyperpolarization is a pre-condition for both responses, and that the change in the E_m is controlled by the P-ATPase.

If the effect of BL on cell-wall expansion and the change in the FLT of BRI1–GFP are causally linked to E_m hyperpolarization, the hormone would be expected to induce an alteration in the E_m *in planta*. We observed a concentration-dependent BL-induced E_m hyperpolarization in wild-type and BRI1–GFP-expressing cells. There was no significant difference between BRI1–GFP-expressing and wild-type cells. This result indicates that, under our assay conditions, the amount of BRI1 receptor molecules is not limiting for induction of E_m hyperpolarization, or that the cells avoid extreme E_m hyperpolarization by compensation using other transport processes across the plasma membrane. Interestingly, the root cells of the BRI1–GFP-expressing seedlings showed BL-dependent changes in the E_m, consistent with the finding that plasma membrane hyperpolarization elicited by two brassinosteroids (28-homobrassinolide and 28-homocastasterone) is concentration-dependent in Arabidopsis suspension cells (Zhang *et al.*, 2005). The loss of E_m sensitivity to increasing BL in wild-type and the BL-dependent hyperpolarization in the BRI1–GFP-expressing cells can be readily understood in the context of the difference in membrane conductances that balance any changes in current caused by the P-ATPase. These results are in agreement with similar studies on the effects of Fc, for example, on secondary conductances (Blatt, 1987; Blatt and Clint, 1989; van den Wijngaard *et al.*, 2005) in addition to P-ATPase. Although a more detailed explanation would require combined measurements under voltage clamp conditions to quantify membrane conductance (Blatt and Clint, 1989), the changes in plasma membrane voltage in the two sets of experiments are nonetheless sufficient to confirm the measured changes in fluorescence lifetime of BRI1-GFP.

Regulation of BL-induced cell-wall expansion is a complex process

BR-induced cell elongation accompanied by proton extrusion and membrane hyperpolarization have been reported for various organs and suspension cells of several plant species (Cerana *et al.*, 1983, 1984, 1985; Katsumi, 1985; Haubrick and Assmann, 2006). However, no reports have been published that described the *in planta* prerequisite for BR-induced cell elongation, i.e. the relaxation and expansion of the wall, at this high spatial resolution. The acidification of the apoplast of hypocotyl cells to pH 5.5, which is naturally observed in the apoplast of cells in the root elongation zone (Li *et al.*, 2005), is not sufficient to cause significant wall expansion. Hyperpolarization of the plasma membrane alone was able to initiate a small but significant wall expansion. However, by combining acidification and E_m hyperpolarization, the degree of response was synergistically enhanced. These data indicate that synergistically acting pH-dependent and E_m-dependent mechanisms participate in the regulation of wall expansion. The pH-dependent mechanism could include activation of the enzymatic activity of apoplastic expansins, leading to wall loosening, water uptake into the apoplast and wall swelling (Cho and Cosgrove, 2004; Zhang *et al.*, 2005; Sanchez-Rodriguez *et al.*, 2010). The E_m-dependent mechanism remains unclear, but could be linked to the membrane transport processes required for continuous wall expansion, such as osmoregulation and maintenance of the wall's capacity to undergo acid-induced wall loosening (Rayle and Cleland, 1992; Zhang *et al.*, 2005). Intriguingly, exogenously applied BL causes even more significant wall expansion than the combination of acidification and HVS-induced E_m hyperpolarization. Either BL is able to initiate an even higher local wall acidification and E_m hyperpolarization, or a third component exists that contributes to the BL-controlled response. This component may be another phytohormone such as auxin. In a variety of bioassays in diverse plant species, auxin has been shown to synergistically promote

cell elongation together with BR at various regulatory levels (Mandava, 1988; Halliday, 2004; Nemhauser *et al.*, 2004; Sanchez-Rodriguez *et al.*, 2010). As shown here, auxin itself is able to cause wall expansion within 30 min of application. It is therefore reasonable to speculate that BL addition causes activation of an auxin response pathway that enhances the BL response in regulation of wall expansion.

BRI1 may regulate P-ATPase activity by phosphorylation via protein–protein interaction

As shown by Goda *et al.* (2008), expression of the P-ATPase genes is not altered within 30 min after BL application. Thus, BL-induced up-regulation of P-ATPase activity for induction of wall expansion and the change in the FLT of BRI1–GFP must be accomplished at the post-translational level. It is well known that P-ATPase activity is kept at a low level by its C-terminal auto-inhibitory domain, and is controlled by reversible phosphorylation of this domain (Portillo, 2000; Speth *et al.*, 2010). Our FRET data, supported by the mbSUS results, indicate that BRI1–GFP interacts specifically with the P-ATPase AHA1 in transiently transformed *N. benthamiana* leaf cells and in yeast. *In planta*, a significant, BL-induced change in the BRI1/AHA1 association was observed. These data suggest that BRI1 and AHA1 may *a priori* form transient complexes in the plasma membrane, which can be modulated by BL. Interestingly, formation of a transient protein complex was also observed for BRI1/BAK1 heteromers in the plasma membrane of Arabidopsis protoplasts (Russinova *et al.*, 2004).

BL-regulated modulation of the BRI1/AHA1 association may be required to enhance activity of the P-ATPase, and could be achieved by phosphorylation of the P-ATPase's C-terminal autoinhibitory domain by BRI1. Although we do not yet have evidence for direct phosphorylation of the P-ATPase, BRI1 kinase activity is required for the change in the FLT of BRI1–GFP and E_m hyperpolarization. As an alternative to direct phosphorylation, BRI1 kinase activity-dependent recruitment of another kinase to the BL-modulated BRI1/P-ATPase complex could induce activation of the pump.

Interestingly, Arabidopsis BRI1–GFP is not able to mediate BL-induced enhancement of the P-ATPase activity and a change in the E_m when expressed in *Nicotiana benthamiana* alone. This is surprising, because tobacco P-ATPase homologues are expected to be present in the plasma membrane of tobacco leaf epidermal cells. This observation emphasizes that either the Arabidopsis BRI1 does not recognize the tobacco P-ATPase sufficiently well to be able to activate the enzyme, or that the amount of tobacco P-ATPase protein is too low in leaf epidermal cells to induce a detectable E_m hyperpolarization in response to BL.

In summary, combination of high-resolution CSSM, one-chromophore FLT spectroscopy and FRET measurements revealed that a BR signalling process exists in the plasma membrane, which rapidly couples BRI1 to P-ATPase to control BL-regulated cell-wall expansion. Use of non-phosphorylatable AHA1 mutants and introduction of the *BRI1–GFP* gene into Arabidopsis lines mutated in other BR signalling elements or components of other hormone signal response pathways will enable us to quantitatively dissect the molecular mechanism of this subcellular physiological process in living plant cells.

EXPERIMENTAL PROCEDURES

Plant material and growth conditions

Wild-type seedlings and seedlings expressing eGFP fusions of BRI1, LTI6b or PMA4 (Cutler *et al.*, 2000; Friedrichsen *et al.*, 2000; Lefebvre *et al.*, 2004) were grown for 5 days at 22°C under 14 h light per 10 h darkness on 0.5× MS agar medium. For measurements, seedlings were prepared as described previously (Elgass *et al.*, 2009). For analysis of cell-wall expansion and FLT in the presence of BL, Fc and *o*V, the seedlings were incubated for the time periods indicated in the figure legends and Results.

Generation of constructs and RT-PCR

AttB sites were added via PCR-mediated ligation to the coding regions of *BRI1* (AT4G39400), *BAK1* (AT4G33430), *AHA1* (AT2G18960) and *LTI6b* (*RCI2B*; AT3G05890), and recombined into pDONR^{TM}201 (http://www.invitrogen.com). The BRI1 kinase-inactive mutant was generated by site-directed mutagenesis using Phusion® high-fidelity DNA polymerase (New England Biolabs, http://www.neb.com/) with the BRI1 BRI1 pDONRTM201 clone as template, resulting in a K911 → E substitution in the BRI1 kinase domain. For FRET analyses, the cDNAs were transferred via LR reactions into the destination vectors pABindGFP, pABindmCherry or pABindFRET (Bleckmann *et al.*, 2010); for the mbSUS study, the cDNAs were transferred into pMetYC-Dest or pXNubA22 (Grefen *et al.*, 2009); for the transient expression of BRI1–GFP, BRI1^{KE}–GFP and AHA1 in tobacco leaf cells, the corresponding cDNAs were transferred into pH7FWG2 or pB7WG2 (Karimi *et al.*, 2002). For RT-PCR, total RNA from leaf discs of transiently transformed tobacco was isolated as described by Chomczynski (1993) and reverse-transcribed using RevertAid^{TM} H Minus reverse transcriptase (Fermentas, http://www.fermentas.de) using oligo(dT) primers. The cDNA was used as a template for PCR, with 28 cycles for amplification of *AHA1* and 22 cycles for *NbActin*. The primer sequences are 5′-GCCACACTGTCCCAATTTATGA-3′ (*NbActin-S*), 5′-GAAGCCAAGATAGAGCCTCCTA-3′ (*NbActin-A*), 5′-GACAATCTCTTGGTCCTCTTG-3′ (*AHA1-S*) and 5′-CACAGTGTAGTGATGTCCTGCTGT-3′ (*AHA1-A*).

Transient transformation of *Nicotiana benthamiana* leaves and yeast mbSUS assay

Agrobacterium tumefaciens strain GV3101 pMP90 was transformed using the expression clones and suspended in AS medium (10 mM $CaCl_2$, 150 μM acetosyringone, 10 mM MES pH 5.7) to an OD_{600} of 0.8 prior to infiltration. *Agrobacterium* strains containing the GFP, mCherry or FRET construct(s) and the p19 silencing inhibitor plasmid were mixed 1:1:1 (triple transformation) or 1:1 (double transformation), respectively, and co-infiltrated into leaves of 2–4-week-old tobacco plants, as described previously (Schütze *et al.*, 2009). Expression was induced using 20 μM β-oestradiol, supplemented with 0.1% Tween-20, 48–96 h after infiltration. FRET studies and imaging were performed within 2–8 h after induction. The mbSUS assay was performed as described previously (Grefen *et al.*, 2009).

Spectro-microscopic measurements, data analysis and FRET-FIDSAM

The spectro-microscopic system and measurement protocols have been described previously (Elgass *et al.*, 2009). Processing of fluorescence intensity images was accomplished using WSxM software (Nanotec Electronica, http://www.nanotec.es). Data analysis was performed as described by Elgass *et al.* (2009). The FRET-FIDSAM analysis is based on a commonly used time correlated single photon counting-FLIM protocol to record fluorescence intensity decay curves in a spatially resolved way. If no acceptor is present, typical donor chromophore fluorescence decay curves obey a basic power law with one single decay time constant and thus can be well described by a mono-exponential fit function (Schleifenbaum *et al.*, 2009):

$$I(t) = I_0 \cdot \exp\left(-\frac{t}{\tau}\right) \quad (1)$$

with t = time and I_0 being the intensity at t = 0. τ represents the characteristic decay time constant. The presence of an acceptor chromophore introduces an additional, non-radiative relaxation path for the excited state of the donor. Due to this additional relaxation pathway, with the time constant $1/k_{ET}$, where k_{ET} is the energy transfer rate, the measured donor fluorescence decay constant decreases in the presence of an acceptor chromophore as soon as k_{ET} is not zero. Due to this additional short decay component, the resulting donor intensity decay no longer obeys a mono-exponential power law but has to be described by at least two decay constants. Thus, fitting the donor intensity decay in the presence of an acceptor to a mono-exponential analytical expression (see eqn 1) results in increasing deviations for increasing FRET rates, which can be quantified by the fitting error value chi-square. Accordingly, this error value can be used directly for robust determination of FRET. The FRET-FLIM and FRET-FIDSAM analyses were performed at the whole-cell level.

Statistics

The statistical analysis was performed using Excel software (http://www.microsoft.com/). The data were analysed using a one-tailed, unpaired *t* test. Unless otherwise noted, the FLT standard deviations shown in the figures do not represent the FLT deviations of all recorded cells but instead represent the FLT error inherent in the measurements itself (e.g. temporal resolution of the avalanche photodiode and/or the FLT recording software). The number of independent FLT measurements (n) and the P values (P) for each experiment and statistical evaluation of ΔFLT values are given in the Results, the figure legends, and the Supporting information. The statistics for the FRET-FIDSAM or FLIM-FRET measurements are given in the Results and the legend to Figure S6.

Electrophysiology

Arabidopsis seedlings were grown under a cycle of 16 h light (65 μmol m^{-2} sec^{-1}), 22°C per 8 h dark, 18°C, and 14–16-day-old plants were used for the E_m measurements. SigmaPlot 11 (http://www.sigmaplot.com) was used to perform *t* tests on the data. The electrophysiological set-up and recording methods were previously described in detail by Blatt (1987). Whole seedlings were affixed by three pieces of rubber to the glass bottom of the experimental chamber after the chamber surface had been coated with pressure-sensitive silicone adhesive. All operations were performed on an Axiovert 35 microscope (Zeiss, http://www.zeiss.com/) fitted with Nomarski differential interference contrast optics. Micro-electrodes were back-filled with 1 M KCl and connected to the head stage of an amplifier via 1 M KCl Ag/AgCl half cells. A 1 M KCl–agar bridge served as the reference electrode. Membrane potential data were continuously collected at a rate of 1 kHz using the Vicar 3 program of Henry's EP Suite software (http://www.psrg.org.uk/henrys-ep-suite.htm). Measurements were performed in continuous flowing solutions controlled by a gravity feeding system at room temperature. The standard perfusion medium contained 0.1 mM KCl and 5 mM 2-(*N*-morpholino)propanesulfonic acid (MES), which was titrated with $Ca(OH)_2$ to a pK_a of 6.1. Statistical analysis was performed using SigmaPlot for *t* tests of the data.

ACKNOWLEDGEMENTS

We thank A. Bleckmann and R. Simon for the FRET vectors, Marc Boutry for the PMA4–GFP construct, and Karin Schumacher for the PMA4–GFP seeds. We also thank Felicity de Courcy for proofreading the manuscript. This work was supported by Deutsche Forschungsgemeinschaft grants to K.H. (HA 2146/10-1) and C.O. (SFB 446), fellowships from the State of Baden-Württemberg and the University of Tübingen to K.C., K.E. and F.S., and Biotechnology and Biological Sciences Research Council grants to M.R.B. (BB/F001673/1, BB/F001630/1). All materials described in this article will be made available for non-commercial research purposes upon request.

SUPPORTING INFORMATION

Additional Supporting Information may be found in the online version of this article:

Figure S1. The FLT of GFP–LTI6b is not influenced by the membrane potential (E_m).

Figure S2. Representative membrane potential measurements recorded from root epidermal cells of Col-0 and BRI1–GFP-expressing plants.

Figure S3. BL induces E_m hyperpolarization in root cells.

Figure S4. The FLT of BRI1–GFP is modulated by P-ATPase activity.

Figure S5. BAK1 forms homomers and interacts with BRI1 in mbSUS.

Figure S6. FRET-FLIM studies demonstrate the association of BRI1–GFP with P-ATPase in the plasma membrane of tobacco leaf cells.

Table S1. ΔFLT values for BRI1–GFP-expressing seedlings treated with BL, sodium acetate, sodium acetate plus BL, and auxin.

Table S2. FLT values recorded in Arabidopsis cells expressing either PMA4–GFP, GFP–LTI6b or BRI1–GFP and exposed to LVS or HVS.

Table S3. FLT values recorded in Arabidopsis cells expressing either BRI1–GFP or GFP–LTI6b and exposed to *o*V or Fc.

Appendix S1. BL-induced changes in the turgor, intracellular pH, temperature and refractive index do not cause alterations in the FLT of BRI1–GFP.

Please note: As a service to our authors and readers, this journal provides supporting information supplied by the authors. Such materials are peer-reviewed and may be re-organized for online delivery, but are not copy-edited or typeset. Technical support issues arising from supporting information (other than missing files) should be addressed to the authors.

REFERENCES

Allen, G.J., Chu, S.P., Harrington, C.L., Schumacher, K., Hoffman, T., Tang, Y.Y., Grill, E. and Schroeder, J.I. (2001) A defined range of guard cell calcium oscillation parameters encodes stomatal movements. *Nature*, **411**, 1053–1057.

Ashby, M.C., Ibaraki, K. and Henley, J.M. (2004) It's green outside: tracking cell surface proteins with pH-sensitive GFP. *Trends Neurosci.* **27**, 257–261.

Blatt, M.R. (1987) Electrical characteristics of stomatal guard-cells – the ionic basis of the membrane-potential and the consequence of KCl leakage from microelectrodes. *Planta*, **170**, 272–287.

Blatt, M.R. and Clint, G.M. (1989) Mechanisms of fusicoccin action – kinetic modification and inactivation of K+ channels in guard-cells. *Planta*, **178**, 509–523.

Bleckmann, A., Weidtkamp-Peters, S., Seidel, C.A. and Simon, R. (2010) Stem cell signaling in Arabidopsis requires CRN to localize CLV2 to the plasma membrane. *Plant Physiol.* **152**, 166–176.

Bobik, K., Boutry, M. and Duby, G. (2010) Activation of the plasma membrane H^+-ATPase by acid stress: antibodies as a tool to follow the phosphorylation status of the penultimate activating Thr. *Plant Signal. Behav.* **5**, 681–683.

Cerana, R., Bonetti, A., Marre, M.T., Romani, G., Lado, P. and Marre, E. (1983) Effects of a brassinosteroid on growth and electrogenic proton extrusion in Azuki bean epicotyls. *Physiol. Plant.* **59**, 23–27.

Cerana, R., Lado, P., Anastasia, M., Ciuffreda, P. and Allevi, P. (1984) Regulating effect of brassinosteroids and of sterols on growth and H^+-secretion in maize roots. *Z. Pflanzenphysiol.* **114**, 221–225.

Cerana, R., Spelta, M., Bonetti, A. and Lado, P. (1985) On the effects of cholesterol on H^+ extrusion and on growth in maize root segements: comparison with brassinosteroid. *Plant Sci.* **38**, 99–105.

Chinchilla, D., Shan, L., He, P., de Vries, S. and Kemmerling, B. (2009) One for all: the receptor-associated kinase BAK1. *Trends Plant Sci.* **14**, 535–541.

Cho, H.T. and Cosgrove, D.J. (2004) Expansins as agents in hormone action. In *Plant Hormones: Biosynthesis, Signal Transduction, Action* (Davies, P.J., ed.). Dordrecht, the Netherlands: Kluwer Academic Publishers, pp. 262–281.

Chomczynski, P. (1993) A reagent for the single-step simultaneous isolation of RNA, DNA and proteins from cell and tissue samples. *BioTechniques*, **15**, 532–534, 536–537.

Cleland, R.E. (2004) Auxin and cell elongation. In *Plant Hormones, Biosynthesis, Signal Transduction, Action* (Davies, P.J., ed.). Dordrecht, the Netherlands: Kluwer Academic Publishers, pp. 204–220.

Clouse, S.D. (2004) Brassinosteroid signal transduction and action. In *Plant Hormones: Biosynthesis, Signal Transduction, Action* (Davies, P.J., ed.). Dordrecht, the Netherlands: Kluwer Academic Publishers, pp. 413–436.

Clouse, S.D. and Sasse, J.M. (1998) Brassinosteroids: essential regulators of plant growth and development. *Annu. Rev. Plant Physiol. Plant Mol. Biol.* **49**, 427–451.

Cutler, S.R., Ehrhardt, D.W., Griffitts, J.S. and Somerville, C.R. (2000) Random GFP::cDNA fusions enable visualization of subcellular structures in cells of Arabidopsis at a high frequency. *Proc. Natl Acad. Sci. USA*, **97**, 3718–3723.

Dixit, R., Cyr, R. and Gilroy, S. (2006) Using intrinsically fluorescent proteins for plant cell imaging. *Plant J.* **45**, 599–615.

Dupre, E. and Schaaf, G. (1996) Influence of ions on the unfolding of the spermatozoa of the rock shrimp, *Rhynchocinetes typus*. *J. Exp. Zool.* **274**, 358–364.

Elgass, K., Caesar, K., Schleifenbaum, F., Stierhof, Y.D., Meixner, A.J. and Harter, K. (2009) Novel application of fluorescence lifetime and fluorescence microscopy enables quantitative access to subcellular dynamics in plant cells. *PLoS ONE*, **4**, e5716.

Elgass, K., Caesar, K., Schleifenbaum, F., Meixner, A.J. and Harter, K. (2010) The fluorescence lifetime of BRI1–GFP as probe for the noninvasive determination of the membrane potential in living cells. *Proc. SPIE*, **7568**, 756804.

Friedrichsen, D. and Chory, J. (2001) Steroid signaling in plants: from the cell surface to the nucleus. *Bioessays*, **23**, 1028–1036.

Friedrichsen, D.M., Joazeiro, C.A., Li, J., Hunter, T. and Chory, J. (2000) Brassinosteroid-insensitive-1 is a ubiquitously expressed leucine-rich repeat receptor serine/threonine kinase. *Plant Physiol.* **123**, 1247–1256.

Giepmans, B.N.G., Adams, S.R., Ellisman, M.H. and Tsien, R.Y. (2006) The fluorescent toolbox for assessing protein location and function. *Science*, **312**, 217–224.

Goda, H., Sasaki, E., Akiyama, K. *et al.* (2008) The AtGenExpress hormone and chemical treatment data set: experimental design, data evaluation, model data analysis and data access. *Plant J.* **55**, 526–542.

Grabov, A. and Blatt, M.R. (1998) Membrane voltage initiates Ca^{2+} waves and potentiates Ca^{2+}increases with abscisic acid in stomatal guard cells. *Proc. Natl Acad. Sci. USA*, **95**, 4778–4783.

Grainger, J.L., Winkler, M.M., Shen, S.S. and Steinhardt, R.A. (1979) Intracellular pH controls protein synthesis rate in the sea urchine egg and early embryo. *Dev. Biol.* **68**, 396–406.

Grefen, C., Obrdlik, P. and Harter, K. (2009) The determination of protein–protein interactions by the mating-based split-ubiquitin system (mbSUS). *Methods Mol. Biol.* **479**, 217–233.

Halliday, K.J. (2004) Plant hormones: the interplay of brassinosteroids and auxin. *Curr. Biol.* **14**, R1008–R1010.

Haruta, M., Burch, H.L., Nelson, R.B., Barrett-Wilt, G., Kline, K.G., Mohsin, S.B., Young, J.C., Otegui, M.S. and Sussman, M.R. (2010) Molecular characterization of mutant Arabidopsis plants with reduced plasma membrane proton pump activity. *J. Biol. Chem.* **285**, 17918–17929.

Haubrick, L.L. and Assmann, S.M. (2006) Brassinosteroids and plant function: some clues, more puzzles. *Plant Cell Environ.* **29**, 446–457.

Johnson, C.H. and Epel, D. (1981) Intracellular pH of sea urchin eggs measured by the dimethyloxazolidinedione (DMO) method. *J. Cell Biol.* **89**, 284–291.

Karimi, M., Inze, D. and Depicker, A. (2002) GATEWAY vectors for *Agrobacterium*-mediated plant transformation. *Trends Plant Sci.* **7**, 193–195.

Katsumi, M. (1985) Interaction of a brassinosteroid with IAA and GA3 in the elongation of cucumber hypocotyl sections. *Plant Cell Physiol.* **26**, 615–625.

Lefebvre, B., Batoko, H., Duby, G. and Boutry, M. (2004) Targeting of a *Nicotiana plumbaginifolia* H^+-ATPase to the plasma membrane is not by default and requires cytosolic structural determinants. *Plant Cell*, **16**, 1772–1789.

Li, J.M. and Jin, H. (2007) Regulation of brassinosteroid signaling. *Trends Plant Sci.* **12**, 37–41.

Li, J., Yang, H., Peer, W.A. *et al.* (2005) Arabidopsis H^+-PPase AVP1 regulates auxin-mediated organ development. *Science*, **310**, 121–125.

MacLennan, D.H., Rice, W.J. and Green, N.M. (1997) The mechanism of Ca^{2+}transport by sarco(endo)plasmic reticulum Ca^{2+}-ATPases. *J. Biol. Chem.* **272**, 28815–28818.

Mandava, N.B. (1988) Plant growth-promoting brassinosteroids. *Annu. Rev. Plant Physiol. Plant Mol. Biol.* **39**, 23–52.

van Manen, H.J., Verkuijlen, P., Wittendorp, P., Subramaniam, V., van den Berg, T.K., Roos, D. and Otto, C. (2008) Refractive index sensing of green fluorescent proteins in living cells using fluorescence lifetime imaging microscopy. *Biophys. J.* **94**, L67–L69.

Marre, E. (1979) Fusicoccin – tool in plant physiology. *Annu. Rev. Plant Physiol. Plant Mol. Biol.* **30**, 273–288.

Meyer, A.J. and Brach, T. (2009) Dynamic redox measurements with redox-sensitive GFP in plants by confocal laser scanning microscopy. *Methods Mol. Biol.* **479**, 93–107.

Moseyko, N. and Feldman, L.J. (2001) Expression of pH-sensitive green fluorescent protein in *Arabidopsis thaliana*. *Plant Cell Environ.* **24**, 557–563.

Nakabayashi, T., Wang, H.P., Kinjo, M. and Ohta, N. (2008) Application of fluorescence lifetime imaging of enhanced green fluorescent protein to intracellular pH measurements. *Photochem. Photobiol. Sci.* **7**, 668–670.

Nemhauser, J.L., Mockler, T.C. and Chory, J. (2004) Interdependency of brassinosteroid and auxin signaling in Arabidopsis. *PLoS Biol.* **2**, 1460–1471.

Oh, M.H., Ray, W.K., Huber, S.C., Asara, J.M., Gage, D.A. and Clouse, S.D. (2000) Recombinant brassinosteroid insensitive 1 receptor-like kinase autophosphorylates on serine and threonine residues and phosphorylates a conserved peptide motif *in vitro*. *Plant Physiol.* **124**, 751–766.

Ohta, N., Nakabayashi, T., Oshita, S. and Kinjo, M. (2010) Fluorescence lifetime imaging spectroscopy in living cells with particular regards to pH dependence and electric field effect. *Proc. SPIE*, **7576**, 75760G.

Orij, R., Postmus, J., Ter Beek, A., Brul, S. and Smits, G.J. (2009) *In vivo* measurement of cytosolic and mitochondrial pH using a pH-sensitive GFP derivative in *Saccharomyces cerevisiae* reveals a relation between intracellular pH and growth. *Microbiology*, **155**, 268–278.

Portillo, F. (2000) Regulation of plasma membrane H^+-ATPase in fungi and plants. *Biochim. Biophys. Acta*, **1469**, 31–42.

Rayle, D.L. and Cleland, R.E. (1992) The acid growth theory of auxin-induced cell elongation is alive and well. *Plant Physiol.* **99**, 1271–1274.

Romani, G., Marré, M.T., Bonetti, A., Cerana, R., Lado, P. and Marré, E. (1983) Effects of a brassinosteroid on growth and electrogenic proton extrusion in maize segments. *Physiol. Plant.* **59**, 528–532.

Russinova, E., Borst, J.W., Kwaaitaal, M., Cano-Delgado, A., Yin, Y., Chory, J. and de Vries, S.C. (2004) Heterodimerization and endocytosis of

Arabidopsis brassinosteroid receptors BRI1 and AtSERK3 (BAK1). *Plant Cell*, **16**, 3216–3229.

Sanchez-Rodriguez, C., Rubio-Somoza, I., Sibout, R. and Persson, S. (2010) Phytohormones and the cell wall in Arabidopsis during seedling growth. *Trends Plant Sci.* **15**, 291–301.

Schaller, A. and Oecking, C. (1999) Modulation of plasma membrane H^+-ATPase activity differentially activates wound and pathogen defense responses in tomato plants. *Plant Cell*, **11**, 263–272.

Schleifenbaum, F., Elgass, K., Sackrow, M., Caesar, K., Berendzen, K., Meixner, A.J. and Harter, K. (2009) Fluorescence intensity decay shape analysis microscopy (FIDSAM) for quantitative and sensitive live-cell imaging. *Mol. Plant*, **3**, 555–562.

Schütze, K., Harter, K. and Chaban, C. (2009) Bimolecular fluorescence complementation (BiFC) to study protein–protein interactions in living plant cells. *Methods Mol. Biol.* **479**, 189–202.

Speth, C., Jaspert, N., Marcon, C. and Oecking, C. (2010) Regulation of the plant plasma membrane H^+-ATPase by its C-terminal domain: what do we know for sure? *Eur. J. Cell Biol.* **89**, 145–151.

Suzuki, T., Matsuzaki, T., Hagiwara, H., Aoki, T. and Takata, K. (2007) Recent advances in fluorescent labeling techniques for fluorescence microscopy. *Acta Histochem. Cytochem.* **40**, 131–137.

Szymanski, D.B. and Cosgrove, D.J. (2009) Dynamic coordination of cytoskeletal and cell wall systems during plant cell morphogenesis. *Curr. Biol.* **19**, R800–R811.

Vert, G., Nemhauser, J.L., Geldner, N., Hong, F.X. and Chory, J. (2005) Molecular mechanisms of steroid hormone signaling in plants. *Annu. Rev. Cell Dev. Biol.* **21**, 177–201.

Wang, X., Goshe, M.B., Soderblom, E.J., Phinney, B.S., Kuchar, J.A., Li, J., Asami, T., Yoshida, S., Huber, S.C. and Clouse, S.D. (2005) Identification and functional analysis of *in vivo* phosphorylation sites of the Arabidopsis BRASSINOSTEROID-INSENSITIVE1 receptor kinase. *Plant Cell*, **17**, 1685–1703.

Wang, Y.X., Shyy, J.Y.J. and Chien, S. (2008) Fluorescence proteins, live-cell imaging, and mechanobiology: seeing is believing. *Annu. Rev. Biomed. Eng.* **10**, 1–38.

van den Wijngaard, P.W., Sinnige, M.P., Roobeek, I., Reumer, A., Schoonheim, P.J., Mol, J.N., Wang, M. and De Boer, A.H. (2005) Abscisic acid and 14-3-3 proteins control K channel activity in barley embryonic root. *Plant J.* **41**, 43–55.

Wurtele, M., Jelich-Ottmann, C., Wittinghofer, A. and Oecking, C. (2003) Structural view of a fungal toxin acting on a 14-3-3 regulatory complex. *EMBO J.* **22**, 987–994.

Zhang, Z., Ramirez, J., Reboutier, D., Brault, M., Trouverie, J., Pennarun, A.M., Amiar, Z., Biligui, B., Galagovsky, L. and Rona, J.P. (2005) Brassinosteroids regulate plasma membrane anion channels in addition to proton pumps during expansion of *Arabidopsis thaliana* cells. *Plant Cell Physiol.* **46**, 1494–1504.

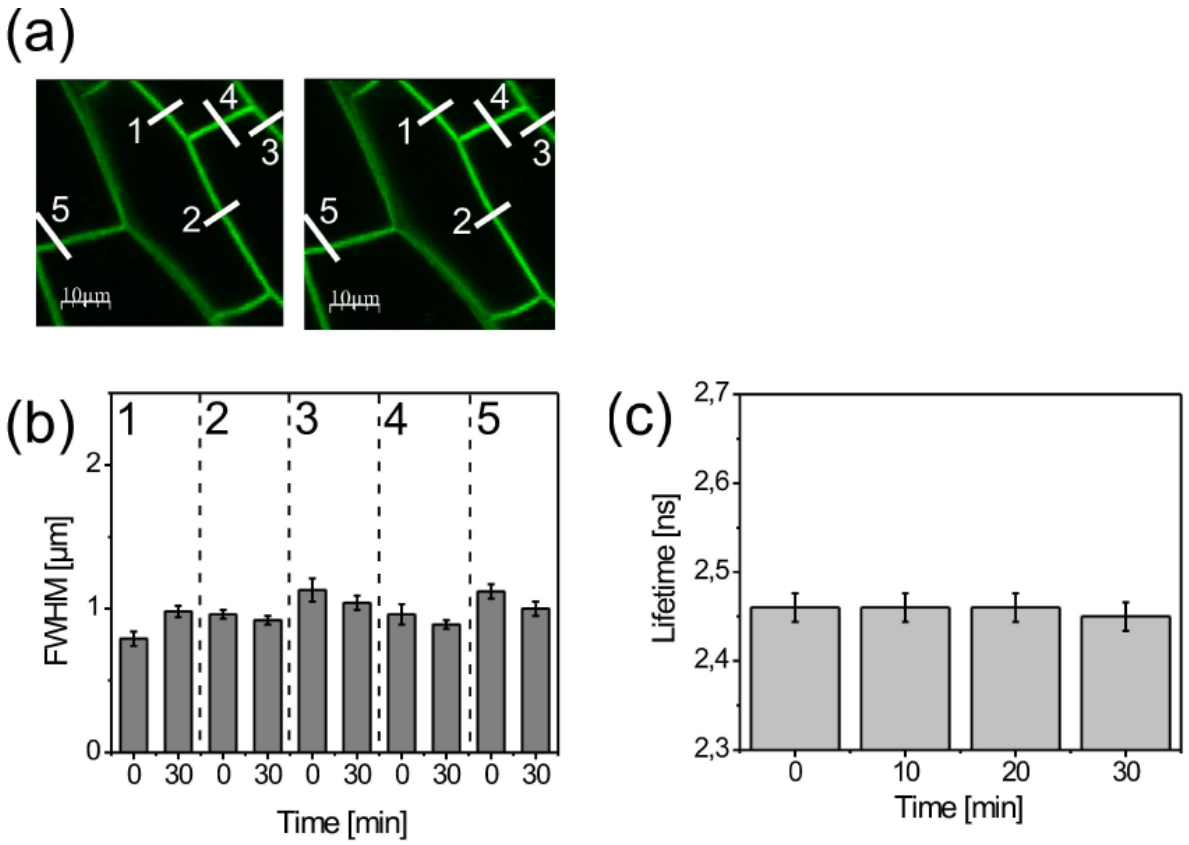

Figure S1. The FLT of GFP-LTI6b is not influenced by the membrane potential (E_m). (a) Confocal images of hypocotyl cells before (0 min) and 30 min after application of high voltage solution (hyperpolarisation). (b) FWHM values of the plasmalemmata-cell wall sections in LTI6B-GFP expressing cells indicated by the white lines in (a) before (0 min) and 30 min after addition of high voltage solution. (c) FLT of GFP-LTI6b recorded before (0 min) and 5, 10, 20 and 30 min after addition of high voltage solution.

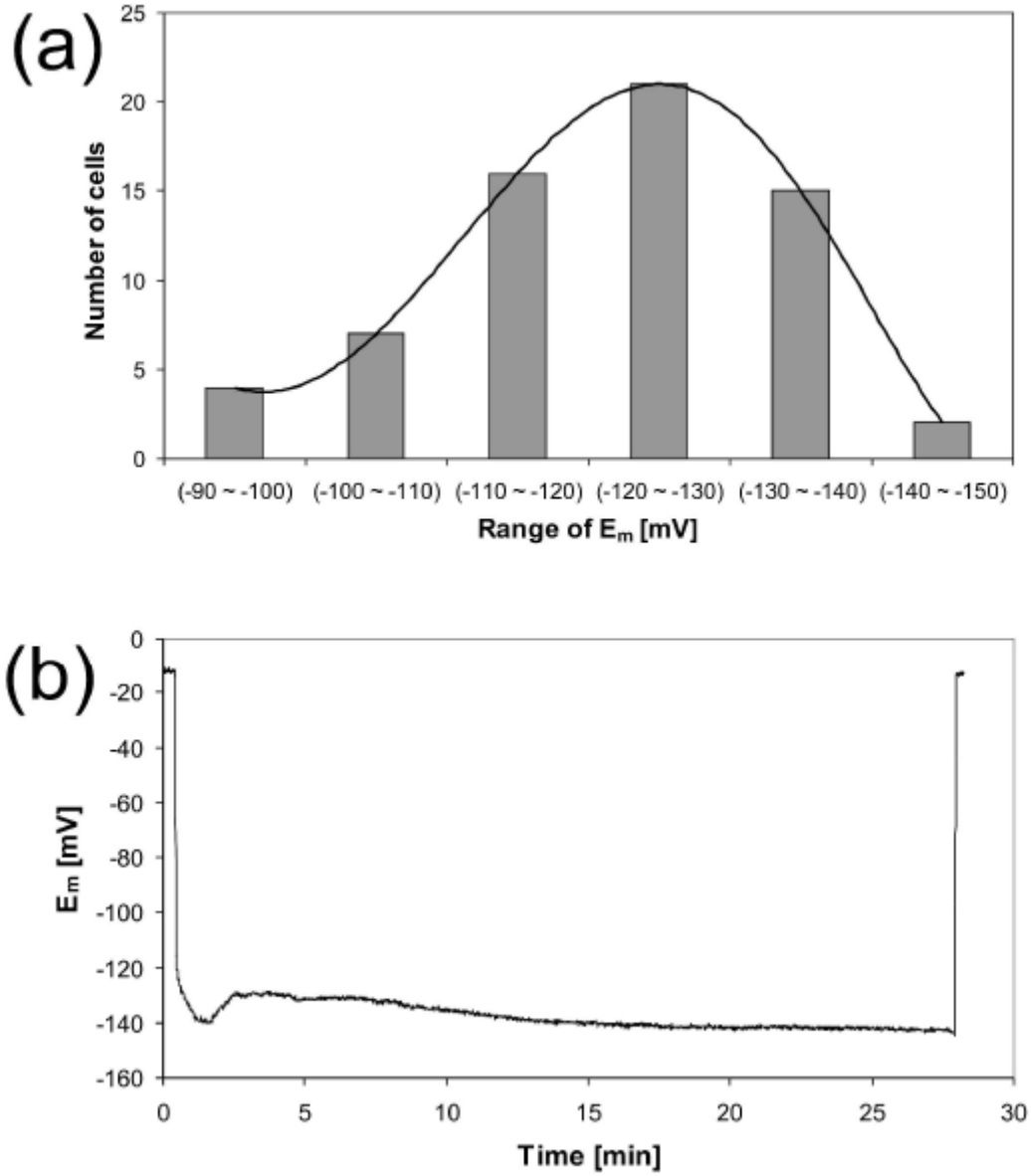

Figure S2. Representative membrane potential measurements recorded from root epidermal cells of Col-0 and BRI1-GFP-expressing plants. (a) The distribution of E_m measured from all root epidermal cells under control condition with 1 mM KCl. (b) A representative E_m measurement in a root epidermal cell of Col-0. The cell was impaled with a single electrode at 1 min in 5 mM Ca^{2+}-MES with 0.1 mM KCl, then switched to 1 mM KCl at 2 min. 10 nM BL was applied at 5 min for a duration over 20 min. Experiment was halted by pulling the electrode out the cell at minute 28.

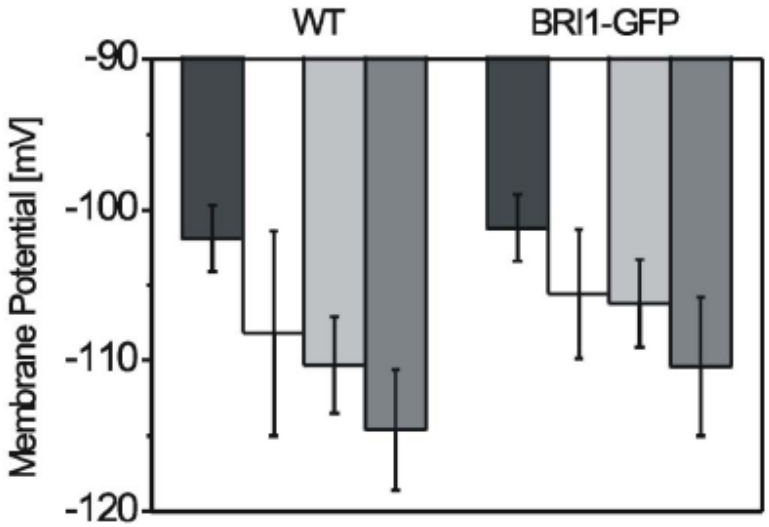

Figure S3. Brassinolide (BL) induces membrane hyperpolarization of root epidermal cells in Col-0 wildtype and BRI1-GFP-expressing plants. Membrane potential values (E_m) of root epidermal cells treated with 10 nM (white bar), 50 nM (grey bar) or 100 nM (dark grey bar) BL. All measurements were undertaken in a 5 mM Ca^{2+}-MES buffer with 1 mM KCl (data are mean ± S.E. n=4 to 14 for each treatment).

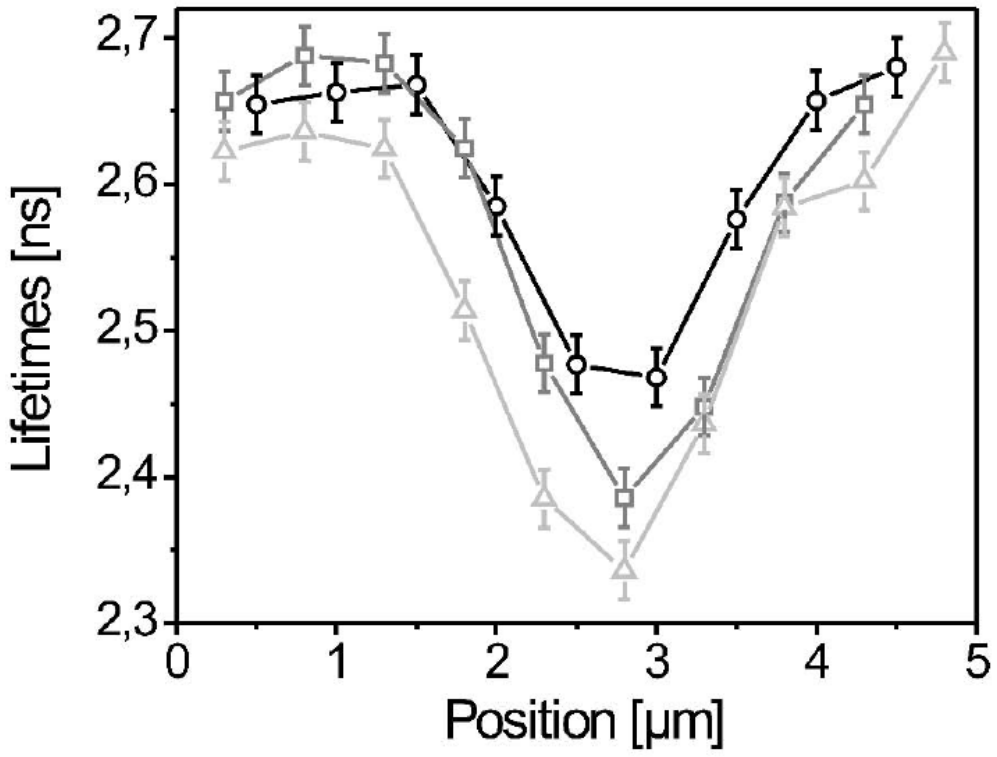

Figure S4. The FLT of BRI1-GFP is modulated by P-ATPase activity in hypocotyl cells. Kinetics of the FLT recovery over a plasmalemmata-cell wall section of two adjacent cells. The seedlings were pre-treated for 30 min with 50 µM *o*V (black circles). After washing out the *o*V, Fc (2 µM) was added and the FLT recorded after 15 min (dark grey squares) and 30 min (grey triangles).

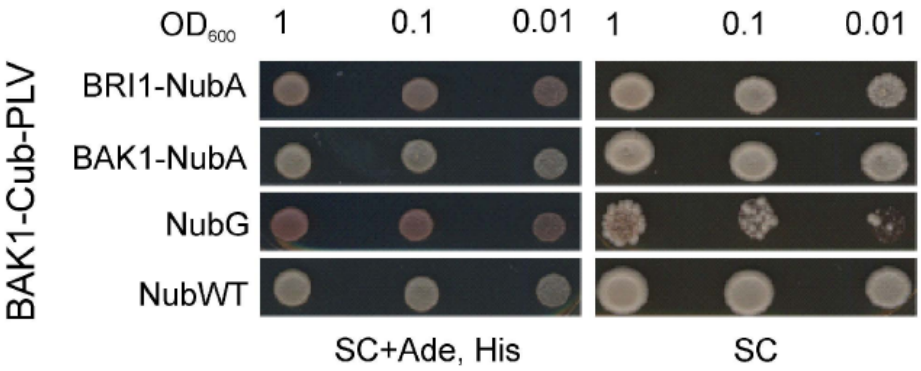

Figure S5. BAK1 forms homomers and interacts with BRI1 in the yeast mating-based split-ubiquitin system (mbSUS). The indicated constructs were co-transformed in yeast. Protein-protein interactions were analyzed by the activation of the reporter gene determined by growth of the transformants in a dilution series (OD_{600nm} from 1 to 0.01) on interaction-selecting medium (SC). The presence of the plasmids were tested by growth on SC+Ade,His medium. The co-transformation of the BAK1-Cub-PLV with NubG served as negative and that with NubWT as positive control.

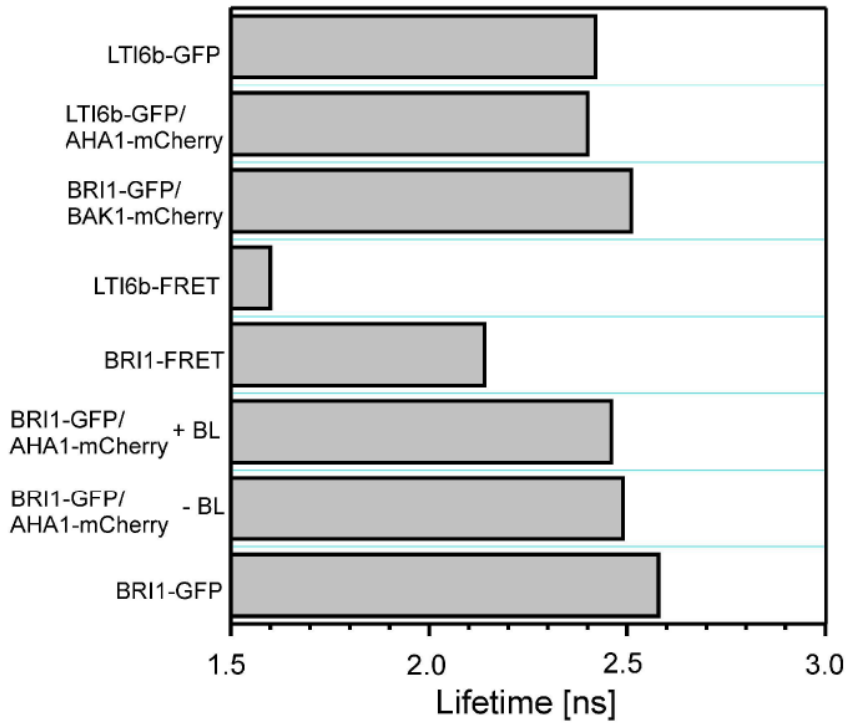

Figure S6. FLIM-FRET indicates interaction of BRI1-GFP with the P-ATPase in the plasma membrane in transiently transformed tobacco epidermal leaf cells. The FRET fusions of BRI1 and LTI6b exhibit strong FRET-FLIM values (BRI1-FRET: n = 28, p = $1.2\ 10^{-21}$; LTI6b-FRET: n = 15, p = $1.2\ 10^{-13}$). The recording of the FLT revealed a significant interaction of BRI1-GFP with AHA1-mCherry in the absence of exogenous BL (n = 77, p = $4.7\ 10^{-11}$). Compared to the non-treated cells, the external application of BL modulated the BRI1-GFP / AHA1-mCherry association (n = 59, p = 0.02). There is no significant interaction of LTI6b-GFP with AHA1-mCherry (n = 14, p = 0.22).

Table S1. FLT and ΔFLT values of BRI1-GFP in transgenic seedlings treated with either 10 nM brassinolide (BL), 10 mM sodium acetate, pH 6.0 (NaAc) plus 10 nM BL or 20 nM auxin (2,4-D). FLT data are shown recorded before and 30 min after addition of the compounds. St. dev.: standard deviation.

BRI1-GFP	FLT [ns] before addition	FLT [ns] 30 min after addition	? FLT [ns]
+ BL	2.64	2.59	-0.05
	2.45	2.38	-0.07
	2.68	2.47	-0.21
	2.64	2.58	-0.06
	2.71	2.67	-0.04
	2.60	2.57	-0.03
	2.65	2.56	-0.09
	2.49	2.39	-0.10
	2.51	2.45	-0.06
mean			**-0.08**
st. dev.			**0.05**
+ NaAc, BL	2.60	2.60	0.00
	2.62	2.64	0.02
	2.68	2.66	-0.02
	2.52	2.51	-0.01
	2.45	2.46	0.01
	2.52	2.51	-0.01
mean			**0.00**
st. dev.			**0.01**
+ 2,4-D	2.61	2.49	-0.12
	2.61	2.52	-0.09
	2.53	2.43	-0.10
	2.55	2.46	-0.09
	2.51	2.39	-0.12
	2.53	2.39	-0.14
mean			**-0.11**
st. dev.			**0.02**

Table S2. FLT values recorded in *Arabidopsis* seedlings expressing plasma membrane-bound PMA4-GFP, LTI6b-GFP or BRI1-GFP. The seedlings were either incubated in low voltage solution (lvs) or high voltage solution (hvs). Only the FLT of BRI1-GFP showed a statistically significant difference (p-value of the difference of the means). St. dev.: standard deviation.

	PMA4-GFP		BRI1-GFP		GFP-LTI6b	
	lvs	hvs	lvs	hvs	lvs	hvs
	2.66	2.67	2.56	2.43	2.54	2.58
	2.67	2.66	2.57	2.38	2.54	2.56
	2.67	2.66	2.57	2.43	2.54	2.54
	2.64	2.66	2.55	2.51	2.52	2.57
	2.64	2.66	2.55	2.45	2.51	2.56
	2.65	2.67	2.50	2.48	2.53	2.58
	2.65	2.66	2.53	2.53	2.52	2.55
	2.66	2.63	2.56	2.50	2.52	2.55
	2.67	2.59	2.55	2.51	2.53	2.55
	2.67	2.61	2.53	2.50	2.55	2.56
	2.66	2.60	2.55	2.49	2.57	2.57
	2.65	2.60	2.56	2.51	2.55	2.59
	2.66	2.58	2.56	2.51	2.54	2.58
	2.69	2.62	2.50	2.50	2.56	2.56
	2.68	2.62	2.52	2.51	2.56	2.60
	2.69	2.65	2.51	2.48	2.55	2.55
	2.66	2.65	2.52	2.47	2.55	2.58
	2.58	2.64	2.52	2.49	2.54	2.58
	2.58	2.66	2.54	2.44	2.55	2.52
	2.56	2.66	2.57	2.44	2.54	2.53
	2.60	2.66	2.53	2.48	2.59	2.53
	2.59	2.69	2.53	2.46	2.57	2.53
	2.59	2.67	2.57	2.52	2.56	2.51
	2.65	2.67	2.57	2.50	2.56	2.52
	2.61	2.66	2.58	2.52	2.58	2.52
	2.64	2.67	2.56	2.43	2.59	2.53
	2.62	2.68	2.58	2.40	2.58	2.53
	2.66	2.68	2.57	2.47	2.56	2.53
	2.63	2.69	2.58	2.42	2.57	2.52
	2.67	2.68	2.57	2.42	2.60	2.53
			2.53	2.38		2.54
			2.57	2.38		2.55
			2.50	2.39		2.54
			2.47	2.43		2.53
			2.48	2.45		2.53
			2.48	2.46		2.50
mean	**2.64**	**2.65**	**2.54**	**2.46**	**2.55**	**2.55**
st. dev.	**0.03**	**0.03**	**0.03**	**0.04**	**0.02**	**0.02**
p-value		0.33		0.00028		0.38

Table S3. FLT values recorded in *Arabidopsis* seedlings expressing plasma membrane-bound GFP-LTI6b or BRI1-GFP. The seedlings were either incubated in 50 µM *ortho*-vanadate (*o*V) or 2 µM Fusicoccin (Fc). Only the FLT of BRI1-GFP showed a statistically significant difference (p-value of the difference of the means). St. dev.: standard deviation.

	BRI1-GFP		**GFP-LTI6b**	
	oV	**Fc**	**oV**	**Fc**
	2.41	2.38	2.50	2.51
	2.43	2.40	2.55	2.56
	2.47	2.35	2.58	2.53
	2.44	2.40	2.65	2.44
	2.43	2.37	2.64	2.40
	2.41	2.35	2.50	2.35
	2.46	2.37	2.39	2.43
	2.44	2.42	2.42	2.45
	2.42	2.33	2.40	2.52
	2.45	2.33	2.37	2.51
	2.47	2.35	2.31	2.54
	2.52	2.30	2.40	2.46
	2.49	2.35	2.39	2.51
	2.47	2.32	2.46	2.55
	2.46	2.30	2.56	2.54
	2.51	2.32	2.42	2.38
	2.49	2.37	2.51	2.32
	2.47	2.28	2.42	2.40
	2.43	2.30	2.47	2.41
	2.43	2.33	2.41	2.47
	2.42	2.40	2.39	2.52
			2.40	2.60
			2.39	2.55
			2.39	2.39
			2.46	2.40
			2.59	2.41
			2.51	2.45
			2.59	2.46
			2.49	2.38
mean	**2.45**	**2.35**	**2.47**	**2.46**
stdev	**0.03**	**0.04**	**0.09**	**0.07**
p-value		9.3×10^{-12}		0.84

Plant Signaling & Behavior 6:7, 1063-1066; July 2011; © 2011 Landes Bioscience

The activation of the Arabidopsis P-ATPase 1 by the brassinosteroid receptor BRI1 is independent of threonine 948 phosphorylation

Janika Witthöft, Katharina Caesar, Kirstin Elgass, Peter Huppenberger, Joachim Kilian, Frank Schleifenbaum, Claudia Oecking and Klaus Harter*

Department of Plant Physiology; Center for Plant Molecular Biology; University of Tübingen; Tübingen, Germany

The plasma membrane-spanning receptor brassinosteroid insensitive 1 (BRI1) rapidly induces plant cell wall expansion in response to brassinosteroids such as brassinolide (BL). Wall expansion is accompanied by a rapid hyperpolarization of the plasma membrane, which is recordable by measuring the fluorescence lifetime (FLT) of the green fluorescent protein (GFP) fused to BRI1. For the BL induction of hyperpolarization and wall expansion, the activation of the plasma membrane P-type H^+-ATPase is necessary. Furthermore, the activation of the P-ATPase requires BRI1 kinase activity and appears to be mediated by a BL-modulated association of BRI1 with the proton pump. Here, we show that BRI1 also associates with a mutant version of the Arabidopsis P-ATPase 1 (AHA1) characterized by an exchange of a well-known regulatory threonine for a non-phosphorylatable residue in the auto-inhibitory C-terminal domain. Even more important, BRI1 is still able to activate this AHA1 mutant in response to BL. This suggests a novel mechanism for the enzymatic activation of the P-ATPase by BRI1 in the plasma membrane. Furthermore, we demonstrate that the FLT of BRI1-GFP can be used as a non-invasive probe to analyze long-distance BL signaling in Arabidopsis seedlings.

Key words: BRI1, fluorescence lifetime, membrane potential, P-ATPase, cell wall expansion

Submitted: 03/29/11

Accepted: 03/29/11

DOI: 10.4161/psb.6.7.15650

*Correspondence to: Klaus Harter;
Email: klaus.harter@zmbp.uni-tuebingen.de

Addendum to: Caesar K, Elgass K, Chen Z, Huppenberger P, Witthöft J, Schleifenbaum F, et al. A fast brassinolide-regulated response pathway in the plasma membrane of *Arabidopsis thaliana*. Plant J 2011; 66:528-40; PMID: 21255166; DOI: 10.1111/j.1365-313X.2011.04510.x.

Using spectro-microscopic technologies, we recently started the quantitative analysis of the properties and subcellular function of GFP fusion of the plasma membrane-localized brassinosteroid (BR) receptor, BRI1, in living plant cells of *Arabidopsis thaliana* and tobacco (*Nicotiana benthamiana*) leaf cells.[1,2] Brassinosteroids, such as brassinolide (BL), are involved in responses to biotic and abiotic stresses and developmental processes, including cell elongation.[3] The present model of the BR response pathway includes the binding of BRs to BRI1, resulting in the autophosphorylation of the receptor and the subsequent recruitment of the co-receptor BRI1-associated receptor kinase 1 (BAK1). This association is followed by trans-phosphorylation between BRI1 and BAK1 and results in the activation of downstream BR signaling processes leading to differential gene expression and, finally, to the execution of the specific responses.[4] However, the molecular events that take place in the plasma membrane immediately after the perception of BL and initiate cell elongation still have to be included in this model.[5] We recently reported a rapid BRI1-GFP-dependent cell wall expansion in Arabidopsis seedlings, which is attributed to wall loosening and water incorporation into the wall, and precedes cell elongation.[1,2] This expansion response was accompanied by a change in the FLT of BRI1-GFP, which reflects an alteration in the plasma membrane potential (E_m).[2,6] For both the FLT change in BRI1-GFP and the wall expansion, the activity of the plasma membrane P-ATPase is crucial. Notably, H^+-pump activation was shown to depend on the kinase activity of BRI1.[2] This suggests a fast BRI1-dependent response pathway in the plasma membrane which links BL perception via P-ATPase activation and

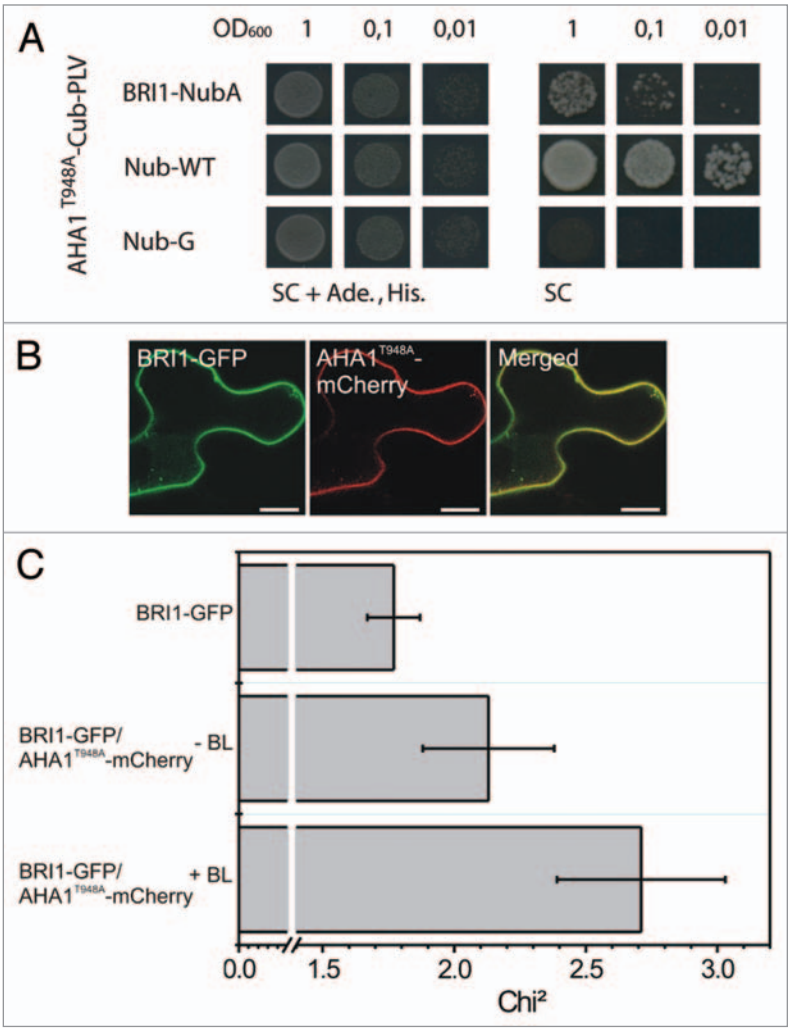

Figure 1. BRI1 interacts with AHA1^{T948A} in vivo. (A) Yeast mbSUS protein-protein interaction analysis: The Cub-PLV construct of AHA1^{T948A} was transformed in the yeast strain THY.AP4 (MATα) and the NubA construct of BRI1 in THY.AP5 (MATα). After mating, the activation of the reporter gene was determined by growth of the transformants in a dilution series ($OD_{600\,nm}$ from 1 to 0.01) on interaction-selective medium (SC). The presence of the plasmids was tested by growth on SC medium supplemented with adenine and histidine (SC + Ade His). The co-transformation of the AHA1^{T948A}-Cub-PLV fusion with Nub-G served as negative and that with Nub-WT as positive control. (B) CLSM image of a representative transiently transformed tobacco (*Nicotiana benthamiana*) epidermal leaf cell co-expressing BRI1-GFP and AHA1^{T948A}-mCherry. Bar represent 10 µm. (C) FRET-FIDSAM protein-protein interaction analysis: The fusion proteins were expressed in tobacco cells as indicated and the fitting error values (chi²) recorded in the absence (-BL) or presence (+BL) of 10 nM brassinolide as described previously.[2] The higher the chi² value, the better is the FRET efficiency. The single transformed GFP fusion of BRI1 was used to determine the background chi². The mean and standard deviation of at least three independent measurements are shown.

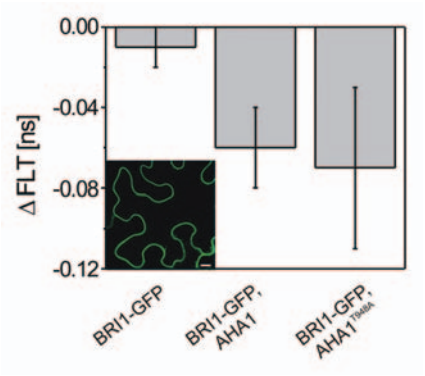

Figure 2. Activation of the Arabidopsis P-ATPase 1 (AHA1) by BRI1 does not require phosphorylation of the conserved threonine 948 in the C-terminal auto-inhibitory domain of the proton pump. The change of the fluorescence lifetime (FLT) of BRI1-GFP in response to BL treatment in transiently transformed tobacco epidermal leaf cells is presented. The cells were transformed with the indicated constructs encoding BRI1-GFP, AHA1 or AHA1^{T948A}. Three days after transformation the FLT was recorded before and 30 min after application of 10 nM BL, and the ΔFLT calculated as described previously.[2] The inlet shows a representative BRI1-GFP-expressing tobacco cell used for the recording of the FLT values. The mean and the standard deviation of three independent ΔFLT measurements from three different cells are shown. The bar represents 10 µm.

E_m hyperpolarization to wall expansion. In this report, we demonstrate that the phosphorylation of a conserved threonine in the auto-inhibitory domain of AHA1 is not required for the enzymatic activation by BRI1 suggesting a novel mechanism by which BRI1 may initiate the activation of the P-ATPase. Furthermore, we show that the FLT of BRI1-GFP is a useful and senstitive probe for the non-invasive analysis of systemic signaling processes in living plants.

BRI1 Activates and Interacts with a Crucial Mutant Version of the P-ATPase

In our recent study we demonstrated that BRI1 interacts with AHA1 in vivo and that the association of BRI1 and AHA1 is modulated by BL in planta.[2] We, therefore, tested, whether BRI1 is also able to interact with the AHA1^{T948A} mutant using the yeast mating-based split-ubiquitin system (mbSUS) and in planta Förster resonance energy transfer-fluorescence intensity decay shape analysis microscopy (FRET-FIDSAM).[2,7,8] Both, the yeast mbSUS and the in planta FRET-FIDSAM approaches revealed an interaction and close spatial association of BRI1 not only with wild-type AHA1 but also with AHA1^{T948A} in vivo (**Fig. 1**).[2] Furthermore, comparable to the results obtained for wild-type AHA1, BL was still able to modify the association of BRI1-GFP with AHA1^{T948A} in planta (**Fig. 1C**).[2]

We recently demonstrated by testing a phosphorylation-inactive version (BRI1^{KE}-GFP) that BRI1 kinase activity is required for the BL-regulated activation of AHA1 and E_m hyperpolarization in tobacco leaf cells.[2] BRI1^{KE}-GFP is still able to interact with AHA1 in vivo (Huppenberger P, Harter K,

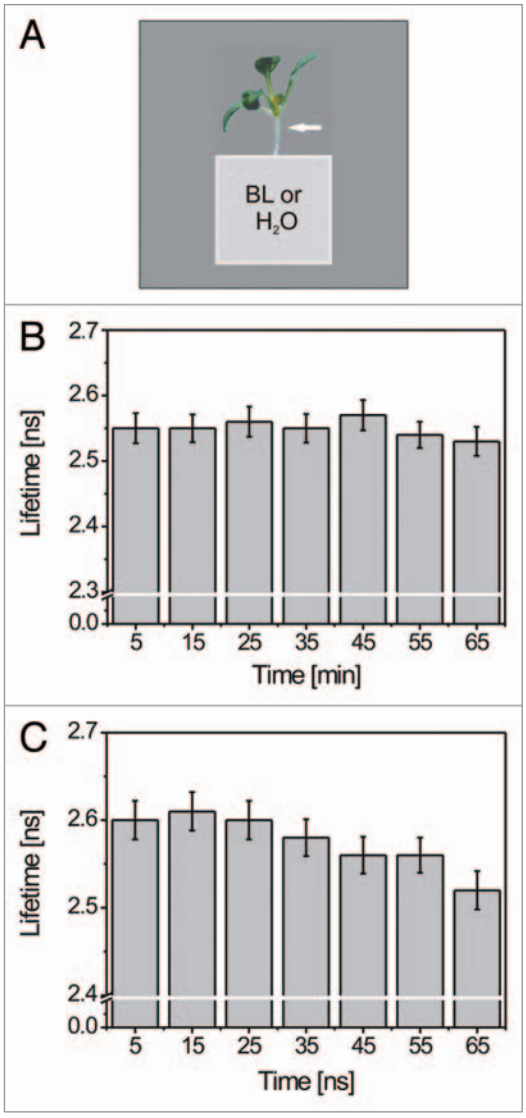

Figure 3. The FLT of BRI1-GFP can be used as sensitive and non-invasive probe for the analysis of systemic brassinosteroid signaling in Arabidopsis. (A) Experimental design: Five-days-old BRI1-GFP-expressing seedlings were placed on a glass slide. Then, a piece of filter paper, soaked in either 10 nM BL or H_2O (mock-treatment), was placed on the seedling's root system. The FLT of BRI1-GFP was recorded in cells of the upper hypocotyl indicated by the arrow. Kinetics of the FLT change in BRI1-GFP after placement of mock-treated filter paper (B) or filter paper soaked with 10 nM BL (C) to the root system. The experiment was repeated at least three times with three independent seedlings with similar results. One representative data set is shown.

unpublished). It is well documented that the phosphorylation of conserved serine or threonine residues in the C-terminal auto-inhibitory domain of P-ATPases, such as AHA1, modulates the enzymatic activity of the proton pumps by inducing or inhibiting association of 14-3-3 proteins.[9] 14-3-3 proteins are known to release the constraint exerted by the autoinhibitory domain of P-ATPases.[9] Since interaction with 14-3-3 requires phosphorylation of the penultimate H^+-ATPase residue (threonine 948 in AHA1) we analyzed whether the modification of this crucial residue is also required for the BL-regulated activation of AHA1 by BRI1. Therefore, the threonine at position 948 was exchanged for alanine by site-directed mutagenesis creating $AHA1^{T948A}$. Non-tagged wild-type AHA1 or $AHA1^{T948A}$ were then transiently co-expressed with BRI1-GFP in tobacco leaf cells. After the application of BL, the ΔFLT of BRI1-GFP was recorded as a probe for E_m hyperpolarization. As shown in **Figure 2**, BRI1-GFP activated not only wild-type AHA1 but also $AHA1^{T948A}$ as indicated by significant alterations in the FLT of BRI1-GFP.

In conclusion, our data indicate that the enzymatic activation of AHA1 by BRI1(-GFP) is not mediated by the phosphorylation of the conserved threonine residue in the C-terminal auto-inhibitory domain of the proton pump. We therefore have to consider alternative P-ATPase activation mechanisms. One possibility is that other serine and threonine phosphosites located in the auto-inhibitory domain or in other cytoplasm-exposed regions of AHA1 might be the target of BRI1. Another mechanism could be the enhancement of the pump's enzymatic activity by a BL-regulated, differential protein-protein interaction between BRI1 and the P-ATPase. The binding of BL could, for instance, induce an auto-phosphorylation-dependent conformational change in BRI1 enabling the receptor to push aside the auto-inhibitory domain and, thereby, to activate the P-ATPase. A comparable mechanism was recently postulated for the auxin-regulated activation of the P-ATPase by the soluble auxin-binding protein ABP_{57}.[10]

The FLT of BRI1-GFP as a Probe for the Analysis of Systemic BL Signaling

The FLT of BRI1-GFP is a sensitive probe for the non-invasive recording of E_m hyperpolarization at subcellular resolution.[1,2] We, therefore, addressed the question, whether recording of the FLT of BRI1-GFP is also applicable for the analysis of in planta long-distance BL signaling. For this purpose, an experimental setup was designed, in which BL or, as a control, H_2O was applied to the root system and the FLT change of BRI1-GFP was recorded in the upper hypocotyl of BRI1-GFP-expressing Arabidopsis seedlings (**Fig. 3A**). As shown in **Figure 3B**, the application of H_2O to the root system did not induce any FLT change in BRI1-GFP in the cells of the upper hypocotyl. In contrast, the application of BL caused a significant alteration in the FLT (**Fig. 3C**). Compared to the FLT change

of BRI1-GFP in hypocotyl cells, which were directly exposed to BL,[2] there was a delay of about 25 min in the appearance of FLT alteration in the upper hypocotyl cells (**Fig. 3C**). Our data, therefore, suggests that a mobile signal originates from the roots cells, which is able to induce the hyperpolarization of the plasma membrane in the non-treated upper hypocotyl cells. Whether this mobile signal is the BL itself remains an open question but it could well be as in herbaceous plants the mean phloem movement velocity is 0.9 meters per hour and the xylem movement velocity between 10 and 60 meters per hour.[11,12] However, independent of the nature of the mobile signal, the FLT of BRI1-GFP can be used to determine systemic signaling processes, which cause alterations in the E_m at the target tissue in living plants.

References

1. Elgass K, Caesar K, Schleifenbaum F, Stierhof YD, Meixner AJ, Harter K. Novel application of fluorescence lifetime and fluorescence microscopy enables quantitative access to subcellular dynamics in plant cells. PLoS One 2009; 4:5716.
2. Caesar K, Elgass K, Chen Z, Huppenberger P, Witthöft J, Schleifenbaum F, et al. A fast brassinolide-regulated response pathway in the plasma membrane of *Arabidopsis thaliana*. Plant J 2011; 66:528-40; DOI: 10.1111/j.1365-313X.2011.04510.x.
3. Clouse SD. Brassinosteroid signal transduction and action. In: Davies RJ, Ed. Plant Hormones, Biosynthesis, Signal Transduction, Action. Dordrecht/Boston/London: Kluwer Academic Publishers 2004:413-36.
4. Li JM, Jin H. Regulation of brassinosteroid signaling. Trends Plant Sci 2007; 12:37-41.
5. Sanchez-Rodriguez C, Rubio-Somoza I, Sibout R, Persson S. Phytohormones and the cell wall in Arabidopsis during seedling growth. Trends Plant Sci 2010; 15:291-301.
6. Elgass K, Caesar K, Schleifenbaum F, Meixner AJ, Harter K. The fluorescence lifetime of BRI1-GFP as probe for the noninvasive determination of the membrane potential in living cells. Proc SPIE 2010; 7568.
7. Grefen C, Obrdlik P, Harter K. The determination of protein-protein interactions by the mating-based split-ubiquitin system (mbSUS). Methods Mol Biol 2009; 479:217-33.
8. Schleifenbaum F, Elgass K, Sackrow M, Caesar K, Berendzen K, Meixner AJ, et al. Fluorescence intensity decay shape analysis microscopy (FIDSAM) for quantitative and sensitive live-cell imaging. Mol Plant 2010; 3:555-62.
9. Speth C, Jaspert N, Marcon C, Oecking C. Regulation of the plant plasma membrane H^+-ATPase by its C-terminal domain: What do we know for sure? Eur J Cell Biol 2010; 89:145-51.
10. Kim YS, Min JK, Kim D, Jung J. A soluble auxin-binding protein ABP_{57}. J Biol Chem 2001; 276:10730-6.
11. Dunford NM. Water balance of plants. In: Taiz L, Zeiger E, Eds. Plant Physiology. Massachusetts: Sinauer Associates Inc. 2010; 5:85-105.
12. Holbrook S. Translocation in the phloem. In: Taiz L, Zeiger E, Eds. Plant Physiology. Massachusetts: Sinauer Associates Inc. 2010; 5:271-303.

frontiers in
PLANT SCIENCE

MINI REVIEW ARTICLE
published: 04 October 2011
doi: 10.3389/fpls.2011.00058

Latest news on *Arabidopsis* brassinosteroid perception and signaling

Janika Witthöft and Klaus Harter*

Zentrum für Molekularbiologie der Pflanzen, Universität Tübingen, Tübingen, Germany

Edited by:
Andreas P. M. Weber, University of Duesseldorf, Germany

Reviewed by:
Georg Groth, University of Duesseldorf, Germany
Christian Hardtke, University of Lausanne, Switzerland
Jan Willem Borst, Wageningen University, Netherlands

****Correspondence:***
Klaus Harter, Zentrum für Molekularbiologie der Pflanzen, Pflanzenphysiologie, Universität Tübingen, Auf der Morgenstelle 1, 72076 Tübingen, Germany.
e-mail: klaus.harter@zmbp.uni-tuebingen.de

Brassinosteroids (BRs) are plant hormones regulating growth and development. In interaction with other hormones, they are involved in environmental cue responses. The present model of the BR response pathway in *Arabidopsis* includes the perception of the hormone by the plasma membrane (PM) receptor brassinosteroid insensitive 1 (BRI1) and its hetero-oligomerization with the co-receptor BRI1-associated receptor kinase 1 (BAK1), followed by the activation of a signaling-cascade finally resulting in the expression of BR-responsive genes. New findings have shed light on the receptor density in the PM and on the molecular mechanism of BR perception, which includes the hormone-induced formation of a platform in the BRI1 extracellular domain for interaction with BAK1. Furthermore, new knowledge on early, BRI1-initiated signaling events at the PM–cytoplasm interface has recently been gained. In addition, a fast BR response pathway that modifies the membrane potential and the expansion of the cell wall – both crucial processes preceding cell elongation growth – have been identified. In this review, these latest findings are summarized and discussed against the background of the present model of BRI1 signaling.

Keywords: brassinosteroids, BAK1, BRI1, membrane potential, cell elongation, P-ATPase, signal transduction, plasma membrane

THE PRESENT MODEL OF BRASSINOSTEROID SIGNALING

Brassinosteroids (BRs) are hormones regulating plant vegetative and reproductive growth and development and are involved in responses to many environmental cues, often in co-action with other hormones (Mandava et al., 1988; Clouse and Sasse, 1998). The present BR signaling-cascade model from the cell surface receptor brassinosteroid insensitive 1 (BRI1) to nuclear transcription factors, has been summarized in three recent reviews (Kim and Wang, 2010; Clouse, 2011; Yang et al., 2011). In short: in the absence of BR, BRI1 is maintained in an inactive state by the BRI1 kinase inhibitor 1 (BKI1). Signaling is initiated by the binding of the ligand to the extracellular domain (ECD) of BRI1, promoting both the recruitment of BAK1 and BRI1-mediated tyrosine phosphorylation of BKI1. The latter leads to dissociation of BKI1 from the plasma membrane (PM) and promotes trans-phosphorylation between BRI1 and BAK1. This process enhances the signaling capacity of the receptor complex and results in the phosphorylation of BR signaling kinase 1 (BSK1) and its release from the receptor complex. BSK1 initiates a complex cascade of signaling events, leading to the activation of the transcription factors BRI1-EMS suppressor 1 (BES1) and brassinazole resistant 1 (BZR1). BES1 and BZR1 are predominantly responsible for eliciting the BR-specific responses that depend on differential gene expression (Sun et al., 2010). Whereas the signaling events downstream of BSKs appear to be well established, novel findings with respect to BR perception by BRI1, early steps in BRI1/BAK1 complex formation and initiation of signaling have emerged. Furthermore, a fast BR response pathway will be discussed that modifies the PM potential (E_m) and the expansion of the wall, both crucial processes preceding cell elongation growth.

BRASSINOSTEROID PERCEPTION BY BRI1

Brassinosteroid insensitive 1 belongs to the large family of leucine-rich repeat receptor-like kinases (LRR-RLKs). Recently Van Esse et al. (2011) estimated the absolute number of BRI1–GFP receptor molecules in the root tip and leaf epidermal cells. Although the number varies from 22,000 in the root meristem up to 130,000 in the elongation zone, the receptor density in the PM is constant at 12 receptors μm^{-2}. Only the quiescent center (6,700 molecules), columella cells (10,800 molecules), and leaf epidermal cells have a lower density of 5 to 6 receptors μm^{-2}(quiescent center, columella) or 10 receptors μm^{-2} (leaf epidermis) (Van Esse et al., 2011). How far BRI1 density in the PM differs for further tissues is not known. However, quantitative analysis of BR-triggered wall expansion in *Arabidopsis* hypocotyl cells demonstrated a correlation between the relative number of BRI1–GFP molecules in the PM and the scale of the response (Elgass et al., 2010a). This indicates that the total amount of BRI1 and/or its density in the PM is of regulatory importance. These differences might also contribute to the differential competence of root and hypocotyl cells to respond to BR in wall expansion (Elgass et al., 2010b).

Brassinosteroid insensitive 1 comprises an ECD with 25 LRRs, with an island domain (ID) between LRRs 21 and 22 followed by a transmembrane domain. Its cytoplasmic domain consists of a juxtamembrane region, a kinase domain and a C-terminal extension (Kim and Wang, 2010; Clouse, 2011; Yang et al., 2011). However, until recently, it was not clear how BR binds to the ECD and by which molecular mechanism BRs cause BRI1 activation. Hothorn et al. (2011) have now been able to present the structure of the BRI1 ECD in its free form and bound to brassinolide (BL). Their

analysis has shed new light on BR perception and BRI1 activation: firstly, the BRI1 ECD does not show the anticipated horse shoe structure but forms a right-handed, highly twisted superhelix. The ID forms a small domain that folds back into the interior of the superhelix, where it interacts extensively with LRRs 13–25. BL binds by one molecule per BRI1 monomer at close proximity to the ID with the extensive contribution of LRRs. This interaction brings the hormone close to the PM (**Figure 1**). Secondly, for several reasons, the structure of the LRR superhelix is incompatible with BRI1–ECD oligomerization even in the presence of BL. This suggests that BRI1 activation is not mediated by ligand-induced homo-dimerization of the ECD or by conformational changes in preformed homodimers. Finally, BL binding induces a conformational rearrangement and fixing of the ID, where large parts of the hormone are still exposed to the solvent. These observations led to the idea that a stable protein–protein interaction platform is created within the BRI1 superhelix in the presence of ID-bound BL. Thus, BRI1 interaction with another protein *via* this platform may be the mechanism for BRI1 activation and initiation of signaling (Hothorn et al., 2011).

ACTIVATION OF BRI1 BY INDUCED PROTEIN–PROTEIN INTERACTION

Brassinolide binding creates a protein–protein interaction platform at the membrane-proximal region of BRI1, which might be crucial for receptor activation. Overwhelming evidence suggests that the favorite protein most likely to dock to the BL-induced platform within the BRI1 superhelix is BAK1 (Kim and Wang, 2010; Clouse, 2011; Yang et al., 2011). How BL-induced interaction with BAK1 transforms BRI1 into an active receptor was recently elucidated by Jaillais et al. (2011a): they studied the molecular basis for the gain-of-function phenotype of the *Arabidopsis bak1*^{elg} mutant. The bak1^{elg} protein carries a substitution of aspartate 122 to asparagine in its ECD. This substitution enhances the affinity of bak1^{elg} to BRI1 and may result, *via* more efficient BRI1/BAK1 receptor complex formation, in a more efficient transformation of BRI1 into an active receptor. Interestingly, this transformation and the full function of the BRI1/BAK1 receptor complex do not only require interaction of the ECDs but also association of the BRI1 and BAK1 kinase domains, as bak1^{elg} cannot overcome the repression of BR signaling by overexpressed BKI1. As mentioned above, BKI1 prevents interaction between the BRI1 and BAK1 kinase domains and, thereby, inhibits the promotion of trans-phosphorylation between BRI1 and BAK1 (Jaillais et al., 2011b). Therefore, Jaillais et al. (2011a) propose a "double-lock" mechanism for BRI1/BAK1 hetero-dimerization and signaling initiation: in the absence of BR, BRI1 is kept in an inactive state by interaction with BKI1 at its C-terminal domain. In this state, BRI1 may form some ligand-independent homo-oligomers but does not interact with BAK1. The binding of BRs creates a BR-containing interaction platform inside the superhelix of BRI1, with high affinity to the ECD of BAK1, and in parallel triggers tyrosine phosphorylation of BKI1. This results in the release of BKI1 from the PM, which is paralleled by the recruitment of BAK1 by BRI1 *via* its interaction platform. The BRI1/BAK1 association promotes trans-phosphorylation between BRI1 and BAK1 and the full activation of the BRI1/BAK1 receptor complex (**Figure 1**). This "double-lock" mechanism is very attractive, as it provides robustness and specificity for the BRI1/BAK1 complex formation and allows the regulatory modification by signals from outside and inside the cell (Jaillais et al., 2011a).

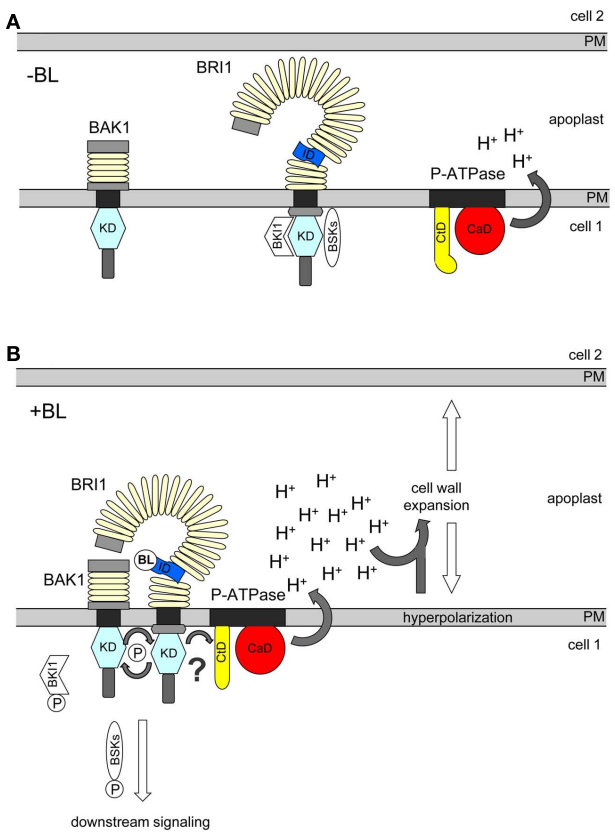

FIGURE 1 | Simplified model of the P-ATPase-independent (left) and P-ATPase-dependent, "short-cut" (right) BR response pathways in plant cells. (A) In the absence of BR, BRI1 is inhibited by its C-terminal domain and BKI1 and sequesters BSKs at the plasma membrane (PM). At this state, BRI1 might also be loosely associated with the P-ATPase (not shown). **(B)** After BL binding, BRI1 interacts with BAK1, phosphorylates BKI1, which is released into the cytoplasm. This promotes trans-phosphorylation between BRI1 and BAK1, establishment of the fully active BRI1/BAK1 signaling complex and the release of phosphorylated BSKs. Phosphorylated BSKs induce the signaling process leading to BR-controlled gene expression. BL binding also triggers the association of BRI1 with the P-ATPase. This suppresses the inhibition of the pump's activity by its C-terminal domain (CtD) and results in the BRI1 kinase activity-dependent activation of the P-ATPase's catalytic domain (CaD) by a yet unknown mechanism (?). The enhanced P-ATPase activity causes proton (H^+) extrusion into the apoplast and hyperpolarization of the PM leading to cell wall expansion. For the full BL-induced expansion response a further, yet unknown component is required in addition to PM hyperpolarization and apoplast acidification (not included). It is unclear whether association with BAK1, release of phosphorylated BKI1 or BKSs and/or direct phosphorylation of the P-ATPase are necessary for its BRI1-dependent activation.

A FAST BR RESPONSE PATHWAY IN THE PLASMA MEMBRANE

Regulation of vegetative growth is a crucial BR function. Vegetative growth can be achieved either by enhanced cell elongation,

cell number increase, or a combination of both. For instance, root length is controlled during organogenesis by components of the BR response pathway, including BRI1. Here, BR might determine the number of meristem cells by promoting cell cycle progression and changing the time of cell differentiation (Gonzalez-Garcia et al., 2011; Hacham et al., 2011). The effect of BL and BRI1 on elongation growth has been shown for the growth rate of BR treated epicotyl or hypocotyl isolates of bean and other plant species (Mandava, 1988; Clouse and Sasse, 1998). In *Arabidopsis*, BR-controlled elongation growth over several hours requires the predominantly BZR1- and BES1-mediated expression of hundreds of genes involved in water uptake, ion transport, wall, and cytoskeleton modifications (Kim and Wang, 2010; Clouse, 2011). With developmentally regulated plasma membrane polypeptide (*DREPP*) a novel BR-upregulated gene was identified whose product appears to be involved in the regulation of BR-mediated elongation growth at the PM–cytoplasm interface (Sun et al., 2010). Although DREPP is discussed to be involved in cytoskeleton reorganization, the molecular mechanism of DREPP elongation growth modification is not yet clear.

Brassinolide-induced elongation growth is preceded by apoplast acidification, hyperpolarization of the PM, and loosening and expansion of the cell wall (Mandava, 1988; Clouse and Sasse, 1998; Cosgrove, 2005). These processes are proposed to be regulated by the activity of PM-located P-Type ATPases (P-ATPases) such as *Arabidopsis* AHA1. These enzymes pump protons from the cytoplasm into the apoplast (Speth et al., 2010). However, a direct mechanistic link between activation of BRI1, up-regulation of P-ATPase activity, E_m hyperpolarization, and wall loosening and expansion was not yet apparent. Recently, micro-spectroscopic methods were applied to analyze the intracellular and intramembrane dynamics, interaction pattern, physico-chemical environment and function of BRI1–GFP in living hypocotyl and root cells of transgenic *Arabidopsis* seedlings and transiently transformed *Nicotiana benthamiana* leaves (Elgass et al., 2009; Caesar et al., 2011): by measuring the dynamic distance between BRI1–GFP-labeled PMs of adjacent cells and the dimension of the wall, a BRI1-dependent expansion of the wall within a few minutes after BL application was observed. In parallel, a decrease in the fluorescence lifetime (FLT) of BRI1–GFP was recorded, which points to an alteration in the receptor's close physico-chemical environment. The parameter that triggers the FLT change in BRI1–GFP in response to BL was identified to be the hyperpolarization of the E_m. By applying an inhibitor or activator of the P-ATPase, BL-regulation of the E_m and expansion of the cell wall could be reversibly modulated. A quantitative analysis of the recorded data revealed that several components, which include the apoplastic pH, the E_m and yet unknown components, contribute synergistically to BL-regulated wall expansion.

Gene expression data indicate that the *P-ATPase* gene family members are not regulated by BRs in *Arabidopsis* within a few minutes after hormone application, suggesting a post-translational control of the P-ATPase activity by BRI1 to trigger E_m hyperpolarization and wall expansion. One way to activate the P-ATPase activity is by BR-regulated interaction with BRI1 followed by the phosphorylation of the pump. Using different approaches, a specific interaction of BRI1 with AHA1 was demonstrated, which was modulated by BL *in planta* (Caesar et al., 2011). Furthermore, kinase activity of BRI1 was required for the BL-regulated change in the FLT of BRI1 and AHA1-caused E_m hyperpolarization. However, the mutation of conserved threonines in the C-terminal auto-inhibitory domain of P-ATPases, which are usually required for P-ATPase activation, did not alter the interaction of mutated AHA1 with BRI1 or its capacity to induce E_m hyperpolarization in the presence of activated BRI1 (Witthöft et al., 2011). Therefore, alternative mechanisms have to be discussed for how BRI1 activates the P-ATPase. In any case, these new findings suggest a "short-cut" BL-regulated signal response pathway within the PM, which is independent of gene expression (**Figure 1**). This pathway links BRI1 to the P-ATPase for the regulation of E_m hyperpolarization and wall loosening and expansion.

The described pathway could also have "wider" consequences. In two recent papers, non-cell autonomous signals were proposed to participate in BR signaling in *Arabidopsis* (Scacchi et al., 2010; Hacham et al., 2011). As most plant cells are electrically coupled through plasmodesmata, they tend to respond in concert to variations in the E_m (Spanswick, 1972). Although there is electrical resistance between the symplasts, it is possible that the BL-induced E_m change in one cell is "communicated" to the neighboring cells. As the E_m is the driving force for many transport processes, this may have significant physiological consequences for the neighboring cells (Blatt, 2004). Changes in the apoplastic pH have similar non-cell autonomous effects (Blatt and Armstrong, 1993; Blatt, 2004). Furthermore, alterations in the rigidity of the cell wall and, thus, the pressure conditions between cells, which occur during BL-induced wall loosening and expansion, may also have non-cell autonomous effects (Braybrook and Kuhlemeier, 2010).

Intriguingly, although the changes in the E_m and wall dimension occur within 15 min after BL application (Elgass et al., 2009; Caesar et al., 2011), the onset of cell elongation is observed at the earliest after 45 min (see References in Clouse, 2011). Furthermore, the BL-triggered E_m hyperpolarization has also been shown for tobacco epidermal leaf cells, which do not elongate (Caesar et al., 2011; Witthöft et al., 2011). This suggests that post-translational regulation of the P-ATPase activity alone is not sufficient to promote BR-triggered cell elongation growth. This probably requires the expression of genes encoding enzymes necessary for production and continuous incorporation of wall material during elongation. Alternatively, an additional growth-promoting hormone such as auxin has first to be produced by up-regulation of the corresponding biosynthetic genes. In a variety of bioassays, auxin has been shown to synergistically promote cell elongation with BRs (Halliday, 2004; Nemhauser et al., 2004; Sanchez-Rodriguez et al., 2010). Nevertheless, E_m polarization and wall expansion are two excellent cell physiological readouts to elucidate the molecular details of the BR/BRI1–P-ATPase response pathway.

PERSPECTIVE

Recently published work provided new insights into BR perception by BRI1 and initiation of signaling by the active BRI1/BAK1 receptor complex at the apoplast-PM-cytoplasm interface. Furthermore, a BR response pathway has been identified that triggers cell wall expansion and E_m polarization. However, there are still

many questions to be addressed: how is BR-binding to the ECD translated into enhanced BRI1 kinase activity? What is the molecular mechanism which results in the release of BSK1? With respect to the "short-cut" pathway: are other components of the early BRI1 signaling pathway, such as BAK1 or BKI1, or elongation growth-modifying proteins, such as DREPP, involved? Which protein domain of BRI1 is responsible for interaction with the P-ATPase and is there also a function of the BR-induced BRI1 protein interaction platform? Is phosphorylation outside the C-terminal auto-inhibitory domain required for activation of the P-ATPase and is BRI1 itself the kinase that phosphorylates the pump? What is the nature of the proposed non-cell autonomous BR signal?

Thus, though the BR response pathway is one of the best understood in plants, its further elucidation will continue to be an exciting undertaking.

ACKNOWLEDGMENTS

We thank Michael R. Blatt for helpful comments and Felicity de-Courcy for proofreading the manuscript. This work was funded by the DFG grant HA2146/10-1 within the framework of the *Arabidopsis* Functional Genomics Network (AFGN).

REFERENCES

Blatt, M. R. (2004). Concepts and techniques in plant membrane physiology. *Annu. Plant Rev.* 15, 1–10.

Blatt, M. R., and Armstrong, F. (1993). K+ channels of stomatal guard cells: abscisic-acid-evoked control of outward rectifier mediated by cytoplasmic pH. *Planta* 191, 330–341.

Braybrook, S. A., and Kuhlemeier, C. (2010). How a plant builds leaves. *Plant Cell* 22, 1006–1018.

Caesar, K., Elgass, K., Chen, Z., Huppenberger, P., Witthöft, J., Schleifenbaum, F., Blatt, M. R., Oecking, C., and Harter, K. (2011). A fast brassinolide-regulated response pathway in the plasma membrane of *Arabidopsis thaliana*. *Plant J.* 66, 528–540.

Clouse, S. D. (2011). Brassinosteroid signal transduction: from receptor kinase activation to transcriptional networks regulating plant development. *Plant Cell* 23, 1219–1230.

Clouse, S. D., and Sasse, J. M. (1998). Brassinosteroids: essential regulators of plant growth and development. *Annu. Rev. Plant Physiol. Plant Mol. Biol.* 49, 427–451.

Cosgrove, D. J. (2005). Growth of the plant cell wall. *Nat. Rev. Mol. Cell Biol.* 6, 850–861.

Elgass, K., Caesar, K., Schleifenbaum, F., Stierhof, Y. D., Meixner, A. J., and Harter, K. (2009). Novel application of fluorescence lifetime and fluorescence microscopy enables quantitative access to subcellular dynamics in plant cells. *PLoS ONE* 4, e5716. doi:10.1371/journal.pone.0005716

Elgass, K., Caesar, K., Stierhof, Y.-D., Meixner, A. J., and Harter, K. (2010a). The fluorescence lifetime of BRI1-GFP as probe for the non-invasive determination of the membrane potential in living cells. *SPIE Proc.* 7568, 756838.

Elgass, K., Caesar, K., Wanke, D., Meixner, A. J., Harter, K., and andSchleifenbaum, F. (2010b). Application of FLIM-FIDSAM for the in vivo analysis of hormone competence of different cell types. *Anal. Bioanal. Chem.* 398, 1919–1925.

Gonzalez-Garcia, M. P., Vilarrasa-Blasi, J., Zhiponova, M., Divol, F., Mora-Garcia, S., Russinova, E., and Cano-Delgado, A. I. (2011). Brassinosteroids control meristem size by promoting cell cycle progression in *Arabidopsis* roots. *Development* 138, 849–859.

Hacham, Y., Holland, N., Butterfield, C., Ubeda-Tomas, S., Bennett, M. J., Chory, J., and Savaldi-Goldstein, S. (2011). Brassinosteroid perception in the epidermis controls root meristem size. *Development* 138, 839–848.

Halliday, K. J. (2004). Plant hormones: the interplay of brassinosteroids and auxin. *Curr. Biol.*14, R1008–R1010.

Hothorn, M., Belkhadir, Y., Dreux, M., Dabi, T., Noel, J. P., Wilson, I. A., and Chory, J. (2011). Structural basis of steroid hormone perception by the receptor kinase BRI1. *Nature* 474, 467–471.

Jaillais, Y., Belkhadir, Y., Balsemao-Pires, E., Dangl, J. L., and Chory, J. (2011a). Extracellular leucine-rich repeats as a platform for receptor/coreceptor complex formation. *Proc. Natl. Acad. Sci. U.S.A.*108, 8503–8507.

Jaillais, Y., Hothorn, M., Belkhadir, Y., Dabi, T., Nimchuk, Z. L., Meyerowitz, E. M., and Chory, J. (2011b). Tyrosine phosphorylation controls brassinosteroid receptor activation by triggering membrane release of its kinase inhibitor. *Genes Dev.* 25, 232–237.

Kim, T. W., and Wang, Z. Y. (2010). Brassinosteroid signal transduction from receptor kinases to transcription factors. *Annu. Rev. Plant Biol.* 61, 681–704.

Mandava, N. B. (1988). Plant growth-promoting brassinosteroids. *Annu. Rev. Plant Physiol. Plant Mol. Biol.* 39, 23–52.

Nemhauser, J. L., Mockler, T. C., and Chory, J. (2004). Interdependency of brassinosteroid and auxin signaling in *Arabidopsis*. *PLoS Biol.* 2, e258. doi:10.1371/journal.pbio.0020258

Sanchez-Rodriguez, C., Rubio-Somoza, I., Sibout, R., and Persson, S. (2010). Phytohormones and the cell wall in *Arabidopsis* during seedling growth. *Trends Plant Sci.* 15, 291–301.

Scacchi, E., Salinas, P., Gujas, B., Santuari, L., Krogan, N., Ragni, L., Berleth, T., and Hardtke, C. (2010). Spatio-temporal sequence of cross-regulatory events in root meristem growth. *Proc. Natl. Acad. Sci. U.S.A.* 107, 22734–22739.

Spanswick, R. M. (1972). Electrical coupling between cells of higher plants: a direct demonstration of intercellular communication. *Planta* 102, 215–227.

Speth, C., Jaspert, N., Marcon, C., and Oecking, C. (2010). Regulation of the plant plasma membrane H+-ATPase by its C-terminal domain: what do we know for sure? *Eur. J. Cell Biol.* 89, 145–151.

Sun, Y., Fan, X. Y., Cao, D. M., Tang, W., He, K., Zhu, J. Y., He, J. X., Bai, M. Y., Zhu, S., Oh, E., Patil, S., Kim, T. W., Ji, H., Wong, W. H., Rhee, S. Y., and Wang, Z. Y. (2010). Integration of brassinosteroid signal transduction with the transcription network for plant growth regulation in *Arabidopsis*. *Dev. Cell* 19, 765–777.

Van Esse, W., Westphal, A. H., Preethi, R., Albrecht, C., van Veen, B., Borst, J. W., and de Vries, S. C. (2011). Quantification of the BRI1 receptor in planta. *Plant Physiol.* 156, 1691–1700.

Witthöft, J., Caesar, K., Elgass, K., Huppenberger, P., Kilian, J., Schleifenbaum, F., Oecking, C., and Harter, K. (2011). The activation of the *Arabidopsis* P-ATPase 1 by the brassinosteroid receptor BRI1 is independent of threonine 948 phosphorylation. *Plant Signal. Behav.* 6, 1063–1066.

Yang, C.-J., Zhang, C., Lu, Y.-N., Jin, J.-Q., and Wang, X.-L. (2011). The mechanism of brassinosteroids´ action: from signal transduction to plant development. *Mol. Plant* 4, 588–600.

Conflict of Interest Statement: The authors declare that the research was conducted in the absence of any commercial or financial relationships that could be construed as a potential conflict of interest.

Received: 29 August 2011; accepted: 10 September 2011; published online: 04 October 2011.

Citation: Witthöft J and Harter K (2011) Latest news on Arabidopsis brassinosteroid perception and signaling. Front. Plant Sci. ***2****:58. doi: 10.3389/fpls.2011.00058*

This article was submitted to Frontiers in Plant Physiology, a specialty of Frontiers in Plant Science.

Nuclear localization signals in A-type response regulators of *Arabidopsis thaliana*

Michael Heunemann[1]*, Virtudes Mira-Rodado*[1]*, Klaus Harter*[1] *and Janika Witthöft*[1,*]

[1]Center for Plant Molecular Biology (ZMBP), Department of Plant Physiology, University of Tübingen, Auf der Morgenstelle 1, 72076 Tübingen, Germany

*Corresponding author:
Janika Witthöft
Center for Plant Molecular Biology (ZMBP)
Department of Plant Physiology
University of Tübingen
Auf der Morgenstelle 1
72076 Tübingen, Germany
Phone: +49 (0)7071 29 76940
FAX: +49 (0)7071 29 3287
E-Mail: janika.witthoeft@zmbp.uni-tuebingen.de

Keywords: A-type response regulators, NLS

Abstract

The *Arabidopsis* response regulators (ARRs) are the output elements of the two-component signal transduction network, represented by a His-to-Asp phosphorelay. One major group, the A-type ARRs localize predominantly to the nucleus, although no functional nuclear localization signals (NLSs) have been reported till present. In this study the A-type response regulators ARR3, 4, 7 and 15 were analysed regarding the presence of a functional NLS. After aligning the amino acid sequences of these A-type ARRs and application of a prediction program, potential NLSs were narrowed down and mutated and the subcellular localization of the corresponding GFP-fusions determined. Some specific mutations caused a re-location of the fusion proteins from the nucleus to the cytoplasm. For ARR4 it was shown by using the reversibly photo-switchable fluorescence marker DRONPA that there is an active nuclear import which is impaired in a NLS-mutated ARR4. This led to the conclusion that the A-type ARRs studied here contain a functional NLS in their short C-terminal extension and suggests that the intracellular distribution of A-type ARRs is regulated, which might be of functional importance. Interestingly, the determined NLS positions are not conserved even between phylogenetically tightly related A-type ARRs.

Introduction

The two-component system (TCS) is an important signal transduction mechanism in plants which is based on a phosphorelay (Hwang *et al.* 2002; Grefen & Harter 2004). The canonical TCS consists of the signal-perceiving histidine kinases (HKs) and the response regulators which mediate the cellular response (Stock *et al.* 2000). In *Arabidopsis thaliana* a more complex type is found which is called multistep TCS. It contains the histidine phosphotransfer proteins (HPs) as an additional component (Stock *et al.* 2000; Hutchison *et al.* 2006). After signal perception, autophosphorylation of a conserved histidine residue in the transmitter domain of the HK is induced. The phosphate is then relayed from histidine to aspartate *via* the HPs to the ARRs (West & Stock 2001; Hutchison *et al.* 2006).

In *Arabidopsis thaliana* 23 canonical response regulators (ARRs) have been described, which are divided into three different types: A-, B- and C-type ARRs (Urao *et al.* 2000; Hwang *et al.* 2002). The B-type ARRs consist of a receiver domain and a large C-terminal output domain, containing a DNA-binding motif, a transactivation domain and at least one NLS and function as transcriptional regulators (Lohrmann *et al.* 1999; Sakai *et al.* 2000; Lohrmann *et al.* 2001). In contrast, A-type ARRs share only the N-terminal receiver domain with the B-type ARRs and lack the C-terminal output domain. Although A-type ARRs contain no obvious NLS they are localized in the cytoplasm and the nucleus (Sweere *et al.* 2001) or accumulate mainly in the nucleus (Imamura *et al.* 2001; Kiba *et al.* 2002; Dortay *et al.* 2008). A-type ARRs are involved in various aspects of plant growth and development and responses to environmental cues, e.g. cytokinin signalling (D'Agostino *et al.* 2000; To *et al.* 2004; To *et al.* 2007), modulation of phytochrome function (Sweere *et al.* 2001; Mira-Rodado *et al.* 2007), the circadian clock (Salome *et al.* 2006; Zheng *et al.* 2006), meristem function (Leibfried *et al.* 2005) and cold stress signalling (Jeon *et al.* 2010).

To enter the nucleus, a protein needs to overcome the nuclear pore. Proteins smaller than 40-60 kDa may passively diffuse into the nucleus (Mattaj & Englmeier 1998; Moore 1998) whereas larger proteins – like the GFP-ARR fusion proteins – require an active nuclear uptake mechanism and, thus, a functional NLS, which is recognized by nuclear import factors such as karyopherins (Macara 2001; Peters 2009). The NLSs can be divided into two major types: The so called classical and non-classical NLSs. Classical NLSs are short peptide motifs consisting of basic amino acids, mostly lysine (K) and arginine (R). They can be further subdivided in mono- and bipartite NLSs (Raikhel 1992; Hicks *et al.* 1995; Macara 2001). A monopartite NLS consists of at least four basic amino acids in series. The continuous basic stretch from the large antigen of the simian virus 40 was the first described monopartite NLS (KKKRK) (Kalderon *et al.* 1984). Other well known monopartite NLSs are the c-myc-like NLSs (KRVK), which contain a basic stretch disrupted by at least one uncharged amino acid (Dang & Lee 1988). A bipartite NLS is defined by two basic regions separated by a linker sequence of variable composition and length, usually 10-30 amino acids (Lange *et al.* 2007; Pawlowski *et al.* 2010). One example is the bipartite NLS of nucleoplasmin (KAVKRPAATKKAGQAKKKKL) (Robbins *et al.* 1991). Non-classical NLSs are not as well defined and show diverse sequence patterns (Mattaj & Englmeier 1998).

In plants, there also exist NLSs that correspond to the categories mentioned above. The maize *trans*-acting factor O2 for instance contains two different types of NLS. NLS A has the structure of a SV40-type NLS (NAIL**RRK**LEEDLE) and NLS B is a bipartite NLS (**RKRK**ESNRESA**RR**S**R**Y**RK**) (Varagona *et al.* 1992).

In this study, we provide evidence that the A-type response regulators ARR3, 4, 7 and 15 contain a functional NLS in their short C-terminal extension. We could show that the mutation of putative NLS positions leads to a cytoplasmic localization of the mutated GFP-ARR fusion protein suggesting that the nuclear accumulation is dependent on a NLS and thus, directed and regulated. This suggests that there are endo- or exogenous stimuli that promote the nuclear import or the movement between the cytoplasm and the nucleus. Therefore, mutation of the NLS most likely interferes with the intranuclear protein function due to the missing ability to enter the nucleus.

Results

ARR4 contains a single monopartite NLS

Arabidopsis A-type response regulators consist of a canonical receiver domain and a short C-terminal extension. The large output domain that can be found in B-type response regulators, containing at least one NLS, is missing (Hwang *et al.* 2002). Despite this, GFP-ARR4, for instance, is not equally distributed between the cytoplasm and the nucleus or found in the cytoplasm but localizes predominantly to the nucleus (Dortay *et al.* 2008). It is therefore supposed to have at least one NLS.

In order to investigate which regions are conserved among the A-type response regulators and which regions could contain a putative NLS, we aligned the protein sequences of all A-type ARRs. As shown in figure 1, the receiver domain is highly conserved between the A-type ARRs and the proteins only differ in

their more diverse C-terminal extension. Taking into account the criteria for a NLS, the sequences supposed to serve as such are mainly found in this C-terminal region of A-type ARRs.

For the prototypical A-type response regulator ARR4 we determined five putative NLSs, each starting with a lysine (Fig. 2A). Compared to wild type GFP-ARR4, which is predominantly detected in the nucleus (Fig. 3A), mutation of all five lysine residues to alanine led to a cytoplasmic localization of the GFP-ARR4$^{K108/147/155/172/252A}$ fusion protein in transiently transformed *Nicotiana benthamiana* leaf cells (Fig. 3B). This observation indicates that at least one of these amino acids is involved in mediating the nuclear accumulation of GFP-ARR4. To identify the amino acid(s) functionally important for the nuclear uptake of GFP-ARR4, single mutants were created and tested for their intracellular distribution, again using the tobacco leaf system. Whereas GFP-ARR4^{K108A}, GFP-ARR4^{K147A}, GFP-ARR4^{K155A} and GFP-ARR4^{K252A} were predominantly localized in the nucleus (Fig. 3C-E, G), the mutation of lysine 172 to alanine led to a distinct change in the subcellular localization of the corresponding GFP fusion protein: GFP-ARR4^{K172A} was mainly localized in the cytoplasm (Fig. 3F). To substantiate these results, we transiently expressed GFP-ARR4, GFP-ARR4$^{K108/147/155/172/252A}$ (mutation of all five lysine residues), GFP-ARR4^{K172A} as well as GFP-ARR4$^{K108/147/155/252A}$ (no mutation of K172) in *Arabidopsis thaliana* seedlings. The subcellular localization of the fusion proteins was identical to that in tobacco (Suppl. Fig. 1A-D) indicating that lysine 172 is required for the nuclear uptake of GFP-ARR4 and potentially part of a functional NLS. These experimental data were supported by applying the NLS prediction tool "cNLS Mapper" (Kosugi *et al.* 2009) to the ARR4 sequence. The program predicted one monopartite NLS reaching from amino acid 169 to 178 (NGN**K**RKLPED) which includes lysine 172.

In order to visualize the nuclear import of ARR4 in comparison to its NLS-mutated version ARR4^{K172A} we C-terminally fused these proteins to DRONPA, a photo-switchable fluorescent marker protein. The DRONPA fluorescence can be "switched-off" by irradiation with light of 488 nm and reactivated with light of 405 nm (Lummer *et al.* 2011). ARR4-DRONPA showed a nucleo-cytoplasmic localization with a very intense fluorescence signal inside the nucleus (Fig. 4). We selectively "switched-off" the nuclear fluorescence and monitored this particular nucleus for a time period of 20 min. The nuclear fluorescence clearly recovered within 20 min which reflects an active nuclear uptake of fluorescing ARR4-DRONPA from the cytoplasm. In contrast, ARR4^{K172A}-DRONPA was neither detectable in the nucleus at the beginning nor could a nuclear import be observed within 20 min after irradiation of the nucleus with 488 nm light (Fig. 4). This shows again that there is an active nuclear import of ARR4 that is severely impaired by mutation of Lysine 172, which is crucial of ARR4 nuclear localization.

The A-type ARRs exhibit different types of NLS

As ARR3 is the closest relative of ARR4, the question arises whether ARR3 also contains a NLS. GFP-ARR3 was localized in the nucleus as well as in the cytoplasm of transiently transformed tobacco leaf cells and *Arabidopsis* seedlings (Fig. 5A, Suppl. Fig. 1E), indicating that ARR3 could contain a nuclear localization signal as well. The KRK motif functioning as NLS of ARR4 also exists within the ARR3 protein at exactly the same position (Fig. 1, 2B). It was, therefore, obvious to test whether lysine 172 is

conserved in its function. Mutation of lysine 172 to alanine led to a wild type like nucleo-cytoplasmic localization of the corresponding GFP-ARR3^{K172A} fusion protein in tobacco leaves (Fig. 5B). Mutation of lysine 172 is therefore not sufficient to exclude ARR3 from the nucleus. On the basis of cNLS Mapper data, which predicted a bipartite NLS from position 152 (DV**K**RLRSYLTRDVKVAAEGN**K**RKLTTPP) in ARR3, we additionally mutated the lysine residue at position 154. Mutation of both lysine 154 and 172 to alanine caused a predominantly cytoplasmic localization of GFP-ARR3$^{K154/172A}$ in transiently transformed tobacco leaf cells and *Arabidopsis* seedlings (Fig. 5D; Suppl. Fig. 1F). To exclude that the mutation of lysine 154 alone is sufficient to keep ARR3 in the cytoplasm, we generated an additional single mutant ARR3 version (GFP-ARR3^{K154A}). GFP-ARR3^{K154A} was found in the nucleus and the cytoplasm of tobacco leaf cells like wild type GFP-ARR3 (Fig. 5C). These results implicate that, in contrast to ARR4, two lysine residues (K154 and K172) are responsible for the nuclear localisation of ARR3.

There are indications in the literature that the A-type response regulator ARR7 contains a NLS in its C-terminus (Imamura *et al.* 2001; Kiba *et al.* 2002). We, therefore, additionally analysed ARR7 and its closest relative ARR15. It has been reported that a GFP fusion of a truncated ARR7 protein, lacking the last 47 amino acids, localizes to the cytoplasm of transiently transformed onion cells, in contrast to wild type GFP-ARR7 that localizes to the nucleus (Imamura *et al.* 2001). Imamura and colleagues (2001) speculated that the KRMK motif (aa 193-196) could function as NLS. We, therefore, mutated lysine 193 to alanine generating ARR7^{K193A}. Similar to wild type GFP-ARR7, GFP-ARR7^{K193A} showed a predominant nuclear localization in transiently transformed tobacco leaf cells (Fig. 6A, C). The C-terminal 47 amino acid long peptide missing in the construct of Imamura and colleagues (2001) also contains a KRK motif that was shown by us to be involved in ARR3 and ARR4 nuclear localization (Fig. 1, 2C). We, therefore, tested whether the mutation of lysine 167, which corresponds to lysine 172 in ARR3 and ARR4, affects the subcellular localization of ARR7. Again GFP-ARR7^{K167A} was mainly localized in the nucleus like wild type GFP-ARR7 (Fig. 6B). In contrast, mutation of both lysine residues (K167 and K193) to alanine led to a cytoplasmic localization of the GFP fusion protein in transiently transformed tobacco leaf cells and *Arabidopsis* seedlings (Fig. 6D; Suppl. Fig. 1H). These results indicate that, similar to ARR3, the nuclear uptake of ARR7 is mediated by a bipartite or by two monopartite NLSs. It has to be noticed that any of the inserted mutations into the ARR7 protein induced the formation of cytoplasmic vesicles. As exemplarily shown for GFP-ARR7$^{K167/193A}$ in supplemental figure 3, they exhibit a perfect overlap with RabA5d-RFP, RabD2a-RFP and VTI12-RFP, which are markers for the endosomal system including recycling endosomes or the prevacuolar compartment (Sanderfoot *et al.* 2000; Rutherford & Moore 2002). We suppose that these vesicles contain misfolded ARR7 proteins that are excluded from the cytoplasm through the endosomal degradation pathway.

For ARR15, the closest homolog of ARR7, Kiba and colleagues (2002) speculated that the KRIK motif (aa 198-201) could serve as NLS but did not substantiate this hypothesis by experiments. Analysis of ARR15 by cNLS Mapper predicted one NLS from position 193 (DTPSS**K**RIKLE) which includes the KRIK motif mentioned above. Mutation of lysine 198 to alanine caused a cytoplasmic localization of GFP-ARR15^{K198A} in transiently transformed tobacco leaf cells and *Arabidopsis* seedlings (Fig. 7C, Suppl.

Fig. 1J), whereas wild type GFP-ARR15 was mainly found in the nucleus (Fig. 7A, Suppl. Fig. 1I). Interestingly, ARR15 only contains KR (aa 162/163) positionally related to the functional KRK motives identified in ARR3, 4 and 7 (Fig.1, 2D). As expected, the mutation of lysine 162 to alanine generating ARR17^{K162A} did not affect the subcellular localization compared to wild type GFP-ARR15 (Fig. 7B) demonstrating that KR does not serve as NLS. Thus, the nuclear uptake of ARR15 is mediated by a monopartite NLS located in the extreme C-terminus of the protein.

To exclude that the differences in the subcellular localization between the mutated and wild type GFP-ARR fusion proteins are due to different expression levels or to free GFP, we performed an immunoblot analysis using extracts from those transiently transformed tobacco leaves, which have been analysed by CLSM before. The fusion proteins were detected by a GFP-specific antibody and, as shown in Suppl. Fig. 2, expressed to very similar levels. No free GFP was detected.

Discussion

Active nuclear import of the nuclear localized A-type ARRs

The A-type response regulators in general are small proteins with a molecular weight between 20 and 30 kDa which in principle would allow passive diffusion into the nucleus. By fusion to GFP, the molecular weight increases to 50-60 kDa which represents the limit for passive diffusion (Mattaj & Englmeier 1998; Moore 1998). However, it has been shown that GFP fusions of several A-type ARRs predominantly localize to the nucleus.

The A-type ARRs share a high sequence homology of the receiver domain but differ in their short C-terminal extension that is supposed to be crucial for their intracellular distribution (Imamura *et al.* 2001; Kiba *et al.* 2002). For instance, the basic motifs that are present in the C-termini of ARR3, 4, 7 and 15 and serve as NLS do not exist within ARR16, which completely lacks the C-terminal extension. Consistent with this observation, GFP-ARR16 was shown to localize predominantly to the cytoplasm of transiently transformed onion cells (Kiba *et al.* 2002; Dortay *et al.* 2008), although it would be small enough to passively diffuse into the nucleus. In contrast, the A-type response regulators ARR5/6 and 8/9 do contain a basic motif in their C-terminal extension – KRAK or KRK, respectively – and localize to the nucleus when fused to GFP (Kiba *et al.* 2002; Dortay *et al.* 2008). Here, we show that mutation of the NLS in ARR3, 4, 7 and 15 causes a predominantly cytoplasmic localization of the corresponding GFP fusion proteins.

Since a single amino acid exchange does not significantly alter the size or structure of a protein but obviously the subcellular localization, we assume that the nuclear accumulation of the A-type ARRs is active and selective and does not represent a passive diffusion.

Subcellular localization of GFP-ARR4$^{K108/147/155/252A}$ (no mutation of lysine 172)

GFP-ARR4 mainly localized to nucleus in transiently transformed tobacco leaf cells and *Arabidopsis thaliana* seedlings whereas mutation of lysine 172 to alanine led to a mostly cytoplasmic localization of the corresponding GFP fusion protein. The mutation of four different putative NLSs within the ARR4

protein led to a more cytoplasmic – in comparison to wild type GFP-ARR4 – but still nuclear localization of the mutated ARR4 protein.

This could mean that one of these mutations hit a NLS with a weak activity and in consequence causes the more cytoplasmic localization. However, since lysine 172 was not mutated, the fusion protein still localizes to the nucleus. The weak NLS could be represented by the KRLR motif containing lysine 155 which is also involved in the nuclear translocation of ARR3 - the closest homolog of ARR4.

The GFP fusion affects ARR4 nuclear localization

It has been reported that ARR4-GFP localizes to the nucleus and the cytoplasm (Sweere *et al.* 2001) whereas N-terminal GFP fusions of ARR4 predominantly localize to the nucleus (Hwang *et al.* 2002; Dortay *et al.* 2008). This difference allowed us to apply several approaches for the analysis of ARR4 nuclear localization signals.

As differences in the subcellular localization appear more clearly if the reference protein is localized in only one compartment, it was suitable to use N-terminal GFP-fusions to analyse whether point mutations within putative NLSs affect the subcellular localization. In contrast, to analyse a protein movement between two compartments by using the photo-switchable fluorescence marker DRONPA, it is necessary that the protein of interest is localized in both compartments. Our DRONPA approach again indicates that ARR4-GFP requires a NLS for nuclear accumulation as ARR4^{K172A}-GFP strictly remains in the cytoplasm.

ARR3 and 7 contain two NLS

Here we provide evidence that ARR3 and 7 contain two basic motifs that are responsible for their nuclear localization and are separated by a linker region as it is commonly known for bipartite NLS. However, for bipartite NLSs it has been shown that mutation of one of the basic sections is sufficient to abolish its NLS activity (Munoz-Fontela *et al.* 2003; Pawlowski *et al.* 2010). In our case, mutation of one of the motifs did not alter the subcellular localization, only mutation of both excluded the corresponding GFP fusion proteins from the nucleus. This suggests that ARR3 and 7 have two monopartite NLS that are functionally redundant.

Conservation of the nuclear localization signals

The 10 A-type response regulators are grouped into five distinct gene pairs which originate from a genome duplication event (Vision 2000; Hwang *et al.* 2002; To *et al.* 2004) leading to the assumption that the NLSs found in this study could be conserved. The examination of a phylogenetic tree revealed that the gene pairs *ARR3/4*, *5/6* and *7/15* are closer related to each other than to *ARR8/9* and *16/17* (Mason *et al.* 2004; To *et al.* 2004).

The KRK motif functioning as NLS in ARR3, 4 and 7 corresponds to KRI in ARR15 and KRE in ARR5 and 6, suggesting original sequence conservation. However, the KRI motif found in ARR15 does not function as NLS most probably since there are only two basic residues in series. On the other hand, the

KRIK motif at the extreme C-terminus shown by us to serve as NLS in ARR15 is not conserved among the A-type response regulators. ARR5 and 6 contain KRAK in their C-terminal extension which is discussed as NLS (Imamura *et al.* 2001). At the conserved position they exhibit KRE that most probably does not serve as NLS as discussed for ARR15.

Summary

Taken together, our results demonstrate the relevance of the A-type response regulators C-terminal extension. It is commonly accepted that the highly conserved receiver domain is crucial for signal transduction since it contains the phosphorylatable aspartate residue. Here, we show in addition that the subcellular distribution of the A-type ARRs is determined by the amino acid composition of their short C-terminal region which elucidates the meaning of this less examined part of the A-type response regulators. The conservation of functional NLSs in these otherwise small proteins suggests that nuclear presence of A-type ARRs is of functional relevance and may even be regulated. Complementation analyses using the described NLS-mutated versions of A-type ARRs will elucidate this hypothesis.

Experimental procedures

Cloning strategy and site directed mutagenesis

All clones were constructed using Gateway™ technology (Invitrogen). The Entry clones were generated by BP-reaction, combining the genes of interest in pDONR207 (Invitrogen). Site-directed mutagenesis of *ARR3* (AT1G59940), *ARR4* (AT1G10470), *ARR7* (AT1G19050) and *ARR15* (AT1G74890) was carried out on the corresponding entry clones using Phusion® High-Fidelity DNA Polymerase (New England BioLabs). To insert a mutation, a pair of fully complementary primers was used containing the desired mutation and, where possible, an additional restriction site (Table 1).

To generate the N-terminal GFP-fusions, the (mutated) cDNAs were recombined *via* LR-reaction into pH7WGF2 (Karimi *et al.* 2002).

The *DRONPA* entry clone was generated by adding *att*B2 and *att*B3 sites *via* PCR to the coding region of DRONPA-s (Lummer *et al.* 2011) and a subsequent BP-reaction with *pDONRP2R-P3* (Invitrogen). To generate C-terminal DRONPA fusions, a Multisite Gateway LR-reaction was performed using the *DRONPA*- and the (mutated) *ARR4* entry clones as well as *pEN-L4-2-R1* containing the 35S-promoter (Karimi *et al.* 2007). The fragments were recombined into the binary vector *pB7m34GW* (Karimi *et al.* 2005).

Transient transformation of *Nicotiana benthamiana* leaves and *Arabidopsis thaliana* seedlings

Transient transformation of *Nicotiana benthamiana* leaves using the *Agrobacterium tumefaciens* strain GV3101 pMP90, transformed with the desired constructs, was carried out as described in Schütze *et al.* (2009). For co-infiltrations with two or more constructs, the corresponding *Agrobacterium* suspensions were mixed 1:1 before infiltration. 2-3 days post infiltration, epidermal leaf cells were analysed for fluorescence by

confocal laser scanning microscopy (CLSM) using a Leica TCS SP2 confocal microscope (Leica Microsystems GmbH). For transient transformation of *Arabidopsis thaliana*, 3 to 4-days-old *efr1* seedlings (Zipfel *et al.* 2006) were transformed *via* vacuum infiltration (Marion *et al.* 2008). The seedlings were analysed for fluorescence by CLSM 3 days post infiltration.

Protein extraction and Western Blot analysis

Proteins were extracted from leaf discs of infiltrated tobacco plants using denaturing SDS sample buffer (Schütze *et al.* 2009). Total protein extract was loaded on a SDS-PAGE with subsequent Western Blot and immunodetection using a GFP-specific antibody (Roche).

Acknowledgements

We thank Dorothee Staiger for providing the DRONPA-plasmids. This work was supported by DFG grant to K.H. (AFGN-HA 2146/10-1) and a fellowship of the University of Tübingen to J.W.

Figure legends

Figure 1 Amino acid alignment of the A-type response regulator family, generated using ClustalW (Chenna *et al.* 2003). The conserved regions are highlighted in blue.

Figure 2 Schematic representation of ARR4, 3, 7 and 15 as well as their amino acid sequences. The putative NLS are underlined in the protein sequence and the lysine residues that were mutated to alanine are highlighted in bold. The arrows mark the positions of the inserted point mutations.

Figure 3 Confocal images of transiently transformed tobacco epidermal leaf cells co-expressing GFP fusions of either wild type ARR4 (A) or a mutated version of ARR4 containing the indicated point mutations (B-H) and mCherryNLS as nuclear marker. The bars represent 10 μm.

Figure 4 Confocal images of transiently transformed tobacco epidermal leaf cells co-expressing ARR4-DRONPA (left) or ARR4^{K172A}-DRONPA (right) and mCherryNLS as nuclear marker. The pictures in the first row were taken before deactivation of the DRONPA-fluorescence by light of 488 nm (before) and the following pictures directly (0 min), 10 or 20 min after deactivation. The bars represent 10 μm.

Figure 5 Confocal images of transiently transformed tobacco epidermal leaf cells co-expressing GFP fusions of either wild type ARR3 (A) or a mutated version of ARR3 containing the indicated point mutations (B-D) and mCherryNLS as nuclear marker. The bars represent 10 μm.

Figure 6 Confocal images of transiently transformed tobacco epidermal leaf cells co-expressing GFP fusions of either wild type ARR7 (A) or a mutated version of ARR7 containing the indicated point mutations (B-D) and mCherryNLS as nuclear marker. The bars represent 10 μm.

Figure 7 Confocal images of transiently transformed tobacco epidermal leaf cells co-expressing GFP fusions of either wild type ARR15 (A) or a mutated version of ARR15 containing the indicated point mutations (B, C) and mCherryNLS as nuclear marker. The bars represent 10 μm.

Supplemental Material

Supplemental Figure 1 Confocal images of transiently transformed *Arabidopsis thaliana* cotyledon cells co-expressing the indicated GFP fusions and mCherryNLS as nuclear marker. The bars represent 10 μm.

Supplemental Figure 2 Western Blot analysis of protein extracts derived from transiently transformed tobacco leaves assayed by CLSM before extraction. The immunodetection of the fusion proteins was carried out with a GFP-specific antibody. In this study, GFP-ARR4 and GFP-ARR3 as well as their mutated versions have an apparent molecular weight of more than 70 kDa instead of the predicted 50-60 kDa. As this phenomenon has already been observed for ARR4 in previous studies (To *et al.* 2007; Ren *et al.* 2009) and no other specific bands could be detected, we considered the 70 kDa bands as the desired ones. Interestingly, GFP-ARR4^{K172A} seems to have a higher molecular weight than wild type GFP-ARR4.

GFP-ARR7 and GFP-ARR15 appear as double bands since the fusion proteins have the same molecular weight as the large subunit of RubisCO. The high amount of RubisCO protein in the leaf extracts might push aside GFP-ARR7 and GFP-ARR15.

Supplemental Figure 3 Confocal images of transiently transformed tobacco epidermal leaf cells co-expressing GFP-ARR7$^{K167/193A}$ and RabA5d-RFP (A), RabD2a-RFP (B) or VTI12-RFP (C). The bars represent 10 μm.

References

CHENNA, R., SUGAWARA, H., KOIKE, T., LOPEZ, R., GIBSON, T.J., HIGGINS, D.G. and THOMPSON, J.D. (2003). Multiple sequence alignment with the Clustal series of programs. *Nucleic Acids Res* **31**(13): 3497-3500.

D'AGOSTINO, I.B., DERUERE, J. and KIEBER, J.J. (2000). Characterization of the response of the Arabidopsis response regulator gene family to cytokinin. *Plant Physiol* **124**(4): 1706-1717.

DANG, C.V. and LEE, W.M. (1988). Identification of the human c-myc protein nuclear translocation signal. *Mol Cell Biol* **8**(10): 4048-4054.

DORTAY, H., GRUHN, N., PFEIFER, A., SCHWERDTNER, M., SCHMÜLLING, T. and HEYL, A. (2008). Toward an Interaction Map of the Two-Component Signaling Pathway of *Arabidopsis thaliana*. *J Proteome Res* **7**(9): 3649-3660.

GREFEN, C. and HARTER, K. (2004). Plant two-component systems: principles, functions, complexity and cross talk. *Planta* **219**(5): 733-742.

HICKS, G.R., SMITH, H.M., SHIEH, M. and RAIKHEL, N.V. (1995). Three classes of nuclear import signals bind to plant nuclei. *Plant Physiol* **107**(4): 1055-1058.

HUTCHISON, C.E., LI, J., ARGUESO, C., GONZALEZ, M., LEE, E., LEWIS, M.W., MAXWELL, B.B., PERDUE, T.D.*, et al.* (2006). The Arabidopsis histidine phosphotransfer proteins are redundant positive regulators of cytokinin signaling. *Plant Cell* **18**(11): 3073-3087.

HWANG, I., CHEN, H.C. and SHEEN, J. (2002). Two-component signal transduction pathways in Arabidopsis. *Plant Physiol* **129**(2): 500-515.

IMAMURA, A., YOSHINO, Y. and MIZUNO, T. (2001). Cellular localization of the signaling components of Arabidopsis His-to-Asp phosphorelay. *Biosci Biotech Biochem* **65**(9): 2113-2117.

JEON, J., KIM, N.Y., KIM, S., KANG, N.Y., NOVAK, O., KU, S.J., CHO, C., LEE, D.J.*, et al.* (2010). A subset of cytokinin two-component signaling system plays a role in cold temperature stress response in Arabidopsis. *J Biol Chem* **285**(30): 23371-23386.

KALDERON, D., ROBERTS, B.L., RICHARDSON, W.D. and SMITH, A.E. (1984). A short amino acid sequence able to specify nuclear location. *Cell* **39**(3 Pt 2): 499-509.

KARIMI, M., BLEYS, A., VANDERHAEGHEN, R. and HILSON, P. (2007). Building blocks for plant gene assembly. *Plant Physiol* **145**(4): 1183-1191.

KARIMI, M., DE MEYER, B. and HILSON, P. (2005). Modular cloning in plant cells. *Trends Plant Sci* **10**(3): 103-105.

KARIMI, M., INZÉ, D. and DEPICKER, A. (2002). GATEWAY™ vectors for Agrobacterium-mediated plant transformation *Trends Plant Sci* **7**(5): 193-195.

KIBA, T., YAMADA, H. and MIZUNO, T. (2002). Characterization of the ARR15 and ARR16 response regulators with special reference to the cytokinin signaling pathway mediated by the AHK4 histidine kinase in roots of Arabidopsis thaliana. *Plant Cell Physiol* **43**(9): 1059-1066.

KOSUGI, S., HASEBE, M., TOMITA, M. and YANAGAWA, H. (2009). Systematic identification of cell cycle-dependent yeast nucleocytoplasmic shuttling proteins by prediction of composite motifs. *PNAS* **106**(25): 10171-10176.

LANGE, A., MILLS, R.E., LANGE, C.J., STEWART, M., DEVINE, S.E. and CORBETT, A.H. (2007). Classical nuclear localization signals: definition, function, and interaction with importin alpha. *J Biol Chem* **282**(8): 5101-5105.

LEIBFRIED, A., TO, J.P., BUSCH, W., STEHLING, S., KEHLE, A., DEMAR, M., KIEBER, J.J. and LOHMANN, J.U. (2005). WUSCHEL controls meristem function by direct regulation of cytokinin-inducible response regulators. *Nature* **438**(7071): 1172-1175.

LOHRMANN, J., BUCHHOLZ, G., KEITEL, C., SWEERE, U., KIRCHER, S., BÄURLE, I., KUDIA, J., SCHÄFER, E.*, et al.* (1999). Differential Expression and Nuclear Localization of Response Regulator-Like Proteins from *Arabidopsis thaliana*. *Plant Biol* **1**: 495-505.

LOHRMANN, J., SWEERE, U., ZABALETA, E., BÄURLE, I., KEITEL, C., KOZMA-BOGNAR, L., BRENNICKE, A., SCHÄFER, E.*, et al.* (2001). The response regulator ARR2: a pollen-specific transcription factor involved in the expression of nuclear genes for components of mitochondrial complex I in *Arabidopsis*. *Mol Genet Genom* **265**: 2-13.

LUMMER, M., HUMPERT, F., STEUWE, C., CAESAR, K., SCHUTTPELZ, M., SAUER, M. and STAIGER, D. (2011). Reversible Photoswitchable DRONPA-s Monitors Nucleocytoplasmic Transport of an RNA-Binding Protein in Transgenic Plants. *Traffic* **12**(6): 693-702.

MACARA, I.G. (2001). Transport into and out of the nucleus. *Microbiol Mol Biol Rev* **65**(4): 570-594, table of contents.

MARION, J., BACH, L., BELLEC, Y., MEYER, C., GISSOT, L. and FAURE, J.D. (2008). Systematic analysis of protein subcellular localization and interaction using high-throughput transient transformation of Arabidopsis seedlings. *Plant J* **56**(1): 169-179.

MASON, M.G., LI, J., MATHEWS, D.E., KIEBER, J.J. and SCHALLER, G.E. (2004). Type-B response regulators display overlapping expression patterns in Arabidopsis. *Plant Physiol* **135**(2): 927-937.

MATTAJ, I.W. and ENGLMEIER, L. (1998). NUCLEOCYTOPLASMIC TRANSPORT: The Soluble Phase. *Annu Rev Biochem* **67**: 265-306.

MIRA-RODADO, V., SWEERE, U., GREFEN, C., KUNKEL, T., FEJES, E., NAGY, F., SCHAFER, E. and HARTER, K. (2007). Functional cross-talk between two-component and phytochrome B signal transduction in Arabidopsis. *J Exp Bot* **58**(10): 2595-2607.

MOORE, M.S. (1998). Ran and Nuclear Transport. *J Biol Chem* **273**: 22857-22860.

MUNOZ-FONTELA, C., RODRIGUEZ, E., NOMBELA, C., ARROYO, J. and RIVAS, C. (2003). Characterization of the bipartite nuclear localization signal of protein LANA2 from Kaposi's sarcoma-associated herpesvirus. *Biochem J* **374**(Pt 2): 545-550.

PAWLOWSKI, R., RAJAKYLA, E.K., VARTIAINEN, M.K. and TREISMAN, R. (2010). An actin-regulated importin alpha/beta-dependent extended bipartite NLS directs nuclear import of MRTF-A. *EMBO J* **29**(20): 3448-3458.

PETERS, R. (2009). Translocation through the nuclear pore: Kaps pave the way. *BioEssays* **31**(4): 466-477.

RAIKHEL, N. (1992). Nuclear targeting in plants. *Plant Physiol* **100**(4): 1627-1632.

REN, B., LIANG, Y., DENG, Y., CHEN, Q., ZHANG, J., YANG, X. and ZUO, J. (2009). Genome-wide comparative analysis of type-A Arabidopsis response regulator genes by overexpression studies reveals their diverse roles and regulatory mechanisms in cytokinin signaling. *Cell Res* **19**(10): 1178-1190.

ROBBINS, J., DILWORTH, S.M., LASKEY, R.A. and DINGWALL, C. (1991). Two interdependent basic domains in nucleoplasmin nuclear targeting sequence: identification of a class of bipartite nuclear targeting sequence. *Cell* **64**(3): 615-623.

RUTHERFORD, S. and MOORE, I. (2002). The Arabidopsis Rab GTPase family: another enigma variation. *Curr Opin Plant Biol* **5**(6): 518-528.

SAKAI, H., AOYAMA, T. and OKA, A. (2000). Arabidopsis ARR1 and ARR2 response regulators operate as transcriptional activators. *Plant J* **24**(6): 703-711.

SALOME, P.A., TO, J.P., KIEBER, J.J. and MCCLUNG, C.R. (2006). Arabidopsis response regulators ARR3 and ARR4 play cytokinin-independent roles in the control of circadian period. *Plant Cell* **18**(1): 55-69.

SANDERFOOT, A.A., ASSAAD, F.F. and RAIKHEL, N.V. (2000). The Arabidopsis genome. An abundance of soluble N-ethylmaleimide-sensitive factor adaptor protein receptors. *Plant Physiol* **124**(4): 1558-1569.

SCHÜTZE, K., HARTER, K. and CHABAN, C. (2009). Bimolecular fluorescence complementation (BiFC) to study protein-protein interactions in living plant cells. *Methods Mol Biol* **479**: 189-202.

STOCK, A.M., ROBINSON, V.L. and GOUDREAU, P.N. (2000). Two-component signal transduction. *Annu Rev Biochem* **69**: 183-215.

SWEERE, U., EICHENBERG, K., LOHRMANN, J., MIRA-RODADO, V., BAURLE, I., KUDLA, J., NAGY, F., SCHAFER, E.*, et al.* (2001). Interaction of the response regulator ARR4 with phytochrome B in modulating red light signaling. *Science* **294**(5544): 1108-1111.

TO, J.P., DERUERE, J., MAXWELL, B.B., MORRIS, V.F., HUTCHISON, C.E., FERREIRA, F.J., SCHALLER, G.E. and KIEBER, J.J. (2007). Cytokinin regulates type-A Arabidopsis Response Regulator activity and protein stability via two-component phosphorelay. *Plant Cell* **19**(12): 3901-3914.

TO, J.P., HABERER, G., FERREIRA, F.J., DERUERE, J., MASON, M.G., SCHALLER, G.E., ALONSO, J.M., ECKER, J.R.*, et al.* (2004). Type-A Arabidopsis response regulators are partially redundant negative regulators of cytokinin signaling. *Plant Cell* **16**(3): 658-671.

URAO, T., YAMAGUCHI-SHINOZAKI, K. and SHINOZAKI, K. (2000). Two-component systems in plant signal transduction. *Trends Plant Sci* **5**(2): 67-74.

VARAGONA, M.J., SCHMIDT, R.J. and RAIKHEL, N.V. (1992). Nuclear localization signal(s) required for nuclear targeting of the maize regulatory protein Opaque-2. *Plant Cell* **4**(10): 1213-1227.

VISION, T.J. (2000). The Origins of Genomic Duplications in Arabidopsis. *Science* **290**(5499): 2114-2117.

WEST, A.H. and STOCK, A.M. (2001). Histidine kinases and response regulator proteins in two-component signaling systems. *Trends Biochem Sci* **26**(6): 369-376.

ZHENG, B., DENG, Y., MU, J., JI, Z., XIANG, T., NIU, Q.-W., CHUA, N.-H. and ZUO, J. (2006). Cytokinin affects circadian-clock oscillation in a phytochrome B- and Arabidopsis response regulator 4-dependent manner. *Physiol Plant* **127**(2): 277-292.

ZIPFEL, C., KUNZE, G., CHINCHILLA, D., CANIARD, A., JONES, J.D., BOLLER, T. and FELIX, G. (2006). Perception of the bacterial PAMP EF-Tu by the receptor EFR restricts Agrobacterium-mediated transformation. *Cell* **125**(4): 749-760.

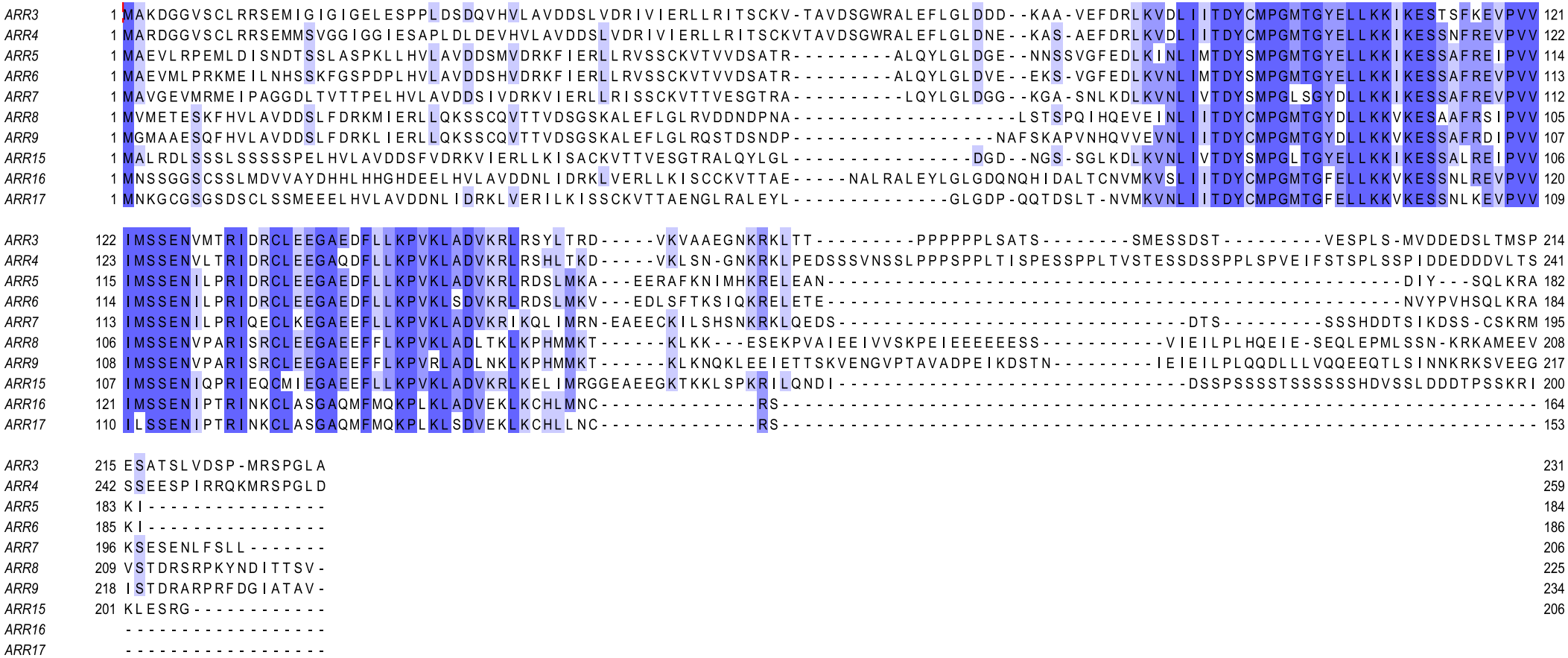
ARR3 1 MAKDGGVSCLRRSEMIGIGIGELESPPLDSDQVHVLAVDDSLVDRIVIERLLRITSCKV-TAVDSGWRALEFLGLDDD--KAA-VEFDRLKVDLIITDYCMPGMTGYELLKKIKESTSFKEVPVV 121
ARR4 1 MARDGGVSCLRRSEMMSVGGIGGIESAPLDLDEVHVLAVDDSLVDRIVIERLLRITSCKVTAVDSGWRALEFLGLDNE--KAS-AEFDRLKVDLIITDYCMPGMTGYELLKKIKESSNFREVPVV 122
ARR5 1 MAEVLRPEMLDISNDTSSLASPKLLHVLAVDDSMVDRKFIERLLRVSSCKVTVVDSATR---------ALQYLGLDGE--NNSSVGFEDLKINLIMTDYSMPGMTGYELLKKIKESSAFREIPVV 114
ARR6 1 MAEVMLPRKMEILNHSSKFGSPDPLHVLAVDDSHVDRKFIERLLRVSSCKVTVVDSATR---------ALQYLGLDVE--EKS-VGFEDLKVNLIMTDYSMPGMTGYELLKKIKESSAFREVPVV 113
ARR7 1 MAVGEVMRMEIPAGGDLTVTTPELHVLAVDDSIVDRKVIERLLRISSCKVTTVESGTRA----------LQYLGLDGG--KGA-SNLKDLKVNLIVTDYSMPGLSGYDLLKKIKESSAFREVPVV 112
ARR8 1 MVMETESKFHVLAVDDSLFDRKMIERLLQKSSCQVTTVDSGSKALEFLGLRVDDNDPNA--------------------LSTSPQIHQEVEINLIITDYCMPGMTGYDLLKKVKESAAFRSIPVV 105
ARR9 1 MGMAAESQFHVLAVDDSLFDRKLIERLLQKSSCQVTTVDSGSKALEFLGLRQSTDSNDP-----------------NAFSKAPVNHQVVEVNLIITDYCMPGMTGYDLLKKVKESSAFRDIPVV 107
ARR15 1 MALRDLSSSLSSSSSPELHVLAVDDSFVDRKVIERLLKISACKVTTVESGTRALQYLGL---------------DGD--NGS-SGLKDLKVNLIVTDYSMPGLTGYELLKKIKESSALREIPVV 106
ARR16 1 MNSSGGSCSSLMDVVAYDHHLHHGHDEELHVLAVDDNLIDRKLVERLLKISCCKVTTAE-----NALRALEYLGLGDQNQHIDALTCNVMKVSLIITDYCMPGMTGFELLKKVKESSNLREVPVV 120
ARR17 1 MNKGCGSGSDSCLSSMEEELHVLAVDDNLIDRKLVERILKISSCKVTTAENGLRALEYL--------------GLGDP-QQTDSLT-NVMKVNLIITDYCMPGMTGFELLKKVKESSNLKEVPVV 109

ARR3 122 IMSSENVMTRIDRCLEEGAEDFLLKPVKLADVKRLRSYLTRD-----VKVAAEGNKRKLTT---------PPPPPPLSATS--------SMESSDST---------VESPLS-MVDDEDSLTMSP 214
ARR4 123 IMSSENVLTRIDRCLEEGAQDFLLKPVKLADVKRLRSHLTKD-----VKLSN-GNKRKLPEDSSSVNSSLPPPSPPLTISPESSPPLTVSTESSDSSPPLSPVEIFSTSPLSSPIDDEDDDVLTS 241
ARR5 115 IMSSENILPRIDRCLEEGAEDFLLKPVKLADVKRLRDSLMKA---EERAFKNIMHKRELEAN--DIY---SQLKRA 182
ARR6 114 IMSSENILPRIDRCLEEGAEDFLLKPVKLSDVKRLRDSLMKV---EDLSFTKSIQKRELETE--NVYPVHSQLKRA 184
ARR7 113 IMSSENILPRIQECLKEGAEEFLLKPVKLADVKRIKQLIMRN-EAEECKILSHSNKRKLQEDS----------------------------DTS---------SSSHDDTSIKDSS-CSKRM 195
ARR8 106 IMSSENVPARISRCLEEGAEEFFLKPVKLADLTKLKPHMMKT------KLKK---ESEKPVAIEEIVVSKPEIEEEEEESS----------VIEILPLHQEIE-SEQLEPMLSSN-KRKAMEEV 208
ARR9 108 IMSSENVPARISRCLEEGAEEFFLKPVRLADLNKLKPHMMKT------KLKNQKLEEIETTSKVENGVPTAVADPEIKDSTN---------IEIEILPLQQDLLLVQQEEQTLSINNKRKSVEEG 217
ARR15 107 IMSSENIQPRIEQCMIEGAEEFLLKPVKLADVKRLKELIMRGGEAEEGKTKKLSPKRILQNDI----------------------------DSSPSSSSTSSSSSSHDVSSLDDDTPSSKRI 200
ARR16 121 IMSSENIPTRINKCLASGAQMFMQKPLKLADVEKLKCHLMNC----------RS---------- 164
ARR17 110 ILSSENIPTRINKCLASGAQMFMQKPLKLSDVEKLKCHLLNC----------RS---------- 153

ARR3 215 ESATSLVDSP-MRSPGLA 231
ARR4 242 SSEESPIRRQKMRSPGLD 259
ARR5 183 KI---------------- 184
ARR6 185 KI---------------- 186
ARR7 196 KSESENLFSLL------- 206
ARR8 209 VSTDRSRPKYNDITTSV- 225
ARR9 218 ISTDRARPRFDGIATAV- 234
ARR15 201 KLESRG---------- 206
ARR16 ----------
ARR17 ----------

Figure 1

A

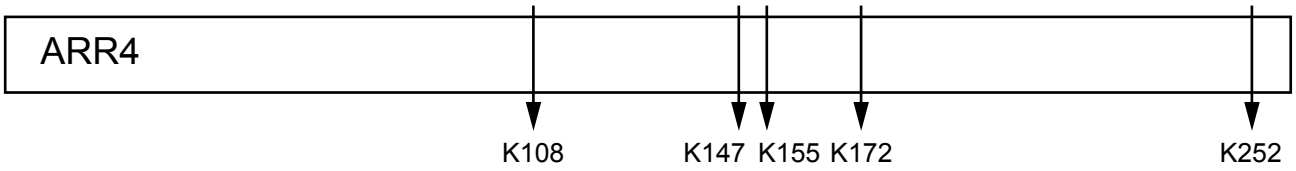

MARDGGVSCLRRSEMMSVGGIGGIESAPLDLDEVHVLAVDDSLVDRIVIERLLRITSCKVTAVDSGWRALEFL
GLDNEKASAEFDRLKVDLIITDYCMPGMTGYELL**K**KIKESSNFREVPVVIMSSENVLTRIDRCLEEGAQDFLL
KPVKLADV**K**RLRSHLTKDVKLSNGN**K**RKLPEDSSSVNSSLPPPSPPLTISPESSPPLTVSTESSDSSPPLSPV
EIFSTSPLSSPIDDEDDDVLTSSSEESPIRRQ**K**MRSPGLD

B

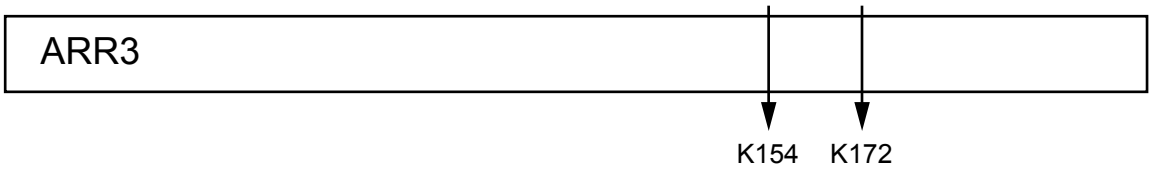

MARDGGVSCLRRSEMMSVGGIGGIESAPLDLDEVHVLAVDDSLVDRIVIERLLRITSCKVTAVDSGW
RALEFLGLDNEKASAEFDRLKVDLIITDYCMPGMTGYELLKKIKESSNFREVPVVIMSSENVLTRIDR
CLEEGAQDFLLKPVKLADV**K**RLRSHLT KDVKLSNGN**K**RKLPEDSSSVNSSLPPPSPPLTISPESSP
PLTVSTESSDSSPPLSPVEIFSTSPLSSPIDDEDDDVLTSSSEESPIRRQKMRSPGLD

C

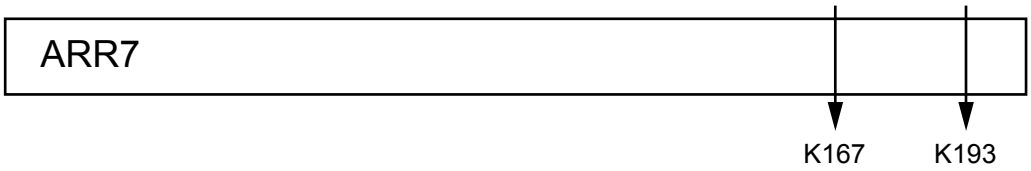

MAVGEVMRMEIPAGGDLTVTTPELHVLAVDDSIVDRKVIERLLRISSCKVTTVESGTRALQYLGLDG
GKGASNLKDLKVNLIVTDYSMPGLSGYDLLKKIKESSAFREVPVVIMSSENILPRIQECLKEGAEEFL
LKPVKLADVKRIKQLIMRNEAEECKILSHSN**K**RKLQEDSDTSSSSHDDTSIKDSSCS**K**RMKSESEN
LFSLL

D

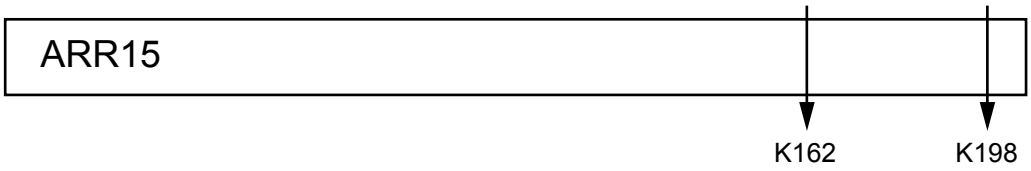

MALRDLSSSLSSSSSPELHVLAVDDSFVDRKVIERLLKISACKVTTVESGTRALQYLGLDGDNGSS
GLKDLKVNLIVTDYSMPGLTGYELLKKIKESSALREIPVVIMSSENIQPRIEQCMIEGAEEFLLKPVKL
ADVKRLKELIMRGGEAEEGKTKKLSP**K**RILQNDIDSSPSSSSTSSSSSSHDVSSLDDDTPSS
KRIKLESRG

Figure 2

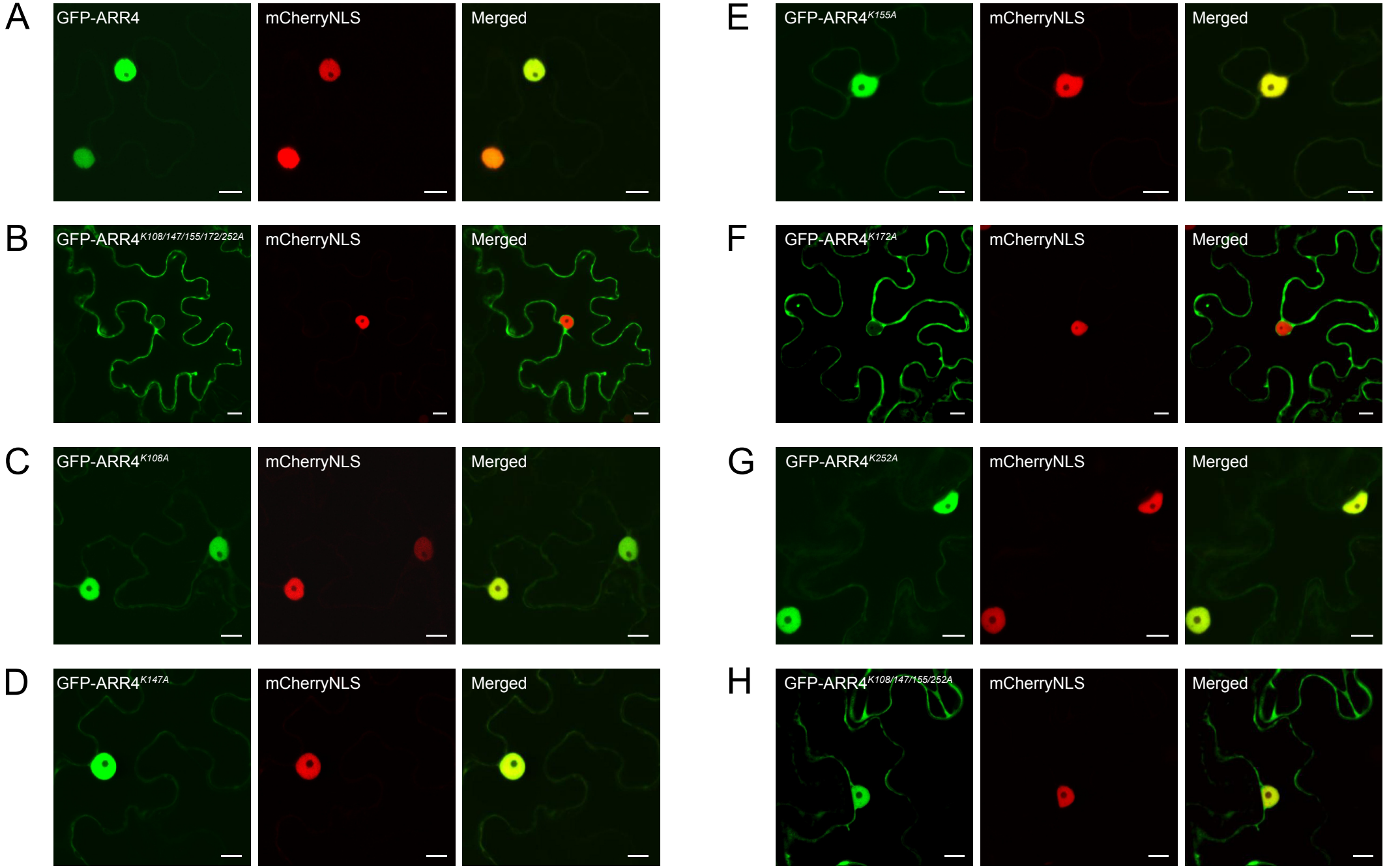
A
GFP-ARR4
mCherryNLS
Merged
B
GFP-ARR4K108/147/155/172/252A
mCherryNLS
Merged
C
GFP-ARR4K108A
mCherryNLS
Merged
D
GFP-ARR4K147A
mCherryNLS
Merged
E
GFP-ARR4K155A
mCherryNLS
Merged
F
GFP-ARR4K172A
mCherryNLS
Merged
G
GFP-ARR4K252A
mCherryNLS
Merged
H
GFP-ARR4K108/147/155/252A
mCherryNLS
Merged

Figure 3

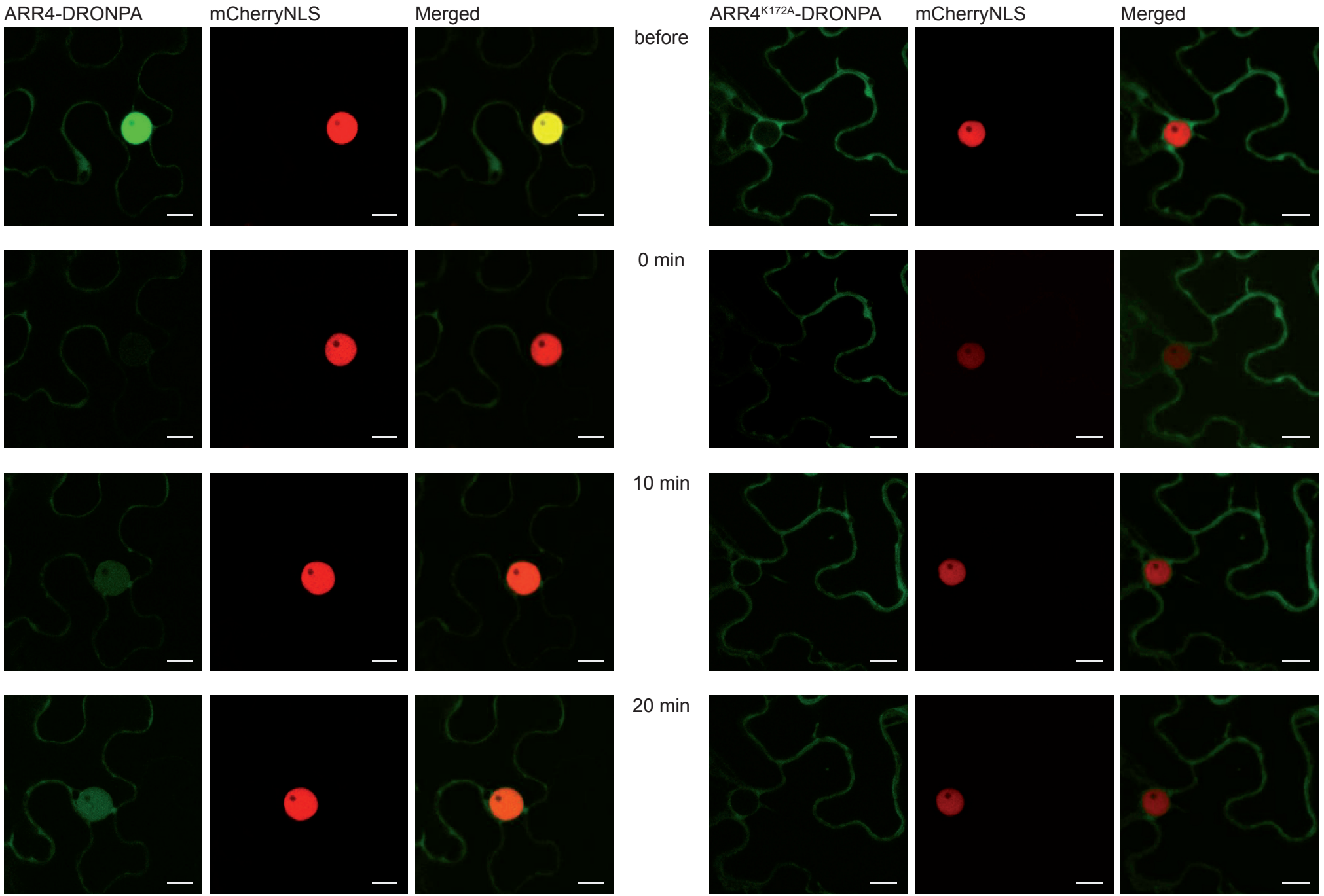
ARR4-DRONPA
mCherryNLS
Merged
before
ARR4K172A-DRONPA
mCherryNLS
Merged
0 min
10 min
20 min

Figure 4

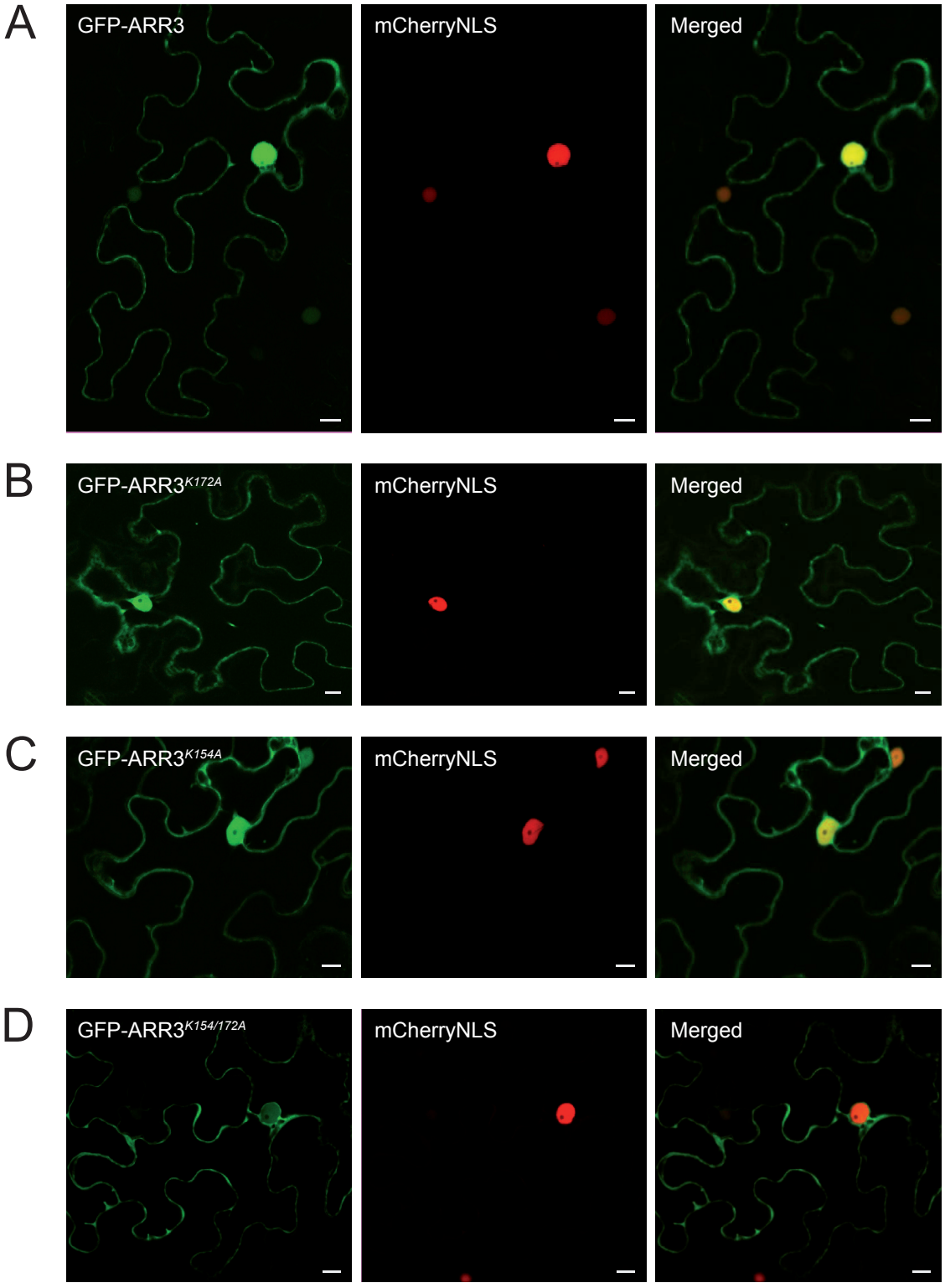
A
GFP-ARR3
mCherryNLS
Merged
B
GFP-ARR3K172A
mCherryNLS
Merged
C
GFP-ARR3K154A
mCherryNLS
Merged
D
GFP-ARR3K154/172A
mCherryNLS
Merged

Figure 5

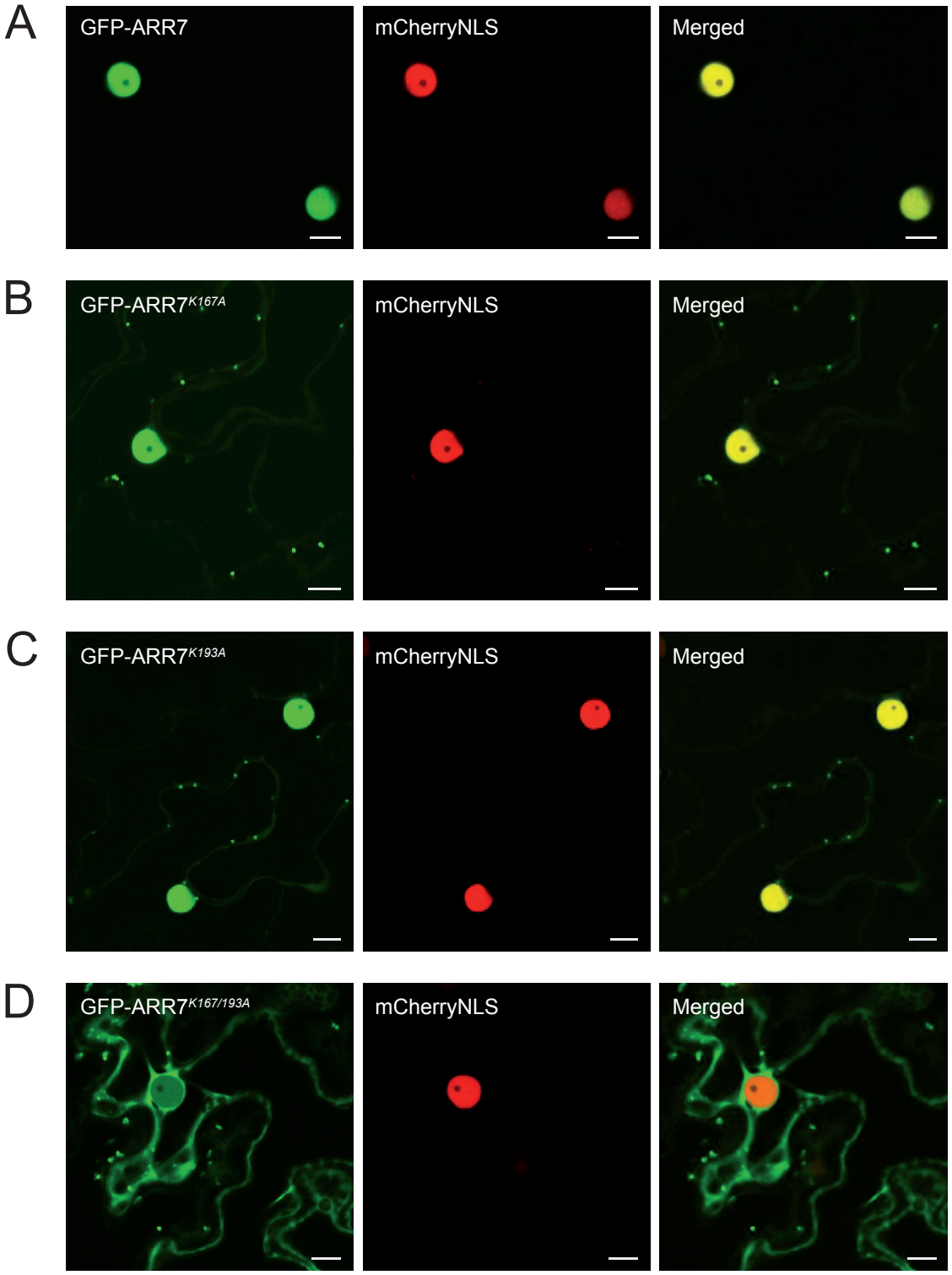
A
GFP-ARR7
mCherryNLS
Merged
B
GFP-ARR7K167A
mCherryNLS
Merged
C
GFP-ARR7K193A
mCherryNLS
Merged
D
GFP-ARR7K167/193A
mCherryNLS
Merged

Figure 6

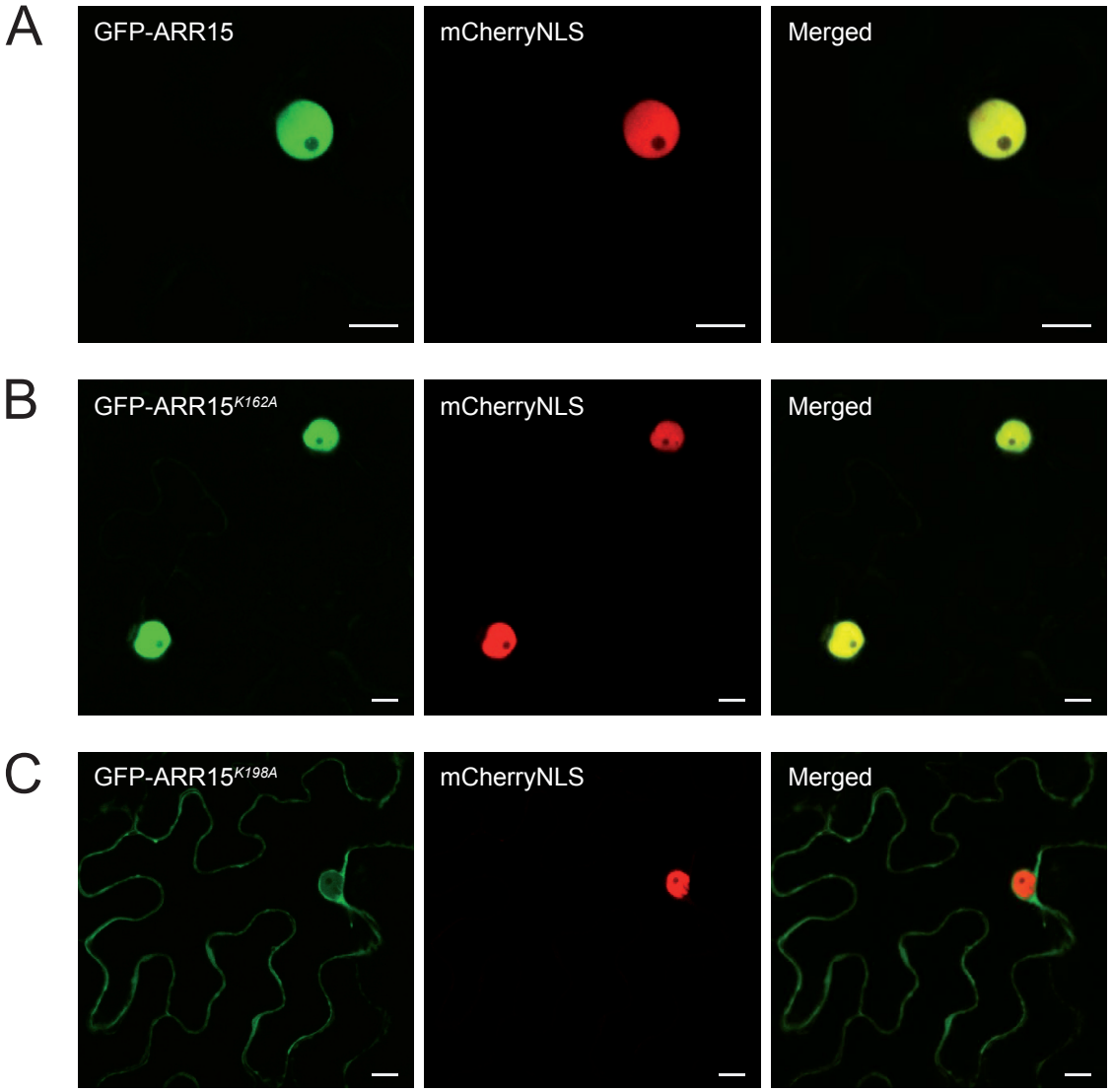
A
GFP-ARR15
mCherryNLS
Merged
B
GFP-ARR15K162A
mCherryNLS
Merged
C
GFP-ARR15K198A
mCherryNLS
Merged

Figure 7

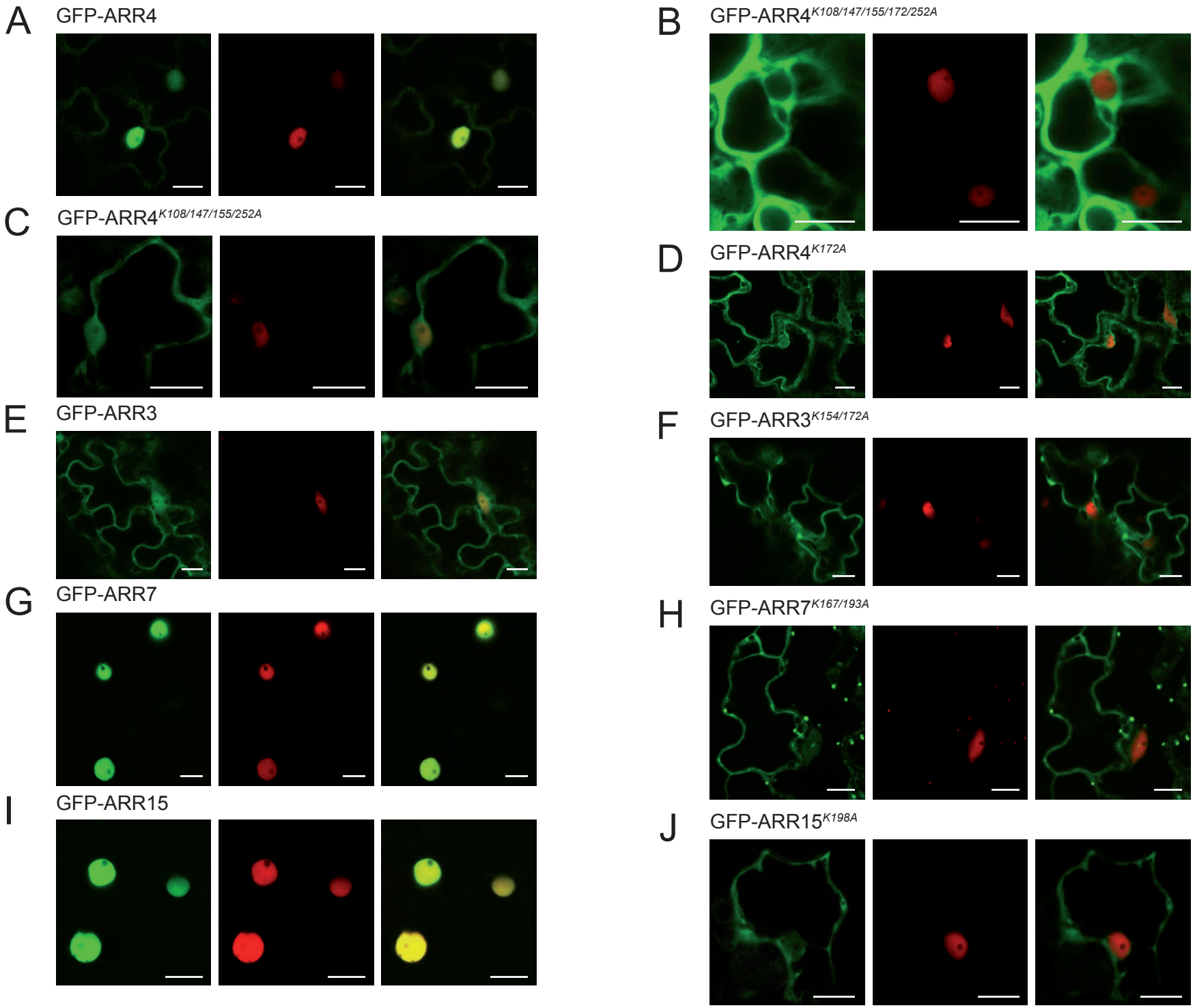
A
GFP-ARR4
B
GFP-ARR4K108/147/155/172/252A
C
GFP-ARR4K108/147/155/252A
D
GFP-ARR4K172A
E
GFP-ARR3
F
GFP-ARR3K154/172A
G
GFP-ARR7
H
GFP-ARR7K167/193A
I
GFP-ARR15
J
GFP-ARR15K198A

Suppl. Fig. 1

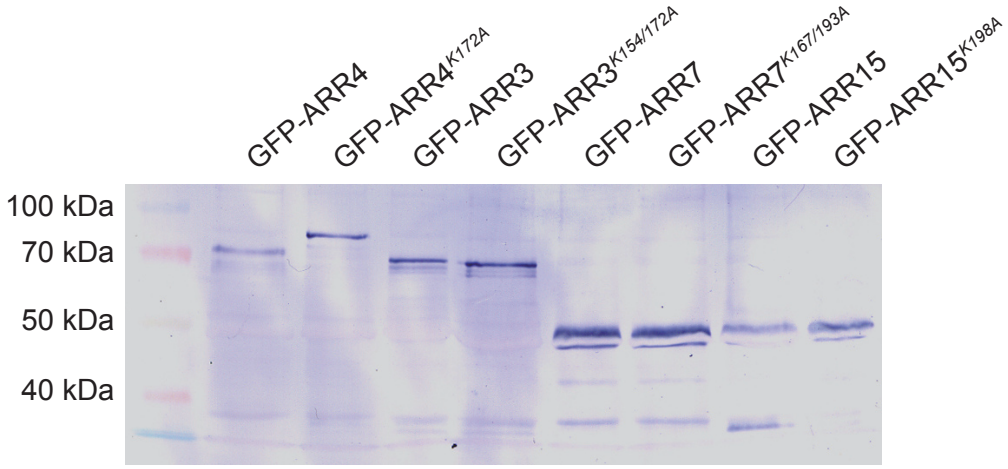

Suppl. Fig. 2

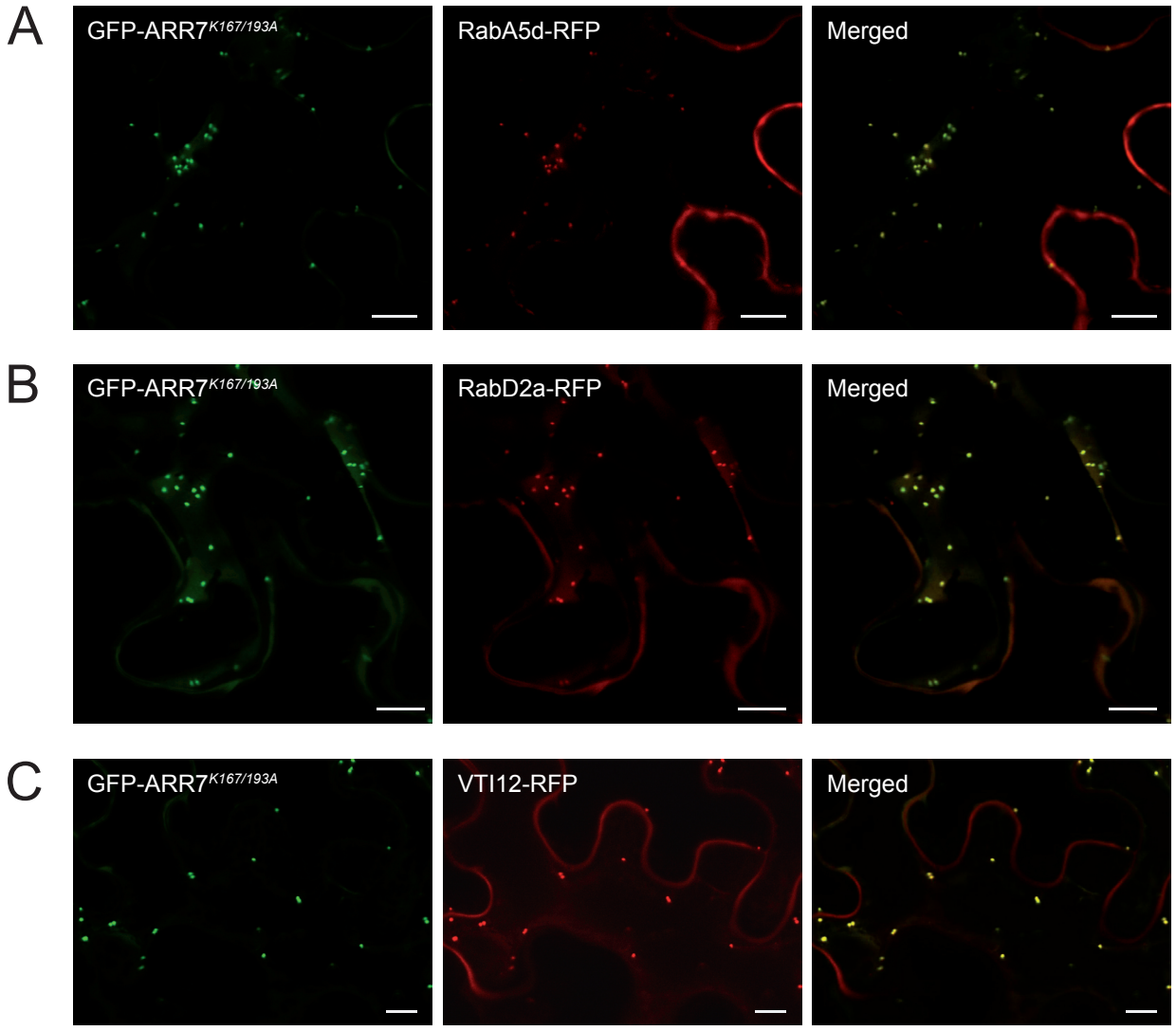

Suppl. Fig. 3

Table 1: Forward primers of the fully complementary primer pairs used for site directed mutagenesis. The mutated nucleotides are highlighted in bold.

***Gene*^{Mutation}**	**Forward Primer (5' to 3')**	**Inserted (+) or removed (-) restriction site**
ARR3^{K172A}	gccgccgaaggaaac**GC**acggaagct**T**accactcc	+ HindIII
ARR3^{K154A}	ctcgccgacgtg**GC**acgtctgaggagttacttgacgagagacg	No modification
ARR4^{K108A}	ggttatgagct**C**ctc**GC**gaagattaagg	+ SacI
ARR4^{K147A}	gaggaagg**A**gctcaagatttcttattg**GC**accggtg	+ SacI
ARR4^{K155A}	ccggtgaaactcgccgacgtg**GC**acgtctgag	+ BglI
ARR4^{K172A}	ccaacggaaac**GC**acggaagct**A**ccggaag	– HindIII
ARR4^{K252A}	cgccgattcg**G**cggcag**GC**gatgaggagtcccgg	+ BglI
ARR7^{K167A}	gccattctaac**GC**gagaaagct**A**caag	– HindIII
ARR7^{K193A}	ggactcttcatgttca**GC**acgaatgaaatcag	No modification
ARR15^{K198A}	ctccatcttcc**GCG**aggatcaaattagagtct**C**gggg	+ AvaI
ARR15^{K162A}	cttagtcct**GC**gagaatcctac	No modification

OPEN ACCESS Freely available online

PLoS one

The Histidine Kinase AHK5 Integrates Endogenous and Environmental Signals in *Arabidopsis* Guard Cells

Radhika Desikan[1,5]*, Jakub Horák[2], Christina Chaban[2], Virtudes Mira-Rodado[2], Janika Witthöft[2], Kirstin Elgass[3], Christopher Grefen[2], Man-Kim Cheung[5], Alfred J. Meixner[3], Richard Hooley[4], Steven John Neill[5], John Travers Hancock[5], Klaus Harter[2]*

1 Division of Biology, Imperial College London, London, United Kingdom, **2** Zentrum für Molekularbiologie der Pflanzen / Pflanzenphysiologie, Universität Tübingen, Tübingen, Germany, **3** Department of Nano Optics, Institute for Physical and Theoretical Chemistry, Universität Tübingen, Tübingen, Germany, **4** Department of Biology and Biochemistry, University of Bath, Bath, United Kingdom, **5** Centre for Research in Plant Science, University of the West of England, Bristol, United Kingdom

Abstract

Background: Stomatal guard cells monitor and respond to environmental and endogenous signals such that the stomatal aperture is continually optimised for water use efficiency. A key signalling molecule produced in guard cells in response to plant hormones, light, carbon dioxide and pathogen-derived signals is hydrogen peroxide (H_2O_2). The mechanisms by which H_2O_2 integrates multiple signals via specific signalling pathways leading to stomatal closure is not known.

Principal Findings: Here, we identify a pathway by which H_2O_2, derived from endogenous and environmental stimuli, is sensed and transduced to effect stomatal closure. Histidine kinases (HK) are part of two-component signal transduction systems that act to integrate environmental stimuli into a cellular response via a phosphotransfer relay mechanism. There is little known about the function of the HK AHK5 in *Arabidopsis thaliana*. Here we report that in addition to the predicted cytoplasmic localisation of this protein, AHK5 also appears to co-localise to the plasma membrane. Although *AHK5* is expressed at low levels in guard cells, we identify a unique role for AHK5 in stomatal signalling. *Arabidopsis* mutants lacking AHK5 show reduced stomatal closure in response to H_2O_2, which is reversed by complementation with the wild type gene. Over-expression of AHK5 results in constitutively less stomatal closure. Abiotic stimuli that generate endogenous H_2O_2, such as darkness, nitric oxide and the phytohormone ethylene, also show reduced stomatal closure in the *ahk5* mutants. However, ABA caused closure, dark adaptation induced H_2O_2 production and H_2O_2 induced NO synthesis in mutants. Treatment with the bacterial pathogen associated molecular pattern (PAMP) flagellin, but not elf peptide, also exhibited reduced stomatal closure and H_2O_2 generation in *ahk5* mutants.

Significance: Our findings identify an integral signalling function for AHK5 that acts to integrate multiple signals via H_2O_2 homeostasis and is independent of ABA signalling in guard cells.

Citation: Desikan R, Horák J, Chaban C, Mira-Rodado V, Witthöft J, et al. (2008) The Histidine Kinase AHK5 Integrates Endogenous and Environmental Signals in *Arabidopsis* Guard Cells. PLoS ONE 3(6): e2491. doi:10.1371/journal.pone.0002491

Editor: Markus Grebe, Umeå Plant Science Centre, Sweden

Received December 6, 2007; **Accepted** May 22, 2008; **Published** June 18, 2008

Funding: This work was funded by a Leverhulme Trust Early Career Fellowship to RD, BBSRC grant to SJN, JTH and RH and DFG grants to KH (AFGN-Ha2146/5, Ha2146/7).

Competing Interests: The authors have declared that no competing interests exist.

* E-mail: r.desikan@ic.ac.uk (RD), klaus.harter@zmbp.uni-tuebingen.de (KH)

Introduction

Plants are constantly exposed to a large multitude of environmental stimuli, and under adverse conditions, are mostly able to survive due to their ability to sense and transduce these signals into cellular and physiological responses. Hydrogen peroxide (H_2O_2) is a form of reactive oxygen species (ROS) generated by plants via several mechanisms, which include metabolic processes such as respiration and photosynthesis as well as reactions to environmental stimuli such as water deficit, high and low temperature, pollutants, UV-B light and pathogen challenge [1]. It is now well accepted that controlled or regulated production of H_2O_2 is beneficial to the plant. H_2O_2 acts as a signal and/or second messenger enabling the plant to activate physiological processes resulting in protection from and adaptation to environmental stress [2].

H_2O_2 regulates a number of molecular and cellular processes in plants ranging from gene expression, programmed cell death, cell division, elongation growth, and stomatal closure [3]. The molecular mechanisms by which each of these processes occurs through H_2O_2 signalling have not been fully clarified. Recently, several targets for H_2O_2 have been identified in *Arabidopsis*, including protein kinases and phosphatases [4–8]. In relation to stomatal closure and redox signalling, the ABI1 and ABI2 members of the protein phosphatase 2C family are redox regulated in response to ABA [9,10]. Moreover, the MAP kinase MPK3 was shown recently to be essential for both ABA and H_2O_2-inhibition of stomatal opening in *Arabidopsis* [11]. The protein kinase OST1 regulates H_2O_2 production in guard cells through signalling pathways requiring the ROS-producing NADPH oxidase subfamily of proteins (namely, AtRBOHD and AtRBOHF [12,13]). Thus, reversible protein phosphorylation appears to be a key

mechanism by which cellular responses to multiple stimuli are regulated via H_2O_2 in guard cells and other cell types.

An alternative mechanism by which H_2O_2 acts on proteins is by oxidation of Cys residues [14]. H_2O_2 oxidation of –SH groups on Cys residues in proteins causes either disulfide bond formation or the formation of sulfenic acid groups. The latter can be sequentially oxidised to sulfinic and sulfonic acid groups at higher concentrations of H_2O_2. Reversal of oxidation occurs under reducing conditions, for example, by reduced glutathione or thioredoxin [14]. Until recently, there was little evidence that H_2O_2 action on Cys residues is responsible for defined physiological responses. In recent work, we have shown that one member of the *Arabidopsis* hybrid histidine kinase (HK) family, the ethylene receptor ETR1, is a potential target for H_2O_2 during stomatal closure [15]. ETR1 is required for H_2O_2-mediated stomatal closure, with the Cys65 residue of ETR1 being essential. Intriguingly the HK domain of ETR1 was not required for H_2O_2-induced closure [15]. In recent developments we have also shown that ETR1 has a dual function in guard cells, that of perceiving ethylene as well as acting as a target for H_2O_2, thereby mediating downstream signalling processes to initiate stomatal closure [16].

The hybrid HK family of receptor proteins are part of the two-component signal perception and transduction system in plants [17]. Perception of a signal by a hybrid HK leads to autophosphorylation of a His residue in the HK domain, followed by a phosphotransfer reaction to an Asp residue on its receiver domain. Subsequently, a relay of the phosphoryl residue occurs to a His residue on a histidine phosphotransfer protein (HP) followed by phosphorylation of an Asp residue on a response regulator (RR) protein [18]. Representative HK family members in plants are the cytokinin and ethylene receptors [17]. However, the plant's two-component signalling network appears to contribute to several other signal response pathways. For instance, recent work has demonstrated functional cross-talk between cytokinin and light (phytochrome B) signalling [19,20]. These overlaps in signalling processes induced by multiple stimuli suggest that two-component proteins are key sensors and transducers of various environmental and endogenous signals.

One mechanism by which different signalling processes and pathways may be integrated is *via* common second messenger molecules. ROS such as H_2O_2 are ideal candidates for such messenger molecules acting as focal points for cross-talk between a wide array of signalling cascades [3]. This is evidenced by a large overlap in the expression of genes that are regulated by ROS on the one hand and by environmental stimuli on the other. For example, H_2O_2-regulated genes are also regulated by drought, cold, UV-B light and pathogen attack [21,22] as well as by ABA [23]. Clearly, there exist multiple targets for H_2O_2 to mediate its effects in specific cells and tissues. Functional overlap is also likely to exist between these pathways, with certain targets acting as integrators of multiple stimuli.

In an attempt to identify further targets for H_2O_2 signalling in guard cells, the function of a least-characterised member of the HK family in *Arabidopsis*, namely AHK5, was investigated. AHK5 is predicted to be the only cytoplasmic HK, with both a canonical HK domain and receiver domain, classifying it as a hybrid HK [17]. Our data here indicate that AHK5 also co-localises to the plasma membrane. Recent work has identified a function for AHK5 in counteracting the ethylene and ABA-regulated growth response in *Arabidopsis* roots [24]. However its role in integrating signalling responses to H_2O_2 is not known.

Using a combination of molecular genetic, cell imaging, biochemical and physiological tools, we show that AHK5 is a key player in H_2O_2 homeostasis in *Arabidopsis* guard cells in response to environmental and endogenous signals, including NO, ethylene, darkness and bacterial flagellin. Intriguingly, AHK5 does not appear to be involved in the ABA signalling pathway in stomata. Our data suggest a regulatory function of AHK5 that is essential for guard cell response to abiotic and biotic environmental stimuli.

Results

Intracellular localisation and tissue-specific expression of AHK5

AHK5 is predicted to be the only cytoplasmic HK amongst the canonical HK class of proteins in *Arabidopsis* [17]. In order to confirm this, we performed *in vivo* localisation studies using 35S promoter-driven GFP fusion constructs of *AHK5*. In transiently transformed *Arabidopsis* protoplasts and tobacco (*Nicotiana benthamiana*) leaf cells the full-length fusion protein was expressed and was present in the cytoplasm, independent of whether the GFP tag was fused to the N-terminus or C-terminus of AHK5 (Fig. 1A and B, and Data S1). To substantiate our cell biological results we also performed cell fractionation experiments with extracts from transiently transformed tobacco leaf cells expressing *35S:GFP-AHK5* or several GFP-marker protein fusion genes. Whereas the ER marker ERS1-GFP [25] and the plasmalemma/endosome marker BRI1-GFP [26] were detected in the microsomal fraction and the cytoplasmic/nucleoplasmic marker ARR4-GFP [19] in the soluble fraction, GFP-AHK5 was found in both fractions (Fig. 1C). This intracellular distribution could be substantiated by recording the wavelength-specific intensity distribution of a cytoplasm-plasmalemma-cell wall section of neighbouring tobacco epidermal cells co-expressing GFP-AHK5 and the red fluorescent plasmalemma marker pm-rk-CD3-1007 (Fig. 1D; [27]). Whereas pm-rk-CD3-1007 showed one distinct peak representing the two plasmalemmata of the adjacent cells, three peaks were observed for GFP-AHK5 (Fig. 1D). The medial GFP-AHK5 peak showed a perfect overlay with pm-rk-CD3-1007, whereas the other two peaks extended to the cytoplasmic sites of the adjacent cells. Our results therefore suggest that AHK5 is a HK that is localised both in the cytoplasm and at the plasmalemma of plant cells.

The expression profile of *AHK5* in different *Arabidopsis* tissues and cell types was analysed by semi-quantitative RT-PCR. *AHK5* transcript was detectable in light-grown but not in etiolated seedlings (Fig. 2A). Furthermore, *AHK5* transcript was present in flowers, siliques and roots and to a lower extent in stems and leaves of 30-days-old *Arabidopsis* plants (Fig. 2A). Increasing the number of PCR cycles showed a detectable level of *AHK5* transcript in mature leaves. As guard cells were the focus of our study, *AHK5* expression was also analysed in guard-cell enriched samples [16]. Compared to whole leaves the *AHK5* transcript level was significantly lower in guard cells. However, *AHK5* expression was increased in guard cell RNA extracted from H_2O_2-treated leaves (Fig. 2A), suggesting that AHK5 might have a function in H_2O_2 signalling in guard cells. The guard cell expression of AHK5 was confirmed by creating an *AHK5* promoter-GFP-AHK5 genomic construct (P_{AHK5}*:GFP-AHK5*) and transiently expressing this in tobacco leaves. As shown in Fig. 2B and comparable to our RT-PCR results, GFP fluorescence was detected in guard cells as well as in epidermal cells indicating that the *AHK5* promoter is active in stomata. Our expression data therefore correlate well with the expression profile of *AHK5* observed in the AtGenExpress developmental data set [28] and adds to that reported earlier [24].

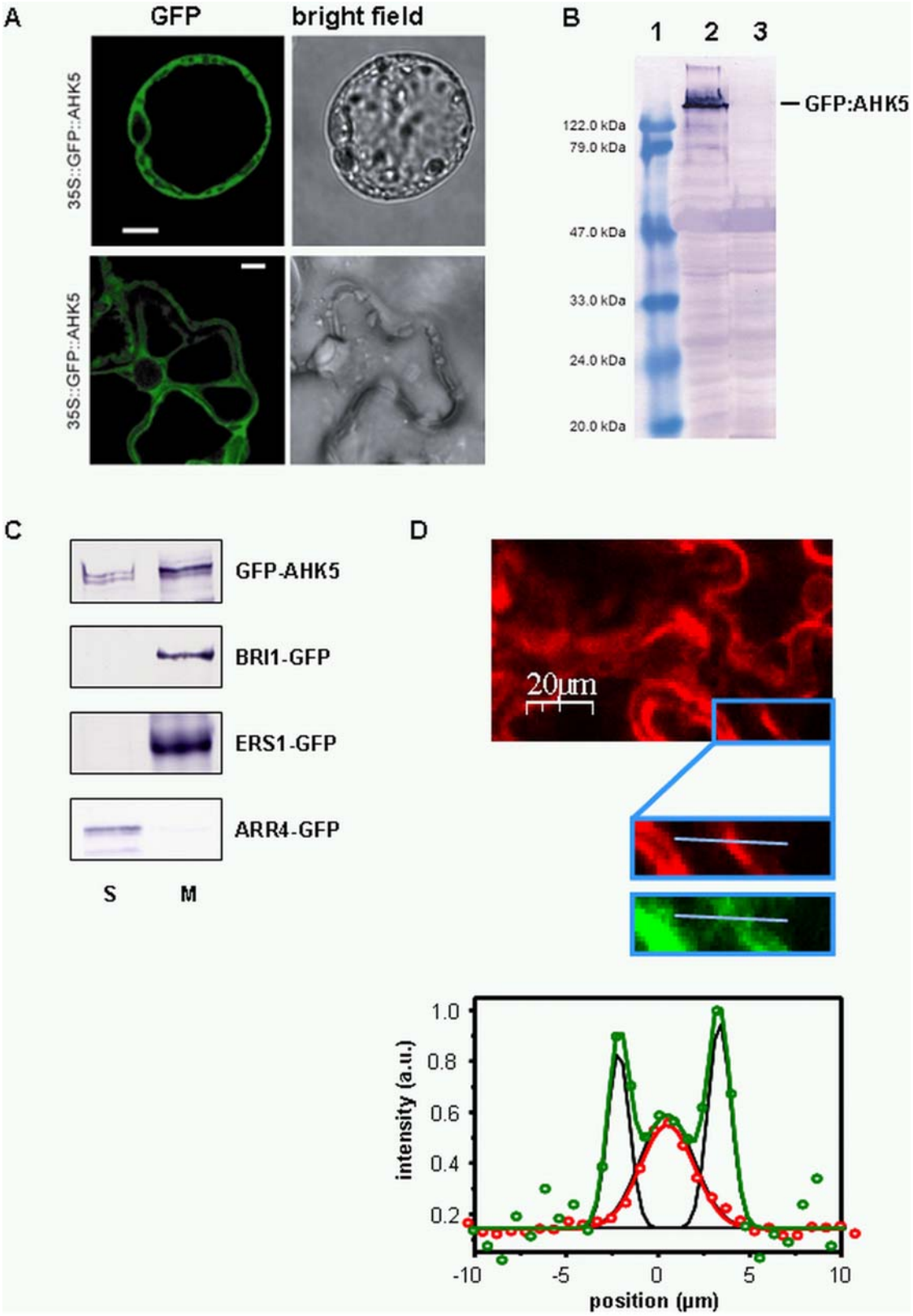

Figure 1. Subcellular localisation of AHK5 in plant cells. (A) Confocal images of *Arabidopsis* protoplasts and tobacco (*Nicotiana benthamiana*) leaf cells transiently transformed with a construct expressing P_{35S}*:GFP-AHK5* cDNA. Left panel, GFP fluorescence; right panel, bright field image. The bars represent 10 µm. (B) Western blot showing the expression of full-length GFP-AHK5 in transiently transformed tobacco leaf cells using anti-GFP antibody. Lane 1, protein standard; lane 2, extracts from cells transformed with a P_{35S}*-GFP-AHK5* construct; lane 3, extracts from cells transformed with the empty vector. (C) Cell fractionation of transiently transformed tobacco leaf cells expressing either GFP-AHK5, the microsomal marker BRI-GFP, the ER marker ERS1-GFP or the soluble marker ARR4-GFP.Two days after the infiltration of the *Agrobacteria* the leaf tissue was harvested and total protein

extracted. The microsomal fraction (M) and the soluble fraction (S) were separated by ultracentrifugation. Equal cell equivalents were loaded per lane. (D) Fluorescence intensity images (upper panel) and the corresponding intensity profiles (lower diagram) of the indicated plasmalemma-cell wall section (blue bar in the magnification) of two adjacent, transiently transformed tobacco leaf cells co-expressing GFP-AHK5 (green dots) and the plasma membrane marker pm-rk-CD3-1007 (red dots). The red line represents the mono-peak Gauss fit of RFP fluorescence and the green line the multi-peak Gauss fit of GFP fluorescence (green). The single fits which compose the multi-peak Gauss fit of GFP, are shown in black.
doi:10.1371/journal.pone.0002491.g001

Identification and characterisation of *ahk5* T-DNA insertion mutants

The functional characterisation of *AHK5* was initiated by the isolation and molecular characterization of *Arabidopsis ahk5* T-DNA insertion lines. Two independent *ahk5* alleles were found, one in the INRA-Versailles T-DNA collection (*ahk5-3* in Ws4 background; [29]) and one in the Syngenta SAIL T-DNA collection (*ahk5-1* in Col-0 background; [30]), respectively. Plants homozygous for the insertion events were identified by PCR on genomic DNA, and the positions of the T-DNA insertions confirmed by sequencing. As shown in Fig. 2C the T-DNA of *ahk5-3* is located in an intron within the predicted HK domain, whereas in *ahk5-1* the T-DNA is inserted in a 3′ exon which encodes a part of the AHK5 receiver domain. The T-DNA insertions did not appear to cause any other changes within the *AHK5* sequence. In addition, the presence of a single T-DNA insertion event in each line was verified by Southern blotting (Data S1). Semi-quantitative RT-PCR was used to determine the level of expression of *AHK5* in the homozygous lines. Fig. 2D shows that across the T-DNA borders there was no amplification of an *AHK5* transcript. Further extensive PCR using different primer pair combinations (of those shown in Fig. 2C) confirmed that no full-length transcript of *AHK5* was present in the mutant lines (Data S1). Therefore a fully functional AHK5 is unlikely to be expressed in *ahk5-1* and *ahk5-3*.

For complementation and functional analyses *ahk5-1* and *ahk5-3* were transformed with a construct expressing the full-length *GFP-AHK5* or *AHK5-TAP* fusion construct respectively under the control of the 35S promoter. In addition, *AHK5* was ectopically expressed in the Ws4 wild type background (Fig. 2D). RT-PCR confirmed that the transformed *ahk5* mutants and wild type expressed *AHK5* to high levels (Fig. 2D).

A functional AHK5 HK is required for H_2O_2 responses in stomatal guard cells

Initially, a pharmacological approach was used to establish whether HK activity is required for H_2O_2 -induced stomatal closure. *Arabidopsis* wild type (Col-0) leaves were pre-treated with the inhibitor 3,3′,4′,5-tetrachlorosalicylanilide (TCSA) [31], followed by exposure to H_2O_2 and stomatal apertures measured. TCSA inhibited H_2O_2-induced closure in a dose-dependent manner (Fig. 3), thereby suggesting that HK activity is indeed required for H_2O_2 signalling to occur in guard cells leading to stomatal closure.

Regulation of *AHK5* expression in guard cells by H_2O_2 led us to investigate whether AHK5 function is necessary for the response of guard cells to exogenous H_2O_2 by performing stomatal bioassays. Compared to wild type, guard cells of *ahk5-1* and *ahk5-3* were dramatically less sensitive to H_2O_2 at various concentrations (Fig. 4 A, B). The sensitivity of both mutant lines to H_2O_2 was restored by the expression of the wild type *AHK5* cDNA under the control of the 35S promoter (Fig. 4C) showing that the GFP-AHK5 fusion protein used for the localisation studies is functional *in planta*. These data also demonstrate that loss of *AHK5* gene function causes the H_2O_2-insensitive mutant phenotype and that AHK5 is required for stomatal response to exogenous H_2O_2. Interestingly, ectopic expression of *AHK5* in wild type background resulted in slightly smaller stomatal apertures compared to wild type Ws4 in the absence of H_2O_2 (Fig. 4C, right columns). This suggests that the guard cells of the *AHK5* overexpressor are more sensitive to endogenous H_2O_2. However, we observed a response of the overexpressor to exogenous H_2O_2 suggesting that ectopic accumulation of AHK5 *per se* does not significantly alter the plant's sensitivity to H_2O_2.

Stomatal responses to NO, ethylene and darkness are impaired in ahk5 mutants

The insensitivity of *ahk5* mutant guard cells to H_2O_2 suggests that AHK5 could be an essential signalling component in the stomatal closure response of *Arabidopsis* to various stimuli. Recently, we have shown that H_2O_2 induces the generation of NO in the response of guard cells to ABA [32]. If AHK5 is acting downstream of H_2O_2, the response to NO might also be affected in the *ahk5* mutants. As shown in Fig. 5A, *ahk5-1* and *ahk5-3* stomata showed a reduced sensitivity to the NO donor sodium nitroprusside (SNP). The NO insensitive phenotype of the *ahk5* mutants was functionally complemented by the wild type *GFP-AHK5* construct (Fig. S1). In addition, experiments with TCSA showed that NO-induced closure required HK activity (Fig. S2). These results indicate a function for AHK5 in both the H_2O_2 and NO response pathway in *Arabidopsis* guard cells. In contrast, the sensitivity of both mutants to ABA was not changed appreciably (Fig. 5A) suggesting the possibility that stimuli other than ABA lead to H_2O_2 and NO generation which might act via AHK5, and that ABA signalling occurs largely independent of AHK5.

In our previous work we demonstrated that pea guard cells exposed to darkness generate H_2O_2 [33]. Our pharmacological data revealed that pre-treatment with TCSA inhibited dark-induced stomatal closure, suggesting a requirement for HK activity in this response (Fig. S2). To investigate the role of AHK5 in dark-induced stomatal closure, the response of *ahk5* mutants to dark conditions were examined. As shown in Fig. 5A, detached leaves of both the *ahk5-1* and *ahk5-3* mutants showed reduced stomatal closure in response to dark conditions, with stomata of *ahk5-1* responding slightly to dark conditions. The experiments were also performed with non-detached leaves. Whilst the stomata of wild type and *ahk5-1* plants were open 30 min prior to transfer to darkness, the light-off conditions induced stomatal closure only in the wild type but not in the mutant (Fig. 5B). These data indicate that AHK5 function also contributes to the dark-induced stomatal closure response in *Arabidopsis*.

We have shown previously that ethylene perceived by the ethylene receptor ETR1 (a hybrid HK) also induces stomatal closure via H_2O_2 synthesis [16]. Furthermore, a functional ETR1 receptor is required to mediate H_2O_2-induced stomatal closure [15]. Experiments with TCSA showed that HK activity is required for ethylene-induced stomatal closure (Fig. S2). We therefore investigated the effect of ethylene on *ahk5-1* and *ahk5-3* guard cells. Treatment with the ethylene-generating compound ethephon induced a stomatal closure response in wild type but not in *ahk5*

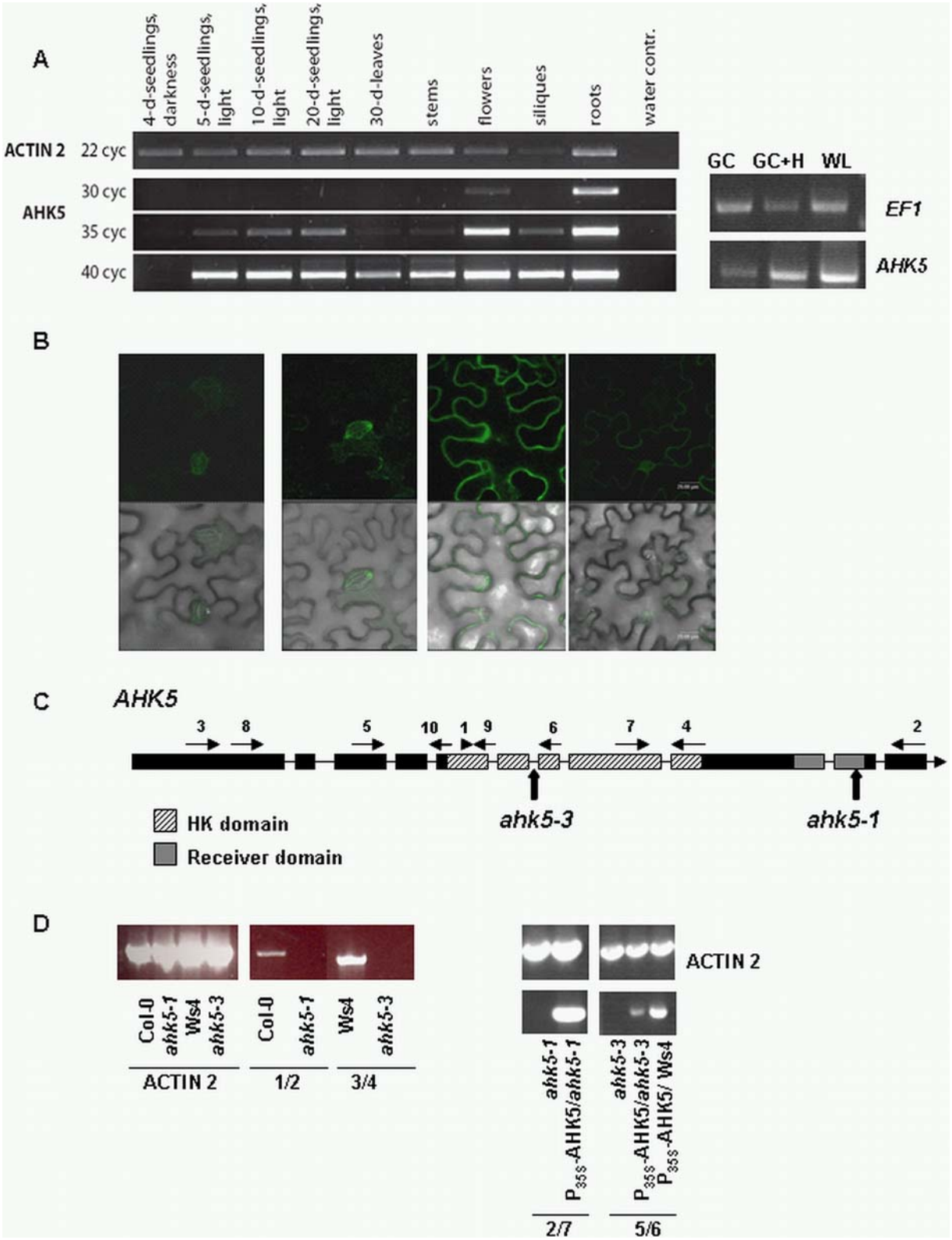

Figure 2. Expression pattern of *AHK5* and characterisation of the T-DNA insertion sites in *ahk5-1* and *ahk5-3*. (A) Steady-state levels of *AHK5* transcript in different tissues and developmental stages of *Arabidopsis* detected by semi-quantitative RT-PCR using different cycle numbers. For the detection of *AHK5*, up to 40 cycles of PCR were performed using primers 3 and 10 (left panel) or primers 8 and 9 and 40 cycles of PCR (right panel). GC, cDNA from guard cell-enriched non-treated leaf sample; GC+H, cDNA from guard cell-enriched leaf samples treated with 0.5 mM H_2O_2 for 2 h; WL, cDNA from whole-leaf sample. ACTIN and EF1 were used as controls. Primer numbers indicated in panel C. (B) Expression of a P_{AHK5}-*GFP-AHK5genomic* construct in transiently transformed tobacco leaf cells. *Agrobacteria* carrying the P_{AHK5}-*GFP-AHK5* construct were infiltrated into the abaxial side of the leaf and the GFP fluorescence analysed by CLSM 2 days later. Top panels = GFP images, lower panels = GFP image overlaying

bright field image. The scale bar represents 20 μm. Images shown from repeat experiments. (C) *AHK5* gene structure, position of primers used for genomic and RT-PCR and T-DNA insertions in *ahk5-1* (Col-0) and *ahk5-3* (Ws4). (D) Analysis of *AHK5* expression in seedlings of wild type, *ahk5-1* and *ahk5-3* mutant, P_{35S}-*AHK5* complemented and AHK5 over-expressing plants using the indicated primer pairs (see Supplementary data for sequences).
doi:10.1371/journal.pone.0002491.g002

guard cells. The sensitivity to ethylene could be restored when the GFP- and TAP-tagged *AHK5* fusion constructs were expressed in the *ahk5* mutants under the control of the 35S promoter (Fig. 5C). These data show that ethylene induces stomatal closure via AHK5 function.

The data so far indicate that AHK5 function is required for H_2O_2, NO, darkness and ethylene-induced stomatal closure, but not for ABA-induced closure. To establish if AHK5 might be regulating redox homeostasis in response to these stimuli, the generation of both H_2O_2 and NO were measured in guard cells. Whilst the source of H_2O_2 in *Arabidopsis* guard cells has been established as *AtrbohD* and *F* for ABA [13], and *AtrbohF* for ethylene [16], it is not known how darkness induces H_2O_2. Figure 6A shows that guard cells of the *atrbohD/F* NADPH oxidase double mutant did not produce H_2O_2 nor close their stomata after transfer into darkness, thereby demonstrating that these homologs regulate dark-induced H_2O_2 synthesis in *Arabidopsis* guard cells. Interestingly, *ahk5* guard cells did generate H_2O_2 following dark adaptation of leaves as in wild type (Fig. 6B), thereby suggesting that AHK5, although involved in dark-induced stomatal closure, is not involved in regulating dark-mediated H_2O_2 synthesis.

H_2O_2 can also induce NO synthesis in the ABA signal transduction pathway in guard cells [32]. Although *ahk5* mutants do not respond to either H_2O_2 or NO (Fig. 4 and 5A), H_2O_2 induced NO synthesis in both mutant alleles (Fig. 6C), thereby positioning AHK5 downstream of H_2O_2 and NO in the signal response pathway. In addition, ethylene-induced H_2O_2 production was investigated in *ahk5-1*. Upon treatment with ethephon we observed a strong increase in H_2O_2-fluorescence in wild type guard cells (Fig. 7D). In contrast, ethylene caused a decrease of H_2O_2 levels in *ahk5-1* in comparison to that of the mock-treated control (Fig. 7D). These data demonstrate that AHK5 contributes to both, the ethylene-induced H_2O_2 production and stomatal closure response in *Arabidopsis*. However, ABA induced H_2O_2 synthesis in *ahk5* mutant, as in wild type guard cells (25% increase over controls; Data S1).

In summary so far, the data presented show that darkness-induced H_2O_2 synthesis, which is generated by ATRBOHD/F, signals through AHK5 to mediate stomatal closure, and that AHK5 is positioned downstream of H_2O_2 and NO in the signal response pathway. Moreover, AHK5 regulates ethylene-induced H_2O_2 synthesis leading to stomatal closure, but is not involved in the ABA signal transduction pathway.

Stomatal responses to PAMPs are impaired in the ahk5 mutants

Bacteria-derived pathogen-associated molecular patterns (PAMPs) such as flagellin and EF-Tu have been shown to induce the synthesis of ethylene [34] and an oxidative burst in *Arabidopsis* leaves, which is mediated by ATRBOHD [35]. Furthermore, recent work by Melotto and colleagues (2006) demonstrated that stomata act as sites of entry for bacteria, and that bacteria and bacteria-derived PAMPs caused a primary stomatal closure response followed by a re-opening, when the plant was attacked by a virulent bacterium [36].

Experiments with the *Pseudomonas syringae* strains *pv* DC3000 and the *hrpA*$^-$ mutant, which lacks a functional type III secretory apparatus, revealed that *ahk5-1* mutant guard cells showed reduced stomatal closure in response to both bacterial strains (Fig. 7A). The reduced stomatal closure response to the *hrpA*$^-$ mutant strain suggests that AHK5 is involved in the basal defence of *Arabidopsis*, which is mediated by PAMPs such as the flagellin peptide 22 (flg22) and the EF-Tu peptide 26 (elf26; [37]).

Flagellin-induced stomatal closure in wild type plants was inhibited by pre-treatment with TCSA (Fig. S2), indicating a requirement for HK activity to mediate this response. To investigate this in more detail, leaves of the *ahk5-1* mutant (Col-0 background) were exposed to flg22 and the stomatal apertures measured. The response to flg22 was not investigated in the *ahk5-3* mutant as the Ws background lacks a functional FLS2 receptor [38]. As reported [36], flg22 induced stomatal closure in Col-0 wild type guard cells (Fig. 7B). This response was not observed in the *ahk5-1* mutant. The loss-of-function phenotype of *ahk5-1* was complemented by the expression of the *GFP-AHK5* fusion construct, which is under the control of the 35S promoter (Fig. 7B). Interestingly, elf26 caused an identical stomatal closure response in wild type (Col-0, Ws4) as well as in the *ahk5-1* and *ahk5-3* mutants (Fig. 7C). These data suggest that AHK5 plays a specific role in the flagellin signal response pathway in guard cells.

PAMP-induced H_2O_2 production was also investigated to study the role of AHK5 in redox homeostasis during basal defence. Interestingly, whereas elf26 caused an identical increase in H_2O_2 fluorescence in guard cells of wild type and *ahk5-1*, treatment with flg22 actually caused a decrease in H_2O_2 fluorescence in *ahk5-1*, when compared with that of the mock-treated control (Fig. 7D). Therefore AHK5 appears to play a role in both the flg22-induced regulation of H_2O_2 production and stomatal closure.

Discussion

An AHK5-dependent signalling pathway acts in stomatal guard cells

We have characterised the canonical HK AHK5 as being a cytoplasmic/membrane protein differentially expressed in various tissues of *Arabidopsis*. Despite the predicted cytoplasmic location

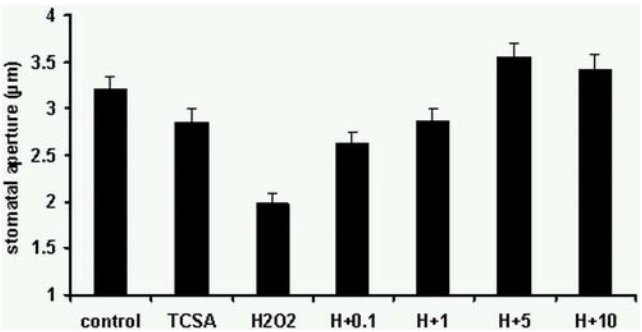

Figure 3. HK activity is required for H_2O_2-induced stomatal closure. Effect of the histidine kinase (HK) inhibitor 3,3′,4′,5-tetrachlorosalicylanilide on H_2O_2-induced stomatal closure in wild type *Arabidopsis* (Col-0). *Arabidopsis* leaves were incubated in stomatal opening buffer for 2.5 h followed by treatment for 15 min with 0.1, 1, 5 or 10 μM of TCSA prior to exposure to 200 μM H_2O_2 (H) for 2.5 h. Control, buffer alone. TCSA, buffer with TCSA alone at 10 μM. Data are expressed as mean +/− S.E. from 3 independent experiments (n = 60–80 guard cells).
doi:10.1371/journal.pone.0002491.g003

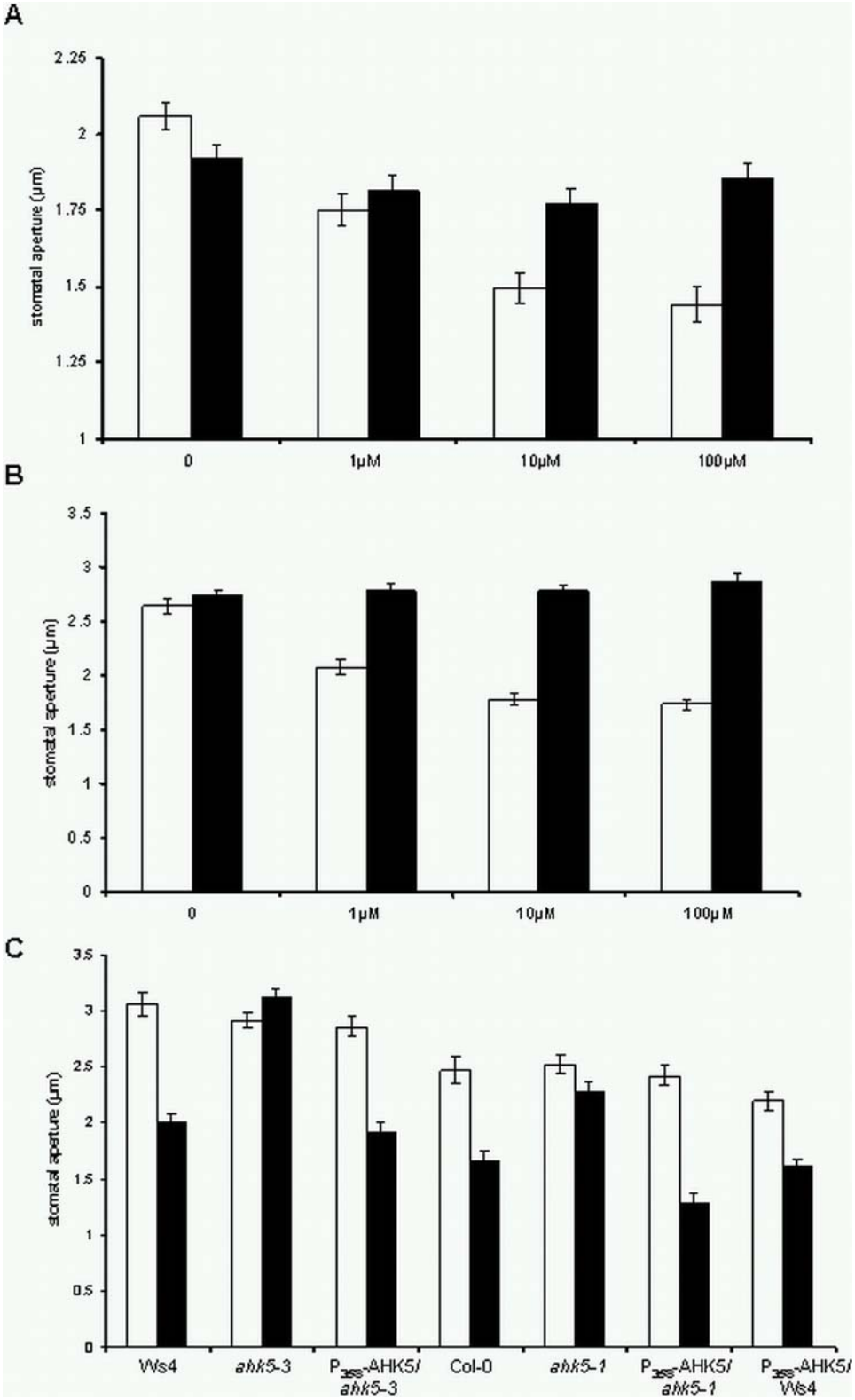

Figure 4. *ahk5* mutant guard cells show reduced sensitivity to H_2O_2. (A) Stomatal closure in wild type Col-0 (white bars) and *ahk5-1* (black bars) leaves 2.5 h after exposure to increasing concentrations of H_2O_2. (B) Stomatal closure in wild type Ws4 (white bars) and *ahk5-3* (black bars) leaves 2.5 h after exposure to increasing concentrations of H_2O_2. (C) Stomatal closure in leaves of wild type (Ws4, Col-0), *ahk5-3* and *ahk5-1* as well as in the *ahk5* mutants and wild type (Ws4) transformed with a construct expressing the *AHK5* cDNA under the control of the *35S* promoter (P_{35S}-*AHK5*). The leaves were either mock-treated (white bars) or exposed to or 100 µM H_2O_2 (black bars). Data are expressed as mean +/− S.E. derived from measuring the apertures of at least 60 guard cells from 3 independent experiments.
doi:10.1371/journal.pone.0002491.g004

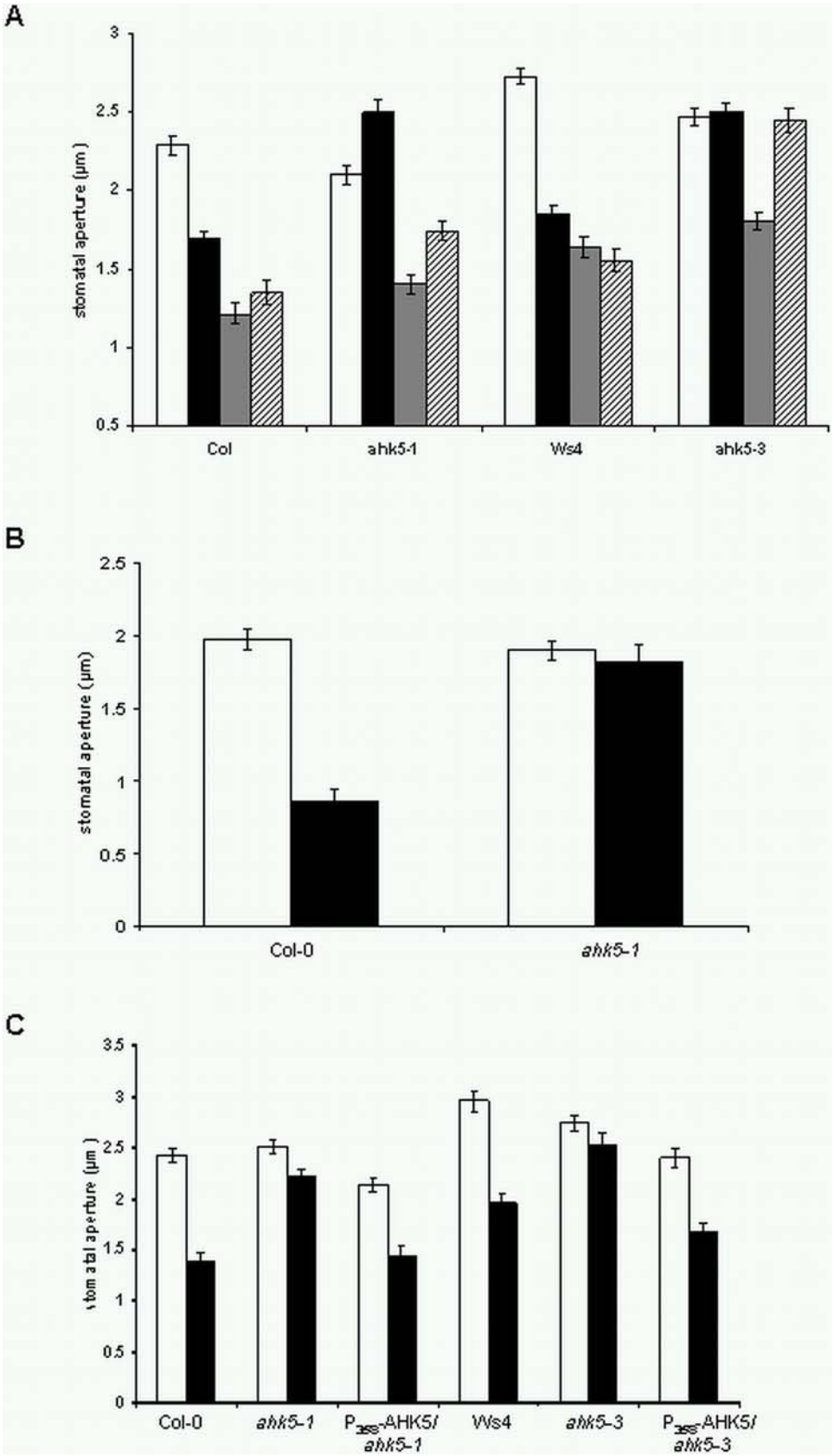

Figure 5. Guard cells of *ahk5* mutants show an altered response to NO, ethylene and darkness. (A) Stomatal closure in wild type (Col-0, Ws4), *ahk5-3* and *ahk5-1* in response to buffer (white bars), 50 µM sodium nitroprusside, (SNP, black bars), 10 µM abscisic acid (ABA, grey bars) and 2.5 h exposure to darkness (striped bars). Data from *ahk5-1* dark treatment are statistically significant (Student's t-test; $p<0.05$) versus dark treatment

of wt, and data from *ahk5* ABA treatment are statistically significant ($p<0.05$) versus controls. (B) Guard cell response in plant-attached leaves in light and after transfer to darkness. Stomatal apertures were measured from wild type (Col-0) or *ahk5-1* leaves either 30 min prior to light off (white bars) or 1 h after transfer to darkness (black bars). Data are expressed as mean +/− S.E. from 3 independent experiments (n = 60 guard cells). (C) Stomatal closure response to ethylene in guard cells of wild type (Col-0, Ws4), *ahk5-1*, *ahk5-3* and *ahk5* mutants transformed with the P_{35S}-*AHK5* construct. White bars, mock-treated; black bars, 3 h treatment with 100 μM ethephon. Data are expressed as mean +/− S.E. from 3 independent experiments (n = 60 guard cells).
doi:10.1371/journal.pone.0002491.g005

[18] and lack of transmembrane domains within the AHK5 sequence, our data suggest that AHK5 co-localises at the plasmalemma as well. Interestingly, putative N-myristoylation sites are predicted for AHK5, suggesting that an association of AHK5 to the plasmalemma is possible. In addition, we cannot exclude the possibility that the interaction with intrinsic membrane proteins including other HKs locates AHK5 to the plasmalemma.

Expression of *AHK5* appears to be regulated by H_2O_2 in guard cells. In addition, we have shown using functional approaches that AHK5 plays a crucial role in mediating H_2O_2-dependent processes in stomatal guard cells which are induced by environmental and hormonal signals such as NO, ethylene, adaptation to darkness and the PAMP flagellin (flg22). Despite its low level of expression, mutations in the *AHK5* gene appear to have profound effects on the guard cell phenotype. The pattern of low expression of a gene in guard cells still resulting in distinct stomatal phenotypes has been observed before – e.g. the nitric oxide (NO)-generating enzyme nitrate reductase (NR). There are two *NR* genes, *NR1* and *NR2*, in the *Arabidopsis* genome. Although *NR1* is expressed at much lower levels than *NR2* in guard cells, mutations in NR1 but not NR2 appear to affect ABA-induced NO responses in stomata [39]. Although *cis* elements found in the promoters of guard cell specific genes [40] are present in the promoter region of *AHK5*, it is possible that other *cis* elements which repress promoter activity in guard cells cause the weak expression pattern, as seen with other guard cell genes [41]. It is also likely that phenotypic effects may be explained by specific protein-protein interactions between a low-expressed protein in guard cells and other proteins of higher abundance. Preliminary data show that expression of the phosphotransfer protein AHP2 and the response regulator ARR4 that AHK5 interact with are of higher abundance than *AHK5* in guard cells (Data S1). Further studies will analyse the functions of *AHK5* promoter, as well as studying the protein interacting two-component partners of AHK5.

AHK5 functions as integrator of H_2O_2- dependent signalling in stomatal guard cells

A lack of functional AHK5 results in altered stomatal responses not only to exogenous H_2O_2 but also to multiple stimuli which are known to generate H_2O_2 in plant tissues. These signals include ethylene [16], the light-off signal (darkness; data shown here and [33]) and the PAMP flg22 [35].

Previously we provided evidence for a role for the plant hormone ethylene in mediating stomatal closure *via* H_2O_2 signalling [16]. Although the HK function of ETR1 is not required for H_2O_2 signalling, the N-terminus of ETR1 appears to be essential for this signalling to occur in guard cells [15]. The pharmacological data presented here with TCSA indicate that HK activity is required for H_2O_2 (and NO)-induced stomatal closure in *Arabidopsis*. As ethylene is able to produce H_2O_2 in wild type guard cells [16], and as shown here, AHK5 is also involved in ethylene-dependent signalling leading to H_2O_2 synthesis and stomatal closure, it is possible that the ethylene-sensing N-terminus of ETR1 functionally and/or physically interacts with H_2O_2-activated AHK5 during ethylene signal transduction in guard cells. This is in agreement with recent work by Iwama et al. [24], who demonstrated a functional interaction of *AHK5* with the ethylene and ABA response in the control of root growth in *Arabidopsis*. The authors propose an "unidentified" stimulus as being sensed by AHK5, which could integrate the ABA and ethylene signalling pathways in roots. On the basis of our data it is likely that this unknown stimulus for AHK5 is H_2O_2, although the *ahk5* phenotype in roots in response to H_2O_2 remains to be determined.

Synthesis of H_2O_2 upon transfer of plants to darkness was found to depend on NADPH oxidase orthologues in pea [33]. By using an *atrbohD/F* double mutant we demonstrate here that dark-induced H_2O_2 formation occurs by a similar mechanism in *Arabidopsis*. We also show that *ahk5* mutants do not close their stomata in response to darkness. This is substantiated by the pharmacological data showing inhibition by TCSA, of dark-induced closure in wild type *Arabidopsis*. Stomata of the H_2O_2-insensitive *etr1-1* mutant still respond to darkness (Data S1), suggesting the possibility that as far as HKs are concerned, AHK5 might have a unique role in the dark-H_2O_2 signalling pathway in guard cells. Although of fundamental physiological and ecological relevance, little is known of the dark-induced signalling processes leading to stomatal closure. The type 2C protein phosphatases ABI1 and ABI2 [42], the outward potassium channel GORK [43] and the MYB transcription factor AtMYB61 [44] have functions in guard cell responses in the dark. However, the mechanism by which AHK5-dependent phosphorelay is linked to proteins such as ABI1, 2, GORK and AtMYB61 in the guard cell signalling network is not yet known.

AHK5 also appears to be essential for mediating flagellin- (flg22) induced stomatal closure in the Col-0 ecotype, again correlating with the TCSA data demonstrating inhibition of flg22-induced stomatal closure. Surprisingly, the AHK5-mediated response seems to be specific for flg22 because the mutants showed a wild type stomatal closure response to the PAMP elf26. This is unexpected because the signalling cascades of flg22 and elf26 overlap considerably in non-guard cell tissue in respect to ethylene and H_2O_2 production, alkalinisation, activation of MAPKs and changes in gene expression [34,37]. However, as noted recently, there are likely to be differences between guard cells and mesophyll cells mediating pre- and post-invasive immunity [45]. Recent work by Melotto et al. [36] indicates that bacterial PAMPs such as flagellin induce stomatal closure in *Arabidopsis*. Our data, therefore, position AHK5 in a signal transduction cascade specific to flagellin in guard cells. The exact mechanism by which AHK5 interacts with this pathway remains to be determined, but it is likely that the interaction occurs with the flg22 receptor FLS2. It is interesting to note that the expression of FLS2 is abundant in guard cells [46]. Given that FLS2 is a plasmalemma-bound and AHK5 is likely to be located at the plasma membrane as well as the cytoplasm, one may speculate that both receptors could physically interact at the plasma membrane allowing AHK5 to perceive high local H_2O_2 concentrations induced by the flg22-activated FLS2/BAK1 receptor complex [47,48]. Importantly, flg22 but not elf26 was unable to induce H_2O_2 accumulation in *ahk5* mutant guard cells. Thus, AHK5 also appears to contribute

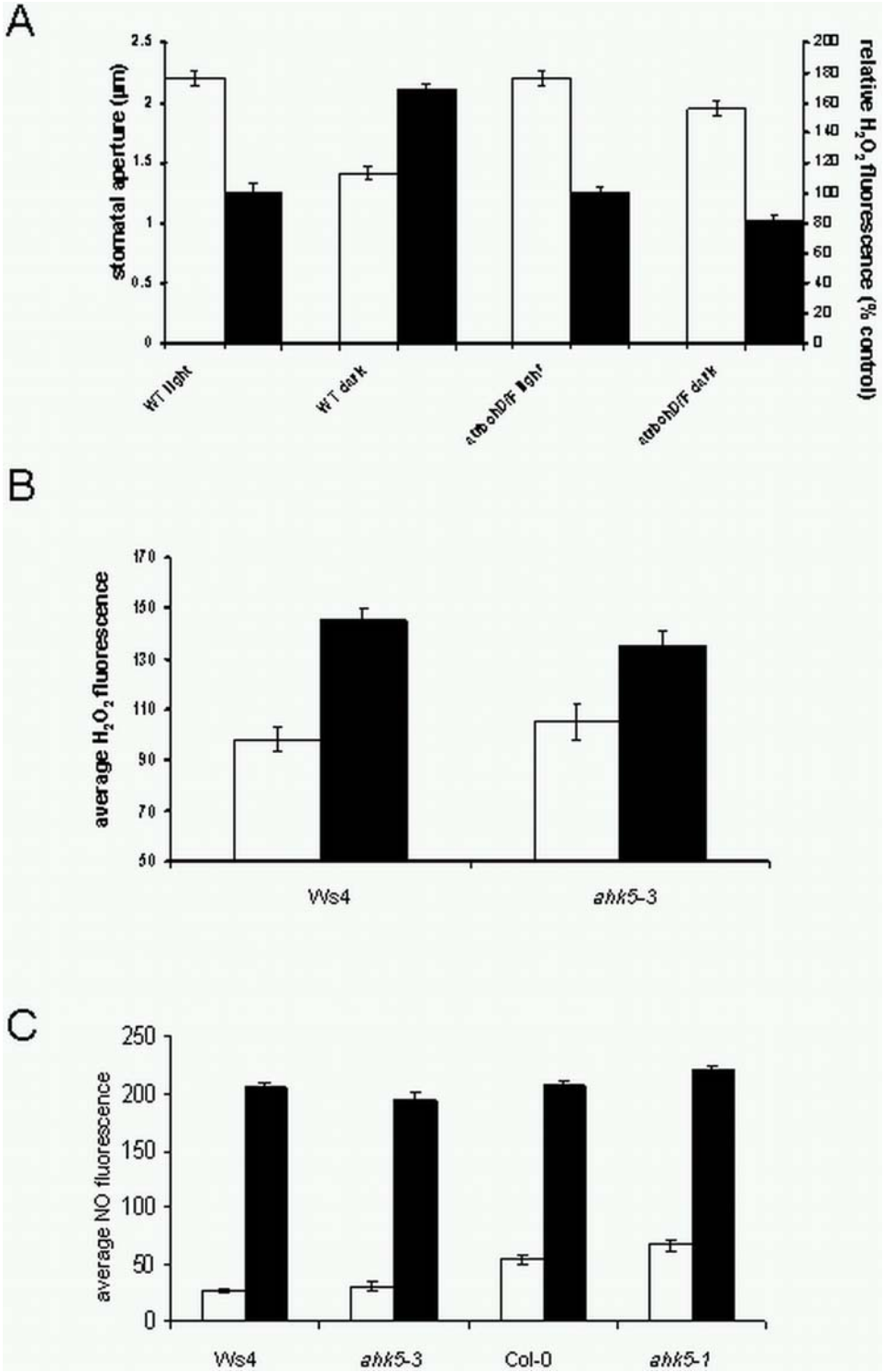

Figure 6. Regulation of H_2O_2 homeostasis by AHK5. (A) Stomatal responses to darkness in wild type (Col-0) and the *atrbohD/F* mutant. White bars, stomatal apertures of guard cells from leaves exposed to light (light) or transferred to darkness for 2 h (dark). Black bars, H_2O_2 fluorescence determined by confocal microscopy from epidermal peels exposed to light (light) or transferred to darkness for 30 min (dark). Data are expressed as mean +/− S.E. (n = 60 guard cells for aperture measurements; n = 40–80 guard cells for average H_2O_2 fluorescence from confocal experiments). (B) Darkness-induced H_2O_2 synthesis in wild type (Ws4) and *ahk5-3* mutant guard cells. H_2O_2 fluorescence from epidermal peels exposed to ambient light (white bars) or darkness (black bars) for 30 min was determined by confocal microscopy using the H_2O_2-sensitive fluorescent dye H_2-DCFDA. Data are expressed as mean +/− S.E. (n = 40–80 guard cells for each treatment). (C) H_2O_2-induced NO fluorescence from guard cells of wild type and *ahk5* mutants using confocal microscopy and the NO-sensitive fluorescent dye DAF2-DA. White bars, mock-treated; black bars, 15 min treatment with 100 µM H_2O_2. Data are expressed as mean +/− S.E. (n = 75–130 guard cells for each treatment.
doi:10.1371/journal.pone.0002491.g006

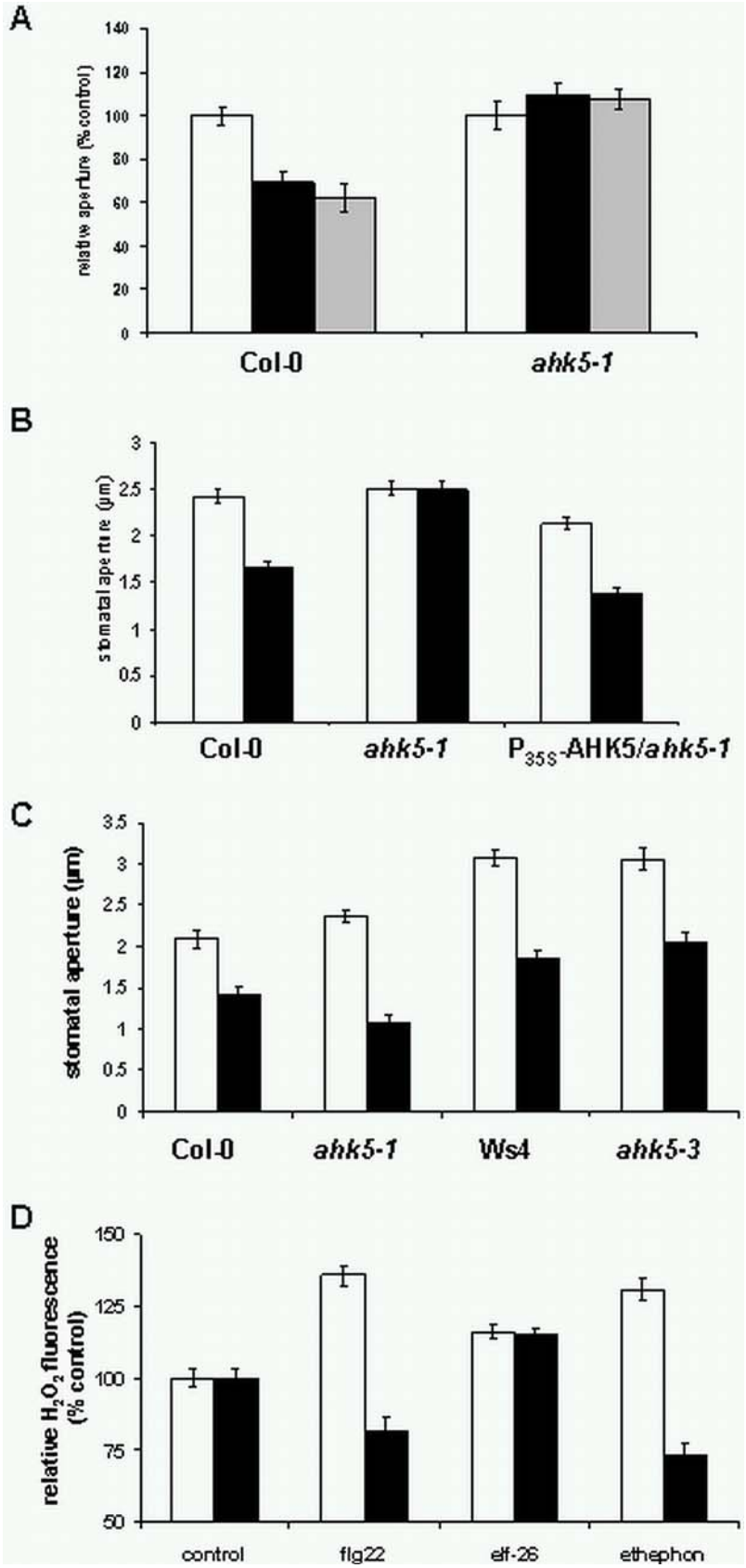

Figure 7. Guard cells of *ahk5* mutant show a differential response to PAMPs. (A) Stomatal aperture of wild type (Col-0) and *ahk5-1* 3 h after exposure to *P. syringae* pv. DC3000 (black bars) or hrpA$^-$ mutant (grey bars). White bars, mock-treatment. ($MgCl_2$). (B) Stomatal closure of wild type (Col-0), *ahk5-1* and *ahk5-1* transformed with a P_{35S}-*AHK5* construct after a 3 h treatment with either buffer (white bars) or 10 nM flg22 peptide (flg22,

black bars). (C) Stomatal closure of wild type (Col-0, Ws4), *ahk5-1* and *ahk5-3* in response to a 3 h treatment with buffer (white bars) or 1 μM elf26 peptide (elf26, black bars). Data are expressed as mean +/− S.E. from 3 independent experiments (n = 60 guard cells), $p<0.05$ (student's t-test) versus appropriate controls. (D) H_2O_2 fluorescence from epidermal peels of wild type (Col-0, white bars) and *ahk5-1* (black bars) treated for 15 min with 10 nM flg22, 1 μM elf26 or for 30 min with 100 μM ethephon. Fluorescence intensity was quantified as described in methods. Data are expressed as relative fluorescence (% control values) +/− S.E. (n = 90–122 guard cells for each treatment).
doi:10.1371/journal.pone.0002491.g007

to the flagellin-induced regulation of H_2O_2 levels in guard cells (see below for detailed discussion). This also implies that an additional H_2O_2 sensor is required for the perception of the H_2O_2 signal derived from the EF-Tu/EFR receptor complex.

As demonstrated by the wild type behaviour of both *ahk5* mutants to ABA, the AHK5-dependent signalling pathway does not contribute to the ABA response pathway in guard cells. This is not entirely surprising, as we have previously observed that mutants of ETR1 also respond normally to ABA [16]. Although ABA signalling requires the synthesis and action of H_2O_2 [13], our data indicate that this function is independent of AHK5.

The complexity of redox signalling in stomatal guard cells

Redox signalling in guard cells is likely to be regulated *via* a number of signalling pathways. This may be because of the nature of H_2O_2 as such, being able to diffuse freely between cellular compartments, and also due to the fact that H_2O_2 is likely to be generated in localised "hot spots" within the cell, thereby leading to localised effects of H_2O_2 on its target proteins [2]. Generation of H_2O_2 in guard cells in response to ABA and darkness occurs *via* the NADPH oxidase orthologues ATRBOHD and ATRBOHF ([13] and this study). ATRBOHF is essential for H_2O_2 generation in response to ethylene and ETR1 functions as a central mediator of H_2O_2 responses [16]. In leaves, flg22-induced H_2O_2 production occurs *via* ATRBOHD [35]. RBOH proteins are localised at the plasma membrane [49], and the proteins involved in H_2O_2 signalling are located at the ER (ETR1; [25,50]), plasma membrane (AHK5, FLS2, [51]) or in the cytosol (AHK5). We have observed that AHK5 function is crucial for ethylene and flg22-induced but not for darkness or elf26-induced H_2O_2 accumulation. Further work using *ahk5* plants crossed with *atrboh* mutants is required to confirm how AHK5 and RBOH signalling interact. However, *AHK5* transcript appears to be regulated by H_2O_2 in guard cells, and AHK5 function is essential for H_2O_2 and NO-dependent signal transduction. Together, the data suggest that AHK5 acts to maintain H_2O_2/redox homeostasis in guard cells in response to multiple stimuli. A positive feedback loop is possible, whereby H_2O_2, generated *via* different stimuli (from RBOH), regulates AHK5 expression (or activity), which in turn regulates H_2O_2 synthesis (for ethylene and flagellin pathways) and action leading to stomatal closure. Regulation of the expression of HKs by the stimulus that induces their activity is not uncommon – expression of the cytokinin receptor CRE1 and ethylene receptors is regulated by cytokinin and ethylene treatments, respectively [22]. Detailed investigations are necessary to elucidate the molecular mechanisms of redox regulation of AHK5, *via* mass spectrometry of the purified protein.

The dual function of AHK5, in regulating H_2O_2 synthesis and action is reminiscent of the role of ETR1, which we have shown previously to have a dual function in guard cells, that of perceiving ethylene as well as H_2O_2 [16]. AHK5 could therefore have multiple functions as well: firstly, AHK5 may contribute to the flagellin- and ethylene-induced H_2O_2 accumulation and, secondly, may sense H_2O_2 produced in the course of the ethylene-, NO-, flg22- and darkness-regulated stomatal closure response. Our evidence that AHK5 plays a role in the inducible accumulation of H_2O_2 comes from our observation that the H_2O_2 level is decreased in *ahk5-1* guard cells upon treatment with ethylene or flg22. It is not yet known whether AHK5 interacts with receptors such as ETR1 or FLS2, H_2O_2-generating enzymes such as ATRBOHD/F and redox-active proteins such as ATGPX3, ABI1 and ABI2 which are located in distinct sub-cellular compartments [9,10,52] or whether AHK5 co-ordinates their functions to integrate H_2O_2 signalling. However, our study provides evidence that AHK5 acts to integrate multiple H_2O_2-dependent processes at different molecular levels.

Summary and concluding remarks

We have shown that AHK5 functions in guard cells to mediate stomatal responses to various stimuli that generate H_2O_2. Evidence is slowly emerging that implicate overlapping signalling pathways during abiotic and biotic stress responses in plants, which include hormone signalling, ROS signalling and protein phosphorylation [22,53]. Our data position AHK5 both upstream and downstream of ROS in integrating bacterial, darkness and hormonal-induced responses which could be achieved by differential protein-protein interactions. This is the first demonstration of a role for a HK two-component signalling pathway in integrating abiotic and biotic signals. Moreover, it is the first identification of a HK mediating H_2O_2 homeostasis to integrate multiple stress responses in guard cells. The data presented here highlight the mechanism and function of the AHK5 two-component signal transduction pathway in stomata, which are ideal model systems to study integration of multiple stimuli.

Materials and Methods

Growth and maintenance of plants

Wild type and mutant seeds of *Arabidopsis thaliana* ecotype Columbia (Col-0) and Wassilewskijia (Ws4) were sown on Levington's F2 compost and grown under a 16 h photoperiod (100–150 μE m^{-2} s^{-1}), 22°C and 65% relative humidity in controlled environment growth chambers (Sanyo Gallenkamp, UK). *atrbohD/F* seeds were obtained from J Jones (Sainsbury Laboratory, Norwich, UK).]. Details of the T-DNA insertion lines in *AHK5* are as follows: *ahk5-1* mutant seeds (SAIL 50_H11) were originally obtained from Syngenta (SAIL collection, now available at ABRC/NASC), and the *ahk5-3* seeds (FLAG_271G11) were obtained from the INRA/FLAG-FST collection at Versailles [29,30].

Stomatal bioassays

Stomatal assays were performed on leaves essentially as described in [15]. Leaves were floated for 2.5 h under continuous illumination (100–150 μE m^{-2} s^{-1}) in Mes/KCl buffer (5 mM KCl/10 mM Mes/50 μM $CaCl_2$, pH 6.15). Once the stomata were fully open, leaves were treated with various compounds for a further 2.5 h. The leaves were subsequently homogenised individually in a Waring blender for 30 s and the epidermal fragments collected on a 100 μm nylon mesh (SpectraMesh, BDH-Merck, UK). Stomatal apertures from epidermal fragments were then measured using a calibrated light microscope attached to an imaging system (Leica QWin software, Leica, UK). Flg22 and

elf-26 peptides were a kind gift from J Mansfield (Imperial College London). Elicitors were added to the incubation buffer at 2.5 h and stomatal apertures measured after a further 3 h.

For bacterial experiments, *Pseudomonas syringae* pv DC3000 or *P. syringae* hrpA$^-$ mutant were grown overnight in LB media and overnight cultures centrifuged, resuspended in 10 mM $MgCl_2$ at an $OD_{600} = 0.2$ (equivalent to 2×10^8 cfu/ml). Silwet (0.002% v/v) was added to cultures or $MgCl_2$ to act as a wetting agent. Bacteria were gently coated onto the abaxial side of leaves on intact plants (controls were $MgCl_2$ with Silwet alone). Plants were left in the growth chambers with a covered lid (to increase humidity) for 3 h, inoculated leaves subsequently detached and stomatal apertures measured.

Measurement of H_2O_2 and NO using confocal/fluorescent microscopy

Epidermal peels from mature leaves, prepared as described above, were incubated in Mes/KCl buffer for 2–3 h. Following this, the fragments were loaded by incubation in 50 μM of the H_2O_2-sensitive fluorescent dye 2′,7′-dichlorodihydrofluorescein diacetate (H_2DCFDA, Molecular Probes, Leiden, The Netherlands) for 10 min. After washing in fresh buffer for a further 20 min, the fragments were challenged with various compounds as indicated in the figure legends. For dark treatments the peels were incubated in darkness for 30 min and microscopy performed. Confocal laser scanning microscopy was used to visualise fluorescence, using an excitation wavelength of 488 nm and an emission wavelength of 515–560 nm (Nikon PCM2000, Nikon Europe B.V. Badhoewvedorp, The Netherlands). Images were acquired and analysed using Scion Image software (Scion Corp., USA) to measure the relative fluorescence intensities in the cells following various treatments. For the data in Figure 7D, fluorescent microscopy (Zeiss Axioskop2, Zeiss, UK) was used with filter set 10 (excitation filter BP 450–490 nm, beam splitter FT 510 nm and emission filter BP 515–565 nm). Images were acquired and analysed using Image J software (NIH, USA). Data represent fluorescence intensities expressed as average fluorescence or as a percent of the control values, from several guard cells analysed in different experiments. For NO fluorescence, epidermal peels were loaded with 10 μM of the NO-sensitive dye diaminofluorescein diacetate (DAF2-DA, Calbiochem, UK) using exactly the same dye loading procedure, and images acquired using confocal microscopy as described above.

Cloning, expression analysis of *AHK5* and characterisation of T-DNA mutants

The *AHK5* Entry clone was constructed using Gateway™ technology (Invitrogen, UK). It was obtained through TOPO-reaction using the pENTR/D-TOPO vector (Invitrogen). PCR was performed using Phusion™ polymerase (Finnzymes, UK) and cDNA from *Arabidopsis* roots as template. Primers were as follow: 5′-*CACC*-ATGGAGACTGATCAGATTGAGGAA-3′, 5′-GTGC-AAATACTGTTGCAAACACTCTC-3′. The *AHK5* Entry clone was verified *via* restriction analysis and sequencing (GATC Biotech). The construct for the expression of the GFP fusion proteins under the control of 35S promoter (*P_{35S}::GFP:AHK5*) was cloned *via* LR-reaction into the destination vector pK7WGF2.0 [54]. For complementation of the mutant line in the Ws4 background, the TAP-tag destination vector pYL436 [55] was used to transform *ahk5-3* plants. The transformants were selected on BASTA and gentamycin and analysed by PCR. For the Col-0 mutant complementation the *P_{35S}::GFP-AHK5* construct in pK7WGF2.0 was used to transform *ahk5-1* plants. The transformants were selected on BASTA and kanamycin and analysed by PCR as described below. For the AHK5 overexpressor in Ws4 background, LR reaction was used to clone the *AHK5* cDNA under the control of 35S promoter into the destination vector pMDC32 [56]. All plant transformations were carried out using *Agrobacterium*-mediated transformation by floral dipping [57].

A four-step procedure was used to generate the *P_{AHK5}::GFP::AHK5* expression cassette. In step 1, a 7117 bp fragment containing the 3.2 kb upstream promoter region of *AHK5*, the full length genomic sequence of *AHK5* and 217 bp of 3′ region was amplified from Col-0 genomic DNA by PCR using KOD Hot Start DNA polymerase (Novagen, Germany) and the primers *AHK.FOR.-3205* (5′-CACC-TCTAGACCCTACACGGGATA-GATTATCG-3′) and *AHK.REV.+219* (5′-TTTGTCGAC-TCTGCTGGATTCGAATGGTGGG-3′) and cloned into the pENTRD/TOPO entry vector (Invitrogen, UK) to generate pMKC101. The entire construct was verified by sequencing. In step 2, a hybrid DNA fragment containing 643 bp upstream promoter region of *AHK5* from pMKC101 was joined to the *GFP* sequence and *AHK5* exon 1 sequence (from the *P_{35S}::GFP::AHK5* construct) by single joint PCR [58]. Briefly, in the 1st round PCR stage, 2 separate PCR reactions were set up. In reaction 1, primer 1 (5′-CCTTTTGCATCTCGAGACTTCATGATTAC-3′) and primer 2 (5′-GGTGAACAGCTCCTCGCCCTTGCTCAC-CATTTCACAGACCATTGATCAAGGTTTCTC-3′) were used to incorporate a XhoI restriction site (underlined in primer 1) and a 27 bp of the 5′ end of *GFP* sequence (underlined in primer 2) onto the 5′- and 3′-ends of the 643 bp *AHK5* promoter region, respectively. In reaction 2, a fragment containing the entire *GFP* sequence and *AHK5* exon 1 was amplified using primer 3 (5′-ATGGTGAGCAAGGGCGAGGAGCTGTTCACC-3′) and primer 4 (5′-GATGAGTCGAATTCAATAGGTTTGGTAA-CC-3′) from the *P_{35S}::GFP::AHK5* construct. Primer 4 contains an EcoRI site (underlined). The products from the two reactions were joined (*via* the 27 bp overlapping 5′ *GFP* sequence common to both PCR products) in the 2nd round PCR stage to generate a hybrid DNA fragment. This fragment was then amplified with the primers 1 and 4 in the 3rd round PCR stage. In step three, the hybrid PCR product was digested with XhoI/EcoRI, and cloned into an XhoI/EcoRI cut pMKC101 plasmid to create the *P_{AHK5}::GFP::AHK5* cassette. The integrity of the hybrid DNA fragment was verified by sequencing. Finally, step 4; the *P_{AHK5}::GFP::AHK5* cassette was cloned into the Gateway destination vector pMDC99 [56] using the LR reaction. This binary vector was then transformed into the *Agrobacterium tumefaciens* strain GV3101, and used in tobacco transient expression studies as described above.

For identification and characterisation of homozygous insertion mutants, genomic DNA isolated from appropriate wild type and mutant plants was used for PCR analysis, using various PCR combinations and primers. T-DNA primers used were those already described [29,30]. Individuals were chosen from homozygote lines by selection on BASTA, Southern analysis confirmed the presence of single T-DNA insertions in these lines and at least 3 generations were followed through to get a homozygote population.

For RT-PCR, total RNA from corresponding tissues and developmental stages of *A. thaliana* was isolated using RNAwiz™ (Ambion, UK) or TRIZOL reagent (Invitrogen, UK) and genomic DNA was removed using TURBO DNA-free™ (Ambion, UK). RNA was isolated from guard cell-enriched epidermal fragments and whole leaves as described previously [16]. Subsequently, 1.5 μg of total RNA was reverse transcribed using oligo-dT primer with SuperScript™ III Reverse Transcriptase (Invitrogen, UK) and the resulting cDNA was used as template for the PCR with

HotStart Taq polymerase (Genaxxon, Germany). PCR products were separated *via* agarose gel electrophoresis after different number of PCR cycles for comparison with *ACTIN2* or *EF1* as described in [59]. The sequences of the primers shown in Figure 2 are in Supplementary data.

Transient transformation of tobacco leaf cells and *Arabidopsis* protoplasts, GFP and RFP analyses

The p19 protein from tomato bushy stunt virus cloned in pBIN61 [60] was used to suppress gene silencing in tobacco (*Nicotiana benthamiana)*. All plasmids were transformed in *Agrobacterium tumefaciens* strain GV3101 pMP90, which was grown in YEB medium to OD_{600} 1.0 and prior to infiltration resuspended in AS medium (10 mM $MgCl_2$, 150 µM acetosyringone and 10 mM MES pH 5.7) to $OD_{600} = 0.8$. The *Agrobacterium* strains containing the GFP or p19 construct were mixed in a 1:1 relationship and co-infiltrated into leaves of 4-week-old tobacco plants as described in [60]. The abaxial epidermis of infiltrated tobacco leaves was assayed for fluorescence by CLSM (confocal laser-scanning microscopy) 2 to 3 days post infiltration according to [61]. *Arabidopsis* protoplasts were transformed using PEG mediated transformation procedure and assayed for fluorescence by CLSM after 20 h [61]. CLSM was performed using a Leica TCS SP2 confocal microscope (Leica Microsystems, Germany). These CLSM images were obtained using the Leica Confocal Software and the HCX PL APO 63×/1.2 W CORR water-immersion objective.

For recording the RFP and GFP intensity profiles a homemade confocal laser-scanning microscope, based on a Zeiss Axiovert was used [62,63]. The microscope was equipped with an avalanche photodiode (APD, SPCM-AQR-14, Perkin Elmer, USA) as a spectrally integrating detector. A pulsed 473 nm diode laser (Picoquant LDH-P-C470) operating at a repetition rate of 10 MHz served as excitation source. Fluorescence intensity images were obtained by raster scanning the sample and detecting emission intensity for every spot on the sampled area. The setup was equipped with a 480 nm long pass filter (Semrock Razor Edge LP02-473RU-25) to block back-scattered excitation light, a 500 nm bandpass filter (Semrock BrightLine BL500/24) to detect GFP-fluorescence and a 590 nm bandpass filter (Semrock FF01-590/20-25) to detect RFP-fluorescence in front of the APD. The processing of the obtained fluorescence intensity images was accomplished with the WSxM software [64].

Protein extraction, cell fractionation, SDS-PAGE and western blotting

For cell fractionation 100 mg tissue of transiently transformed tobacco leafs were homogenised in liquid nitrogen and the homogenate was extracted in 2 ml homogenization buffer (25 mM MOPS, 0.1 mM $MgCl_2$, 8 mM L-cysteine, 2.5 mM EDTA, 2× protease inhibitor mix (Roche), 250 mM sucrose; pH 7.8). The crude extract was cleared from debris by centrifugation (4000x*g*, 40 min, 4°C). The microsomal fraction was separated from the soluble fraction by ultracentrifugation (100,000x*g*, 30 min, 4°C). The pellet was washed three times in homogenization buffer supplemented with 0.05% Triton X-100 and resuspended in 50 µl SDS-PAGE sample buffer. The soluble fraction was mixed with SDS-PAGE sample (ratio: 2:1 v/v). For SDS-PAGE 18 µl of the soluble fraction and 10 µl of microsomal fraction were loaded. Western blot analysis and immunodetection were performed according to [61] using anti-GFP antibody (Roche, Switzerland) to detect GFP-AHK5, BRI1-GFP, ERS1-GFP and ARR4-GFP. An anti-mouse-AP conjugate (BioRad, UK) was used as secondary antibody.

Statistical analysis

All data from stomatal bioassays and fluorescence measurements were statistically analysed by using Student's t-test analysis. Data are statistically significant ($p<0.01$) for all treated versus control responses for wild type and complemented lines, and not significant ($p>0.01$) for mutant treated (H_2O_2, ethephon, NO, darkness and flg22) versus mutant controls, unless otherwise indicated.

Supporting Information

Figure S1 The NO insensitive stomatal closure response phenotype of the ahk5-1 mutant is complemented by the 35S promoter-driven expression of the AHK5 cDNA. Stomatal closure in wild type Col-0, ahk5-1 mutant or ahk5-1 transformed with a construct expressing GFP-AHK5 under the control of the 35S promoter (P35S-AHK5/ahk5-1) in response to mock treatment (white bars) or SNP (50 µM, black bars) for 2.5 h.
Found at: doi:10.1371/journal.pone.0002491.s001 (1.42 MB TIF)

Figure S2 Histidine kinase (HK) activity is required for NO-, dark- and flg22-induced stomatal closure. Effect of the HK inhibitor 3,3′,4′,5-tetrachlorosalicylanilide (TCSA) on stomatal closure in wild type Arabidopsis (Col-0). Arabidopsis leaves were incubated in stomatal opening buffer for 2.5 h followed by treatment for 15 min with 10 µM of TCSA prior to exposure to darkness, ethephon (eth, 100 µM), flg22 (100nM) or SNP (50 µM) for 2.5 h. Control, buffer alone. Data are expressed as mean +/− S.E. from 3 independent experiments (n = 60 guard cells).
Found at: doi:10.1371/journal.pone.0002491.s002 (0.61 MB TIF)

Data S1
Found at: doi:10.1371/journal.pone.0002491.s003 (0.02 MB DOC)

Acknowledgments

We acknowledge Arabidopsis Biological Resource Center, USA and INRA-Versailles, France for the T-DNA lines used in this study and J Mansfield (Imperial College London) for the bacteria and PAMPs.

Author Contributions

Conceived and designed the experiments: SN KH RD RH JH. Performed the experiments: RD JH CC VM CG JW KE MC. Analyzed the data: KH RD JH CC VM CG KE AM. Contributed reagents/materials/analysis tools: AM. Wrote the paper: SN KH RD RH JH.

References

1. Apel K, Hirt H (2004) Reactive oxygen species: metabolism, oxidative stress, and signal transduction. Annu. Rev Plant Biol 55: 373–399.
2. Neill S, Desikan R, Hancock J (2002) Hydrogen peroxide signalling. Curr Opin Plant Biol 5: 388–395.
3. Desikan R, Hancock J, Neill S (2005b) Reactive oxygen species as signaling molecules. In "Antioxidants and Reactive Oxygen Species in Plants" 169–196, Smirnoff N, ed. Blackwell Publishing, UK.
4. Desikan R, Clarke A, Hancock JT, Neill SJ (1999) H_2O_2 activates a MAP kinase-like enzyme in *Arabidopsis thaliana* suspension cultures. J Exp Bot 50: 1863–1866.
5. Desikan R, Hancock JT, Ichimura K, Shinozaki K, Neill SJ (2001) Harpin induces activation of the Arabidopsis mitogen-activated protein kinases AtMPK4 and AtMPK6. Plant Physiol 126: 1579–1587.
6. Kovtun Y, Chiu W-L, Tena G, Sheen J (2000) Functional analysis of oxidative stress-activated mitogen-activated protein kinase cascade in plants. Proc Natl Acad Sci USA 97: 2940–2945.
7. Rentel MC, Lecorieux D, Ouaked F, Usher SL, Petersen L, et al. (2004) OXI1 kinase is necessary for oxidative burst-mediated signalling in *Arabidopsis*. Nature 427: 858–861.

8. Gupta R, Luan S (2003) Redox control of protein tyrosine phosphatases and mitogen activated protein kinases in plants. Plant Physiol 132: 1149–1152.
9. Meinhard M, Grill E (2001) Hydrogen peroxide is a regulator of ABI1, a protein phosphatase 2C from *Arabidopsis*. FEBS Letts 508: 443–446.
10. Meinhard M, Rodriguez PL, Grill E (2002) The sensitivity of ABI2 to hydrogen peroxide links the abscisic acid-response regulator to redox signalling. Planta 214: 775–782.
11. Gudesblat GE, Iusem ND, Morris PC (2007) Guard cell-specific inhibition of Arabidopsis MPK3 expression causes abnormal stomatal responses to abscisic acid and hydrogen peroxide. New Phytol 173: 713–721.
12. Mustilli A-C, Merlot S, Vavasseur A, Fenzi F, Giraudat J (2002) *Arabidopsis* OST1 protein kinase mediates the regulation of stomatal aperture by abscisic acid and acts upstream of reactive oxygen species production. Plant Cell 14: 3089–3099.
13. Kwak JM, Mori IC, Pei Z-M, Leonhardt N, Torres MA, et al. (2003) NADPH oxidase *AtrbohD* and *AtrbohF* genes function in ROS-dependent ABA signaling in *Arabidopsis*. EMBO J 22: 2623–2633.
14. Cooper CE, Patel RP, Brookes PS, Darley-Usmar VM (2002) Nanotransducers in cellular redox signalling: modification of thiols by reactive oxygen and nitrogen species. Trends Biochem Sci 27: 489–492.
15. Desikan R, Hancock JT, Bright J, Harrison J, Weir I, et al. (2005a) A role for ETR1 in hydrogen peroxide signalling in stomatal guard cells. Plant Physiol 137: 831–834.
16. Desikan R, Last K, Harrett-Williams R, Tagliavia C, Harter K, et al. (2006) Ethylene-induced stomatal closure in Arabidopsis occurs via AtrbohF-mediated hydrogen peroxide synthesis. Plant J 47: 907–916.
17. Grefen C, Harter K (2004) Plant two-component systems: principles, functions, complexity and cross talk. Planta 219: 733–742.
18. Hwang I, Chen H-C, Sheen J (2002) Two-component signal transduction pathways in *Arabidopsis*. Plant Physiol 129: 500–515.
19. Sweere U, Eichenberg K, Lohrmann J, Mira-Rodado V, Bäurle I, et al. (2001) Interaction of the response regulator ARR4 with phytochrome B in modulating red light signaling. Science 294: 1108–1111.
20. Mira-Rodado V, Sweere U, Grefen C, Kunkel T, Fejes E, et al. (2007) Functional cross-talk between two-component and phytochrome B signal transduction in *Arabidopsis*. J Exp Bot 58: 2595–2607.
21. Desikan R, A-H Mackerness S, Hancock JT, Neill SJ (2001b) Regulation of the *Arabidopsis* transcriptome by oxidative stress. Plant Physiol 127: 159–172.
22. Kilian J, Whitehead D, Horak J, Wanke D, Weinl S, et al. (2007) The AtGenExpress global stress expression data set: protocols, evaluation and model data analysis of UV-B light, drought and cold stress responses. Plant J 50: 347–363.
23. Wang P-C, Du Y-Y, An G-Y, Zhou Y, Miao C, et al. (2006) Analysis of global expression profiles of *Arabidopsis* genes under abscisic acid and H_2O_2 applications. J Int Plant Biol 48: 62–74.
24. Iwama A, Yamashino T, Tanaka Y, Sakakibara H, Kakimoto T, et al. (2007) AHK5 His-kinase regulates root elongation through an ETR1-dependent abscisic acid and ethylene signaling pathway in *Arabidopsis thaliana*. Plant Cell Physiol 48: 375–380.
25. Grefen C, Städele K, Ruzicka K, Obrdlik P, Harter K, et al. (2008) Subcellular localization and *in vivo* interactions of the *Arabidopsis thaliana* ethylene receptor family members. Molecular Plant 1: 308–320.
26. Geldner N, Hyman DL, Wang X, Schumacher K, Chory J (2007) Endosomal signaling of plant steroid receptor kinase BRI1. Genes Develop. 21: 1598–1602.
27. Nelson BK, Cai X, Nebenführ A (2007) A multicolored set of *in vivo* organelle markers for co-localization studies in Arabidopsis and other plants. Plant J. 51: 1126–1136.
28. Schmid M, Davison TS, Henz SR, Pape UJ, Demar M, et al. (2005) A gene expression map of *Arabidopsis thaliana* development. Nat Genetics 37: 501–506.
29. Samson F, Brunaud V, Balzergue S, Dubreucq B, Lepiniec L, et al. (2002) FLAGdb/FST a database of mapped flanking insertion sites (FSTs) of Arabidopsis thaliana T-DNA transformants. Nucleic Acids Res 30: 94–97.
30. Sessions A, Burke E, Presting G, Aux G, McElver J, et al. (2002) A high-throughput Arabidopsis reverse genetics system. Plant Cell 14: 2985–94.
31. Papon N, Clastre M, Gantet M, Rideau M, Chenieux J-C, et al. (2003) Inhibtiion of the plant cytokinin transduction pathway by bacterial histidine kinase inhibitors in *Catharantheus roseus* cell cultures. FEBS Letts 537: 101–105.
32. Bright J, Desikan R, Hancock JT, Neill SJ (2006) ABA-induced NO generation and stomatal closure in *Arabidopsis* are dependent on H_2O_2 synthesis. Plant J 45: 113–122.
33. Desikan R, Cheung M-K, Clarke A, Golding S, Sagi M, et al. (2004) Hydrogen peroxide is a common signal for darkness and ABA-induced stomatal closure in *Pisum sativum*. Functional Plant Biol 31: 913–920.
34. Felix G, Duran JD, Volko S, Boller T (1999) Plants have a sensitive perception system for the most conserved domain of bacterial flagellin. Plant J 18: 265–276.
35. Zhang J, Shao F, Li Y, Cui H, Chen L, et al. (2007) A *Pseudomonas syringae* effector inactivates MAPKs to suppress PAMP-induced immunity in plants. Cell Host Micr 1: 175–185.
36. Melotto M, Underwood W, Koczan J, Nomura K, He SY (2006) Plant stomata function in innate immunity against bacterial invasion. Cell 126: 969–980.
37. Zipfel C, Kunze G, Chinchilla D, Caniard A, Jones JDG, et al. (2006) Perception of the bacterial PAMP EF-Tu by the receptor EFR restricts Agrobacterium-mediated transformation. Cell 125: 749–760.
38. Gomez-Gomez L, Boller T (2002) Flagellin perception: a paradigm for innate immunity. Trends Plant Sci 7: 251–256.
39. Bright J (2006) Nitric oxide signalling in *Arabidopsis thaliana* guard cells. PhD thesis. .
40. Plesch G, Ehrhardt T, Mueller-Roeber B (2001) Involvement of TAAAG elements suggests a role for Dof transcription factors in guard cell specific gene expression. Plant J 28: 455–464.
41. Yang Y, Costa A, Leonhardt N, Siegel RS, Schroeder JI (2008) Isolation of a strong Arabidopsis guard cell promoter and its potential as a research tool. Plant Methods 4: 6.
42. Leymarie J, Vavasseur A, Lasceve G (1998) CO_2 sensing in stomata of *abi1-1* and *abi2-1* mutants of *Arabidopsis thaliana*. Plant Physiol Biochem 36: 539–543.
43. Hosy E, Vavasseur A, Mouline K, Dreyer I, Gaymard F, et al. (2003) The *Arabidopsis* outward K^+ channel *GORK* is involved in regulation of stomatal movements and plant transpiration. Proc Natl Acad Sci USA 100: 5549–5554.
44. Liang Y-K, Dubos C, Dodd IC, Holroyd GH, Hetherington AM, et al. (2005) *At*MYB61, an R2R3-MYB transcription factor controlling stomatal aperture in *Arabidopsis thaliana*. Curr Biol 15: 1201–1206.
45. Bittel P, Robatzek S (2007) Microbe-associated molecular patterns (MAMPs) probe plant immunity. Curr Opin Plant Biol 10: 335–341.
46. Robatzek A, Chinchilla D, Boller T (2006) Ligand-induced endocytosis of the pattern recognition receptor FLS2 in Arabidopsis. Genes Dev 20: 537–542.
47. Chinchilla D, Zipfel C, Robatzek S, Kemmerling B, Nurnberger T, et al. (2007) A flagellin-induced complex of the receptor FLS2 and BAK1 initiates plant defence. Nature 448: 497–501.
48. Heese A, Hann D, Gimenez-Ibanez S, Jones AME, He K, et al. (2007) The receptor-like kinase SERK3/BAK1 is a central regulator of innate immunity in plants. Proc Natl Acad Sci USA 104: 12217–12222.
49. Keller T, Damude HG, Werner D, Doerner P, Dixon RA, et al. (1998) A plant homolog of the neutrophil NADPH oxidase gp91-*phox* subunit gene encodes a plasma membrane protein with Ca^{2+} binding motifs. Plant Cell 10: 255–266.
50. Chen Y-F, Randlett MD, Findell JL, Schaller GE (2002) Localisation of the ethylene receptor ETR1 to the endoplasmic reticulum of Arabidopsis. J Biol Chem 27: 19861–19866.
51. Gomez-Gomez L, Boller T (2000) FLS2: an LRR receptor-like kinase involved in the perception of the bacterial elicitor flagellin in Arabidopsis. Mol Cell 5: 1003–1011.
52. Miao Y, Lv D, Wang P, Wang X-C, Chen J, et al. (2006) An Arabidopsis glutathione peroxidase functions as both a redox transducer and a scavenger in abscisic acid and drought stress responses. Plant Cell 18: 2749–2767.
53. Fujita M, Fujita Y, Noutoshi Y, Takahashi F, Narusaka Y, et al. (2006) Crosstalk between abiotic and biotic stress responses: a current view from the points of convergence in the stress signalling networks. Curr Opin Plant Biol 9: 436–442.
54. Karimi M, Inze D, Depicker A (2002) GATEWAY vectors for *Agrobacterium*-mediated plant transformation. Trends Plant Sci 7: 193–195.
55. Rubio V, Shen Y, Saijo Y, Liu Y, Gusmaroli G, et al. (2005) An alternative tandem affinity purification strategy applied to Arabidopsis protein complex isolation. Plant J 41: 767–778.
56. Curtis MD, Grossniklaus U (2003) A Gateway cloning vector for high-throughput functional analysis of genes *in planta*. Plant Physiol 133: 462–469.
57. Clough SJ, Bent AF (1998) Floral dip: a simplified method for *Agrobacterium*-mediated transformation of *Arabidopsis thaliana*. Plant J 16: 735–743.
58. Yu J-H, Hamari Z, Han K-H, Seo J-A, Reyes-Dominguez Y, et al. (2004) Double-joint PCR: a PCR-based tool for gene manipulations in filamentous fungi. Fungal Genetics and Biol 41: 973–981.
59. Horák J, Brzobohatý B, Lexa M (2003) Molecular and physiological characterisation of an insertion mutant in the ARR21 putative response regulator gene from *Arabidopsis thaliana*. Plant Biol 5: 245–254.
60. Voinnet O, Lederer C, Baulcombe DC (2000) A viral movement protein prevents spread of the gene silencing signal in *Nicotiana benthamiana*. Cell 103: 157–67.
61. Walter M, Chaban C, Schütze K, Batistic O, Weckermann K, et al. (2004) Visualization of protein interactions in living plant cells using bimolecular fluorescence complementation. Plant J 40: 428–438.
62. Blum C, Stracke F, Becker S, Müllen K, Meixner AJ (2001) Discrimination and interpretation of spectral phenomena by room-temperature single-molecule spectroscopy. J Phys Chem A 105: 6983–6990.
63. Schleifenbaum F, Blum C, Elgass K, Subramanian V, Meixner AJ (2008) New insights into the photophysics of DsRed by multiparameter spectroscopy on single proteins. J Phys Chem B in press. .
64. Horcas I, Fernandez R, Gomez-Rodriguez JM, Colchero J, Gomez-Herrero J, et al. (2007) WSXM: A software for scanning probe microscopy and a tool for nanotechnology. Rev Sci Instrum 78: 013705.

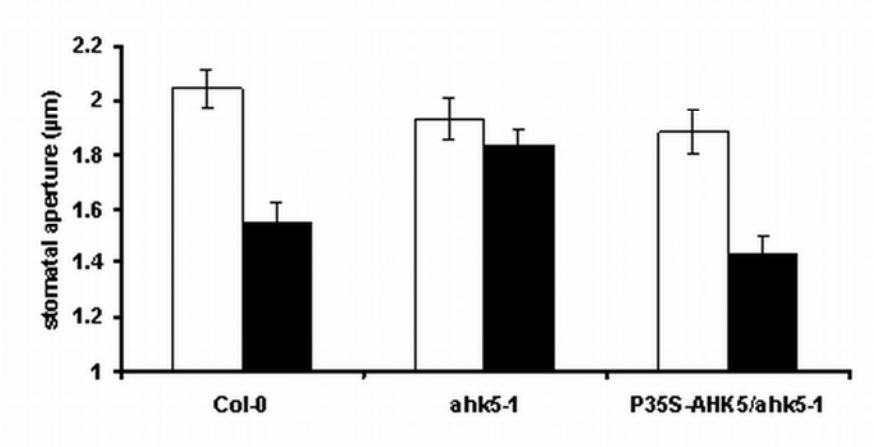

Figure S1 The NO insensitive stomatal closure response phenotype of the *ahk5-1* mutant is complemented by the 35S promoter-driven expression of the AHK5 cDNA. Stomatal closure in wild type Col-0, *ahk5-1* mutant or *ahk5-1* transformed with a construct expressing GFP-AHK5 under the control of the 35S promoter (P35S-AHK5/ahk5-1) in response to mock treatment (white bars) or SNP (50 µM, black bars) for 2.5 h.

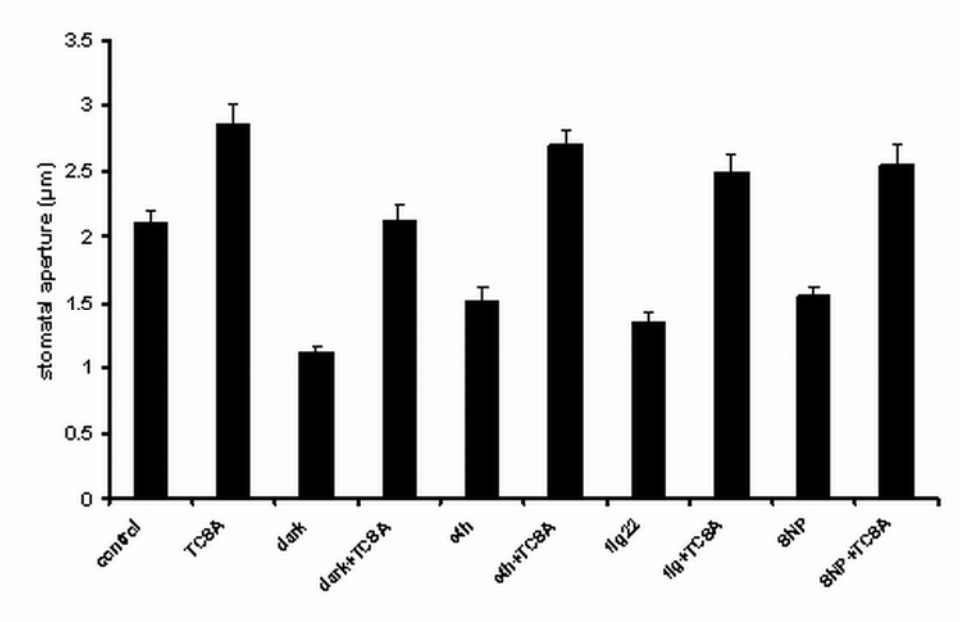

Figure S2 Histidine kinase (HK) activity is required for NO-, dark- and flg22-induced stomatal closure. Effect of the HK inhibitor 3,3′,4′,5-tetrachlorosalicylanilide (TCSA) on stomatal closure in wild type *Arabidopsis* (Col-0). *Arabidopsis* leaves were incubated in stomatal opening buffer for 2.5 h followed by treatment for 15 min with 10 µM of TCSA prior to exposure to darkness, ethephon (eth, 100 µM), flg22 (100nM) or SNP (50 µM) for 2.5 h. Control, buffer alone. Data are expressed as mean +/− S.E. from 3 independent experiments (n = 60 guard cells).

Primer sequences used for PCR in Figure 2

1	GTCAGGAGTAGTGGGAATGGCTGAG
2	CTCAGTGCAAATACTGTTGC
3	AAATGCTTGAGGCGAGTACTGA
4	GTTGGCCTCCCATTAACTCAACCAG
5	TGTTTACAACAAAGCTGGCG
6	CAAATTGGTGAGGATCTGCC
7	GCTGTGACGTATGGGACACTGG
8	CGGTCCAAGAGCTTACTCAG
9	AAAGTATCTCAGCCATTCCC
10	TCATGAGACATCGTCGCTAGC
ACT2F	CTGCTCAATCTCATCTTCTTCC
ACT2R	GACCTGCCTCATCATACTCG
EF1FOR	AGCACGCTCTTCTTGCTTTC
EF1REV	GGGTTGTATCCGACCTTCTTC

Identification of two-component system elements downstream of AHK5 in the stomatal closure response

Virtudes Mira-Rodado[1], Manikandan Veerabagu[1], Janika Witthöft[1], Julia Teply[1], Klaus Harter[1], Radhika Desikan[2]**

[1] Center for Plant Molecular Biology (ZMBP), Department of Plant Physiology, University of Tübingen, Auf der Morgenstelle 1, 72076 Tübingen, Germany, Phone: +49-(0)7071-29-76940

[2] Department of Life Sciences, Imperial College London, South Kensington, London SW7 2AZ, United Kingdom, Phone: +44(0)207 594 3895

*Corresponding authors:
r.desikan@imperial.ac.uk
virtudes.mira-rodado@zmbp.uni-tuebingen.de

Abstract

To optimize water use efficiency, plants regulate stomatal closure through a complex signaling process. Hydrogen peroxide (H_2O_2) is produced in response to several environmental stimuli and has been identified to be a key second messenger involved in the regulation of stomatal aperture. The *Arabidopsis* histidine kinase 5 (AHK5) has been related to the regulation of stomatal closure in response to H_2O_2 and other stimuli, that depend on H_2O_2. AHK5 is a member of the two-component system (TCS) in *Arabidopsis*. The plant TCS comprises three different protein types: the hybrid histidine kinases (HKs), the phosphotransfer proteins (HPs) and the response regulators (RRs). Here we determined TCS elements involved in the H_2O_2- and ethylene-dependent stomatal closure downstream of AHK5. By yeast and *in planta* interaction assays and functional studies, AHP1, 2 and ARR4 were identified acting downstream of AHK5 in the guard cell ethylene and H_2O_2 response pathways. Furthermore, we could demonstrate that aspartate phosphorylation of ARR4 was only required for the H_2O_2- but not for the ethylene-induced stomatal closure response. Our data suggest the presence of a complex TCS signaling network comprising of at least AHK5, several AHPs and ARRs, which modulates stomatal closure in response to H_2O_2 and ethylene.

Introduction

Stomata are openings in leaves that regulate gas exchange and water loss between the plant and the environment. Guard cells surrounding stomatal pores regulate stomatal movements *via* swelling and shrinking in response to changes in turgor pressure, depending on the stimulus. Guard cells have been extensively used to not only understand plant responses to drought stress *via* the hormone abscisic acid (ABA) but also other abiotic (salinity, ozone, light/dark) and biotic stimuli (bacteria, fungi and pathogen-derived elicitors) (Schroeder *et al.* 2001b; Underwood *et al.* 2007) The extreme robustness of guard cell signaling networks, cell autonomy and the advantage of having a quick physiological read-out (stomatal aperture) make guard cells an extremely attractive system to study signal transduction pathways. This is over-ridden by the overall importance of transpirational water loss through stomata being crucial for plant survival under a constantly changing environment.

The signal transduction network has been extensively studied for ABA, and is nowhere being complete (Schroeder *et al.* 2001b). However this has been a driving force to understand mechanisms of signal perception and transduction in other situations, e.g. the hormone ethylene (Desikan *et al.* 2005) and bacteria (Underwood *et al.* 2007). Inevitably, cross-talk does occur between signaling pathways in guard cells; for example, between ABA and ethylene, as well as ABA and jasmonic acid (JA) and bacterial elicitors. One of the key elements common to signal transduction cross-talk is the reactive oxygen species (ROS) hydrogen peroxide (H_2O_2). H_2O_2 has been shown to act as a central node integrating plant responses to both abiotic and biotic stimuli (Desikan *et al.* 2004) The mechanisms, by which plant cells perceive ROS and trigger various signaling pathways, are slowly being unraveled, particularly in guard cells (Pham & Desikan 2009).

In an attempt to understand redox signaling, we have recently shown that the hybrid histidine kinase AHK5 functions in *Arabidopsis* guard cells to integrate endogenous and environmental cues *via* redox homeostasis (Desikan *et al.* 2008). Although protein phosphorylation is a key signal transduction component in ABA-induced stomatal closure (Schroeder *et al.* 2001a), there is not much evidence for the two-component system (TCS) functioning in guard cells. The TCS network in plants consists of hybrid histidine kinases (HKs), histidine-containing phosphotransfer proteins (HPs) and response regulators (RRs). Signal perception by a HK leads to a phosphorelay from the HK, *via* HPs to a RR, modulating gene expression and other cellular reactions. The RR family in *Arabidopsis* (ARR) is divided into three subgroups, the A-, B- and C-type ARRs, according to their protein structure. The type-A ARRs are quite small proteins with a short receiver domain that contains the phosphorylatable aspartate residue and a short C-terminal extension (Grefen & Harter 2004). They are up-regulated by cytokinin and, apart from their function as negative regulators of cytokinin signaling (Hwang & Sheen 2001), they have also been related to other processes such as red light signaling (Sweere *et al.* 2001; Mira-Rodado *et al.* 2007), circadian clock (Salome *et al.* 2006; Ishida *et al.* 2008), lateral root formation (Ren *et al.* 2009), cold stress (Jeon *et al.* 2010) and leaf senescence (Ren *et al.* 2009).

The type-B response regulator proteins (type-B ARRs) also comprise a receiver domain along with an extended C-terminal output region (Grefen & Harter 2004). They act as transcription factors that induce transcription of type-A ARRs upon cytokinin treatment (D'Agostino *et al.* 2000). Structurally and functionally, the type-C ARRs resemble type-A ARRs, however, unlike type-A ARRs, their expression does not depend on cytokinin (Müller 2011).

Our recent data show that the *Arabidopsis* HK (AHK) ETR1 functions in ethylene and H_2O_2-regulated stomatal closure (Desikan *et al.* 2005), and the HK AHK5 functions in H_2O_2, NO, darkness, bacteria- and ethylene-induced stomatal closure (Desikan *et al.* 2008). Intriguingly, both these HKs appear not to be required for the ABA signal response pathway in guard cells (Desikan *et al.* 2005; Desikan *et al.* 2008).

AHK5 is a unique HK protein in the *Arabidopsis* TCS family. It is the only HK that was predicted to have a cytosolic location; yet recent experiments showed that it is cytosolic and also associates with the plasma membrane (Desikan *et al.* 2008). This intracellular distribution pattern would make it unique in its ability to integrate various signals, both from within and outside the cell (Desikan *et al.* 2008). As AHK5 is a canonical HK, it is assumed to function within the TCS network. We therefore aimed to investigate the two-component elements in this signal transductome and how the interactors may function in the stomatal closure response. We show that AHK5 interacts with the *Arabidopsis* HP (AHP) proteins AHP1, AHP2, and AHP5 *in vivo* and that *Arabidopsis* plants carrying loss-of-function alleles of the *AHP* genes have defects in stomatal closure in response to ethylene and H_2O_2. Downstream of the AHK5-interacting AHPs, we identified ARR4 as at least one RR involved in the regulation of stomatal closure. In addition, the phosphorylation of ARR4 appears to be required for at least some of AHK5 signal transduction to occur.

Results

Identification of AHPs that associate with the AHK5 protein

AHK5 is a canonical hybrid histidine kinase and, thus, proposed to be the first element in a phosphorelay process that also consist of AHPs and ARRs. This opens the question of whether AHK5 function in stomatal closure rests upon a classical TCS pathway. Until now, no TCS element has been described acting downstream of AHK5. The TCS elements acting immediately downstream of hybrid AHKs are the AHPs. To elucidate whether and which of the 5 canonical AHPs (AHP1, 2, 3, 4, 5) and pseudo-AHP (AHP6) may act down-stream of AHK5, we first performed AHK5-AHP interaction studies using the yeast two-hybrid system (Y2H). As shown in Figure 1A, AHK5 interacted with AHPs 1, 2, 3 and 5 and the pseudo-AHP6 but not with AHP4 in Y2H, although AHP4 was expressed in the yeast cells (Figure 1B).

To substantiate the yeast results with an independent technique, we also performed *in planta* protein-protein interaction studies based on a bimolecular fluorescence complementation (BiFC) assay in transiently transformed tobacco (*Nicotiana benthamiana*) leaf epidermal cells (Walter *et al.* 2004; Schütze *et al.* 2009). Although AHK5 and the different AHP proteins co-accumulated to a similar level in the independently co-transformed tobacco leaves (Figure 2B), BiFC signals were only observed in the case where AHK5 was co-expressed with AHP1, 2 and 5 (Figure 2A). This indicates that AHP1, 2 and 5 are the specific interaction partners of AHK5 *in planta* and that the interaction of AHK5 with AHP3, 4 and 6 is a yeast artifact. The divergence of the yeast and *in planta* results could be due to the fact that yeast represents a heterologous system lacking plant components which are required to achieve a more specific interaction pattern in the TCS network.

Behavior of *ahp* mutants to the AHK5-dependent ethylene and H_2O_2-induced stomatal closure response

The data above suggest a putative TCS signaling pathway that would initiate with AHK5 and carry on with AHP1, 2 and 5. As mentioned above, AHK5 is involved in H_2O_2-induced as well as in the ethylene-induced stomatal closure response in *Arabidopsis*. To test if AHK5-AHPs interactions are of physiological relevance for the ethylene-induced stomatal closure response, we analysed the phenotypic behavior of *ahp1, 2* and *5* single, double and triple mutants (Hutchison *et al.* 2006) in the presence of the hormone. In *ahk5* mutants, the ethylene response is impaired resulting in plants that, opposite to the wild type, do not close their stomata in response to the hormone (Desikan *et al.* 2008). Interestingly, both *ahp1* and *ahp2* single mutants displayed no significant stomatal closure response to the synthetic ethylene ethephon, compared to Ws and Col-0 controls respectively (Figure 3A). In contrast, *ahp5* mutants displayed significant response to ethephon, despite the control apertures being considerably smaller than wild type Col-0. The double mutant *ahp1,5* was insensitive to ethylene as was the *ahp1,2* double mutant. The *ahp2,5* double mutant however, showed a slight response to ethylene, whereas in the *ahp1,2,5* triple mutant the ethylene response was virtually abolished (Figure 3A).

In order to determine the role of the AHK5-interacting AHPs in the H_2O_2-dependent stomatal closure pathway, the above mutants were tested for their response to exogenous H_2O_2. Figure 3B shows that *ahp1* stomata closed significantly to H_2O_2, similar to wild type Ws guard cells. However compared to wild type Col-0, the *ahp2* mutant did not respond to H_2O_2 treatment, but the *ahp5* mutant showed a significant response to H_2O_2. Moreover, the *ahp1,5* double mutant phenotype reflected that of *ahp5*, and the *ahp1,2* and *ahp2,5* double mutants' response to H_2O_2 reflected that of *ahp2* single mutant. The *ahp1,2,5* triple mutant showed no response to H_2O_2, although their stomata were constitutively more closed (as with *ahp5* and *ahp2,5*), compared to Col-0 (Figure 3B).

Identification of putative ARRs that could be involved in the AHK5-two component system

After elucidating the AHP components that were involved in the stomatal response, it remained open to identify the final TCS output element, in this case the specific ARR, responsible to conclude the TCS pathway. There are a total of 32 ARRs that have been described in *Arabidopsis* (To & Kieber 2008) and of these, ARR2 was shown to be functioning as a positive element downstream of ETR1 in the ethylene and H_2O_2 signal transduction pathway in guard cells (Desikan *et al.* 2006). To be downstream of the AHK5-AHP signaling pathway, the ARR must be able to interact and function with AHP1 or AHP2. By Y2H assays it has been shown that 10 ARRs interacted in yeast with AHP1 and 2, namely ARR1, 2, 3, 4, 5, 7, 8, 9, 14 and 16 (Dortay *et al.* 2006). From these, only ARR1, 2, 4, and 7 are expressed in stomatal guard cells (Leonhardt *et al.* 2004). We recently demonstrated that the A-type response regulator ARR4 is not only able to interact with AHP1 in the Y2H system but also accepts phosphoryl residues from the phosphotransfer protein AHP1 in a plant cell-derived *in vitro* phosphorelay system (Mira-Rodado *et al.* 2007). This makes ARR4 a promising candidate as a putative downstream element of the AHK5-AHP1 phosphorelay.

As the Y2H system showed discrepancies to *in planta* interaction studies with respect to the AHK5-AHP interactions (Figure 1 and 2), it was therefore crucial to verify that ARR4 actually interacts with those AHPs which also associated with AHK5 in plant cells. To do so, we repeated the Y2H interaction assays and in addition, carried out *in planta* BiFC interaction studies in tobacco. We could confirm that ARR4 interacts with AHP1, 2, 3 and 5 (Dortay *et al.* 2006), excluded AHP4 as an interaction partner and identified AHP6 as a new ARR4-interacting protein in yeast (Figure 4). In this case, the results of the *in planta* BiFC interaction studies corroborated the yeast interaction data: ARR4 interacted *in planta* with AHP1, 2, 3, 5 and 6 but not with AHP4 (Figure 5). Together with the above AHK5-AHP data, the possibility therefore arises that AHK5, AHP1, AHP2 and ARR4 comprise a TCS signaling pathway, which might regulate guard cell activity in response to H_2O_2 and ethylene.

ARR4 contributes to the ethylene- and H_2O_2-induced stomata closure response

To test the significance of ARR4 in the ethylene-induced stomatal closure response, we tested the response of the *arr4* T-DNA insertion mutant (To *et al.* 2004) to ethylene. In contrast to wild type Col-0 plants, *arr4* stomata did not close when treated with ethephon (Figure 6A). Plants overexpressing ARR4

(ARR4ox) (Sweere *et al.* 2001) had their stomata constitutively more closed compared to wild type Col-3, but nevertheless showed a reduced, but significant closure response to ethephon treatment (Figure 6A).

TCS signaling mechanisms are based on a phosphorelay that transfers the signal from the hybrid histidine kinase, over the phosphotransfer proteins, to the response regulators. It was, therefore, important to determine whether the phosphorylation of ARR4 is required for ethylene-induced stomatal closure and to investigate whether the response was affected in a transgenic line, which ectopically expresses a non-phosphorylatable, loss-of-function version of ARR4 ($ARR4^{D95N}$) (Mira-Rodado *et al.* 2007). Surprisingly, the $ARR4^{D95N}$-expressing line behaved as wild type Ws plants closing its stomata normally upon ethylene treatment (Figure 6A). This suggests that, although ARR4 is involved in the signaling pathway, its activation through aspartate phosphorylation is not required for the ethylene response.

To test the function of ARR4 in the H_2O_2 signaling pathway leading to stomatal closure, leaves from the above mutants were treated with exogenous H_2O_2 and their stomatal closure response was measured. The *arr4* mutant clearly displayed insensitivity to H_2O_2 treatment, compared to wild type Col-0 (Figure 6B). Furthermore, H_2O_2-treated ARR4ox plants closed their stomata as wild type Col-3 plants. Interestingly, the transgenic line which ectopically expresses non-phosphorylatable $ARR4^{D95N}$, showed an impaired stomatal closure response upon H_2O_2 treatment (Figure 6B), suggesting that phosphorylation of ARR4 is necessary for H_2O_2-induced stomatal closure.

In conclusion, our biochemical, genetic and physiological data show that AHK5 interacts with AHPs 1, 2 and ARR4, to regulate stomatal closure responses.

Discussion

AHK5 is a unique histidine kinase, in that it is the only predicted cytosolic HK known in *Arabidopsis*. In previous work we showed that AHK5 is not only located in the cytosol, but is also associated with the plasma membrane (Desikan *et al.* 2008). Our previous genetic and physiological analyses showed that AHK5 acts to integrate endogenous and external cues to regulate stomatal closure (Desikan *et al.* 2008). The mechanism of AHK5 action in guard cells remained to be elucidated. Here we demonstrate that AHK5 acts as part of a two-component system, physically interacting with the phosphotransfer proteins AHP1, AHP2 and AHP5. These AHPs subsequently interact with the response regulator protein ARR4. We also show that functional AHP1 and AHP2 as well as ARR4 proteins are required for stomatal closure response.

The yeast interaction data shown here demonstrate that further validation of this assay is required in order to get results meaningful for plant cells. Previously, numerous studies have used yeast two-hybrid assays and *in vitro* co-purification experiments with recombinant proteins to determine interaction of plant HKs with AHPs and AHPs with ARRs (Urao *et al.* 2000; Dortay *et al.* 2006; Dortay *et al.* 2008). However the functional relevance of these interactions needs to be verified *in planta*, in most cases. Our data here and elsewhere (Grefen *et al.* 2010) show that the BiFC assay is reliable to demonstrate physical interaction between these partner proteins. AHK5 has been shown to have histidine kinase activity (Iwama *et al.* 2007) and shown to complement yeast SLN1 mutants (Tran *et al.* 2007). Therefore it was necessary to show that

AHK5 does indeed function in a two-component system – our results show for the first time that AHK5 interacts with AHP1,2 and 5 *in planta* (but not AHPs 3, 4 and 6).

To extend the biochemical interaction data to functional significance, we tested the response of single, double and triple mutants of these AHPs for their stomatal response to ethylene and H_2O_2, two different stimuli shown to affect the stomatal response of *ahk5* (Desikan *et al.* 2008). For the ethylene response, it appears that AHP1 and AHP2 function are essential, but AHP5 function is not required. Single and double mutant data indicate that when AHP1 and AHP2 are absent, a null response is attained, reflecting the importance of the individual genes. An identical effect is also observed when AHP1 and AHP5 are mutated together; however, when AHP2 and AHP5 are together not functional, the stomata are still able to respond to a slight extent to ethylene. This implies that AHP5 is epistatic to AHP2 but not to AHP1 in this signaling pathway. The null phenotype in the triple mutant suggest that the epistatic effect of AHP5 to AHP2 is masked when AHP1 is also mutated implying that the signaling mechanism involving AHP1is the main pathway followed in the response to ethylene.

H_2O_2 is a key signaling molecule generated in response to multiple stimuli, and of relevance to this work, shown to be required for a stomatal closure response to ethylene (Desikan *et al.* 2006). Previously we showed that AHK5 regulates redox homeostasis in stomatal guard cells in response to ethylene and the bacterial elicitor flagellin (Desikan *et al.* 2008). Here we find that the signaling pathway for H_2O_2-induced stomatal closure *via* AHK5-interacting AHPs appears to be different to that seen for ethylene. It seems that AHP1 and AHP5 are clearly not involved in H_2O_2-induced closure. However AHP2 function is essential for H_2O_2-induced closure. In contrast to the ethylene response, when AHP2 and AHP5 are both absent, there is a null response to H_2O_2, indicating that the function of AHP5 is redundant for the H_2O_2 pathway to be operational. This is also reflected in the triple mutant, where the *ahp1* phenotype is clearly masked.

Together the above complex observations suggest that there are different routes to the AHK5-dependent TCS, depending on the input stimulus. So whilst AHP2 appears to be overlapping in both signaling pathways, AHP1 appears to be unique to the ethylene signaling arm alone (Figure 7). Although we observed an epistatic effect of AHP5 on AHP2 in the ethylene response, AHP5 does not seem to be essential for either the ethylene or H_2O_2 pathways *via* AHK5 to be operational. It is quite possible that the AHK5-AHP5 interaction is required for another stimulus-response pathway, perhaps not in stomata. The AHP1-dependent ethylene pathway indicates that there is a H_2O_2-independent pathway operating downstream of ethylene in guard cells. Ongoing work in our laboratory indicates that nitric oxide (NO) is also generated following ethylene-stimulation of guard cells. It is possible that the NO pathway occurs independent of the H_2O_2 branch in the pathway, where AHP1 might fit in.

Completing the AHK5 TCS pathway

To identify the last component of the AHK5-dependent TCS pathway, yeast interaction assays and BiFC experiments were performed. We demonstrated that AHPs 1, 2 and 5 interact with ARR4. ARR4 is an A-type response regulator, having only a receiver domain and a very short output domain (Hwang *et al.*

2002). ARR4 has been shown to not only participate as a negative regulator in cytokinin signaling, but also as a positive regulator modulating the phytochrome B and other environmental signaling pathways (Mira-Rodado *et al.* 2007). Here we provide functional evidence that ARR4 functions as a positive regulator in the ethylene- and H_2O_2-induced stomatal closure pathways. However, rather surprisingly, our genetic data demonstrate that phosphorylation of ARR4 is required only for the H_2O_2 response, but not for the ethylene response in stomata. This suggests that ARR4 may function *via* phosphorylation-independent interference with other proteins (Dortay *et al.* 2008) in the stomatal ethylene response pathway.

Ethylene signaling occurs *via* ethylene perception by its cognate receptors, of which ETR1 has been shown to play a pivotal role in guard cells (Desikan *et al.* 2006). Ethylene signaling required H_2O_2 generation, and was also shown to involve the B-type response regulator ARR2 in guard cells (Desikan *et al.* 2006). Previously, a phosphorelay downstream of ETR1 was shown to be operational *via* ARR2 (Hass *et al.* 2004). Furthermore, ETR1 and ARR2 have also been shown to interact with AHP1 and AHP2 *in vitro* (Dortay *et al.* 2008; Scharein *et al.* 2008). Together with our observations, it appears that the ethylene signaling pathway could operate *via* AHP1, AHP2 and ARR2, independent of ARR4 phosphorylation (Figure 7). Another possibility is that the (post-translational) activation of ARR2 by ethylene, which encodes a transcriptional regulator known to activate A-type *ARR* genes, results in the enhanced *ARR4* expression and followed by enhanced ARR4 protein accumulation. ARR4 could then mediate the stomatal ethylene response in the stomata in a phosphorylation-independent way (Figure 7). On the other hand, the phosphorylation-dependent ARR4 pathway occurring *via* H_2O_2 must be occurring in response to other stimuli (such as bacterial elicitors); this remains to be determined.

The complexity arising from these new data in the ethylene signaling pathway in guard cells suggest that cross-talk between the HKs AHK5 and ETR1 are occurring. It has been shown that AHK5 acts to inhibit the ETR1-dependent ethylene pathway leading to root growth inhibition (Iwama *et al.* 2007). The HK function of ETR1 appears to be required at least for the ethylene triple response and leaf development (Qu & Schaller 2004). However in stomatal guard cells, the HK domain of ETR1 appeared to not be essential for H_2O_2-induced stomatal closure (Desikan *et al.* 2005). We therefore postulated that the N-terminus of ETR1 may interact with the H_2O_2-activated AHK5 in the ethylene signaling pathway in guard cells (Desikan *et al.* 2008). Our data here support this hypothesis, in that the downstream components of AHK5 are essential for ethylene signaling. However, robustness of guard cell signaling dictates that there is always more than one signal transduction pathway triggered in response to a given stimulus. Therefore the alternative H_2O_2-independent pathway downstream of ethylene could be independent of AHK5 (Figure 7).

To summarize this data, we identified TCS downstream elements of the AHK5-dependent ethylene- and H_2O_2-induced stomatal closure response in *Arabidopsis*. We describe a novel ethylene-induced stomatal closure response that is independent of H_2O_2. Our data highlight new complexities in the ethylene signal transduction pathway which have not been described before. Stomatal guard cells have proven to be a valuable system to identify new components in signaling pathways. Nevertheless to understand the robust-

ness of this system and to unravel which of the key nodes are essential for ethylene signaling, mathematical modeling is needed alongside detailed quantification of various key steps leading to stomatal closure.

Methods

Plant growth conditions

Nicotiana benthamiana plants that were used for BiFC-constructs transient transformation were cultivated in the greenhouse in a day/night cycle of 14h/10h. Temperature: day 25°C/night 19°C; 60% humidity. For growth of *Arabidopsis* plants, seeds were sown on Levington's F2 compost + sand and maintained in controlled environment growth rooms for 4 weeks under short day conditions of 10 hours light/14 hours dark cycles with a light intensity of 120-150 μE m^{-2} s^{-1} at a temperature of 23°C and 55-65% relative humidity.

Stomatal bioassays

Leaves were floated for 2h under continuous illumination (120-150 μE m^{-2} s^{-1}) in Mes/KCl buffer (5 mM KCl/10 mM Mes/50 μM $CaCl_2$, pH 6.15). Once the stomata were fully open, leaves were treated with either ethephon or H_2O_2 for further 2h. The leaves were subsequently homogenised individually in a Waring blender for 30 s and the epidermal fragments collected on a 100 μm nylon mesh (SpectraMesh, BDH-Merck, UK). Stomatal apertures from epidermal fragments were then measured using a calibrated light microscope attached to an imaging system (Leica QWin software, Leica, UK).

Cloning strategy

All clones were constructed using Gateway™ technology (Invitrogen). The Entry clones were generated by BP-reaction, combining the genes of interest in pDONR207 (Invitrogen). All genes were amplified using cDNA preparations from *Arabidopsis* plant material. To avoid spontaneous mutations, the Entry clone of AHK5 was cloned and propagated using the *E. coli* strain CopyCutter™ (Epicentre).

For the BiFC assays, the *AHP* cDNAs were recombined *via* LR-reaction into pSPYNE-35S and *AHK5* into pSPYCE-35S, which C-terminally express the N- and C-terminal YFP-fragments respectively (Walter *et al.* 2004). The *ARR4* cDNA was combined into pSpyCe-GW binary destination vector, which N-terminally expresses the C-terminal YFP-fragment (Wanke *et al.* 2011).

Yeast-two-hybrid experiments were performed using the Matchmaker™System (Clontech). The *BD-AHK5* and *BD-ARR4* plasmids were constructed by LR-reaction using the corresponding Entry clones and the destination vector pGBKT7-DEST. To generate *AD-AHP1-6*, the destination vector pGADT7-DEST was used.

Yeast-two-hybrid analysis

The BD- and AD-destination clones were co-transformed into the yeast strain PJ69-4A, using lithium acetate/SS-DNA/PEG method (Grefen *et al.* 2009). After transformation, the yeast was grown on vector selective medium (CSM-L$^-$, W$^-$) and incubated for 3 days at 28°C. Subsequently, 5 independent yeast

clones were pooled and grown in liquid vector selective medium to an OD_{600} of 1.0. To test protein interaction, 7,5 µl of each culture were dropped on interaction selective medium (CSM-L$^-$, W$^-$, Ade$^-$) and incubated for 2 days at 28°C and. As a control for testing the presence of the AD- and BD-fusion proteins, the yeast culture was also dropped on vector selective medium.

Infiltration of BiFC-constructs into *Nicotiana benthamiana* leaves

Transient transformation of *Nicotiana benthamiana* leaves using the *Agrobacterium tumefaciens* strain GV3101 pMP90, previously transformed with the desired BiFC-constructs, was carried out as previously described (Schütze *et al.* 2009).

2-3 days post infiltration, *Nicotiana benthamiana* epidermal leaf cells were analysed for fluorescence (protein interaction) by confocal laser scanning microscopy using a Leica TCS SP2 confocal microscope (Leica Microsystems GmbH). The microscopy was done as previously described (Horák *et al.* 2008).

Protein extraction, SDS-PAGE, Western blot and immunodetection

Western Blot analysis was used to verify the correct expression of the desired fusion proteins in BiFC- and Y2H-assays. Leaf discs were excised from infiltrated tobacco plants and proteins were extracted using denaturing SDS sample buffer (Schütze *et al.* 2009). Total protein extract was loaded on a SDS-PAGE and subsequent Western Blot and immunodetection using HA- and c-myc-specific antibodies (Roche) was carried on as described by Schütze and colleagues (2009). The protein extraction from transformed yeast cells was done according to Grefen et al. (2009).

Acknowledgements

We thank J. Kieber and G.E. Schaller for *arr4* and *ahp* seeds. This work was funded by a Leverhulme Trust Early Career Fellowship to R.D., by a DFG grant to K.H. (HA 2146/10-1), a DAAD PhD fellowship to M.V. and PhD fellowship of the state Baden-Württemberg and the University of Tübingen to J.W.

Figure legends

Figure 1 AHK5 interacts with a set of AHP proteins in yeast-two-hybrid assays. (A) Yeast-two-hybrid assay with yeast cells co-expressing BD::AHK5 (AHK5 protein fused to the BD domain of the Gal4 DNA) and the indicated AD::AHP (AHP1 to 6 proteins fused to the AD domain of the Gal4 DNA) fusion proteins. Yeast cells were incubated for 4 days at 28°C on either vector selective (L-, W-) or interaction selective media (L-, W-, Ade-) (B) Western-blot analysis using crude extracts from transformed yeast cells co-expressing the indicated AD::AHP (AHP1 to 6) and BD::AHK5 fusion proteins. The AD::AHP (upper panel) and the BD::AHK5 (lower panel) fusions were detected with a HA- and c-myc-specific antibody respectively.

Figure 2 AHK5 interacts with a set of AHP proteins in a Bimolecular Fluorescence Complementation Assay (BiFC). (A) Confocal images of epidermal tobacco leaf cells (*Nicotiana benthamiana*) co-expressing the indicated YFP-N and YFP-C fusion proteins. The left panels show the fluorescence signal, the middle panels the bright field images of identical cells and the right panels the overlay of both. YFP-N, N-terminal YFP fragment fused to the different AHP proteins; YFP-C, C-terminal YFP fragment fused to the AHK5 protein. The bars represent 10 μm. (B) Western-blot analysis using crude protein extracts from transiently transformed tobacco leaves analysed for BiFC before extraction. The AHP::YFP-N (upper panel) and the AHK5::YFP-C (lower panel) fusions were detected with a c-myc and HA-specific antibody respectively. M, protein marker.

Figure 3 The ethylene and H_2O_2-induced stomatal response pathway downstream of AHK5. (A) Stomatal aperture in leaves of wild type (WS, Col-0) and different *ahp* single, double and triple *Arabidopsis* mutants. The leaves were either mock-treated (black bars) or exposed to 100 μM ethephon (white bars). Data are expressed as mean +/- SE derived from measuring the aperture of at least 60 guard cells from 3 independent experiments. ***** Statistical difference (p-value ≤ 0.001) compared to the non-treated control. (B) Stomatal aperture in leaves of wild type (WS, Col-0) and different *ahp* single, double and triple *Arabidopsis* mutants. The leaves were either mock-treated (black bars) or exposed to 100 μM H_2O_2 (white bars). Data are expressed as mean +/- SE derived from measuring the aperture of at least 60 guard cells from 3 independent experiments. ***** Statistical difference (p-value ≤ 0.001) compared to the non-treated control.

Figure 4 ARR4 interacts with a set of AHP proteins in yeast-two-hybrid assays. (A) Yeast-two-hybrid assay with yeast cells co-expressing BD::ARR4 (ARR4 protein fused to the BD domain of the Gal4 DNA) and the indicated AD::AHP (AHP1 to 6 proteins fused to the AD domain of the Gal4 DNA) fusion proteins. They were incubated for 4 days at 28°C on either vector selective (L-, W-) or interaction selective media (L-, W-, Ade-) (B) Western-blot analysis using crude extracts from transformed yeast cells co-expressing the indicated AD::AHP (AHP1 to 6) and BD::ARR4 fusion proteins. The AD::AHP (upper panel) and the BD::ARR4 (lower panel) fusions were detected with a HA- and c-myc-specific antibody respectively.

Figure 5 ARR4 interacts with a set of AHP proteins in a Bimolecular Fluorescence Complementation Assay (BiFC). (A) Confocal images of epidermal tobacco leaf cells (*Nicotiana benthamiana*) co-expressing the

indicated YFP-N and YFP-C fusion proteins. The left panels show the fluorescence signal, the middle panels the bright field images of identical cells and the right panels the overlay of both. YFP-N, N-terminal YFP fragment fused to the different AHP proteins; YFP-C, C-terminal YFP fragment fused to the ARR4 protein. The bars represent 10 μm. (B) Western-blot analysis using crude extracts from transiently transformed tobacco cells co-expressing the indicated AHP::YFP-N (AHP1 to 6) and YFP-C::ARR4 fusion proteins. The AHP::YFP-N (upper panel) and the YFP-C::ARR4 (lower panel) fusions were detected with a c-myc- and HA-specific antibody respectively. M, protein marker.

Figure 6 The ethylene and H_2O_2-induced stomatal response pathway downstream of AHK5 involves ARR4. (A) Stomatal aperture in leaves of wild type (Col-0, Col-3, WS), *arr4*, ARR4ox (ARR4 overexpressor) and ARR4^{D95N} (non-phosphorylatable ARR4 overexpressor) *Arabidopsis* plants. The leaves were either mock-treated (black bars) or exposed to 100 μM ethephon (white bars). Data are expressed as mean +/- SE derived from measuring the aperture of at least 60 guard cells from 3 independent experiments. ***** Statistical difference (p-value ≤ 0.001) compared to the non-treated control. (B) Stomatal aperture in leaves of wild type (Col-0, Col-3, WS), *arr4*, ARR4ox (ARR4 overexpressor) and ARR4^{D95N} (non-phosphorylatable ARR4 overexpressor) *Arabidopsis* plants. The leaves were either mock-treated (black bars) or exposed to 100 μM H_2O_2 (white bars). Data are expressed as mean +/- SE derived from measuring the aperture of at least 60 guard cells from 3 independent experiments. ***** Statistical difference (p-value ≤ 0.001) compared to the non-treated control.

Figure 7 Hypothetical model of ethylene and H_2O_2-induced stomatal closure responses *via* HKs. The H_2O_2 branch of the pathway occurs *via* AHK5 or ETR1-activated AHP2 signaling leading to activation and phosphorylation ARR4, and thus resulting in stomatal closure. The stimulus which generates H_2O_2 in guard cells and functioning *via* ARR4 phosphorylation remains to be determined. Ethylene stimulates H_2O_2 production *via* ETR1/AHK5. Ethylene response occurs *via* AHK5-AHP1/AHP2-ARR4 pathway, independent of ARR4 phosphorylation. Blue arrows indicate the ethylene response pathway and the red arrows indicate the H_2O_2-dependent pathway leading to stomatal closure. Dashed lines indicate intermediates in an independent ETR1 pathway that includes ARR2 and is based on data not shown in this paper. Black arrows represent transcriptional control. +P, phosphorelay dependent, -P, phosphorelay independent.

References

D'AGOSTINO, I.B., DERUERE, J. and KIEBER, J.J. (2000). Characterization of the response of the Arabidopsis response regulator gene family to cytokinin. *Plant Physiol* **124**(4): 1706-1717.

DESIKAN, R., CHEUNG, M.K., BRIGHT, J., HENSON, D., HANCOCK, J.T. and NEILL, S.J. (2004). ABA, hydrogen peroxide and nitric oxide signalling in stomatal guard cells. *J Exp Bot* **55**(395): 205-212.

DESIKAN, R., HANCOCK, J.T., BRIGHT, J., HARRISON, J., WEIR, I., HOOLEY, R. and NEILL, S.J. (2005). A role for ETR1 in hydrogen peroxide signaling in stomatal guard cells. *Plant Physiol* **137**(3): 831-834.

DESIKAN, R., HORAK, J., CHABAN, C., MIRA-RODADO, V., WITTHOFT, J., ELGASS, K., GREFEN, C., CHEUNG, M.K.*, et al.* (2008). The histidine kinase AHK5 integrates endogenous and environmental signals in Arabidopsis guard cells. *PloS one* **3**(6): e2491.

DESIKAN, R., LAST, K., HARRETT-WILLIAMS, R., TAGLIAVIA, C., HARTER, K., HOOLEY, R., HANCOCK, J.T. and NEILL, S.J. (2006). Ethylene-induced stomatal closure in Arabidopsis occurs via AtrbohF-mediated hydrogen peroxide synthesis. *Plant J* **47**(6): 907-916.

DORTAY, H., GRUHN, N., PFEIFER, A., SCHWERDTNER, M., SCHMÜLLING, T. and HEYL, A. (2008). Toward an Interaction Map of the Two-Component Signaling Pathway of *Arabidopsis thaliana*. *J Proteome Res* **7**(9): 3649-3660.

DORTAY, H., MEHNERT, N., BURKLE, L., SCHMULLING, T. and HEYL, A. (2006). Analysis of protein interactions within the cytokinin-signaling pathway of *Arabidopsis thaliana*. *FEBS J* **273**(20): 4631-4644.

GREFEN, C., DONALD, N., HASHIMOTO, K., KUDLA, J., SCHUMACHER, K. and BLATT, M.R. (2010). A ubiquitin-10 promoter-based vector set for fluorescent protein tagging facilitates temporal stability and native protein distribution in transient and stable expression studies. *Plant J* **64**(2): 355-365.

GREFEN, C. and HARTER, K. (2004). Plant two-component systems: principles, functions, complexity and cross talk. *Planta* **219**(5): 733-742.

GREFEN, C., OBRDLIK, P. and HARTER, K. (2009). The determination of protein-protein interactions by the mating-based split-ubiquitin system (mbSUS). *Methods Mol Biol* **479**: 217-233.

HASS, C., LOHRMANN, J., ALBRECHT, V., SWEERE, U., HUMMEL, F., YOO, S.D., HWANG, I., ZHU, T.*, et al.* (2004). The response regulator 2 mediates ethylene signalling and hormone signal integration in Arabidopsis. *EMBO J* **23**(16): 3290-3302.

HORÁK, J., GREFEN, C., BERENDZEN, K.W., HAHN, A., STIERHOF, Y.D., STADELHOFER, B., STAHL, M., KONCZ, C.*, et al.* (2008). The *Arabidopsis thaliana* response regulator ARR22 is a putative AHP phospho-histidine phosphatase expressed in the chalaza of developing seeds. *BMC Plant Biol* **8**: 77.

HUTCHISON, C.E., LI, J., ARGUESO, C., GONZALEZ, M., LEE, E., LEWIS, M.W., MAXWELL, B.B., PERDUE, T.D.*, et al.* (2006). The Arabidopsis histidine phosphotransfer proteins are redundant positive regulators of cytokinin signaling. *Plant Cell* **18**(11): 3073-3087.

HWANG, I., CHEN, H.C. and SHEEN, J. (2002). Two-component signal transduction pathways in Arabidopsis. *Plant Physiol* **129**(2): 500-515.

HWANG, I. and SHEEN, J. (2001). Two-component circuitry in Arabidopsis cytokinin signal transduction. *Nature* **413**(6854): 383-389.

ISHIDA, K., YAMASHINO, T. and MIZUNO, T. (2008). Expression of the cytokinin-induced type-A response regulator gene ARR9 is regulated by the circadian clock in Arabidopsis thaliana. *Biosci Biotechnol Biochem* **72**(11): 3025-3029.

IWAMA, A., YAMASHINO, T., TANAKA, Y., SAKAKIBARA, H., KAKIMOTO, T., SATO, S., KATO, T., TABATA, S.*, et al.* (2007). AHK5 histidine kinase regulates root elongation through an ETR1-dependent abscisic acid and ethylene signaling pathway in *Arabidopsis thaliana*. *Plant Cell Physiol* **48**(2): 375-380.

JEON, J., KIM, N.Y., KIM, S., KANG, N.Y., NOVAK, O., KU, S.J., CHO, C., LEE, D.J.*, et al.* (2010). A subset of cytokinin two-component signaling system plays a role in cold temperature stress response in Arabidopsis. *J Biol Chem* **285**(30): 23371-23386.

LEONHARDT, N., KWAK, J.M., ROBERT, N., WANER, D., LEONHARDT, G. and SCHROEDER, J.I. (2004). Microarray expression analyses of Arabidopsis guard cells and isolation of a recessive abscisic acid hypersensitive protein phosphatase 2C mutant. *Plant Cell* **16**(3): 596-615.

MIRA-RODADO, V., SWEERE, U., GREFEN, C., KUNKEL, T., FEJES, E., NAGY, F., SCHAFER, E. and HARTER, K. (2007). Functional cross-talk between two-component and phytochrome B signal transduction in Arabidopsis. *J Exp Bot* **58**(10): 2595-2607.

MÜLLER, B. (2011). Generic signal-specific responses: cytokinin and context-dependent cellular responses. *J Exp Bot* **62**(10): 3273-3288.

PHAM, J. and DESIKAN, R. (2009). ROS signalling in stomata. Reactive oxygen Species in Plant Signalling. pp 55-71, eds Rio, LD and Puppo, A. Springer-Verlag, Berlin.

QU, X. and SCHALLER, G.E. (2004). Requirement of the histidine kinase domain for signal transduction by the ethylene receptor ETR1. *Plant Physiol* **136**(2): 2961-2970.

REN, B., LIANG, Y., DENG, Y., CHEN, Q., ZHANG, J., YANG, X. and ZUO, J. (2009). Genome-wide comparative analysis of type-A Arabidopsis response regulator genes by overexpression studies reveals their diverse roles and regulatory mechanisms in cytokinin signaling. *Cell Res* **19**(10): 1178-1190.

SALOME, P.A., TO, J.P., KIEBER, J.J. and MCCLUNG, C.R. (2006). Arabidopsis response regulators ARR3 and ARR4 play cytokinin-independent roles in the control of circadian period. *Plant Cell* **18**(1): 55-69.

SCHAREIN, B., VOET-VAN-VORMIZEELE, J., HARTER, K. and GROTH, G. (2008). Ethylene signaling: identification of a putative ETR1-AHP1 phosphorelay complex by fluorescence spectroscopy. *Anal Biochem* **377**(1): 72-76.

SCHROEDER, J.I., ALLEN, G.J., HUGOUVIEUX, V., KWAK, J.M. and WANER, D. (2001a). Guard Cell Signal Transduction. *Annu Rev Plant Physiol Plant Mol Biol* **52**: 627-658.

SCHROEDER, J.I., KWAK, J.M. and ALLEN, G.J. (2001b). Guard cell abscisic acid signalling and engineering drought hardiness in plants. *Nature* **410**(6826): 327-330.

SCHÜTZE, K., HARTER, K. and CHABAN, C. (2009). Bimolecular fluorescence complementation (BiFC) to study protein-protein interactions in living plant cells. *Methods Mol Biol* **479**: 189-202.

SWEERE, U., EICHENBERG, K., LOHRMANN, J., MIRA-RODADO, V., BAURLE, I., KUDLA, J., NAGY, F., SCHAFER, E.*, et al.* (2001). Interaction of the response regulator ARR4 with phytochrome B in modulating red light signaling. *Science* **294**(5544): 1108-1111.

TO, J.P., HABERER, G., FERREIRA, F.J., DERUERE, J., MASON, M.G., SCHALLER, G.E., ALONSO, J.M., ECKER, J.R.*, et al.* (2004). Type-A Arabidopsis response regulators are partially redundant negative regulators of cytokinin signaling. *Plant Cell* **16**(3): 658-671.

TO, J.P. and KIEBER, J.J. (2008). Cytokinin signaling: two-components and more. *Trends Plant Sci* **13**(2): 85-92.

TRAN, L.S., URAO, T., QIN, F., MARUYAMA, K., KAKIMOTO, T., SHINOZAKI, K. and YAMAGUCHI-SHINOZAKI, K. (2007). Functional analysis of AHK1/ATHK1 and cytokinin receptor histidine kinases in response to abscisic acid, drought, and salt stress in Arabidopsis. *Proc Natl Acad Sci U S A* **104**(51): 20623-20628.

UNDERWOOD, W., MELOTTO, M. and HE, S.Y. (2007). Role of plant stomata in bacterial invasion. *Cell Microbiol* **9**(7): 1621-1629.

URAO, T., MIYATA, S., YAMAGUCHI-SHINOZAKI, K. and SHINOZAKI, K. (2000). Possible His to Asp phosphorelay signaling in an Arabidopsis two-component system. *FEBS Lett* **478**(3): 227-232.

WALTER, M., CHABAN, C., SCHUTZE, K., BATISTIC, O., WECKERMANN, K., NAKE, C., BLAZEVIC, D., GREFEN, C.*, et al.* (2004). Visualization of protein interactions in living plant cells using bimolecular fluorescence complementation. *Plant J* **40**(3): 428-438.

WANKE, D., HOHENSTATT, M.L., DYNOWSKI, M., BLOSS, U., HECKER, A., ELGASS, K., HUMMEL, S., HAHN, A.*, et al.* (2011). Alanine Zipper-Like Coiled-Coil Domains Are Necessary for Homotypic Dimerization of Plant GAGA-Factors in the Nucleus and Nucleolus. *PLoS One* **6**(2): e16070.

Figure 1

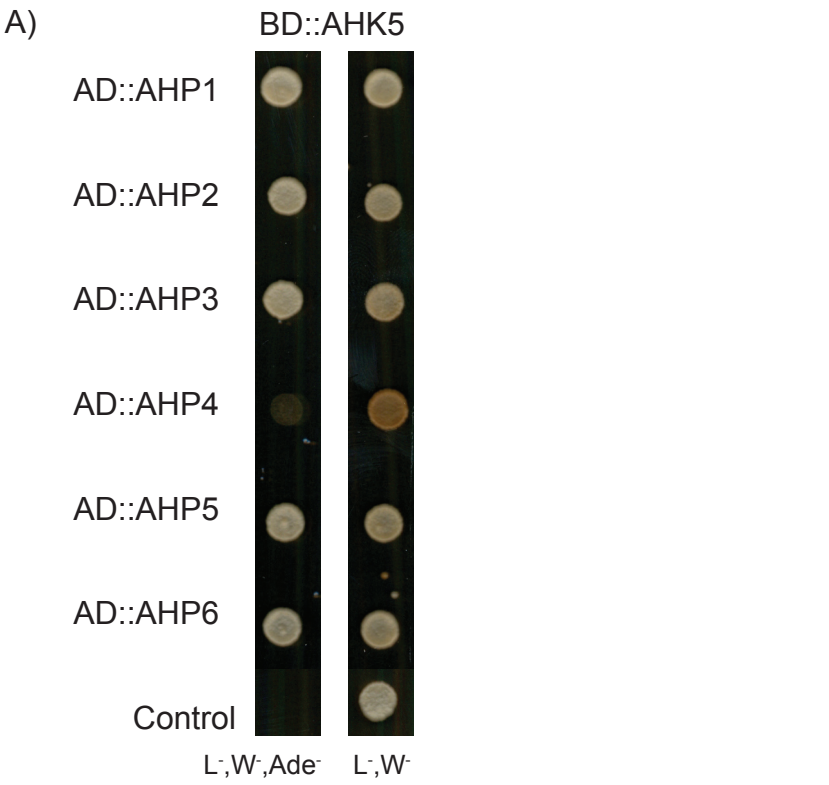
A)
BD::AHK5
AD::AHP1
AD::AHP2
AD::AHP3
AD::AHP4
AD::AHP5
AD::AHP6
Control
L-,W-,Ade-
L-,W-
B)
AD: AHP1 2 3 4 5 6
α-HA
α-myc
BD: AHK5

Figure 2

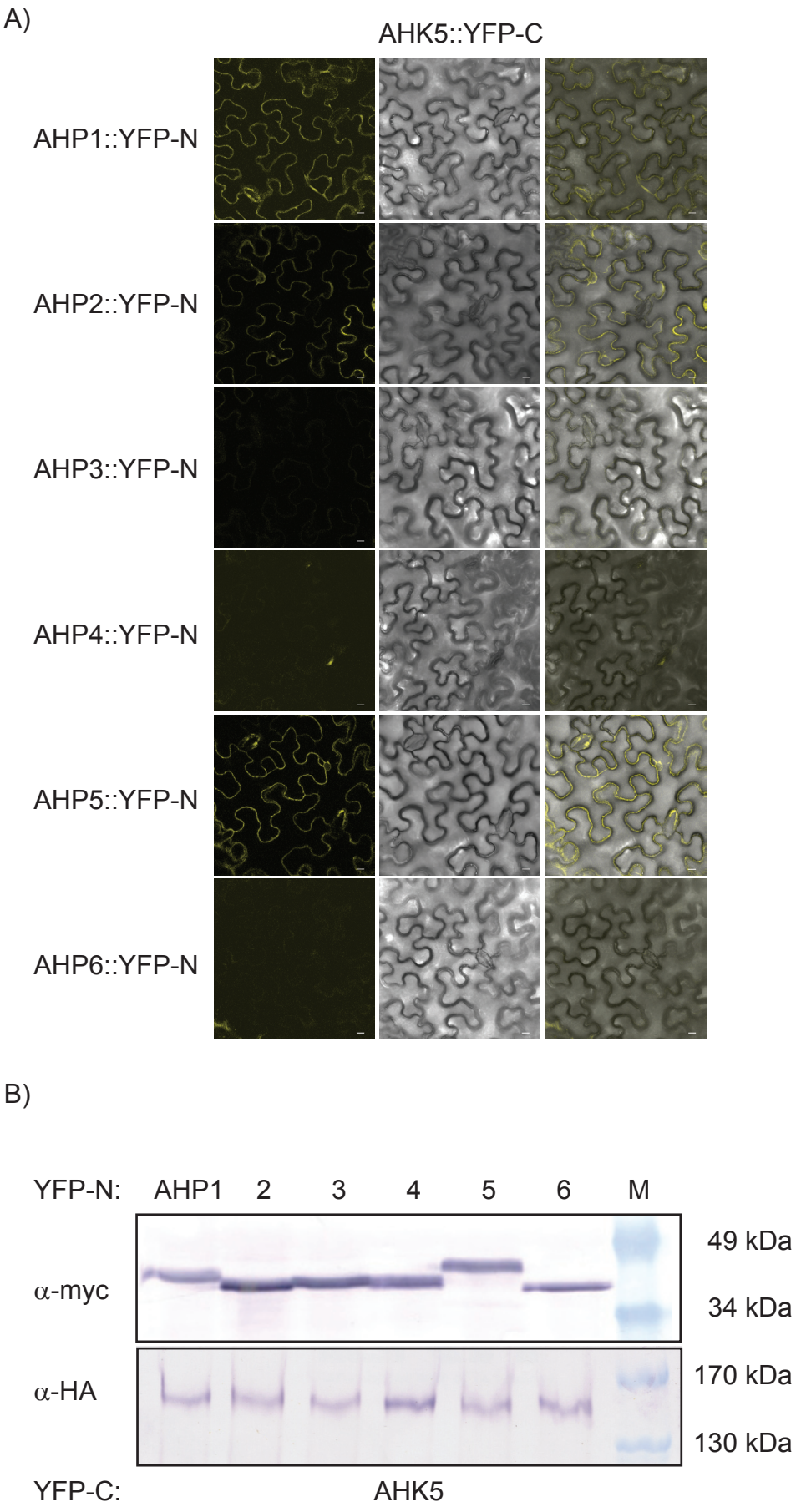
A)
AHK5::YFP-C
AHP1::YFP-N
AHP2::YFP-N
AHP3::YFP-N
AHP4::YFP-N
AHP5::YFP-N
AHP6::YFP-N
B)
YFP-N:
AHP1
2
3
4
5
6
M
α-myc
α-HA
49 kDa
34 kDa
170 kDa
130 kDa
YFP-C:
AHK5

Figure 3

A)

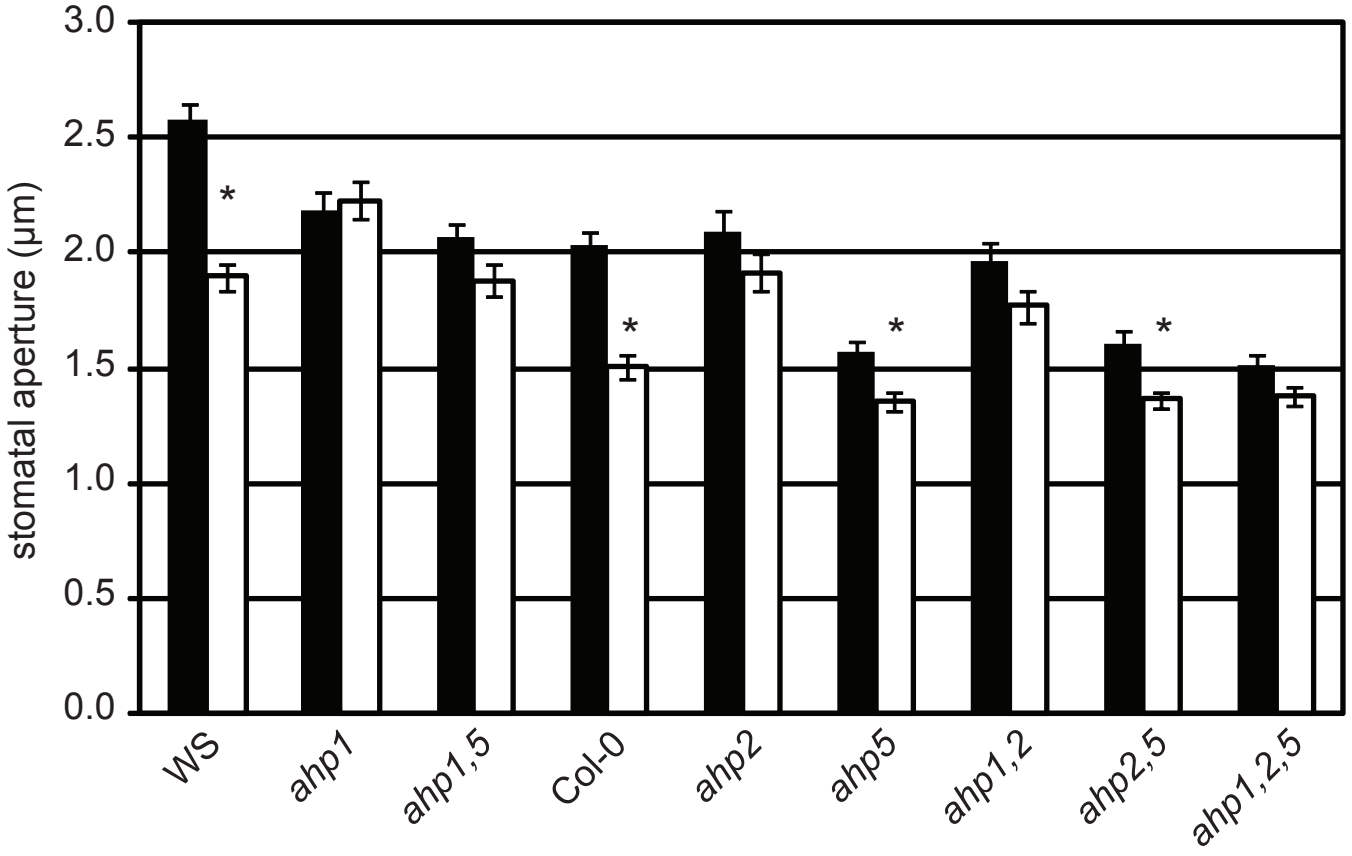
3.0
2.5
2.0
1.5
1.0
0.5
0.0
stomatal aperture (µm)
*
*
*
*
WS
ahp1
ahp1,5
Col-0
ahp2
ahp5
ahp1,2
ahp2,5
ahp1,2,5

B)

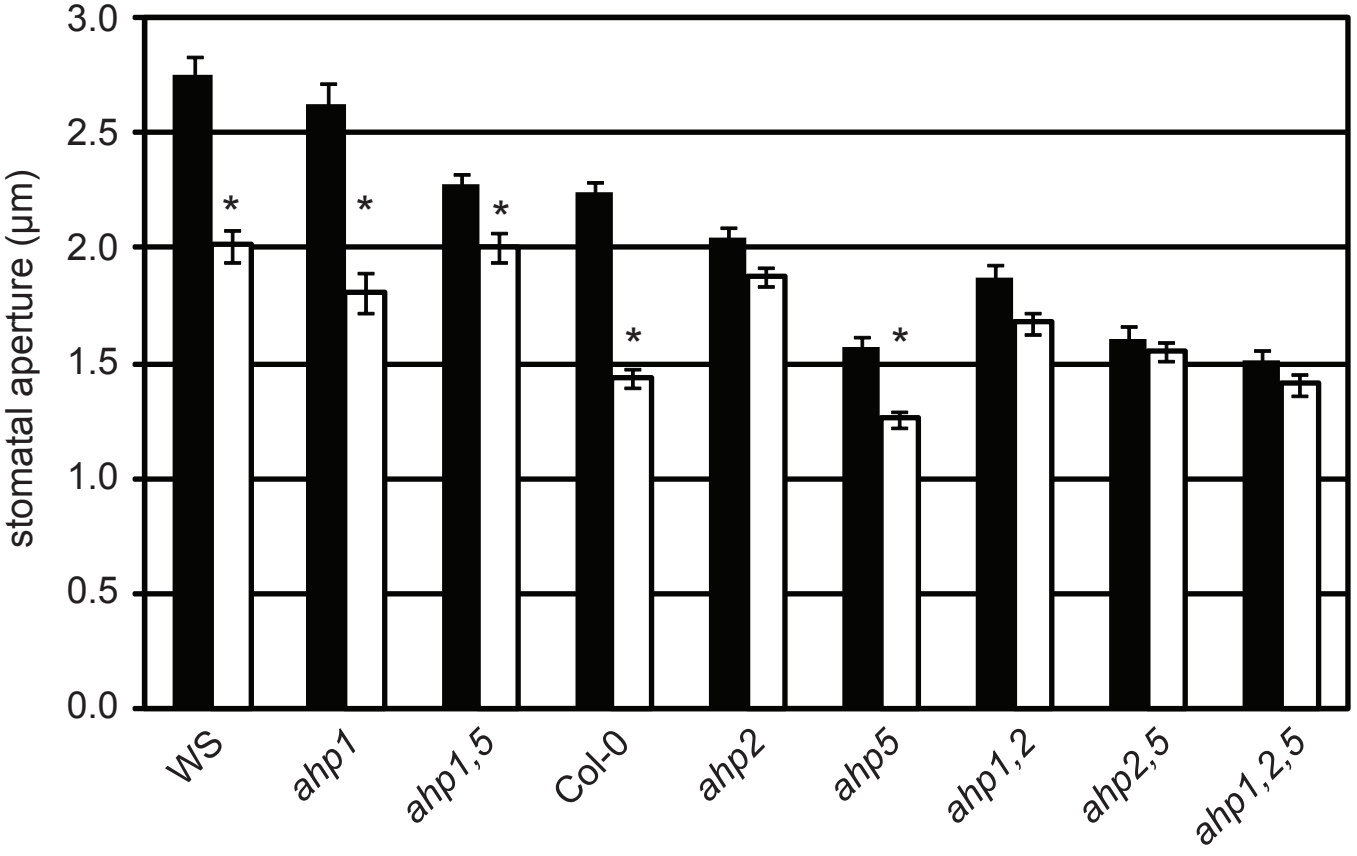
3.0
2.5
2.0
1.5
1.0
0.5
0.0
stomatal aperture (µm)
*
*
*
*
*
WS
ahp1
ahp1,5
Col-0
ahp2
ahp5
ahp1,2
ahp2,5
ahp1,2,5

Figure 4

A)

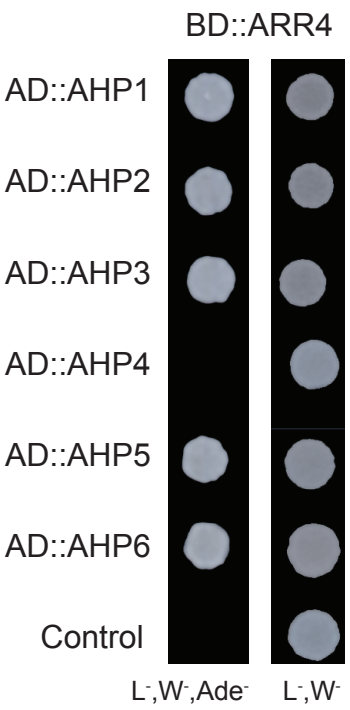
BD::ARR4
AD::AHP1
AD::AHP2
AD::AHP3
AD::AHP4
AD::AHP5
AD::AHP6
Control
L-,W-,Ade-
L-,W-

B)

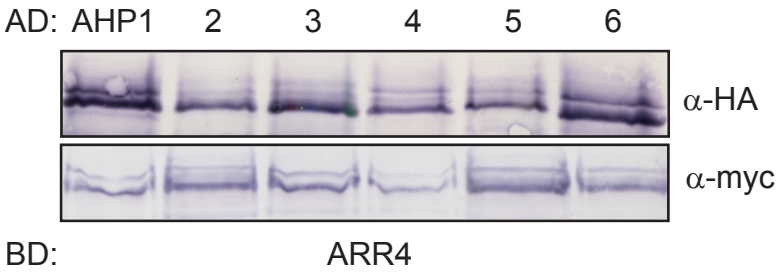
AD: AHP1 2 3 4 5 6
α-HA
α-myc
BD: ARR4

Figure 5

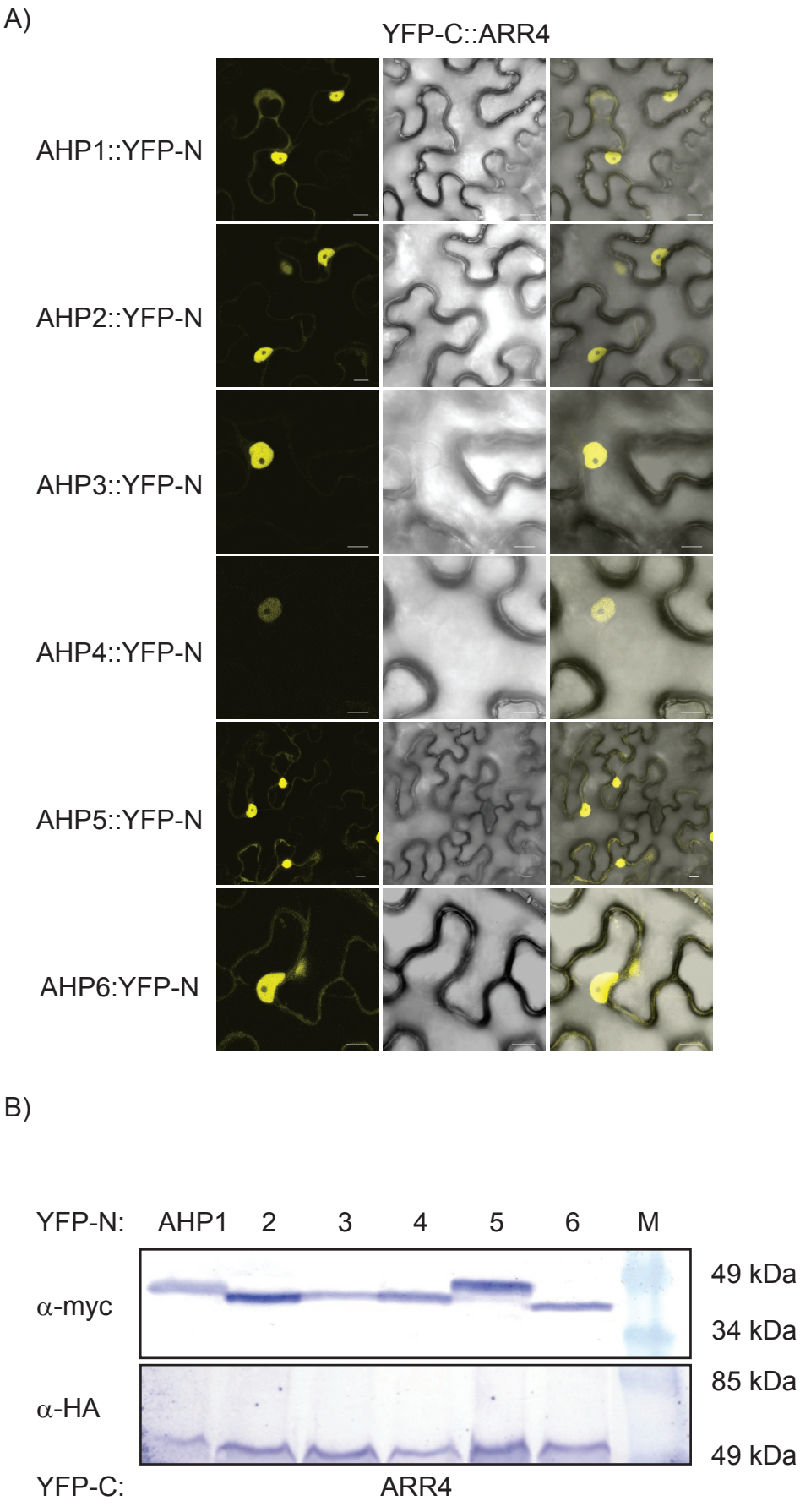
A)
YFP-C::ARR4
AHP1::YFP-N
AHP2::YFP-N
AHP3::YFP-N
AHP4::YFP-N
AHP5::YFP-N
AHP6:YFP-N
B)
YFP-N: AHP1 2 3 4 5 6 M
α-myc
α-HA
49 kDa
34 kDa
85 kDa
49 kDa
YFP-C: ARR4

Figure 6

A)

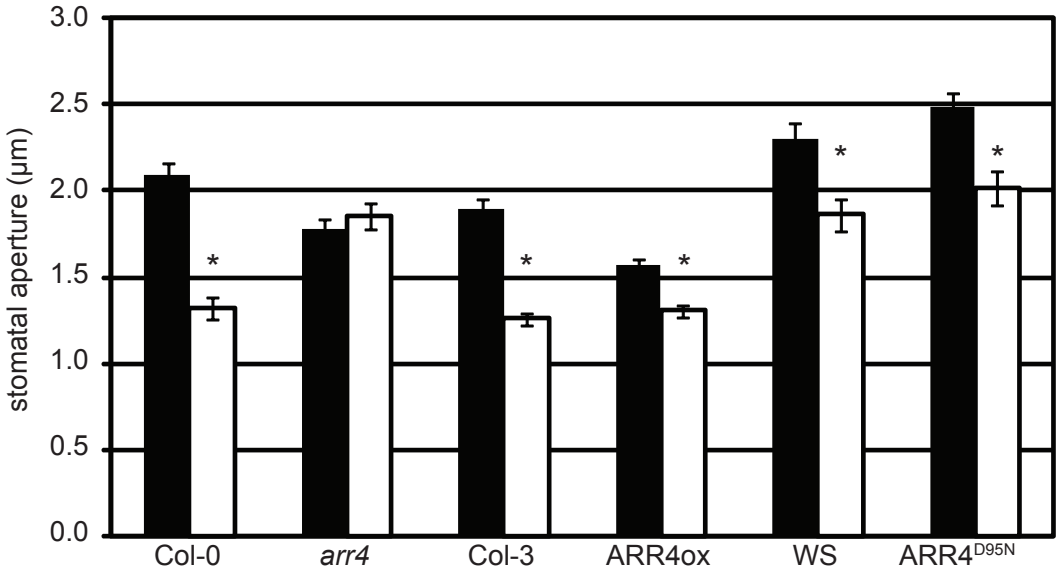
3.0
2.5
2.0
1.5
1.0
0.5
0.0
stomatal aperture (µm)
*
*
*
*
*
Col-0
arr4
Col-3
ARR4ox
WS
ARR4D95N

B)

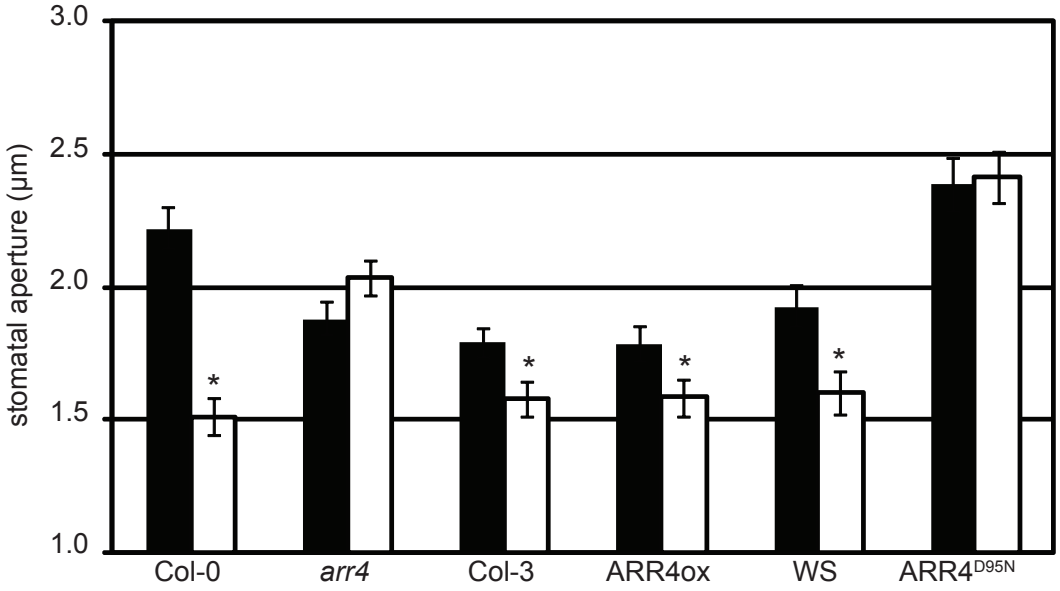
3.0
2.5
2.0
1.5
1.0
stomatal aperture (µm)
*
*
*
*
Col-0
arr4
Col-3
ARR4ox
WS
ARR4D95N

Figure 7

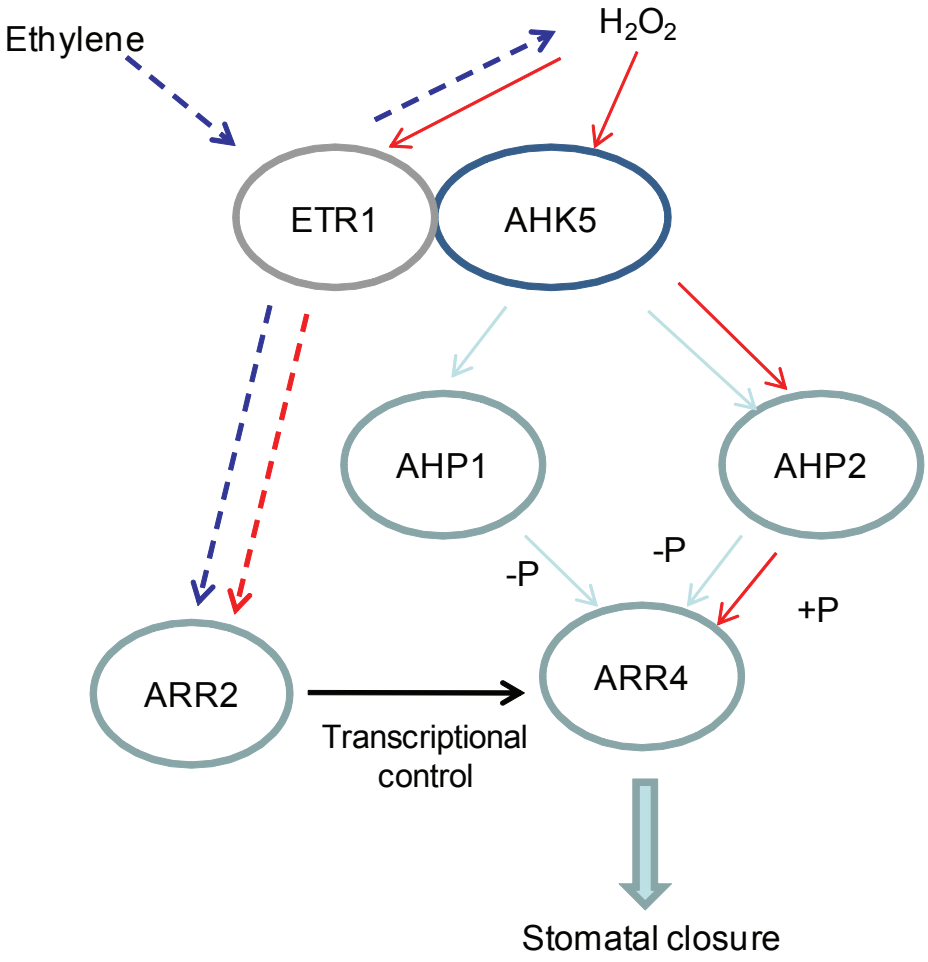
Ethylene
H_2O_2
ETR1
AHK5
AHP1
AHP2
-P
-P
+P
ARR2
ARR4
Transcriptional control
Stomatal closure